Physical, optical and chemical properties of atmospheric aerosols in the western Mediterranean continental background

Anna Ripoll Roca

Aquesta tesi doctoral està subjecta a la llicència ***Reconeixement- NoComercial – CompartirIgual 4.0. Espanya de Creative Commons***.

Esta tesis doctoral está sujeta a la licencia ***Reconocimiento - NoComercial – CompartirIgual 4.0. España de Creative* Commons**.

This doctoral thesis is licensed under the ***Creative Commons Attribution-NonCommercial-ShareAlike 4.0. Spain License***.

Institut de Diagnosi Ambiental i Estudis de l'Aigua

Departament d'Astronomia i Meteorologia

Physical, optical and chemical properties of atmospheric aerosols in the western Mediterranean continental background

Anna Ripoll Roca

PhD Thesis

Barcelona, April 2015

Supervisors:

Dr. Andrés Alastuey Urós

Dr. María Cruz Minguillón Bengochea

Tutor:

Dr. Maria Rosa Soler Duffour

Programa de doctorat en Física

Physical, optical and chemical properties of atmospheric aerosols in the western Mediterranean continental background

Memòria presentada per

Anna Ripoll Roca

per optar al grau de
Doctor per la Universitat de Barcelona

Barcelona, abril 2015

Directors de tesis:
Dr. Andrés Alastuey Urós
Dra. María Cruz Minguillón Bengochea

Tutora:
Dra. Maria Rosa Soler Duffour

Als qui m'han donat la vida.

Be less curious about people

and more curious about ideas.

Marie Sklodowska-Curie (1867-1934),
the first woman who won a Nobel Prize.

Abstract

Atmospheric aerosols have played a key role in the development of the Earth's atmosphere. Without atmospheric particles rainfall would not exist and the climate would be very different. However, anthropogenic emissions have changed the chemical composition of atmospheric aerosols significantly through emissions of particles and precursor gases, particularly since the industrial revolution. Moreover, numerous studies have demonstrated that specific atmospheric aerosols do not only influence Earth's climate, but also have adverse effects on air quality, and consequently on human health and ecosystems. For these reasons, regional to continental policies have been implemented in an effort to combat the negative effects associated with atmospheric aerosols.

Because of the vast amounts of anthropogenic emissions combined with the efficient atmospheric long-range transport, it is nowadays very difficult to find areas of the Earth that are not measurably impacted by aerosols. Urban atmospheric monitoring sites are employed to determine the average exposure of general population to urban aerosols, although they are inadequate to identify the origin of regional and long-range-transported aerosols, as local sources prevail in this type of environments. To this end, monitoring sites isolated from the direct influence of local anthropogenic sources, such as regional and continental background sites, are needed. This type of sites are representative of the air quality of a wide area; however regional background sites are frequently more influenced by regional transport of pollutants than continental background sites.

In southern Europe, and in particular in the western Mediterranean region, the meteorological conditions with warmer temperatures and lower precipitation, together with the abrupt topography around the Mediterranean Sea, hinder aerosol dispersion and prevent atmospheric wet-scavenging processes. Moreover, the Mediterranean region is highly influenced by large anthropogenic emissions from shipping, power generation, industrial processes and urban agglomerations, among others; and natural emissions from the Mediterranean Sea and the biosphere, as well as, regularly impacted by African dust outbreaks, soil resuspension and wildfires. This peculiar and complex atmospheric scenario results in higher concentrations of aerosols around the Mediterranean Basin than in northern Europe.

A detailed study of the physical, optical and chemical properties of the continental background aerosols measured at Montsec (MSC) monitoring station is presented in this work. The MSC mountain site (1570 m a.s.l.) was established during the development of this thesis; it is located in the western Mediterranean and became a member of the GAW (Global Atmosphere Watch) network in 2014. The relatively long-term series of measurements were analyzed, with the aim of identifying seasonal, weekly and intra-day variations of the aerosol properties, and the main factors influencing these variations were deduced. Greater emphasis was placed on the evaluation of the impact of different atmospheric episodes on the aerosol properties. This work also aims to discriminate natural and anthropogenic aerosol contributions affecting continental background aerosols in the western Mediterranean, with a focus on the partitioning of the chemical components into different size fractions. Moreover, an aerosol chemical speciation monitor (ACSM) was used during almost a year for the first time in Europe at a remote site, with the aim of identifying intra-day variations of submicron aerosol chemical composition. This instrument provides real-time mass concentration of submicron particulate organics, nitrate, sulfate, ammonium and chloride. The identification of different types of organic aerosols was also undertaken using receptor modelling. All these results were compared with those simultaneously recorded at the Montseny (MSY) monitoring station located in the western Mediterranean in order to discriminate regional and continental contributions. This station was installed in 2002 and it has become a reference site for characterizing regional background aerosols, participating in several international campaigns. Furthermore, results obtained at MSC were also compared with those obtained at other remote European sites.

Aerosol measurements (particle mass (PM), particle number, absorption (σ_{ap}), scattering (σ_{sp}) and chemical composition) from MSC were found to be comparable in magnitude to those from other remote sites in Europe, when removing African dust

outbreaks influence. This suggests that a *continental background* designation for MSC site is applicable. Nevertheless, differences between MSC and the other European remote sites highlight the importance of new particle formation processes as a source of particles, the lower contribution of combustion and industrial processes, the greater impact of shipping emissions, and the higher influence of biogenic emissions. Moreover, these differences corroborate the important contribution of long-range transport of mineral dust and reveal an impact of regional dust resuspension in the western Mediterranean region.

Continental background aerosols in this region are affected by natural and anthropogenic emissions. Whereas PM_1 (PM of diameter less than 1 µm) is made of (in decreasing concentrations) organic matter, sulfate, ammonium, mineral matter, nitrate, elemental carbon, sea salt and trace elements; PM_{1-10} (PM of diameter between 1 and 10 µm) is constituted by mineral matter, followed by organic matter, nitrate, sulfate, sea salt, ammonium and elemental carbon. Comparison of σ_{ap} measurements with those of elemental carbon revealed an average mass absorption cross section at MSC of 9.1 $m^2\ g^{-1}$. The continental to regional background increase in the western Mediterranean was estimated in 1.1 µg m^{-3} for PM_1 and 4.0 µg m^{-3} for PM_{10} (PM of diameter less than 10 µm). The PM_1 increase is attributed mostly to the higher concentrations of sulfate, elemental carbon, organic matter, and some anthropogenic trace elements (V, Ni, Cu, Zn, and Pb) at the regional background environment, whereas the PM_{10} increase is attributed to higher concentrations of organic matter, sulfate, nitrate and sea salt. This is due to the fact that the regional background site is located closer to the anthropogenic sources and the sea, and that it is within the planetary boundary layer most of the days.

The simultaneous measurements of aerosol chemical composition at regional and continental background environments demonstrated, for the first time in the western Mediterranean, that the impact of air masses from Africa and Europe is frequently larger in the higher parts of the troposphere than in the lower parts. This is reflected in the higher average concentrations of PM_{1-10} mineral matter at MSC (14 µg m^{-3}, 1570 m a.s.l.) than at MSY (8 µg m^{-3}, 720 m a.s.l.) under African dust outbreaks. Moreover, the net contribution of Saharan dust to annual averaged PM_{10} concentrations is estimated in 16% at MSC and 11% at MSY. Under European episodes concentrations of PM_1, black carbon, nitrate, organic matter, and industrial and traffic-related trace elements undergo an increase, which is usually more evident at the continental background site than at the regional background station.

A clear seasonal variation is observed for the majority of the aerosol parameters measured at MSC, with the highest values in summer and the lowest in winter, except

for nitrate, in agreement with previous studies in the western Mediterranean. The higher nitrate concentrations in winter than in summer are attributed to the high volatility of ammonium nitrate at low humidity and relatively high temperature. The summer maximum of the rest of aerosol measurements is caused by a variety of factors: 1) the increase in the planetary boundary layer height, which favors the transport of surface pollutants towards high-altitude sites; 2) the higher intensity of convection processes that increase the regional dust resuspension; 3) the regional recirculation of air masses over the western Mediterranean inducing the accumulation of pollutants across the region; 4) the higher intensity of solar radiation, which enhances atmospheric photochemistry, promoting the formation of secondary inorganic and organic aerosols; 5) the higher temperature that increases biogenic emissions; 6) the lower number of precipitation events that prevents atmospheric wet-scavenging processes, and 7) the higher frequency of African dust episodes. In winter very different conditions drive the aerosol phenomenology at MSC. The combination of (1) the higher frequency of thermal inversions and (2) the lower vertical development of the PBL, which leave MSC in the free troposphere most of the day, together with (3) the higher occurrence and intensity of Atlantic advections, accounts for the markedly reduced aerosol concentrations in winter.

Coarse PM showed more enhanced seasonal variation than fine PM and black carbon due to the higher influence of resuspended and long-range-transported dust in this fraction, whereas PM_1 and black carbon are more associated with anthropogenic emissions, which have less marked seasonal variation but better defined weekly patterns. The reduced human activity at the weekend is reflected in the concentrations of PM_1 and black carbon with a delay of one day (minimum on Sunday and Monday), which confirms that MSC is located at a sufficient distance from direct anthropogenic emissions, although it is still affected by them.

At MSC the intra-day variation of PM_x, black carbon, σ_{sp} and PM_1 major inorganic components (sulfate, nitrate, ammonium and chloride) is not equally influenced by the emission sources and atmospheric processes influencing particle number and submicron organic aerosol variations. Thus, in the western Mediterranean continental background environment these aerosol parameters are governed by different factors. Whereas daily patterns of PM_x, black carbon, σ_{sp}, and PM_1 major inorganic components are driven by mountain breezes, planetary boundary layer evolution, and air mass origin, diurnal cycles of particle number and submicron organic aerosol concentrations are less affected by the air mass origin and depend more on meteorological variables such as temperature and solar radiation. As a result, poorly defined daily patterns were observed in summer and clearer in winter, except for

particle number and submicron organic aerosol concentrations, which show marked diurnal cycles throughout the year and regardless of the air mass origin, with a clear increase around midday. This midday increase was partially attributed to new particle formation processes.

Source apportionment studies of the organic fraction based on the ACSM mass spectra led to the identification of three types of submicron organic aerosols in summer, namely hydrocarbon-like organic aerosol (HOA), semivolatile oxygenated organic aerosol (SV-OOA) and low-volatility oxygenated organic aerosol (LV-OOA), and three types in winter, namely HOA, biomass burning organic aerosol (BBOA) and one single oxygenated organic aerosol (OOA). The OOA in winter showed a higher degree of oxidation than any of the two OOA types in summer, which confirms that OA at MSC had a dominant aged character during winter. During summer, the major organic aerosol constituent was the LV-OOA, with 64% on average, followed by SV-OOA (26%) and HOA (10%), whereas in winter OOA accounted for 71%, BBOA contributed 24%, and HOA contribution decreased to 5%. A clear daily pattern of organic components, with a maximum at midday, was found throughout the year regardless of the air mass origin, except for Atlantic advections in winter. Nevertheless, in summer the maximum SV-OOA concentrations were measured between 11:00 and 12:00 UTC, whereas those of LV-OOA and HOA were measured between 12:00 and 13:00 UTC. Conversely, in winter, the maximum concentrations of HOA, BBOA, and OOA were observed simultaneously around 14:00 UTC. The different daily patterns between seasons can be attributed to the higher production of secondary organic aerosol (SOA) in summer as opposed to winter, when the maximum daily concentrations are reached later driven by the mountain breezes.

Resum

Els aerosols atmosfèrics han jugat un paper crucial en el desenvolupament de l'atmosfera terrestre. Sense les partícules atmosfèriques la pluja no hauria existit i el clima seria molt diferent. No obstant això, les emissions antropogèniques han canviat de forma significativa la composició química dels aerosols atmosfèrics degut a l'emissió de partícules i de gasos precursors, sobretot des de la revolució industrial. A més a més, nombrosos estudis han demostrat que els aerosols atmosfèrics, tant naturals com antropogènics, no només influencien el clima de la Terra, sino que també provoquen efectes perjudicials per la qualitat de l'aire, i per tant, per la salut humana i els ecosistemes. Per aquests motius, la legislació a nivell nacional i europeu ha fet un gran esforç per regular i controlar els aerosols atmosfèrics.

Degut a la gran quantitat d'emissions antropogèniques i a l'eficient transport atmosfèric de llarga distància, avui en dia és molt difícil trobar alguna regió del planeta que no estigui afectada per l'impacte dels aerosols. Les estacions de mesura dels contaminants atmosfèrics situades a les zones urbanes s'utilitzen per determinar l'exposició mitjana de la població als aerosols urbans. Tanmateix, aquestes estacions no són apropiades per identificar l'origen dels aerosols regionals ni dels transportats a llarga distància, perquè en aquest tipus d'ambients predominen les fonts locals. Per aquest motiu, son necessàries les estacions de mesura allunyades de la influència directa de les fonts antropogèniques locals, com ara les estacions rurals i remotes. Aquest tipus d'estacions són representatives de la qualitat de l'aire d'una àmplia zona. No obstant això, les estacions rurals es troben més influenciades pel transport regional dels contaminants que les estacions remotes.

Al sud d'Europa, i en particular a la zona de l'oest del Mediterrani, les condicions meteorològiques amb altes temperatures i baixes precipitacions, conjuntament amb la brusca topografia que envolta el mar Mediterrani, dificulten els processos de rentat de l'atmosfera i de dispersió dels aerosols. A més a més, la regió del Mediterrani està summament influenciada tant per les emissions antropogèniques dels vaixells, la indústra i el trànsit rodat, entre d'altres, com per les emissions naturals procedents de les intrusions de pols del Sàhara, la resuspensió del sòl, els incendis forestals o la vegetació. Tots aquests processos generen una dinàmica atmosfèrica particular i complexa, que provoca que les concentracions d'aerosols al voltant del Mediterrani siguin més altes que les del nord d'Europa.

En aquesta tesi doctoral es presenta un estudi detallat de les propietats físiques, òptiques i químiques dels aerosols de fons continental mitjançant les mesures realitzades a l'estació del Montsec (MSC, 1570 m s.n.m.). Aquesta estació de muntanya està situada a l'oest del Mediterrani, es va establir durant el desenvolupament d'aquesta tesi i forma part de la xarxa GAW (Global Atmosphere Watch) des de 2014. Les sèries de mesures relativament llargues van ser analitzades amb l'objectiu d'identificar les variacions estacionals, setmanals i intradiàries de les propietats dels aerosols, i així deduir els principals factors que influencien aquestes variacions. L'avaluació de l'impacte dels diferents episodis atmosfèrics sobre les propietats dels aerosols va ser realitzada amb especial atenció i tenint en compte la distribució dels compostos químics en diferents fraccions granulomètriques. Aquest treball també té com a objectiu distingir les emissions naturals i antropogèniques que afecten als aerosols del fons continental a l'oest del Mediterrani. Finalment, es va dur a terme un estudi detallat de les variacions intradiàries dels principals components químics que formen els aerosols submicromètrics. Amb aquest objectiu, es va utilitzar un monitor d'especiació química dels aerosols (angl., aerosol chemical speciation monitor, ACSM) en un lloc remot per primera vegada a Europa durant gairebé un any. Aquest equip és capaç de mesurar en temps real la concentració màssica dels components no refractaris de les partícules submicromètriques, diferenciant la matèria orgànica, el nitrat, el sulfat, l'amoni i el clorur. A més a més, aquest últim estudi també inclou la identificació dels diferents tipus d'aerosol orgànic (angl., organic aerosol, OA) mitjançant l'ús de models receptors. Tots els resultats obtinguts van ser comparats amb els obtinguts simultàniament a l'estació de mostreig del Montseny (MSY), localitzada a l'oest del Mediterrani, per tal de distingir la contribució regional i la de fons continental. Aquesta estació va ser instal·lada l'any 2002, i ha esdevingut una estació fonamental per a la caracterització dels aerosols del fons regional de l'oest del Mediterrani, participant en nombroses campanyes de mesura internacionals. Per últim,

els resultats obtinguts al MSC també van ser comparats amb els obtinguts a altres estacions remotes d'Europa.

Les propietats dels aerosols (massa (PM), nombre de partícules, absorció (σ_{ap}), dispersió (σ_{sp}) i composició química) mesurades al MSC van presentar magnituds comparables a les obtingudes a altres llocs remots d'Europa, una vegada eliminada la influència de les intrusions de pols sahariana. Per tant, la designació de *fons continental* és aplicable per a l'estació del MSC. Tanmateix, algunes diferències entre les propietats mesurades al MSC i les mesurades a altres estacions remotes europees van revelar que els processos de formació de noves partícules com a font de partícules són molt importants a la regió oest del Mediterrani. També van destacar que els processos industrials i de combustió tenen una menor contribució a la matèria particulada (angl., particulate matter, PM) ambiental, mentre que les emissions biogèniques i dels vaixells tenen un major impacte. A més a més, van corroborar que el transport de llarga distància de la pols del Sàhara és la font natural de partícules més important en aquesta regió, i van revelar que la pols de resuspensió regional té un impacte considerable.

Els aerosols del fons continental d'aquesta zona estan afectats tant per les emissions naturals com per les antropogèniques, la qual cosa va donar com a resultat un PM_1 (PM amb diàmetre inferior a 1 µm) constituït per (en ordre de més concentració a menys) matèria orgànica, sulfat, amoni, matèria mineral, nitrat, carboni elemental, sal marina i elements traça, i un PM_{1-10} (PM amb diàmetre entre 1 i 10 µm) format per matèria mineral, matèria orgànica, nitrat, sulfat, sal marina, amoni i carboni elemental. La comparació de les mesures d'absorció amb les de carboni elemental va revelar una MAC (angl., mass absorption cross section) mitjana de 9.1 m^{-2} g^{-1} al MSC. Les concentracions mitjanes d'aerosols al fons regional de l'oest del Mediterrani van ser 1.1 µg m^{-3} pel PM_1 i 4.0 µg m^{-3} pel PM_{10} (PM de diàmetre inferior a 10 µm) més altes que les del fons continental. L'increment del PM_1 s'atribueix a les majors concentracions de sulfat, carboni elemental, matèria orgànica i alguns elements traces (V, Ni, Cu, Zn i Pb) trobades al fons regional, mentre que l'increment de PM_{10} s'associa a les concentracions més elevades de matèria orgànica, sulfat, nitrat i sal marina. Això és degut al fet que el MSY està més a prop de les fonts antropogèniques i del mar, i a que es troba dins la capa límit planetària la major part dels dies.

La mesura simultània de la composició química dels aerosols a un lloc representatiu del fons continental i a un del fons regional va permetre demostrar, per primera vegada en la zona d'estudi, que l'impacte de les masses d'aire procedents d'Àfrica i d'Europa és molt sovint major a les parts altes de la troposfera que a les parts baixes. Això es veu reflectit en les majors concentracions mitjanes de PM_{1-10} de

matèria mineral al MSC (14 µg m^{-3}, 1570 m s.n.m.) respecte al MSY (8 µg m^{-3}, 720 m s.n.m.) durant les intrusions de pols sahariana. A més a més, la contribució neta de pols sahariana estimada pel PM_{10} és del 16% al MSC i del 11% al MSY. Quan la zona d'estudi es veu afectada per episodis europeus, les concentracions de PM_1, carboni negre, nitrat, matèria orgànica, i elements traça relacionats amb les emissions industrials i del trànsit rodat experimenten un increment que normalment és més evident al fons continental que al regional.

La majoria dels paràmetres mesurats al MSC mostren una clara variació estacional, amb els valors més alts a l'estiu i els més baixos a l'hivern, excepte el nitrat, tal i com s'ha vist en altres estudis sobre l'oest del Mediterrani. Les majors concentracions de nitrat a l'hivern que a l'estiu s'atribueixen a l'alta volatilitat del nitrat amònic quan la humitat és baixa i la temperatura és relativament alta. Els valors màxims registrats per la resta de mesures durant l'estiu són causats per la combinació dels següents factors: 1) l'augment de l'altura de la capa límit planetària, que afavoreix el transport dels contaminants antropogènics des de les zones baixes de la troposfera a les zones altes; 2) la major intensitat dels processos de convecció, els quals incrementen la resuspensió del sòl a nivell regional; 3) la recirculació de masses d'aire damunt de l'oest del Mediterrani, que indueix l'acumulació de contaminants a aquesta regió; 4) la intensitat més elevada de la radiació solar, que fa augmentar la fotoquímica atmosfèrica i, per tant, la formació d'aerosols secundaris, tant inorgànics com orgànics; 5) la major temperatura, la qual cosa provoca un increment de les emissions biogèniques; 6) la disminució de la precipitació, que dificulta l'eliminació dels aerosols; i 7) les intrusions de pols sahariana, que afecten aquesta zona molt freqüentment a l'estiu. A l'hivern, per contra, les condicions atmosfèriques al MSC són molt diferents. La combinació de (1) la major freqüència d'inversions tèrmiques i (2) un menor desenvolupament vertical de la capa límit planetària fan que el MSC es trobi a la troposfera lliure (angl., free troposphere, FT) la major part del temps. A més a més, a l'hivern, (3) les adveccions atlàntiques són més freqüents i de més intensitat, de manera que es produeix una disminució molt marcada de les concentracions dels aerosols durant aquesta estació de l'any.

Tot i tenir una variació estacional similar, la fracció grollera del PM va presentar un patró més accentuat que la fracció fina i el carboni negre. Això és degut a que la fracció grollera està més influenciada per les aportacions de la pols sahariana i de la resuspensió del sòl, les quals tenen una clara estacionalitat. Per contra, el PM_1 i el carboni negre s'associen més a emissions antropogèniques, que tenen menys variacions estacionals però un patró setmanal més definit. Això es veu reflectit en les concentracions de PM_1 i de carboni negre, ja que mostren un mínim estadísticament

significatiu el diumenge i el dilluns, corresponent a la disminució de l'activitat humana durant el cap de setmana. El fet que la disminució de les emissions antropogèniques durant el cap de setmana arribi al MSC amb un dia de retard confirma que és un lloc situat a suficient distància de les fonts antropogèniques, malgrat que continuï rebent la seva influència.

Al MSC les variacions intradiàries de PM_x, carboni negre, σ_{sp} i de la majoria de compostos inorgànics del PM_1 (sulfat, nitrat, amoni i clorur) no es veuen influenciades per les mateixes fonts ni pels mateixos processos atmosfèrics que influencien les variacions intradiàries del nombre de partícules i dels aerosols submicromètrics orgànics. Per tant, al fons continental de l'oest del mediterrani aquests paràmetres depenen de factors diferents. D'una banda, els cicles diaris de PM_1, carboni negre, σ_{sp} i de la majoria de compostos inorgànics del PM_1 són governats pels vents de muntanya, l'evolució de la capa límit planetària, i l'origen de la massa d'aire; mentre que, per l'altra banda, els patrons diaris del nombre de partícules i dels aerosols submicromètrics orgànics es veuen menys afectats per l'origen de la massa d'aire i depenen més de les condicions meteorològiques, com ara la temperatura i/o la radiació solar. Com a resultat s'observa una alta variabilitat dels cicles diaris, amb patrons poc definits a l'estiu però més clars a l'hivern, excepte pel nombre de partícules i pels aerosols submicromètrics orgànics que mostren un cicle diari tot l'any, independentment de l'origen de la massa d'aire, amb un màxim al migdia. Aquest increment a migdia va ser atribuït en part als processos de formació de noves partícules.

La caracterització dels OA va ser possible gràcies a les dades obtingudes amb l'ACSM. Aquest estudi va permetre identificar tres tipus de compostos orgànics diferents a l'estiu, anomenats aerosol orgànic similar als hidrocarburs (angl., hydrocarbon-like organic aerosol, HOA), aerosol orgànic oxigenat semivolàtil (angl., semivolatile oxygenated organic aerosol, SV-OOA), i aerosol orgànic oxigenat de baixa volatilitat (angl., low-volatility oxygenated organic aerosol, LV-OOA), i tres tipus a l'hivern, anomenats HOA, aerosol orgànic de crema de biomassa (angl., biomass burning organic aerosol, BBOA), i un únic aerosol orgànic oxigenat (angl., oxygenated organic aerosol, OOA). L'OOA identificat a l'hivern té un major grau d'oxidació que els dos OOA trobats a l'estiu, la qual cosa confirma que l'OA al MSC te un caràcter envellit durant l'hivern. Durant l'estiu, el major constituent d'OA va ser el LV-OOA amb un 64% de mitjana, seguit del SV-OOA amb un 26%, i del HOA amb un 10%, metre que a l'hivern la proporció d'OOA va ser del 71%, la de BBOA del 24%, i la d'HOA del 5%. Aquests compostos orgànics van mostrar una clara variació intradiària, amb un màxim al migdia durant tot l'any i independentment de l'origen de la massa d'aire, excepte

durant les adveccions atlàntiques a l'hivern. No obstant, durant l'estiu les concentracions més elevades de SV-OOA van ser mesurades entre les 11:00 i les 12:00 UTC, mentre que les de LV-OOA i HOA van ser entre les 12:00 i les 13:00 UTC. Per altra banda, durant l'hivern, les concentracions màximes de HOA, BBOA i OOA es van registrar simultàniament al voltant de les 14:00 UTC. Les diferències entre els patrons diaris trobats a l'estiu i a l'hivern poden ser degudes a la major producció d'aerosols orgànics secundaris (angl., secondary organic aerosol, SOA) durant l'estiu en comparació a l'hivern, quan les concentracions màximes es produeixen més tard perquè depenen dels vents de muntanya.

Resumen

Los aerosoles atmosféricos han jugado un papel crucial en el desarrollo de la atmósfera terrestre. Sin las partículas atmosféricas la lluvia no habría existido y el clima sería muy diferente. A pesar de esto, las emisiones antropogénicas han cambiado de forma significativa la composición química de los aerosoles atmosféricos debido a la emisión de partículas y de gases precursores, sobretodo desde la revolución industrial. Además, numerosos estudios han demostrado que los aerosoles atmosféricos, tanto naturales como antropogénicos, no solo influyen en el clima de la Tierra sino que también provocan efectos perjudiciales para la calidad del aire, y por lo tanto, para la salud humana y los ecosistemas. Por estos motivos, la legislación a nivel nacional y europeo ha hecho un gran esfuerzo para regular y controlar los aerosoles atmosféricos.

Debido a la gran cantidad de emisiones antropogénicas y a la eficiencia del transporte atmosférico de larga distancia, hoy en día es muy difícil encontrar alguna región del planeta que no esté afectada por el impacto de los aerosoles. Las estaciones de medida de los contaminantes atmosféricos situadas en las zonas urbanas se utilizan para determinar la exposición media de la población a los aerosoles urbanos. Sin embargo, estas estaciones no son apropiadas para identificar el origen de los aerosoles regionales ni de los transportados a larga distancia, porque en este tipo de ambientes predominan las fuentes locales. Asi pues, son necesarias las estaciones de medida alejadas de la influencia directa de las fuentes antropogénicas locales, como las estaciones rurales y remotas. Este tipo de estaciones son representativas de la calidad del aire de una amplia zona. No obstante,

las estaciones rurales acostumbran a estar más influenciadas por el transporte regional de los contaminantes que las estaciones remotas.

En el sur de Europa, y en particular en la zona oeste del Mediterráneo, las condiciones meteorológicas, con altas temperaturas y bajas precipitaciones, conjuntamente con la brusca topografía que rodea el mar Mediterráneo, dificultan los procesos de lavado de la atmósfera y de dispersión de los aerosoles. Además, la región del Mediterráneo está sumamente influenciada tanto por las emisiones antropogénicas de los barcos, la industria y el tráfico rodado, entre otras, como por las emisiones naturales procedentes de las intrusiones de polvo del Sahara, la resuspensión del suelo, los incendios forestales o la vegetación. Todos estos procesos generan una dinámica atmosférica particular y compleja que provoca que las concentraciones de aerosoles en el Mediterráneo sean más elevadas que las del norte de Europa.

En esta tesis doctoral se presenta un estudio detallado de las propiedades físicas, ópticas y químicas de los aerosoles de fondo continental mediante las medidas realizadas en la estación del Montsec (MSC, 1570 m s.n.m.). Esta estación de montaña está situada al oeste del Mediterráneo, se estableció durante el desarrollo de esta tesis y forma parte de la red GAW (Global Atmosphere Watch) desde 2014. Las series de medidas relativamente largas fueron analizadas con el objetivo de identificar las variaciones estacionales, semanales e intradiarias de las propiedades de los aerosoles, y así deducir los principales factores que determinan dichas variaciones. La evaluación del impacto de los diferentes episodios atmosféricos sobre las propiedades de los aerosoles fue realizada con especial atención y teniendo en cuenta la distribución de los compuestos químicos en diferentes fracciones granulométricas. Este trabajo también tiene como objetivo distinguir las emisiones naturales y antropogénicas que afectan a los aerosoles del fondo continental al oeste del Mediterráneo. Finalmente, se llevó a cabo un estudio detallado de las variaciones intradiarias de los principales componentes químicos que forman los aerosoles submicrométricos. Con este fin, se utilizó un monitor de especiación química de aerosoles (ingl., aerosol chemical speciation monitor, ACSM) en un lugar remoto por primera vez en Europa durante casi un año. Este equipo es capaz de medir en tiempo real la concentración másica de los componentes no refractarios de las partículas submicrométricas, diferenciando la materia orgánica, el nitrato, el sulfato, el amonio y el cloruro. Además, este último estudio también incluye la identificación de los diferentes tipos de aerosol orgánico (ingl., organic aerosol, OA) mediante el uso de modelos receptores. Todos los resultados obtenidos fueron comparados con los obtenidos simultáneamente en la estación del Montseny (MSY), localizada en el oeste

del Mediterráneo, a fin de distinguir la contribución regional y la de fondo continental. Esta estación fue instalada en el año 2002 y se ha convertido en una estación fundamental para la caracterización de los aerosoles de fondo regional al oeste del Mediterráneo, participando en numerosas campañas de medida internacionales. Por último, los resultados obtenidos en el MSC también fueron comparados con los obtenidos en otras estaciones remotas de Europa.

Las propiedades de los aerosoles (masa (PM), número de partículas, absorción (σ_{ap}), dispersión (σ_{sp}) y composición química) medidas en el MSC presentaron magnitudes comparables a las obtenidas en otros sitios remotos de Europa, una vez eliminada la influencia de las intrusiones de polvo sahariano. Por tanto, la designación de *fondo continental* es aplicable para la estación del MSC. Sin embargo, algunas diferencias entre las propiedades medidas en el MSC y las medidas en otras estaciones remotas europeas revelaron que los procesos de formación de nuevas partículas como fuente de partículas son muy importantes en la región oeste del Mediterráneo. También destacaron que los procesos industriales y de combustión tienen una menor contribución al PM ambiental (ingl., particulate matter, PM), mientras que las emisiones biogénicas y las de los barcos tienen un mayor impacto. Además, corroboraron que el transporte de larga distancia de polvo del Sahara es la fuente natural de partículas más importante en la región, y revelaron que el polvo de resuspensión regional tiene un impacto considerable.

Los aerosoles de fondo continental de esta zona están afectados tanto por las emisiones naturales como por las antropogénicas, lo cual dio como resultado un PM_1 (PM con diámetro inferior a 1 µm) constituido por (en orden de mayor a menor concentración) materia orgánica, sulfato, amonio, materia mineral, nitrato, carbono elemental, sal marina y elementos traza, y un PM_{1-10} (PM con diámetro entre 1 y 10 µm) formado por materia mineral, materia orgánica, nitrato, sulfato, sal marina, amonio y carbono elemental. La comparación de las medidas de absorción con las de carbono elemental reveló una MAC (ingl., mass absorption cross section) promedio de 9.1 m^{-2} g^{-1} en el MSC. Las concentraciones promedias de los aerosoles de fondo regional del oeste del Mediterráneo fueron 1.1 µg m^{-3} para el PM_1 y 4.0 µg m^{-3} para el PM_{10} (PM con diámetro inferior a 10 µm) más altas que las del fondo continental. El incremento del PM_1 se atribuye a las mayores concentraciones de sulfato, carbono elemental, materia orgánica y algunos elementos traza (V, Ni, Cu, Zn y Pb) encontradas en el fondo regional, mientras que el incremento de PM_{10} se asocia a las concentraciones más elevadas de materia orgánica, sulfato, nitrato y sal marina. Esto se debe al hecho de que el MSY está más cerca de las fuentes antropogénicas y del mar, y a que se encuentra dentro de la capa límite planetaria la mayor parte de los días.

La medida simultánea de la composición química de los aerosoles en un sitio representativo del fondo continental y en uno del fondo regional permitió demostrar, por primera vez en la zona de estudio, que el impacto de las masas de aire procedentes de África y de Europa es a menudo mayor en las partes altas de la troposfera que en las bajas. Esto se ve reflejado en los promedios de las concentraciones de PM_{1-10} de materia mineral ya que son mayores en el MSC (14 µg m^{-3}, 1570 m s.n.m.) que en el MSY (8 µg m^{-3}, 720 m s.n.m.) durante las intrusiones de polvo sahariano. Además, la contribución neta de polvo sahariano estimada para el PM_{10} es del 16% en el MSC y del 11% en el MSY. Cuando la zona de estudio se ve afectada por episodios europeos las concentraciones de PM_1, carbono negro, nitrato, materia orgánica, y de elementos traza relacionados con las emisiones industriales y del tráfico rodado experimentan un incremento que normalmente es más evidente en el fondo continental que en el regional.

La mayoría de los parámetros medidos en el MSC mostraron una clara variación estacional, con los valores más altos en verano y los más bajos en invierno, excepto el nitrato, tal y como se ha visto en otros estudios sobre el oeste del Mediterráneo. Las mayores concentraciones de nitrato en invierno que en verano se atribuyen a la alta volatilidad del nitrato amónico cuando la humedad es baja y la temperatura relativamente alta. Los valores máximos registrados por el resto de medidas durante el verano son causados por la combinación de los siguientes factores: 1) el aumento de la altura de la capa límite planetaria, que favorece el transporte de los contaminantes antropogénicos de las zonas bajas de la troposfera a las zonas altas; 2) la mayor intensidad de los procesos de convección, los cuales incrementan la resuspensión del suelo a nivel regional; 3) la recirculación de masas de aire en el oeste del Mediterráneo, que provocan la acumulación de contaminantes en esta región; 4) la intensidad más elevada de la radiación solar, que aumenta la fotoquímica atmosférica y por tanto la formación de aerosoles secundarios, tanto inorgánicos como orgánicos; 5) la mayor temperatura, lo cual provoca un incremento en las emisiones biogénicas; 6) la disminución de la precipitación, que dificulta la eliminación de los aerosoles; y 7) las intrusiones de polvo sahariano que afectan esta zona muy frecuentemente en verano. En invierno, por el contrario, las condiciones atmosféricas en el MSC son muy diferentes. La combinación de (1) una mayor frecuencia de inversiones térmicas y (2) un menor desarrollo vertical de la capa límite planetaria, hacen que el MSC se encuentre en la troposfera libre (ingl., free troposphere, FT) la mayor parte del tiempo. Además, en invierno, (3) las advecciones atlánticas son más frecuentes y de más intensidad, de manera que se produce una disminución muy marcada de las concentraciones de los aerosoles en esta estación del año.

A pesar de tener una variación estacional similar, la fracción gruesa del PM presentó un patrón más acentuado que la fracción fina y el carbono negro. Esto es debido a que la fracción gruesa está más influenciada por los aportes de polvo sahariano y de la resuspensión del suelo, los cuales tienen una clara estacionalidad, mientras que el PM_1 y el carbono negro están más asociados a emisiones antropogénicas que tienen una menor estacionalidad pero un patrón semanal más definido. Esto se ve reflejado en las concentraciones de PM_1 y de carbono negro, ya que muestran un mínimo estadísticamente significativo el domingo y el lunes, correspondiente a la disminución de la actividad humana durante el fin de semana. El hecho de que la disminución de las emisiones antropogénicas durante el fin de semana llegue al MSC con un día de retraso confirma que es un sitio situado a suficiente distancia de las fuentes antropogénicas, aunque continúe recibiendo su influencia.

En el MSC las variaciones intradiarias de PM, carbono negro, σ_{sp} y de la mayoría de los compuestos inorgánicos del PM_1 (sulfato, nitrato, amonio i cloruro) no están influenciados por las mismas fuentes ni por los mismos procesos atmosféricos que determinan las variaciones intradiarias del número de partículas y de los aerosoles submicrométricos orgánicos. Por tanto, en el fondo continental del oeste del Mediterráneo estos parámetros dependen de factores diferentes. Por un lado, los ciclos diarios de PM_1, carbono negro, σ_{sp} y de la mayoría de los compuestos inorgánicos del PM_1 son gobernados por los vientos de montaña, la evolución de la capa límite planetaria y el origen de la masa de aire, mientras que por el otro lado los patrones diarios del número de partículas y de los aerosoles submicrométricos orgánicos están menos afectados por el origen de la masa de aire y dependen más de las condiciones meteorológicas como la temperatura y/o la radiación solar. Todos estos procesos dan lugar a una alta variabilidad de los ciclos diarios, con patrones poco definidos en verano pero más claros en invierno, excepto para el número de partículas y para los aerosoles submicrómetros orgánicos que muestran un ciclo diario todo el año, independientemente del origen de la masa de aire, con un máximo al mediodía. Este incremento al mediodía se atribuye en parte a los procesos de formación de nuevas partículas.

La caracterización del OA fue posible gracias a los datos obtenidos con el ACSM. Este estudio permitió identificar tres tipos de compuestos orgánicos diferentes en verano, nombrados aerosol orgánico similar a los hidrocarburos (ingl., hydrocarbon-like organic aerosol, HOA), aerosol orgánico oxigenado semivolátil (ingl., semivolatile oxygenated organic aerosol, SV-OOA) y aerosol orgánico oxigenado de baja volatilidad (ingl., low-volatility oxygenated organic aerosol, LV-OOA), y tres tipos en

invierno, nombrados HOA, aerosol orgánico de quema de biomassa (ingl., biomass burning organic aerosol, BBOA) y un único aerosol orgánico oxigenado (ingl., oxygenated organic aerosol, OOA). El OOA identificado en invierno tiene un mayor grado de oxidación que los dos OOA encontrados en verano, lo cual confirma que el OA en MSC tiene un carácter envejecido durante el invierno. Durante el verano, el mayor constituyente del OA fue el LV-OOA con un 64% en promedio, seguido por el SV-OOA con un 26% y por el HOA con un 10%, mientras que en invierno la proporción de OOA fue del 71%, la de BBOA del 24% y la del HOA del 5%. Estos compuestos orgánicos mostraron una clara variación intradiaria, con un máximo al mediodía, durante todo el año e independientemente del origen de la masa de aire, excepto durante las advecciones atlánticas en invierno. Sin embargo, en verano las concentraciones más elevadas de SV-OOA se midieron entre las 11:00 y las 12:00 UTC, mientras que las de LV-OOA y HOA fueron entre las 12:00 y las 13:00 UTC. Por otro lado, en inverno, las concentraciones máximas de HOA, BBOA y OOA se registraron simultáneamente alrededor de las 14:00 UTC. Las diferencias entre los patrones diarios encontrados en verano y en invierno pueden ser debidas a la mayor producción de aerosol orgánico secundario (ingl., secondary organic aerosol, SOA) durante el verano en comparación al invierno, cuando las concentraciones máximas se producen más tarde porque dependen de los vientos de montaña.

Contents

1. Introduction _____ 5

1.1. Atmospheric aerosols 5

1.1.1. Aerosol emission sources 5
1.1.2. Global aerosol distribution 7
1.1.3. Aerosol processes 8
1.1.4. Aerosol chemical composition 10
1.1.5. Aerosol size distribution 12

1.2. Effects of aerosols 15

1.2.1. Human health effects 15
1.2.2. Climate effects 17

1.3. European air quality standards for aerosols 21
1.4. Continental background environments 23
1.5. Peculiarities of the western Mediterranean aerosols 25
1.6. Previous knowledge and studies on atmospheric aerosols in the western Mediterranean basin by IDAEA-CSIC group 28
1.7. Gaps in current knowledge 32
1.8. Objectives 33
1.9. Structure of the thesis 35

2. Methodology 39

2.1. Montsec (MSC) monitoring station 39

2.2. Measurements of aerosol physical properties 43

2.2.1. Offline particle mass concentration 43

2.2.2. Real-time particle mass concentration 44

2.2.3. Particle number concentration 44

2.2.4. Particle number size distribution 46

2.3. Measurements of aerosol optical properties 48

2.3.1. Aerosol absorption coefficient measurements 48

2.3.2. Aerosol scattering coefficient measurements 49

2.4. Offline aerosol chemical composition and data analyses 50

2.4.1. Aerosol chemical composition analyses 50

2.4.2. Aerosol composition data analysis 52

2.5. Real-time aerosol chemical composition and data analyses 53

2.5.1. Aerosol chemical composition measurements 53

2.5.2. ACSM data processing 54

2.5.3. ACSM intercomparison study 55

2.5.4. Source apportionment of organic aerosol 57

2.6. Classification of atmospheric episodes 59

2.6.1. Backward trajectories: Hysplit model 59

2.6.2. Boundary layer height 59

2.6.3. Aerosol dispersion models 60

3. Articles included in this thesis 63

3.1. Author's contribution to the articles 63

3.2. Article 1: Three years of aerosol mass, black carbon and particle number concentrations at Montsec (southern Pyrenees, 1570 m a.s.l.) 65

3.3. Article 2: Joint analysis of continental and regional background environments in the western Mediterranean: PM_1 and PM_{10} concentrations and composition 97

3.4. Article 3: Long-term real-time chemical characterization of submicron aerosols at Montsec (Southern Pyrenees, 1570 m a.s.l.) 133

3.5. Article 4: Climatology of aerosol optical properties and black carbon mass absorption cross section at a remote high-altitude site in the western Mediterranean Basin 163

4. Summarized results and discussion ***187***

4.1. Average concentrations of aerosols and comparison with other high-altitude and regional background European sites *188*

4.2. Seasonal variation of aerosols *192*

4.3. Intra-day variation of aerosols *196*

5. Conclusions ***203***

Future prospects ***209***

Scientific contributions ***213***

References ***219***

Agraïments/Acknowledgments ***245***

Appendix ***251***

A. Appendix: List of acronyms and symbols *251*

B. Appendix: List of detection limit and uncertainty for PM components *254*

1

Introduction

1.1. Atmospheric aerosols

Atmospheric aerosols are defined as a suspension of fine solid and/or liquid particles in the atmosphere (Seinfeld and Pandis, 2006). Atmospheric aerosols comprise particles that range from a few nanometers (nm) to tens of micrometers (μm) in diameter. These particles can be emitted directly to the atmosphere (primary aerosols) or formed from gaseous precursors (secondary aerosols). Sources of particulate matter (PM) include both natural and anthropogenic emissions. Once released into the atmosphere, aerosols are subjected to many processes that affect their spatial distribution, time of residence, chemical, physical and optical properties (Levin and Cotton, 2009), and hence their influence on human health (WHO, 2013), climate (Boucher et al., 2013) and ecosystems (Burkhardt and Pariyar, 2014). Compared to trace gases, aerosols are relatively complex to characterize because of their multi-component chemical composition, and their large range in particle size.

1.1.1. Aerosol emission sources

On a global scale, natural primary emissions are the dominant sources, whereas anthropogenic emissions contribute with a low proportion to the total and cause mainly secondary aerosols (Huneeus et al., 2012). Aerosols of natural origin include sea salt, mineral matter (mostly desert dust), biogenic emissions (spores, pollens and organics from biogenic gases), volcanic emissions (dust and sulfates from volcanic SO_2) and naturally occurring biomass burning (such as wild forest fires) (Seinfeld and Pandis,

2006). PM emissions attributable to the human activities (anthropogenic aerosols) can be fuel combustion emissions, industrial processes, nonindustrial fugitive sources (such as road dust resuspension, wind erosion of cropland, construction, etc.), domestic emissions (from cooking, heating, etc.), transportation sources (automobiles, shipping, etc.) among others (Seinfeld and Pandis, 2006). The type of source will largely govern the physical and optical properties of the aerosols (mass, size, density, scattering, absorption, etc.) as well as the chemical composition. The estimated global annual emission fluxes of aerosols carry significant uncertainty and therefore range from 8257 to 18600 Tg y^{-1} (Boucher et al., 2013). However, all estimations coincide with the fact that sea salt and mineral matter contribute the largest amount to the global aerosol loading.

Marine aerosols are produced at the sea surface by bubble bursting induced mostly, but not exclusively, by breaking waves. The effective emission flux of sea salt particles to the atmosphere depends on the surface wind speed, sea state and atmospheric stability, and to a lesser extent on the temperature and composition of the sea water (De Leeuw et al., 2011). On a regional scale, the contribution of marine aerosol to the PM mass will depend on the geographical area, proximity to the coast and meteorology.

Mineral dust particles arise mainly from natural disintegration of aggregates following creeping and saltation of larger soil particles over desert and other arid surfaces (Kok, 2011). The principal arid and semi-arid surfaces of the Earth are located in the so-called ‘dust belt’ (North Africa, Middle East, and Central and South Asia) and in South and North America, Namibia and Australia (Prospero et al., 2002). The magnitude of dust emissions to the atmosphere depends on the surface wind speed and many soil-related factors such as its texture, moisture and vegetation cover (Marticorena, 2014). Despite its main natural origin, mineral matter can have an anthropogenic origin such as construction and demolition processes, road dust resuspension, and/or wind erosion of cropland (Ginoux et al., 2012).

Carbonaceous aerosols represent also an important fraction of the atmospheric aerosols, however, their global emission fluxes estimations carry significant uncertainties (Boucher et al., 2013). Carbonaceous aerosols are usually divided into organic compounds, collectively referred to as organic aerosol (OA) or organic matter (OM), and elemental carbon (EC) or black carbon (BC). Organic aerosols comprise a myriad of organic compounds that can be directly emitted from sources (primary organic aerosol (POA)) or formed from photochemical atmospheric reactions (secondary organic aerosol (SOA)) (Jimenez et al., 2009). POA and SOA have both natural and anthropogenic origin including bioaerosols, biomass burning, and fossil fuel

combustion, among others, and involving gaseous organic precursors such as volatile organic compounds (VOCs). EC or BC particles are produced from the incomplete combustion of fossil fuels and biomass (Goldberg, 1985) and therefore they are only primary. The main sources of EC or BC in the atmosphere are vehicle emissions (mainly diesel engines), power generation (especially coal-fuelled power plants), certain industrial processes, natural and anthropogenic biomass combustion and domestic emissions (Bond et al., 2013).

Primary anthropogenic aerosols are produced mainly by fossil fuel combustion, energy plants, metallurgic industry and other industrial activities (mainly cement, ceramic and brick production), road traffic (brake and tyre wear and pavement erosion), agricultural activities, waste treatment plants and fertilizer production plants (Gieré and Querol, 2010). However, the highest proportion of anthropogenic aerosols is made up of secondary particles produced chemically from gaseous precursors such as sulfur dioxide (SO_2), ammonia (NH_3), nitrogen oxides (NO_x) and VOCs. SO_2 is emitted by coal and fuel oil combustion used for power generation and shipping (Huneeus et al., 2012), NH_3 is mostly produced from agricultural emissions although it can be from sewage and waste in urban areas (Reche et al., 2012b), and NO_x are principally emitted by road traffic and industrial processes (EEA Technical report, 2013).

On a local scale, the relative contribution of different sources to the ambient PM differs from the proportion of global scale emissions shown by emission inventories. Therefore, the application of source apportionment techniques is required to assess such contributions (Belis et al., 2013).

1.1.2. Global aerosol distribution

Because the time for air parcels to circle the Earth on winds in the troposphere is of the same order of magnitude as the residence time of atmospheric aerosols, there is no location on the globe that is not influenced by aerosol sources (Levin and Cotton, 2009). Once released, particles are dispersed in the atmosphere through processes of advection, convection and turbulence. As a result, long-range transport can occur and particles may reach remote locations.

Hemispheric-scale differences in land area (39% of the northern hemisphere is covered by land vs. 19% in the southern hemisphere) and in human population have led to large inter-hemispheric differences in primary aerosol source strengths (Figure 1.1). This involves both natural and anthropogenic aerosols, but the greatest differences are seen for fossil fuel and aircraft emissions. According to data summarized by Boucher et al. (2013), more than 90% of the aircraft emissions and

~99% of the fossil fuel emissions are emitted into the atmosphere over the northern hemisphere. More than 80% of the mineral dust is produced in the northern hemisphere (Jickells et al., 2005), and <20% of the dust flux into the oceans occurs in the southern hemisphere. In contrast, biomass burning emissions are more evenly distributed between hemispheres, with a split of nearly 50%:50%. Sea salt is the only primary aerosol produced in greater quantities in the southern hemisphere (Figure 1.1).

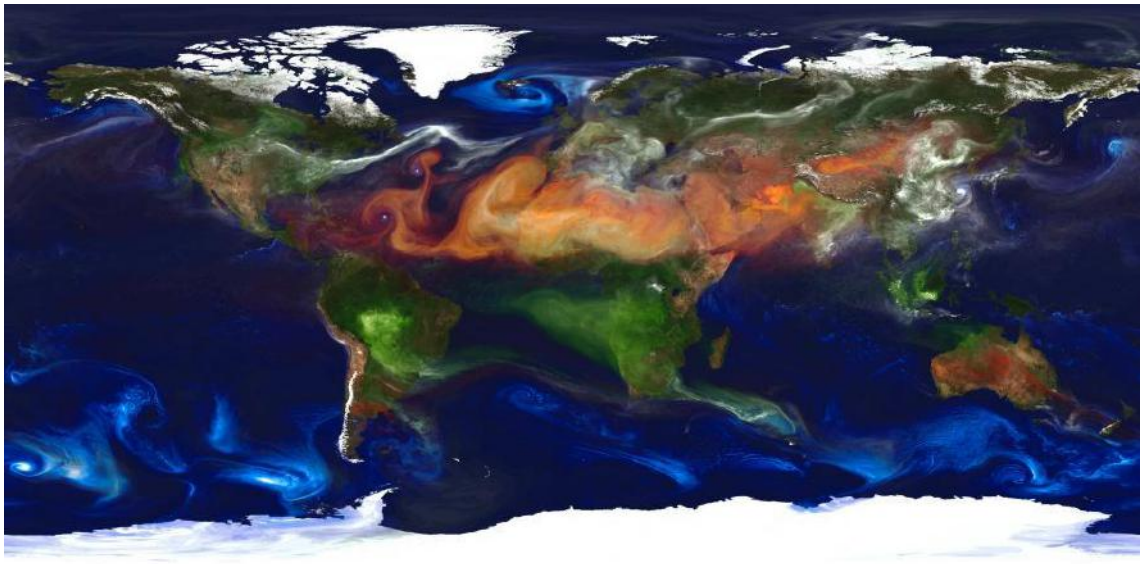

Figure 1.1 Image of the global aerosol distribution produced by NASA. The image was produced using high-resolution global atmospheric modeling run on the Discover supercomputer at the NASA Center for Climate Simulation by William Putman from NASA/Goddard. The colors show aerosol particles as dust (gold/brown), sea-spray (blue), biomass burning/wildfires (green) and industrial/urban (white).

1.1.3. Aerosol processes

New particle formation (NPF) is the process by which low-volatility vapors nucleate spontaneously into stable molecular clusters (e.g., Zhang et al., 2012). These low-volatility vapors include sulfuric acid, amines, ammonia, and organic acids (Kulmala et al., 2013), and are produced from photo-oxidation of atmospheric gaseous precursors (SO_2, NH_3, VOCs, etc.). The molecular clusters can be formed from the original gas phase (gas-to-particle conversion processes), which are referred to as homogeneous nucleation, or can be produced from pre-existing small particles, which are referred to as heterogeneous nucleation. Several nucleation mechanisms have been proposed, including homogeneous water-sulfuric acid nucleation, homogeneous water-sulfuric acid-ammonia nucleation, ion-induced nucleation of organic or inorganic vapors, or kinetically controlled homogeneous nucleation (Kulmala et al., 2013). Pre-existing

particles in the atmosphere can scavenge the gaseous precursors necessary for nucleation through condensation processes and thus clean air conditions are often more favorable for NPF processes (Birmili et al., 2003). The occurrence of nucleation depends on a number of variables. Ambient air conditions, such as temperature, relative humidity and solar radiation are believed to be influential factors on nucleation processes (Easter and Peters, 1994). Photochemistry plays also a pivotal role in NPF as it generates free radicals in the atmosphere that can react with gaseous precursors to produce the vapors necessary for nucleation (Kulmala and Kerminen, 2008).

Nucleation has been observed to occur in almost all environments, including: the Polar Regions (Wiedensohler et al., 1996), high-altitude sites (Venzac et al., 2009), continental boreal forests (Kulmala et al., 1998), remote areas (Birmili et al., 2001), and urban environments (Dall'Osto et al., 2013; Pey et al., 2008), among many others. In urban environments, traffic emissions contribute significantly to nucleation processes through emissions of precursor gases necessary for nucleation, while also emitting primary particles with a typical size distribution in the nucleation mode (Casati et al., 2007). The residence time of these particles is typically short as they grow rapidly through condensation and coagulation processes (Zhang and Wexler, 2004). In rural and remote regions, nucleation episodes are typically favored under clean air conditions, as nucleation and the condensation of gaseous precursors on pre-existing particles are competing processes (Birmili et al., 2001; Rodríguez et al., 2005). However, nucleation can still occur under polluted atmospheric conditions (e.g., Cusack et al., 2013b).

After aerosol particles are formed they undergo various physical and chemical interactions and transformations (atmospheric aging), changing in composition, structure and size. Chemical transformation refers to chemical reactions on the surface or in the volume of aerosol particles that can increase aerosol mass, and/or change the ability of aerosols to act as cloud condensation nuclei (CCN) or ice nuclei (IN). Condensation is the main process transferring low-volatility vapors to aerosol particles, and also usually the dominant process for growth to larger sizes, together with collision and coagulation processes. Coagulation is produced by Brownian motion and diffusion, and is the most common removal process for nanoparticles (Mészáros, 1999).

The average residence times of atmospheric aerosols are on the order of a few hours to about two weeks, depending on their size and location (Boucher et al., 2013). Aerosols are removed from the atmosphere by wet and dry deposition. Wet deposition removes aerosols from the atmosphere by below-cloud scavenging, when falling rain droplets or snow particles collide with aerosol particles through Brownian diffusion, interception, impaction and turbulent diffusion, and in-cloud scavenging, when aerosol

particles get into cloud droplets or cloud ice crystals, with increasing efficiency for soluble aerosols. In the absence of precipitation, dry deposition removes aerosols by mechanical processes such as gravimetry and wind dispersion and diffusion (Levin and Cotton, 2009).

1.1.4. Aerosol chemical composition

Owing to the broad range of aerosol sources and formation processes, the chemical composition of atmospheric aerosols is often complex and varied. The main constituents of the atmospheric particulate matter are sea salt, mineral species, organic species, BC or EC, secondary inorganic species (such as sulfate, nitrate, and ammonium), trace elements and water. The predominance of any of these major components will depend heavily on the prevailing emission sources affecting the aerosols and the formation mechanism of the particles.

Sea salt is constituted mainly of NaCl, with minor contributions of other salts such as $MgCl_2$, $MgSO_4$, and Na_2SO_4 (Mészáros, 1999). Dimethyl sulfide (DMS) is an important marine aerosol precursor, and is the most abundant biological sulfur compound emitted to the atmosphere, specifically by phytoplankton (Simpson et al., 1999). DMS is oxidized in the marine atmosphere to various sulfur-containing compounds such as sulfur dioxide, dimethyl sulfoxide, dimethyl sulfone, methanesulfonic acid and sulfuric acid (Lucas and Prinn, 2005).

Mineral dust is comprised of primary particles and its composition varies depending on local geology, soils and anthropogenic activities. The most abundant element components are Al, Ca, Si, Fe, Ti, K and Mg, and the most abundant trace elements are Co, Rb, Ba, Sr, Li, Sc, Cs and rare earth elements (Moreno et al., 2006). The major mineral components of PM are calcite, quartz, dolomite, clay minerals and feldspars. Minor components include calcium sulfate, iron oxides and other oxides and salts (Alfaro et al., 2004; Scheuvens and Kandler, 2014).

Carbonaceous aerosols are so called owing to the presence of carbon as the major component, although mineral carbon from carbonates is excluded as they are categorized as mineral matter. Thus, carbonaceous aerosols comprise a wide variety of organic compounds and EC or BC.

Organic aerosols include organic compounds such as polycyclic aromatic hydrocarbons (PAH), alkanes, alkenes and organic acids, cellulose and humic acids, among others (Seinfeld and Pandis, 2006). Nevertheless, only a minor part of this complex mixture, in the range of 10 to 40%, has been identified at the molecular level (Levin and Cotton, 2009). POA and SOA are influenced by both natural and

anthropogenic sources. Among th e natural sources of VOCs, vegetation is regarded as the greatest source on a global scale (Guenther et al., 2000). Oxidation of both natural and anthropogenic VOCs in the atmosphere produces less-volatile compounds which can, in turn, undergo gas-to-particle transformation, forming SOA and contributing to the particle mass loading. Formation and evolution of SOA is an area of study with a large degree of uncertainty (Jimenez et al., 2009). The formation of low-volatility compounds that make up SOA is governed by a complex series of reactions involving a large number of organic species, so the experimental characterization and theoretical description of SOA formation presents a substantial challenge (Volkamer et al., 2006). The most commonly studied mechanism of SOA formation is the oxidation of VOCs, but reactions of less-volatile organic compounds may lead to the formation of particulate matter as well. Therefore, SOA may also be formed from chemical reactions or organic compounds emitted originally in the condensed phase (Robinson et al., 2007).

BC or EC component is operationally defined as light-absorbing (‘‘black’’) or thermally refractory (‘‘elemental’’) carbon, and is generally thought to consist of aggregates of 20–50 nm granules with a graphite-like crystal structure and near-elemental composition (Bond et al., 2013). These particles are associated with ‘‘soot’’ particles, which are BC or EC particles with an external coating of organic carbon (OC) and originate from various types of combustion (Andreae and Gelencsér, 2006).

Secondary inorganic aerosols are formed in the atmosphere from precursor gaseous species through gas-to-particle processes (Hidy, 1994). The major secondary inorganic compounds in the atmosphere are sulfate (SO_4^{2-}), nitrate (NO_3^-) and ammonium (NH_4^+), and they are formed from their precursor gaseous species (SO_2, NO_x and NH_3, respectively).

The atmospheric oxidation of SO_2 can proceed through different pathways to form H_2SO_4 (Seinfeld and Pandis, 2006). Some of these pathways are shown below:

1) $SO_2 + OH \rightarrow HO\text{-}SO_2$
   $HO\text{-}SO_2 + O_2 \rightarrow SO_3 + HO_2$
   $SO_3 + H_2O \rightleftarrows H_2SO_4$
2) $2SO_2 + O_2 \rightarrow 2SO_3$
   $SO_3 + H_2O \rightleftarrows H_2SO_4$

The H_2SO_4 is readily neutralized in the atmosphere by the NH_3 to form particulate $(NH_4)_2SO_4$, and to a lesser extent $CaSO_4$ or Na_2SO_4 after reaction with $CaCO_3$ or NaCl (Junge, 1963):

1) $H_2SO_4 + NH_3 \rightleftarrows (NH_4)_2SO_4$
2) $H_2SO_4 + CaCO_3 \rightleftarrows CaSO_4 + H_2O + CO_2$
3) $H_2SO_4 + 2NaCl \rightleftarrows Na_2SO_4 + 2HCl$

The atmospheric oxidation of NO_x can proceed through different pathways to form HNO_3 (Seinfeld and Pandis, 2006). Some of these pathways are shown below:

1) $NO_2 + OH \rightarrow HNO_3$
2) $NO_2 + O \rightarrow NO_3$
   $NO_2 + NO_3 \rightarrow N_2O_5$
   $N_2O_5 + H_2O \rightarrow 2HNO_3$

The HNO_3 is subsequently neutralized by forming particulate NH_4NO_3, $Ca(NO_3)_2$ or $NaNO_3$ after reaction with $CaCO_3$ or NaCl (Junge, 1963):

1) $HNO_3 + NH_3 \leftrightarrows NH_4NO_3$
2) $2HNO_3 + CaCO_3 \rightleftarrows Ca(NO_3)_2 + H_2O + CO_2$
3) $HNO_3 + NaCl \leftrightarrows NaNO_3 + HCl$

As NH_4NO_3 is thermally unstable at relatively high ambient temperature (>20-25ºC) and low humidity, under warm and dry conditions HNO_3 reacts mainly with marine and/or mineral species (Zhuang et al., 1999b).

1.1.5. Aerosol size distribution

Atmospheric aerosols are typically categorized according to their size. Particle sizes can range from a few nanometers (nm) to tens of micrometers (μm). The specific ranges of particle sizes are called modes, which include the nucleation mode (<20 nm), the Aitken mode (20-100 nm), the accumulation mode (100 nm – 1000 nm) and the coarse mode (1-10 μm) (Seinfeld and Pandis, 2006). Particles can also be classified as nanoparticles, for particles with diameter <50 nm, ultrafine (<100 nm), fine (<1 μm) and coarse for particles of diameter 1-10 μm (Figure 1.2). Air quality studies normally refer to mass concentrations of particulate matter with aerodynamic diameters less than 1 μm, 2.5 μm and 10 μm as PM_1, $PM_{2.5}$ and PM_{10} respectively.

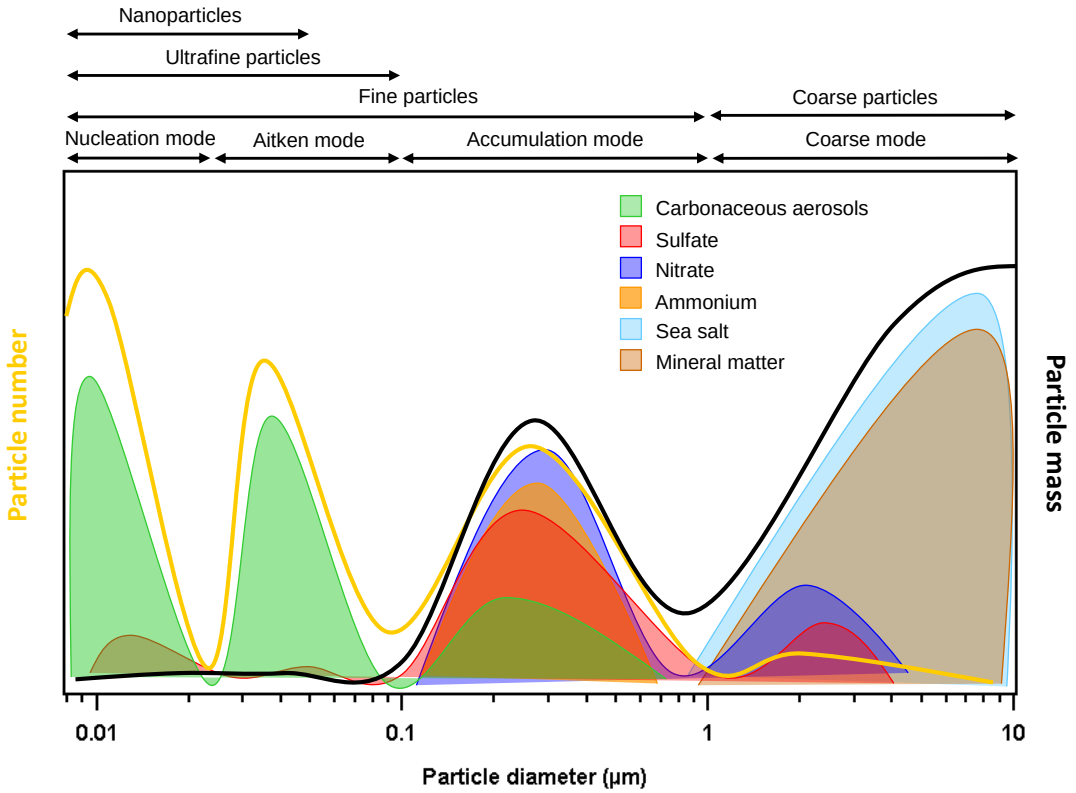

Figure 1.2 Simplified schematic illustration of aerosol size distribution (modified from Seinfeld and Pandis, 2006).

The nucleation mode particles (with diameter <20 nm) are typically formed from gaseous precursors which nucleate spontaneously in the atmosphere (Kulmala et al., 2013), thus nucleation mode is mainly constituted of secondary particles (mostly sulfate and organic compounds). Nevertheless, particles in this size mode can be also emitted by traffic as primary particles since the typical size of traffic particles range from 13 to 100 nm (Dall'Osto et al., 2012).

The Aitken mode particles (with diameter between 20-100 nm) result from primary emissions, processes of coagulation between pre-existing particles, usually from the nucleation mode, and condensation of gaseous species on nucleated particles (Morawska et al., 1999). In the urban environment this mode is prevalent owing to primary emissions from traffic, specially soot from the incomplete combustion of fuels associated with diesel engines (Kerminen et al., 2007; Lingard et al., 2006).

The accumulation mode particles (with diameter between 100-1000 nm) are those resulting from processes of coagulation between other particles, and/or from condensation and adsorption processes of semivolatile compounds on the surface of these particles (Seinfeld and Pandis, 2006). Consequently, the particle number concentration decreases and the particle mass concentration increases (Figure 1.2).

Accumulation mode particles are typically constituted of secondary inorganic aerosols (SO_4^{2-}, NO_3^-, and NH_4^+) (Harrison and Pio, 1983), and to lesser extent carbonaceous aerosols. The accumulation mode is so named because particle removal mechanisms are least efficient in this regime and thus have a long residence time in the atmosphere compared to the finer and coarser size modes (Seinfeld and Pandis, 2006).

Coarse particles (with diameter >1 μm) are mostly primary and are generated from mechanical processes such as resuspended mineral dust, marine aerosol, products from tyre and brake abrasion and biogenic emissions. However, coarse secondary particles can occur when gases chemically react with particles of marine or crustal origin forming $NaNO_3$, Na_2SO_4, $Ca(NO_3)_2$, and/or $CaSO_4$ (Zhuang et al., 1999a).

1.2. Effects of aerosols

Atmospheric aerosols have played a key role in the development of the Earth's atmosphere. Without atmospheric particles rainfall would be non existent and the climate would be very different (Mészarós, 1999). However, anthropogenic emissions have changed the chemical composition of atmospheric aerosols significantly through emissions of particles and precursor gases, particularly since the industrial revolution (Pöschl, 2005). Numerous studies have demonstrated that atmospheric aerosols, both natural and anthropogenic, do not only influence Earth's climate (Boucher et al., 2013), but also have adverse effects on air quality, and consequently on human health (WHO, 2013) and ecosystems (e.g., Burkhardt and Pariyar, 2014). Many of these effects will be referred to in the following sections.

1.2.1. Human health effects

Epidemiological and toxicological studies have consistently evidenced a wide range of adverse health outcomes on the human cardiovascular and respiratory systems linked to exposure to ambient PM (Lim et al., 2012). Worldwide, it has been estimated that air pollution represents up to 8% of lung cancer deaths, 5% of cardiopulmonary deaths and 3% of respiratory infection deaths (WHO, 2009). A recent review on evidence of health aspects of air pollution (WHO, 2013) suggested a possible link with neurodevelopment, cognitive function and diabetes, and strengthened the link between $PM_{2.5}$ and cardiovascular respiratory deaths. Recent estimates suggest that 3.5 million cardiopulmonary and 220,000 lung cancer annual deaths globally can be attributed to the anthropogenic component of $PM_{2.5}$ (Anenberg et al., 2010).

Research results evidence that these health effects from airborne particles depend on the chemical composition and the physical properties (particulate number, size, shape) of the particles, but also on the extent of the exposure (Krishnan et al., 2012). Short-term exposure of aerosols is related to acute health effects, whereas long-term PM exposures are associated with chronic diseases (Kloog et al., 2013).

The complex chemical composition of particles makes it difficult to identify which components are responsible for the adverse health effects (Heal et al., 2012). However, some studies have focused on the direct health effects of specific aerosol components, such as a report commissioned by WHO (2012) on the health implications of exposure to BC. The report suggested that BC may not be a major directly toxic component of PM, but it may operate as a universal carrier of a wide variety of chemicals of varying toxicity to the lungs, the body's major defense cells and possibly

the systematic blood circulation. Furthermore, the different chemical composition of particles can generate reactive oxidative species, such as metallic particles (Fu et al., 2014), and mineral dust particles have been associated with cardiovascular and respiratory mortality (Perez et al., 2008).

Inhalation of airborne particles is the main mode of exposure, for this reason particles size is the most determinant factor to evaluate the penetration of aerosols into human body (Figure 1.3). Whereas coarse aerosols impact mostly on the respiratory system, ultrafine particles have the ability to penetrate deeper and enter the circulatory system stream (Cassee et al., 2013). Consequently, ultrafine particles health effects can be much more serious than those of coarse particles because once they are in the circulation system can induce inflammation (Samet et al., 2009), translocate to other organs (Kreyling et al., 2006) and deposit in them (Oberdörster et al., 2004). Also, ultrafine particles fraction usually contain components such as certain organic compounds and trace metals (Daher et al., 2013), which are believed to increase the risk of diseases (Ostro et al., 2006; Ovrevik and Schwarze, 2006) owing to their potential oxidative stress (Daher et al., 2014).

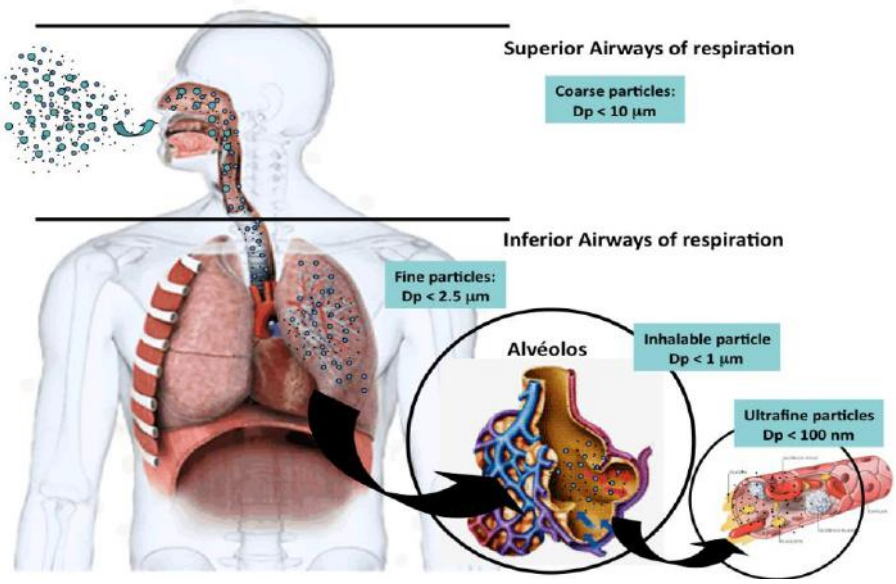

Figure 1.3 Areas where airborne particles are deposited in human body (Guarieiro, 2013).

1.2.2. Climate effects

Atmospheric aerosols can affect the climate in multiple and complex ways through their interactions with radiation and clouds. Overall, models and observations indicate that anthropogenic aerosols have exerted a cooling influence on the Earth since pre-industrial times, which has masked some of the global mean warming from greenhouse gases that would have occurred in their absence. The projected decrease in emissions of anthropogenic aerosols in the future, in response to air quality policies, would eventually unmask this warming (Boucher et al., 2013).

There are a variety of ways to examine how aerosols affect climate, however, radiative forcing (RF) is one of the most widely used metrics. RF is the net change in the energy balance of the Earth system due to some imposed perturbations. The total aerosol effect (excluding BC on snow and ice) estimated by the IPCC fifth assessment report (AR5) (Stocker et al., 2013) is -0.9 (-1.9 to -0.1) W m^{-2}, which results in a cooling net effect, however, it has a larger uncertainty range than the greenhouse gases effect, and therefore the total anthropogenic effect results in a higher uncertainty range (Figure 1.4).

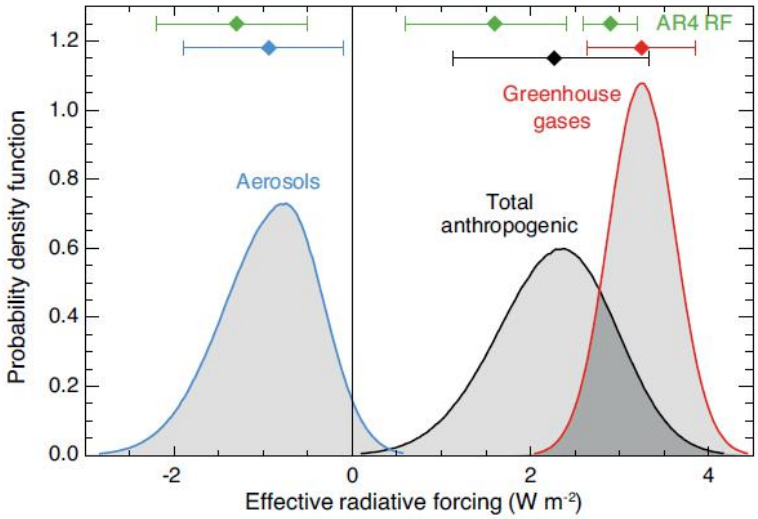

Figure 1.4 Probability density functions for the effective radiative forcing, for the aerosol, greenhouse gas and total. The green lines show the IPCC (2007) radiative forcing 90% confidence intervals and can be compared with the red, blue and black lines which show the IPCC (2013) effective radiative forcing 90% confidence intervals (Myhre et al., 2013).

In the IPCC fourth assessment report (AR4) (Forster et al., 2007), RF estimates were provided for three aerosol effects. These effects were the direct aerosol effect (in the AR5 denoted as RF of aerosol–radiation interaction), the indirect or cloud albedo

effect (in the AR5 denoted as RF of the aerosol–cloud interaction), and the semi-direct effect (Figure 1.5).

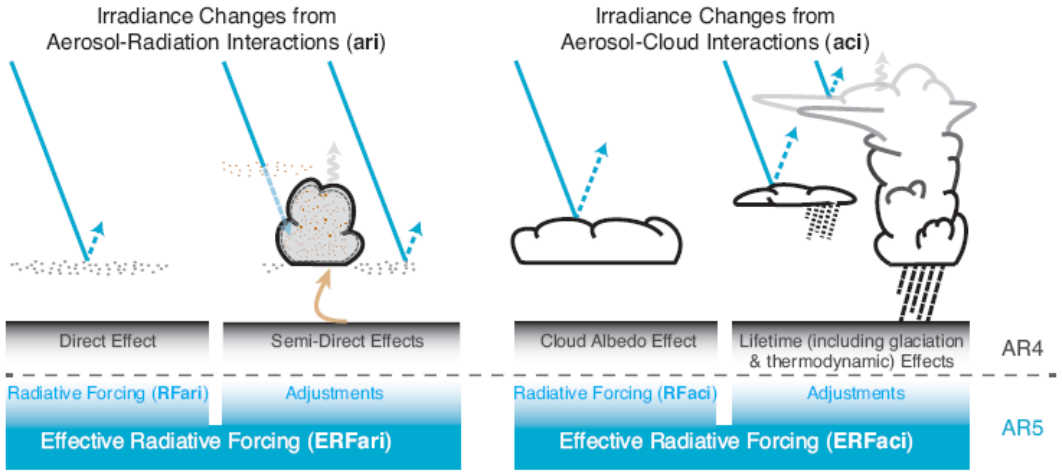

Figure 1.5 Schematic of the new terminology used in the IPCC (2013) for aerosol-radiation and aerosol-cloud interactions. The blue arrows depict solar radiation, the grey arrows represent terrestrial radiation, and the brown arrow symbolizes the importance of couplings between the surface and the clouds layer for rapid adjustments (Boucher et al., 2013).

The RF due to aerosol–radiation interactions is the scattering and absorption of shortwave (solar) and longwave (terrestrial) radiation by atmospheric aerosols (Figure 1.5). Aerosol scattering and reflection generally makes the planet more reflective, and tends to cool the climate (negative radiative forcing), while aerosol absorption has the opposite effect, and tends to warm the climate system (positive radiative forcing).

The balance between cooling and warming depends on aerosol properties and environmental conditions. Many observational studies have quantified local radiative effects from anthropogenic and natural aerosols, but determining their global impact carries significant uncertainties because the majority of the aerosols are emitted from the same sources and/or are mixed during their transportation. BC, for example, is an absorbing aerosol, but it is usually emitted with other particles that cause cooling, therefore it is difficult to estimate their total radiative forcing (Bond et al., 2013). Nevertheless, the mean RF estimate of the aerosol-radiation interactions reported by the AR5 (Myhre et al., 2013) is -0.35 (-0.85 to 0.15) W m^{-2}. This estimate is smaller in magnitude than that reported by the AR4 (Forster et al., 2007), -0.55 W m^{-2}, however, with a larger uncertainty range (-0.75 to -0.25 W m^{-2}). The RF from the different atmospheric components estimated by the AR5 (Myhre et al., 2013) is shown in Figure 1.6.

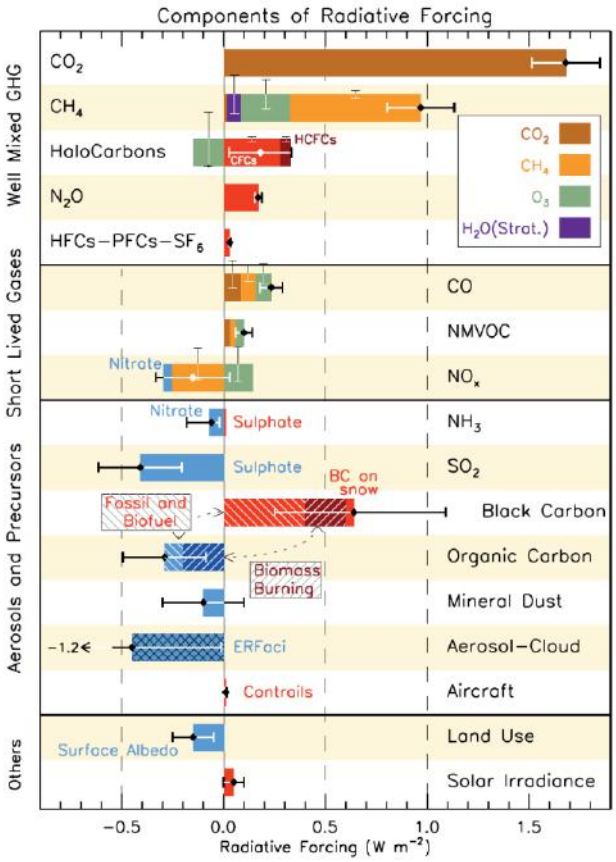

Figure 1.6 RF bar chart for the period 1750-2011 based on emitted compounds (gases, aerosols or aerosol precursors) or other changes. Red (positive RF) and blue (negative RF) are used for emitted components which affect few forcing agents, whereas for emitted components affecting many compounds, several colors are used as indicated by the legend. The vertical bars indicate the relative uncertainty of the RF induced by each component. The net impact of the individual contributions is shown by a diamond symbol and its uncertainty (5 to 95% confidence range) is given by the horizontal error bar (Myhre et al., 2013).

The RF due to aerosol-cloud interactions results from aerosols acting as CCN or IN, on which cloud droplets and ice particles can form, and thus indirectly changing cloud formation and lifetimes. When influenced by more aerosol particles, clouds of liquid water droplets tend to have more, but smaller droplets, which cause these clouds to reflect more solar radiation. There are however many other pathways for aerosol-cloud interactions, particularly in ice (or mixed liquid and ice) clouds, where phase changes between liquid and ice water are sensitive to aerosol concentrations and properties (Boucher et al., 2013). The initial view that an increase in aerosol concentration will also increase the amount of low clouds has been challenged because a number of counteracting processes come into play. Quantifying the overall impact of aerosols on cloud amounts and properties is understandably difficult. Nevertheless, available studies, based on climate models and satellite observations, generally indicate that the

net effect of anthropogenic aerosols on clouds is to cool the climate system. The AR5 (Myhre et al., 2013) reported a mean RF estimation of aerosol-cloud interactions of -0.45 (-1.2 to 0.0) W m^{-2}.

Because aerosols are distributed unevenly in the atmosphere, they can heat and cool the climate system in patterns that can drive changes in the weather. These effects are complex, and hard to simulate with current models, but several studies suggest significant effects at regional scale (Boucher et al., 2013). As a result, certain regions, such as the Mediterranean area, are expected to experiment substantial weather changes in the next years.

1.3. European air quality standards for aerosols

Considering the detrimental health effects of atmospheric aerosols and their ability to disrupt the Earth's radiative budget, many countries aim to control and regulate ambient concentrations of atmospheric aerosols and specific emission sources. In order to reduce the negative effects of air pollution, the European Union (EU) has drawn up the European air quality directives 2008/50/EC and 2004/107/EC with the specific aim of regulating ambient concentrations of air pollutants. Member states are obliged to adhere to these regulations by implementing effective means to reduce air pollution at local, national and European levels. In the above air quality directives, criteria from previous directives were unified, while also taking into consideration the most recent scientific research and combined experience of member states. Thus, the parameters currently regulated at a European level include ambient concentrations of: PM_{10}, $PM_{2.5}$, C_6H_6, O_3, Pb, As, Cd, Hg, Ni, PAH, SO_2, NO_2, CO and NO_X. Furthermore, monitoring of NO_3^-, SO_4^{2-}, NH_4^+, Cl^-, Na^+, K^+, Mg^{2+}, Ca^{2+}, OC and EC concentrations in $PM_{2.5}$ for rural areas has become mandatory (Annex IV of the 2008/50/EC Directive).

Air quality standards for PM_{10} require that an annual mean limit value of 40 μg m^{-3} must not be exceeded, and a daily limit value of 50 μg m^{-3} must not be exceeded more than 35 times a year. Since 1 January 2015, an annual mean limit value of 25 μg m^{-3} for $PM_{2.5}$ must not be exceeded. This annual limit value will be 20 μg m^{-3} by 2020.

In order to meet the above limit values, emission standards were implemented by the EU under specific directives. Vehicular emissions from new light duty vehicles (passenger cars and light commercial vehicles) were controlled under the Euro 1 standards (also known as EC 93) whereby Directives 91/441/EEC (passenger cars only) or 93/59/EEC (passenger cars and light trucks), Euro 2 standards (EC 96) through Directives 94/12/EC or 96/69/EC, and Euro 3/4 standards (2000/2005) whereby Directive 98/69/EC, further amendments in 2002/80/EC. Currently these directives have been repaled and replaced by Euro 5/6 standards (2009/2014) through Regulation 715/2007 and several comitology regulations. Emissions from new heavy duty vehicles were controlled under the Euro I standards introduced by the Directive 88/77/EEC, followed by the Euro II/III standards introduced by the Directive 1999/96/EC, and re-casted and consolidated by the Euro IV/V standards whereby Directive 2005/55/EC. Currently new emissions limits are controlled under Euro VI standards introduced by the Regulation 595/2009, with technical details specified in Regulation 582/2011. Emissions of NO_x, total hydrocarbon, non-methane hydrocarbon, CO and PM are currently regulated for most vehicle types. Industrial emissions are

controlled by the industrial emissions Directive (also known as IED) whereby the Directive 2010/75/EC, which replaces the integrated pollution prevention and control (IPPC) Directive (Directive 2008/1/EC). This Directive requires industrial and agricultural activities with a high pollution potential to have a specific permission, and this permit can only be issued if certain environmental conditions are met. The Directive establishes emissions ceilings for each specific type of industry, while taking into consideration BATNEEC (Best Available Techniques Not Exceeding Excessive Costs), which require industries to employ efficient pollution control that are economically viable.

Currently, there is much debate surrounding the inclusion of specific components of PM, other than those mentioned earlier, that should be controlled by environment agencies. As outlined previously, BC is a known contributor to radiative forcing (Bond et al., 2013), and there are continuing studies in the adverse health effects of BC (WHO, 2012). Shindell et al. (2012) have shown how implementing specific practical emissions reductions chosen to maximize climate benefits would have important mutual benefits for near-term climate, human health and agriculture, among others. Bond et al. (2013) suggests that diesel engine and biomass burning sources of BC appear to offer the best mitigation potential to reduce near-term climate forcing. Furthermore, control of BC emissions would bring health benefits by additionally reducing PM exposure.

As discussed previously, ultrafine particles are believed to be the most harmful to human health, to the extent that the World Health Organization (WHO) has called for further research to establish the links between ultrafine particles, exposure and human health (WHO, 2013). The significance of fine and ultrafine aerosol concentrations in the context of impacts on human health has been well established in numerous studies which have outlined possible abatement measures (Cassee et al., 2013). However, there is no current legal threshold for controlling particle number concentrations (as opposed to particle mass concentrations which are controlled) even though there is evidence to suggest that ultrafine particles can be even more harmful to health (Samet et al., 2009).

1.4. Continental background environments

Because of the vast amounts of anthropogenic emissions of aerosol particles and their gaseous precursors, combined with efficient long-range transport, it is nowadays very difficult to find areas of the Earth that are not measurably impacted by pollutant aerosols (Levin and Cotton, 2009). Aerosol particles have typical lifetime on the order of a few hours to about two weeks (Boucher et al., 2013), and air masses can easily travel several thousand km in 15 days. Consequently, there are really no places where we can expect to find pristine conditions, at least in the northern hemisphere where few places are located more than a few thousand km from major pollution sources. However, aerosol concentration and composition may vary significantly as a function of location.

Atmospheric monitoring stations can be classified as urban, regional/rural, and continental/remote background sites and industrial and traffic hotspot sites. Urban background sites are located in urban areas separated from direct emissions from traffic or industry, with the aim of determining the average exposure of the general population to urban aerosols. According to the criteria outlined in Directive 2008/50/EC, Van Dingenen et al. (2004) and Putaud et al. (2010), regional or rural background sites should be isolated from the direct influence of local anthropogenic emission sources, and should represent background pollutant levels from across the region in which they are located, with a distance of 10-50 km from significant pollution sources. Finally, continental or remote background sites can be described as representative of the air quality of a wide area of hundreds of km, with a distance of more than 50 km from local emissions (Putaud et al., 2010). In many cases the monitoring sites chosen to represent continental background environments are located in mountaintops over 1000 m a.s.l., and therefore they are also called high-altitude sites (Nyeki et al., 1998) or free troposphere (FT) environments (Andrews et al., 2011). The relevance of the FT environments is that they are more representative of the global atmosphere (Laj et al., 2009) because residence time of aerosols is longer in the FT, i.e., several weeks (Kent et al., 1998).

The importance of monitoring continental background aerosols is highlighted by the existence of international networks of remote observatories. The National Oceanic and Atmospheric Administration (NOAA) from USA has been continuously monitoring and collecting data related to continental background aerosols since the 1950's. Nowadays, NOAA has observatories located at remote sites across the planet, which includes locations in the arctic and antarctic. Currently, these observatories are included in the

GAW (Global Atmosphere Watch) network, which has 25 years of global coordinated atmospheric composition observations and analyses. The main goal of the GAW aerosol programme is to determine the spatio-temporal distribution of aerosol properties related to climate forcing and air quality up to multidecadal time scales. The GAW network consists of 29 global stations and more than 400 regional stations located at more than 80 different countries.

The ACTRIS (Aerosols, Clouds and Trace gases Research InfraStructure) project also aims to meet the challenges posed by global climate change, air quality, and long-range transport of pollutants (http://www.actris.net). ACTRIS (and ACTRIS-2) is building the next generation of the ground-based component of the EU observing system by integrating three existing research infrastructures EUSAAR, EARLINET, CLOUDNET, and a new trace gas network component into a single coordinated framework. This network is funded within the EC 7th Framework Programme under "Research Infrastructures for Atmospheric Research". The parameters measured under the ACTRIS network and currently monitored under the ACTRIS-2 project include remote sensing of the vertical aerosol distribution, in-situ chemical, physical and optical properties of aerosols (such as aerosol light absorption, size distribution, OC and EC), trace gases (NOxy, VOCs) and cloud observations.

In Europe traditionally atmospheric composition observations have been performed in the northern and central part of the continent, however during the last decades a growing number of aerosol observatories have been located in southern Europe. Most of these monitoring stations are considered urban and regional background sites, and very few continental background sites exist.

1.5. Peculiarities of the western Mediterranean aerosols

As described previously, atmospheric aerosols are complex in nature owing to the wide variety of natural and anthropogenic emission sources and atmospheric processes, both largely influencing the physical and chemical nature of the aerosols. The nature of atmospheric aerosols in any given region, in terms of both concentration and composition, will also largely depend on other variables such as meteorology (temperature, humidity, solar radiation/photochemistry, precipitation, or air mass origin) and geography (complex topography, proximity to the coast or to arid areas, soil cover, or land use).

The characteristics and variability of the physical properties and chemical composition of atmospheric aerosols have been studied for many sites across Europe (Asmi et al., 2013, 2011; Barmpadimos et al., 2012; Birmili et al., 2001; Collaud Coen et al., 2013; Van Dingenen et al., 2004; Putaud et al., 2010, 2004; Querol et al., 2009a). These studies have highlighted the wide variations in aerosol physical properties and chemical composition across the European continent.

In northern Europe the higher arrival of weather fronts from the Atlantic Ocean brings westerly winds and relatively high levels of precipitation that enhances aerosol dispersion and scavenging. In southern Europe, and in particular in the Mediterranean region, the meteorological conditions with higher temperatures and lower precipitation, together with the abrupt topography around the Mediterranean Sea, hinder aerosol dispersion and prevent atmospheric wet-scavenging processes. Moreover, Mediterranean region is very much influenced by both anthropogenic (large coastal urban agglomerations, shipping, power generation and industrial processes, biomass burning, among others) and natural (African dust, soil resuspension, wildfires, sea spray, biogenic organic compounds) emissions (Garcia-Hurtado et al., 2014; Pey et al., 2013a, 2013b; Rodríguez et al., 2011; Steinbrecher et al., 2009). As a result, higher concentrations of atmospheric aerosols are reported around the Mediterranean Basin compared to northern Europe.

The western Mediterranean basin has peculiar atmospheric dynamics that are atypical and complex owing to its geographical position, isolated from mainland Europe and close to the Africa continent. Meteorology and atmospheric dynamics in this region have been previously described in detail (Jiménez et al., 2006; Jorba et al., 2013; Millán et al., 2000, 1997; Pérez et al., 2004; Rodríguez et al., 2002b, 2003; Sicard et al., 2006; Toll and Baldasano, 2000). Atmospheric circulation over the western

Mediterranean is highly influenced by the Azores high pressure system and is balanced between two synoptic systems.

During the cold season, the displacement of the Azores high pressure system to the lower latitudes allows for the frequent movement of depression systems from the Atlantic across the Iberian Peninsula (Lopez-Bustins et al., 2008). This scenario brings fresh, typically clean air masses to the western Mediterranean and consequently results in the renovation of air masses and removal of pollution. Displacement of the Azores high pressure system can also result in the movement of central and northern European air masses to the western Mediterranenan, which are typically cold and polluted air masses, leading to an increment of pollutant concentrations on a regional level. However, in some instances, the Azores high can become displaced over the Iberian Peninsula, and this situation can continue for several days. Pey et al. (2010a) describes this scenario as Winter Anticyclonic Episodes (WAE). WAE are associated with calm, sunny weather with little air mass renovation and thermal inversions, giving rise to stagnant conditions across the region. Due to the lack of advection, pollution emitted from urban and industrialized areas accumulates in the mixing layer, and a subsequent increase in pollutants is observed at surface level, lasting for several days until dispersed by advection of air masses from the Atlantic Ocean. Although the pollution typically remains close to the emission sources, local circulation can transport this contaminated air mass to rural areas. Owing to the mountainous topography of the Mediterranean coast and the meteorological conditions associated with WAE, mountain and sea breezes can be activated by insolation. These breezes can thus transport the accumulated pollution in the industrialized valleys and depressions to rural areas (Pérez et al., 2008; Pey et al., 2010a).

During the warmer months, the Azores high is situated further to the north east, causing thermal lows to develop over the Iberian Peninsula and the Sahara. This scenario favors a very weak pressure gradient over the western Mediterranean and consequently, local and regional circulations dominate the atmospheric dynamics (Pérez et al., 2004). Recirculation of air masses across the region are caused by the interaction of sea and mountain breezes, the topography of the region, the dominant north-western atmospheric air flows at high altitudes and the uplift of air masses in the central Iberian Peninsula (Millán et al., 1997). This recirculation gives rise to aerosol aging and accumulation of pollutants across the region, and combined with low summer rainfall, intensified solar radiation inducing photochemical processes and increased soil resuspension, induce an aerosol seasonal pattern characterized by elevated levels of background aerosols during the summer in the western Mediterranean region (Pérez et al., 2008; Pey et al., 2009; Querol et al., 2009a;

Rodríguez et al., 2002a; Viana et al., 2005). Furthermore, elevated concentrations of aerosols during the summer months are also atributted to the higher frequency of Saharan dust intrusions, owing to the Iberian Peninsula's close proximity to the African continent, giving rise to sizeable increases in ambient aerosol concentrations often exceeding the EU Directive's daily limit value, especially in the PM_{10} fraction (Escudero et al., 2006, 2007; Querol et al., 2009b; Rodríguez et al., 2001; Viana et al., 2002). Elevated concentrations of mineral matter are also a result of local dust resuspension, owing to the low rainfall and dry and arid soils across the region (Querol et al., 2004). The presence of a high load of mineral matter in the atmosphere favors the interaction with gaseous pollutants and increases the secondary PM_{10} load (Harrison and Pio, 1983; Wall et al., 1988; Zhuang et al., 1999b).

All these characteristics of the western Mediterranean region cause a particular aerosol phenomenology that may have specific impacts on human health and climate system.

1.6. Previous knowledge and studies on atmospheric aerosols in the western Mediterranean basin by IDAEA-CSIC group

The study of atmospheric aerosols in urban, regional and continental environments in the western Mediterranean basin has been one of the main objectives of the Environmental Geochemistry research group at the Institute of Environmental Assessment and Water Research (IDAEA-CSIC). Numerous scientific articles have been published and PhD theses have been defended since the measurements of atmospheric aerosols started in 1995 (Querol et al., 1996, 1998a, 1998b). These works have improved our understanding of the physical and chemical processes affecting atmospheric aerosols in the western Mediterranean region. The foremost studies carried out until now are briefly described in this section.

The first few studies of IDAEA-CSIC group on atmospheric aerosols focused on the regional background air quality around power plants (Querol et al., 1998a, 1998b). Subsequently, research focused on the urban air quality of the Barcelona Metropolitan area. The variability of PM_{10}, $PM_{2.5}$ and PM_1 concentrations and the chemical composition of PM_{10} and $PM_{2.5}$ was described in great detail by Querol et al. (2001b). The results from that work revealed a high number of exceedances of the European daily PM_{10} limit value. The high PM_{10} concentrations at Barcelona Metropolitan area were partially attributed to traffic and industrial emissions and to Saharan dust outbreaks. Hence, the study concluded that measures on road traffic were necessary in Barcelona, and that $PM_{2.5}$ measurements were more appropriate for the control of the anthropogenic aerosols. Moreover, Rodríguez et al. (2001) investigated the Saharan dust contribution to PM_{10} in southern and eastern Spain, and afterwards Escudero et al. (2007) proposed a method to quantify the net African dust load in air quality monitoring networks. The comparison between the PM_{10} and $PM_{2.5}$ chemical composition in several cities in southern Europe with those obtained in central and northern European areas was done by Querol et al. (2004). This work concluded that concentrations of mineral matter were higher in Southern Europe and highlighted a significant presence of secondary inorganic aerosols in intensively industrialized regions or heavily polluted urban areas. Furthermore, Querol et al. (2007) studied the source origin of trace elements in PM from regional background, urban and industrial sites of Spain. In order to better understand the aerosols sources and formation processes in the urban environment of the western Mediterranean, Pey et al. (2008) studied the particle number size distribution and concentration of fine and ultrafine aerosols in Barcelona. One of the most interesting findings of that study was the

occurrence of intense photochemical nucleation episodes after midday, especially in summer, which could be an important source of ultrafine particles. Pérez et al. (2010) also observed photochemical nucleation episodes in the afternoon in Barcelona urban background environment and found a good correlation of BC concentrations with some road traffic tracers such as CO, NO and NO_2. As a consequence, BC was proposed to be included in the air quality measurement networks as a tracer of combustion processes. A source apportionment study in the urban background environment of Barcelona revealed the contribution of eight sources to the urban aerosols: mineral, vehicle exhaust, road dust, secondary sulfate, secondary nitrate, aged sea salt, fuel oil combustion, and industrial (Amato et al., 2009). Results from the international field campaign DAURE (Determination of the sources of atmospheric Aerosols in Urban and Rural Environments in the western Mediterranean) (Pandolfi et al., 2014a), also provided evidence of the influence of three PM sources to the urban aerosols: road traffic, construction-demolition works and shipping emissions (Reche et al., 2011). Moreover, during DAURE campaign five sources of urban organic aerosol (OA) were identified: LV-OOA, related to regional, aged secondary OA; SV-OOA, a fresher oxygenated OA; HOA, related to traffic emissions; BBOA from domestic heating or agricultural biomass burning activities; and cooking organic aerosol (COA) (Mohr et al., 2012; Reche et al., 2012a). The contribution of fossil sources to OC in Barcelona was 40% and 48%, in winter and summer, respectively (Minguillón et al., 2011).

In order to quantify more accurately the local and external contributions in the western Mediterranean, a monitoring station was installed at Montseny Natural Park (MSY, 720 m a.s.l.) in 2002 as a regional background site. Years later, the station was incorporated into the EUSAAR, ACTRIS and ACTRIS-2 projects and participated in regular EMEP (European Monitoring and Evaluation Programme) intensive measurements campaigns. Nowadays, it is part of the GAW network. The variability of PM_{10}, $PM_{2.5}$ and PM_1 as a function of different meteorological scenarios and seasons at this regional background site was described in detail by Pérez et al. (2008). Pey et al. (2009) studied the chemical composition and source origin of regional background aerosols in the western Mediterranean. Results from that study suggested that a regional background designation for Montseny site is applicable and that it is representative of regional background aerosols in the western Mediterranean. However, the urban and industrial contribution to the regional background aerosols in the western Mediterranean was found to be higher than those at other European regions, especially concerning the coarse fraction (Pey et al., 2010b). The meteorological episodes affecting the regional background aerosols in the western Mediterranean, were evaluated in detail by Pey et al. (2010a) focusing on the intense

winter atmospheric pollution episodes. The characteristics of regional background aerosols in the western Mediterranean were compared with those in the eastern Mediterranean by Querol et al. (2009a). This work showed higher concentrations of crustal material and sulfate in the eastern Mediterranean, whereas nitrate and OC+EC concentrations were relatively constant across the Mediterranean. Querol et al. (2009a) also demonstrated why the Mediterranean is included among the most vulnerable regions globally in the context of climate destabilization, as well as the significant and complicated role that aerosols play as a forcing driver. Furthermore, Pandolfi et al. (2011) investigated the variability of aerosol optical properties in the western Mediterranean regional background. In that work the change in aerosol optical properties as a function of meteorological scenarios and as a function of aerosol chemical composition was studied. The aerosol transport patterns at Montseny during winter and summer were described by Jorba et al. (2013) using results from the DAURE field campaign. During this international campaign, Seco et al. (2011) also studied the effect of local biogenic emissions at Montseny. This work concluded that short-chain oxygenated VOCs presented higher mixing ratios in summer, presumably due to greater emission by vegetation and increased photochemistry, both enhanced by the high temperatures and solar radiation in summer. The higher contribution of biogenic emissions to fine secondary OC at Montseny in summer, was confirmed by Minguillón et al. (2011), reporting a contribution of biogenic OC to the total non-fossil OC of 59% and 76%, in winter and summer, respectively. Recent publications have shown that regional background aerosols in the western Mediterranean have been steadily decreasing over almost a decade, with statistical significance (Cusack et al., 2012). The source apportionment analysis of fine PM at Montseny resulted in six sources, namely: secondary sulfate, traffic + biomass burning, industrial, secondary organic aerosol, secondary nitrate and fuel oil combustion (Cusack et al., 2013a). Moreover, Cusack et al. (2013b) studied the particulate number size distribution variations at Montseny site, revealing the importance of NPF processes as a source of particles at regional scale in the western Mediterranean, especially in summer. During the warmer months the nucleation mode concentrations incremented due to increased photochemical reactions, with enhanced subsequent growth owing to elevated concentrations of condensable organic vapors produced from biogenic VOCs.

As aerosol characterization at Montseny showed relatively high influence of reginal anthropogenic emissions, a mobile laboratory equipped with aerosol monitoring instrumentation was set up at Montsec mountain range (MSC, 1570 m a.s.l.) for intensive measurements campaigns in November 2005. The study of aerosols in this remote environment together with the measurements at the urban and regional

background sites was thought to be a useful strategy to understand the aerosol phenomenology across the western Mediterranean. Results on real-time concentrations of PM_{10}, $PM_{2.5}$ and PM_1 and chemical composition of PM_{10} were published in the thesis of Pérez (2010). This work concluded that continuous measurements of PM concentrations and chemical composition as well as other aerosol properties were needed to gain further insight into the continental background aerosols in the western Mediterranean.

1.7. Gaps in current knowledge

An extensive literature, including all the studies described above, has contributed to characterize aerosol phenomenology in the western Mediterranean urban and regional background environments. However, the following significant gaps on continental background aerosols still remain in our understanding:

- The research on continental background aerosols is scarce, especially in the western Mediterranean.
- The investigation of aerosols at high-altitude sites in the western Mediterranean is almost nonexistent.
- The transport processes of aerosols between Africa and Europe and how mesoscale and synoptic meteorological conditions affect continental background aerosols have not been widely studied in the western Mediterranean.
- The understanding of the aerosol origins and sources in the western Mediterranean continental background is limited by the lack of the aerosol chemical composition information in the region.
- The study of the ultrafine aerosol processes occurring in the atmosphere, such as NPF mechanisms and growth processes does not exist in the western Mediterranean continental background.
- The knowledge on organic aerosol formation, sources, and atmospheric processing is still very incomplete in general and in particular at continental background environments, especially for secondary organic aerosols formed from chemical reactions of gas-phase species.
- The lack of aerosol optical properties measurements, such as aerosol absorption, scattering and backscattering coefficients, is especially clear in the western Mediterranean continental background.

1.8. Objectives

The present study aims to fill a number of the knowledge gaps identified in the previous section through the installation of a station equipped with aerosol monitoring instrumentation at Montsec mountain range (MSC, 1570 m a.s.l.). This allows for the investigation of the continental background aerosols in the western Mediterranean. Thus, this study aims to achieve the following specific objectives:

1) To set up the Montsec sampling station as a continental background monitoring site and representative of the air quality of a wide area in the western Mediterranean.
2) To deduce the main factors governing variations of aerosol properties at a site with no direct influence of local emissions.
3) To identify ultrafine aerosol processes, such as NPF, growth and particle transformation, in the western Mediterranean continental background.
4) To study the aerosol optical properties in order to provide data for investigating the role of continental background aerosols on the Earth's radiative balance.
5) To discriminate natural and anthropogenic emissions affecting continental background aerosols in the western Mediterranean, with a focus on the partitioning of the chemical components into different size fractions.
6) To identify the similarities and differences in regional and continental background aerosols by jointly analyzing the variations in composition and properties at both environments in the western Mediterranean.
7) To further investigate the origin of the fine aerosols in the continental background environment by studying their chemical composition with a high time resolution instrument.
8) To characterize the fine organic aerosols in the western Mediterranean continental background environment.

The following tasks were carried out in order to reach the objectives outlined above:

- The setting up of a permanent station equipped with aerosol monitoring instrumentation at Montsec mountain range.
- The measurement of real-time PM_{10}, $PM_{2.5}$ and PM_1 concentrations and offline PM_{10} and PM_1 chemical composition.

- The introduction of continuous real-time measurements of concentrations of BC, submicron particle number, and gaseous pollutants.
- The measurements of aerosol absorption coefficient and aerosol scattering and backscattering coefficients, which allow for determining the direct radiative forcing effect for climate system.
- The quantification of PM_{10} source contribution by using multivariate source apportionment techniques.
- The measurements with an ACSM during one year, at a remote site, for the first time in Europe. This instrument provides real-time mass concentration of submicron particulate organics, nitrate, sulfate, ammonium and chloride.
- The identification and quantification of PM_1 organic aerosols origin by applying source apportionment techniques to ACSM mass spectra.
- The performance of intensive campaigns with additional aerosol instrumentation, such as a scanning mobility particle sizer (SMPS) and an AiRRmonia that measures real-time gas-phase NH_3.

1.9. Structure of the thesis

Following this introduction, a methodology section will describe the monitoring site in detail, and outline the measurements and experimental techniques employed to reach the aforementioned objectives. Despite the fact that some measurements were compared with those obtained at the MSY regional background site, the methodology section will focus on MSC site since MSY have been described in numerous scientific articles (e.g., Pérez et al., 2008; Pey et al., 2009) and theses (Castillo, 2006; Pey, 2007; Pérez, 2010; Cusack, 2013).

The structure of this current work is that of a compilation of scientific articles published in peer-reviewed journals on atmospheric sciences. Taking this into consideration, the following methodology section will focus on principles of operation for the instruments employed in order to avoid repetition, as the methodology is also described in each publication. Thus, the main body of this thesis is made up of four specific scientific articles. A summary discussion of the main findings in each article, and how these findings relate to each other, will be presented, followed by the main conclusions of this thesis. Afterwards, a brief section will discuss future research directions and implications of the work presented here. Finally, a references section will provide the references used in this work except for the once used in each article since they are already provided in each publication. At the end of this work it can be find an appendix that includes the list of acronyms and symbols, and the detection limit and the uncertainties of the chemical species analyzed.

The scientific articles included in this thesis are briefly described below:

- **Article 1: Ripoll, A., Pey, J., Minguillón, M. C., Pérez, N., Pandolfi, M., Querol, X. and Alastuey, A.: Three years of aerosol mass, black carbon and particle number concentrations at Montsec (southern Pyrenees, 1570 m a.s.l.), Atmos. Chem. Phys., 14(8), 4279–4295, doi:10.5194/acp-14-4279-2014, 2014.** The variation of PM, BC, and N concentrations measured over a period of three years (2010-2012) at MSC, as a representative of the western Mediterranean continental background, was interpreted in this article. The annual, seasonal, weekly, and daily variations in the concentrations of continental background aerosols were investigated and the main factors influencing these variations were deduced.

- **Article 2: Ripoll, A., Minguillón, M. C., Pey, J., Pérez, N., Querol, X. and Alastuey, A.: Joint analysis of continental and regional background environments in the western Mediterranean: PM_1 and PM_{10} concentrations and composition, Atmos. Chem. Phys., 15, 1129–1145, doi:10.5194/acp-15-1129-2015, 2015.** This article focused on the investigation of the temporal and spatial variations of aerosol chemical composition in the western Mediterranean basin during Janyary 2010 – March 2013. Seasonal patterns of PM_1 and PM_{10} concentrations, as well as their major chemical components and trace elements, from MSC and MSY GAW stations, were interpreted. Greater emphasis was placed on the evaluation of the influence of different atmospheric episodes, with a focus on the partitioning of the chemical components into different size fractions in order to discriminate natural and anthropogenic contributions.

- **Article 3: Ripoll, A., Minguillón, M. C., Pey, J., Jimenez, J. L., Day, D. A., Sosedova, Y., Canonaco, F., Prévô, A. S. H., Querol, X., and Alastuey, A.: Long-term real-time chemical characterization of submicron aerosols at Montsec (Southern Pyrenees, 1570 m a.s.l.), Atmos. Chem. Phys., 15, 2935-2951, doi:10.5194/acp-15-2935-2015, 2015.** Real-time submicron aerosol chemical composition over a period of ten month (July 2011 – April 2012) at MSC high-altitude site was investigated in this article. The variation of inorganic and organic submicron components was interpreted, with a focus on the analysis of diurnal pattern and seasonal variations. Special emphasis was placed on the characterization of organic aerosol (OA) components, and their different types were deduced.

- **Article 4: Pandolfi, M., Ripoll, A., Querol, X. and Alastuey, A.: Climatology of aerosol optical properties and black carbon mass absorption cross section at a remote high-altitude site in the western Mediterranean Basin, Atmos. Chem. Phys., 14(12), 6443–6460, doi:10.5194/acp-14-6443-2014, 2014.** This article presented results from two-year measurements of aerosol optical properties performed at the high-altitude site of Montsec (MSC). Seasonal and diurnal variation of extensive (scattering, absorption, extinction) and intensive (single-scattering albedo (SSA), scattering Ångström exponent (SAE), backscattering-to-scattering ratio (B/S), and asymmetry parameter (g))

aerosol properties as well as mass scattering cross section (MSCS) and mass absorption cross section (MAC) were identified and discussed.

2

Methodology

2.1. Montsec (MSC) monitoring station

In order to characterize continental background aerosols in the western Mediterranean, a monitoring station was placed at the Montsec Astronomical Observatory (Observatori Astronòmic del Montsec, OAdM) facilities (Figure 2.1), supported by the Catalan Government (Generalitat de Catalunya). Several research units are installed at the OAdM (http://www.oadm.cat) including inter alia an automatic weather station from the Catalonian Meteorological Service (Servei Meteorologic de Catalunya, SMC http://www.meteocat.com), and an automatic gaseous pollutants unit from the Network of Control and Surveillance of Air Quality (XVPCA) of the Department of Environment (Departament de Territori i Sostenibilitat) of the Catalan Government (Generalitat de Catalunya) (http://mediambient.gencat.cat).

Figure 2.1 The OAdM facilities with the monitoring station inside.

The OAdM facilities are located on the highest part of the Montsec d'Ares mountain range, at an altitude of 1570 m a.s.l. (42º 03' 04.8'' N, 0º 43' 46.4'' E) (Figure 2.2), in a plain near the edge of a 1000 m cliff to the south, with no wind obstructions present

around. This mountain range has a west-to-east orientation and is found 50 km south of the central Pyrenees. The region is sparsely populated and isolated from large urban and industrial agglomerations: 140 km northwest of the Barcelona metropolitan area, 50 km northeast of the largest city in the region (Lleida, 139176 inhabitants), and 30 km north of the closer town (Balaguer, 15769 inhabitants).

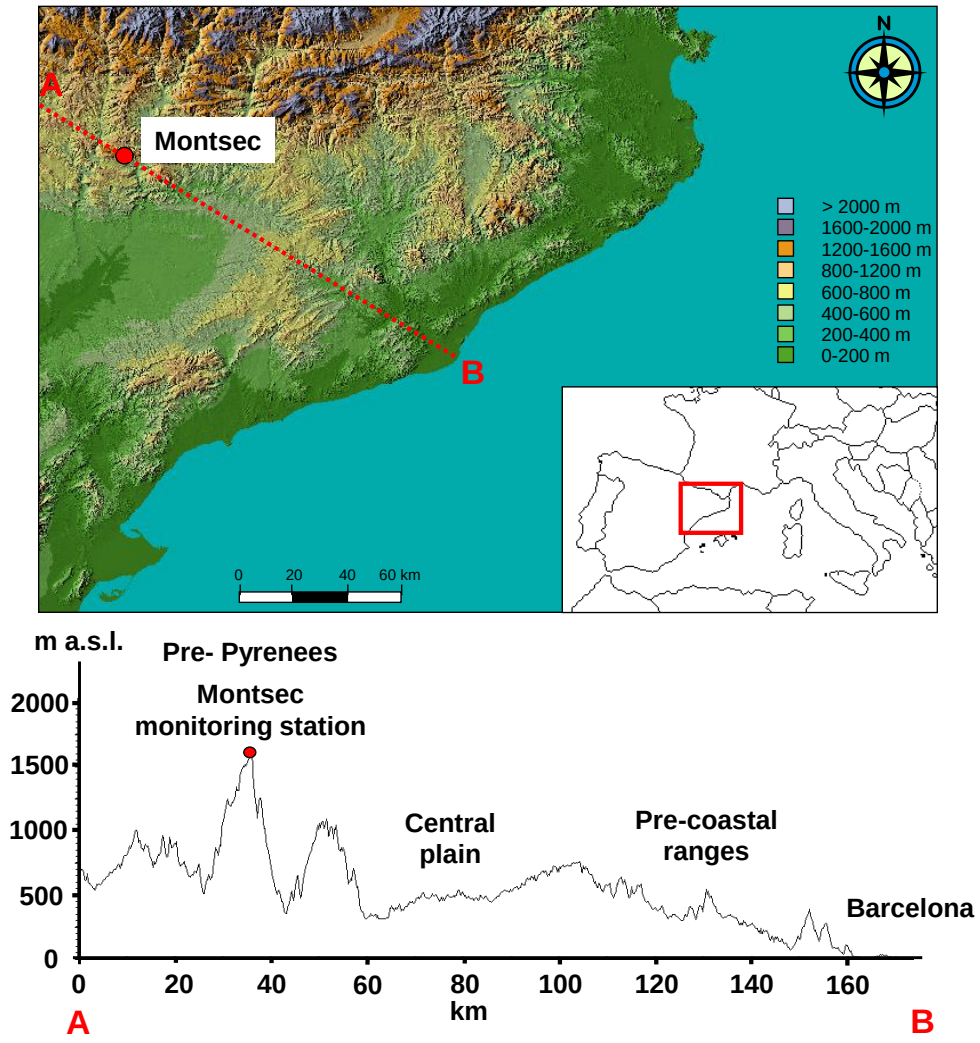

Figure 2.2 Top: location of the MSC monitoring station. Bottom: topography of the Montsec area following the red line.

Light pollution in the OAdM was found to be very low (Colomé et al., 2010), which is an indicator of the very low anthropogenic impact at this site. The station is surrounded by forest (mainly pine and oak) and Cretaceous calcareous rock formations. There is a marked prevalence, especially in the colder seasons (autumn and winter), of Atlantic advections owing to its latitudinal and longitudinal position, at mid-latitude in the Ferrel cell between the sub-polar lows belt and the subtropical highs belt, where westerly

trade winds prevail. The meteorological conditions are governed by the typical Mediterranean climate, with long dry periods and sporadic but intense rains. The average annual temperature is 8.7 ºC (maximum temperature of 27.7 ºC and minimum of -8.7 ºC), and the average annual relative humidity and precipitation are 66 % and 627 mm, respectively (based on meteorological data from 2006 to 2014).

A mobile laboratory equipped with aerosol monitoring instrumentation was placed for the first time at this site from November 2005 to September 2007 under the framework of the DAMOCLES (CGL-2005-03428-C04-03/CLI) project. Results from this campaign were compared with those simultaneously obtained at an urban and regional background site in the western Mediterranean, and were published in the thesis of Pérez (2010). This work concluded that measurements at MSC were representative of the western Mediterranean and were necessary to better understand aerosol processes in this region. For this reason, in November 2009 the same mobile laboratory was situated again in this site, but at this time with some more instruments. In November 2010 the mobile laboratory was replaced by a permanent station, and new instruments have been installed into the station since then. This station is operated in collaboration with the Catalan Government (Generalitat de Catalunya) that jointly installed an automatic gaseous pollutants unit into the station since January 2011 as a part of the XVPCA network. This unit supplies continuous real-time measurements of O_3, NO, NO_2, CO, and SO_2 using a MCV 48AV UV photometry analyzer, a Thermo Scientific instrument (42i-TL), a Teledyne 300 EU Gas filter correlation analyzer; and a Teledyne 100 EU UV fluorescence analyzer, respectively. The MSC station is also operated in collaboration with the University of Barcelona, as a Cimel CE-318 sun photometer is installed into the station since November 2011 as a part of the global aerosol monitoring network (AERONET) and the Iberian network for sun photometers (RIMA). This instrument supplies continuous real-time measurements of aerosol optical properties at 8 different wavelengths. Moreover, meteorological data are supplied by the SMC from the Montsec d'Ares meteorological station, which is also located in the facilities of the OAdM as mentioned earlier.

Currently, the IDAEA-CSIC group is measuring continuous real-time PM_{10}, $PM_{2.5}$, PM_1, and N concentrations, and absorption and scattering coefficients by an optical counter, a condensation particle counter, a multi-angle absorption photometer, a Nephelometer, and an Aethalometer, respectively. Furthermore, 24 h PM_{10} and PM_1 samples are collected using high-volume samplers equipped with PM_{10} and PM_1 cut-off inlets. All these measurements are implemented following the guidelines of ACTRIS, with standardized procedures, in order to obtain high-quality data which can be comparable to those obtained at other stations. From July 2011 to April 2012 an

aerosol chemical speciation monitor was deployed at the MSC station in order to further investigate the real-time chemical composition of submicron particles. In addition to the continuous measurements, five intensive campaigns were performed during March–April 2011, July–August 2011, January–February 2012, June–July 2012, and January–February 2013. During these intensive campaigns 24 h PM_{10} and PM_1 samples were daily collected, and additional aerosol instrumentation, such as a scanning mobility particle sizer (SMPS) and an AiRRmonia, was used. A detailed sampling schedule of MSC measurements is shown in Figure 2.3.

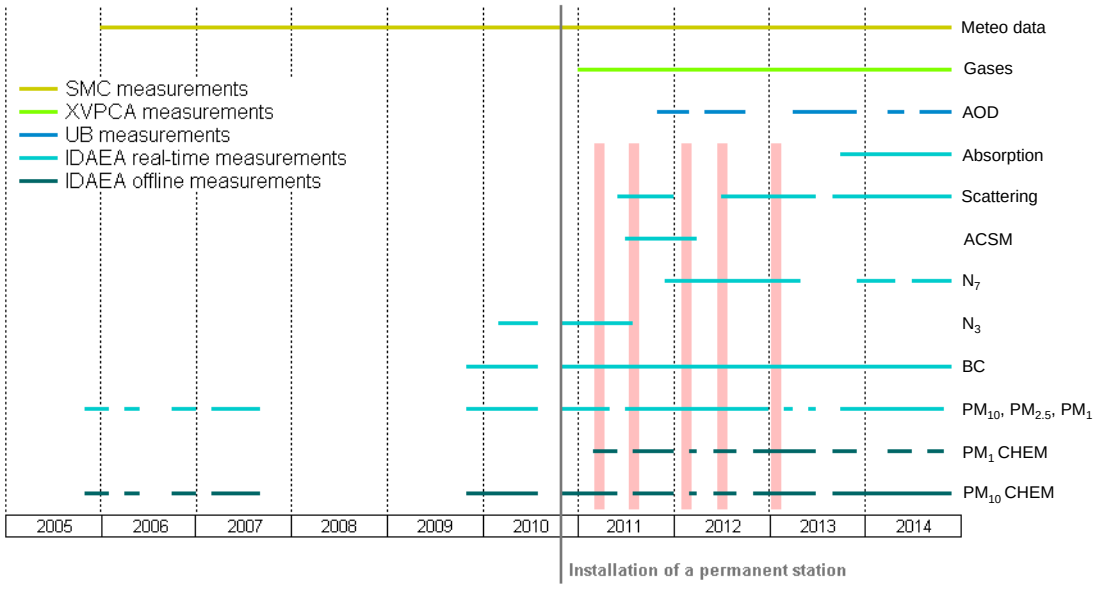

Figure 2.3 Data availability of measurements of aerosol properties at MSC station. Red lines indicate when the intensive campaigns took place.

Finally, MSC monitoring station has been a member of the GAW network since 2014 as a regional station named MSA.

2.2. Measurements of aerosol physical properties

2.2.1. Offline particle mass concentration

Samples of PM_{10} and PM_1 were collected every 4 days using two automatic sequential high-volume samplers model MCV CAV-A/MSb equipped with MCV PM_{10} and PM_1 cut-off inlets, respectively. Samples were collected on quartz microfiber filters of 150 mm of diameter (Pallflex QAT) . Before being used, these filters were baked in an oven at 200ºC for at least four hours to eliminate volatile impurities. After that, filters were conditioned in a climate controlled chamber with temperature of 20ºC and relative humidity of 50% for 24 hours. Then, filters were weighed three times on three consecutive days in the same climate controlled chamber according to the EN 12341 standard (CEN, 1999). After sampling, filters were conditioned once again for 24 hours, and then they were weighed twice on two consecutive days under the same conditions mentioned above. The mass concentration was determined from the increase in filter mass and the volume of air sampled. Overall, about 600 and 470 samples of PM_{10} and PM_1, respectively, were collected throughout the study period.

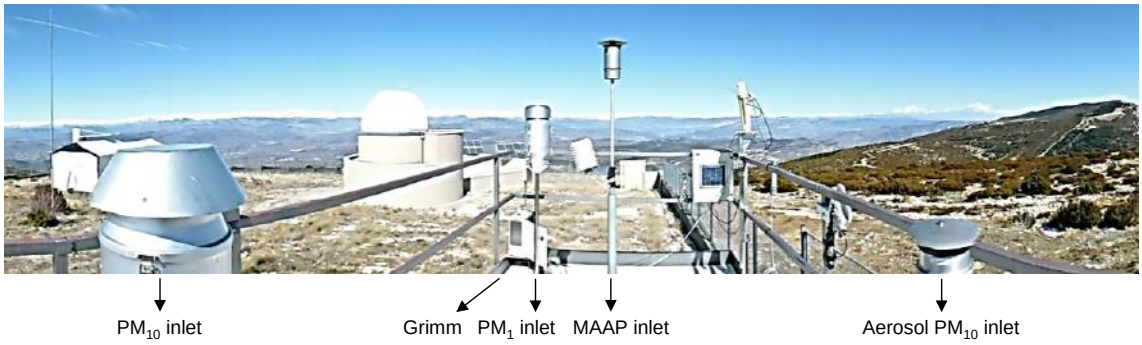

Figure 2.4 Aerosol monitoring inlets protruding above the station roof.

Air is sampled at a flow rate of 30 m^3 h^{-1} through the inlets (Figure 2.4) by means of an in-built pump, through the nozzles of the sampling head. The geometric design of the nozzles determine the cut-off diameter for the particle size fraction being sampled, whereby particles larger than those impact and adhere to a plate daubed with vaseline. The desired particles pass through and are collected on the filter. The PM_1 inlet has a 2-stage impactor inlet whereby larger particles (>$PM_{2.5}$) are removed in the first impactor stage and subsequently particles $PM_{1\text{-}2.5}$ are removed in the second stage. Sampling heads were cleaned once a month and flow rate control was done ever six months.

2.2.2. Real-time particle mass concentration

Real-time measurements of PM_{10}, $PM_{2.5}$, and PM_1 mass concentrations were obtained using an optical particle counter (OPC) model GRIMM 1.107 set to 30 minutes time resolution. GRIMM dust monitor measures light scattered by individual particles as they traverse a tightly focused beam of light. A fraction of the scattered light is collected at a 90º angle by a mirror and transferred to a photodetector (Figure 2.5), where it is converted to a proportional voltage pulse (McMurry, 2000). Particle size is determined from the number of single particle counts registered in each channel, by a 15 channel pulse height analyzer, and it is converted to mass by using a calibration curve obtained from different polystyrene latex (PSL) with refraction index 1.59. These instruments measure particles of diameters between 0.3 and 15 µm. In the present study, PM_{10}, $PM_{2.5}$, and PM_1 mass concentrations were averaged daily and subsequently corrected by comparison with insitu 24 h gravimetric mass measurements of PM_{10} and PM_1.

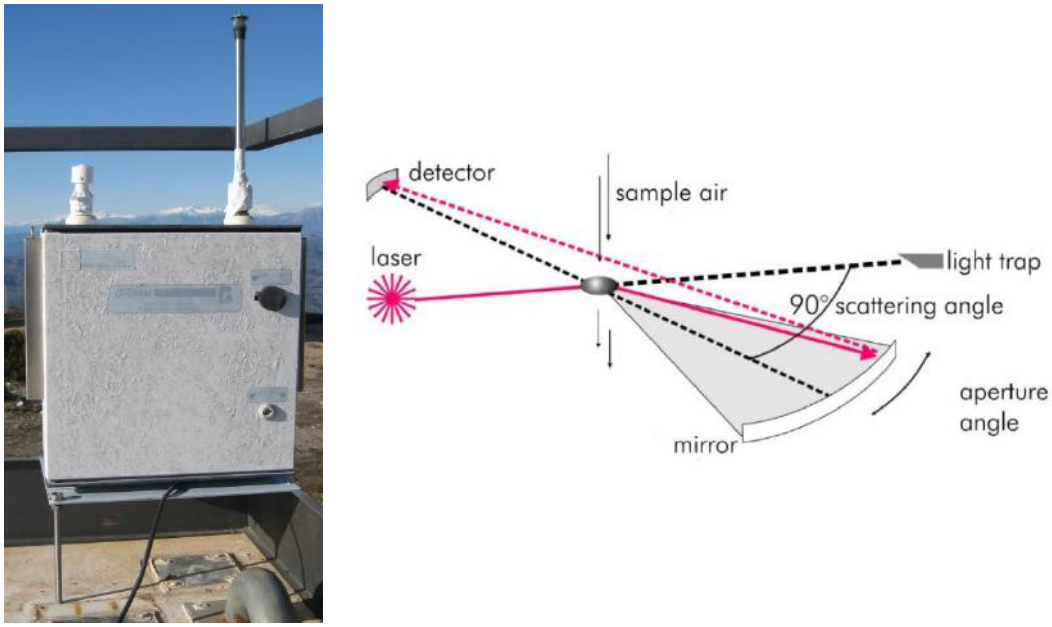

Figure 2.5 GRIMM and schematic diagram of the GRIMM detector block (GRIMM, 2007).

2.2.3. Particle number concentration

The particle number (N) concentration was measured continuously using a condensation particle counter (CPC) with a time resolution of 5 minutes and an inlet with a PM_1 cyclone. From March 2010 to August 2011 the instrument used was a low-size detection or ultrafine CPC (UCPC), which detects particles with an aerodynamic diameter (Dp) higher than 3 nm (model TSI 3776). Afterwards, this instrument was

replaced by an environmental particle counter (EPC), which counts particles larger than Dp 7 nm (model TSI 3783). Both instruments were maintained following the guidelines of ACTRIS, doing flow rate controls and zero checks.

The model 3776 UCPC is a continuous-flow condensation particle counter that is able to count each single particle. The operation of this instrument is quite complex (Figure 2.6). The aerosol flow is saturated with butanol in a slightly heated saturator. The temperature of the butanol-aerosol mixture is decreased down to 10 °C in the condenser of the CPC. Here, the butanol become supersaturated and condenses onto the particles, which grow to droplets large enough to be detectable. The droplet flow passes through a laser beam, and each single particle creates a light pulse. The pulses with an amplitude above a certain threshold are counted by a counting optic. The particle number concentration is then calculated by knowing the aerosol flow rate (Mordas et al., 2008). This instrument participated in the intercomparison workshop conducted within the European infrastructure project ACTRIS held in Leipzig in September-October 2011 (Wiedensohler et al., 2012).

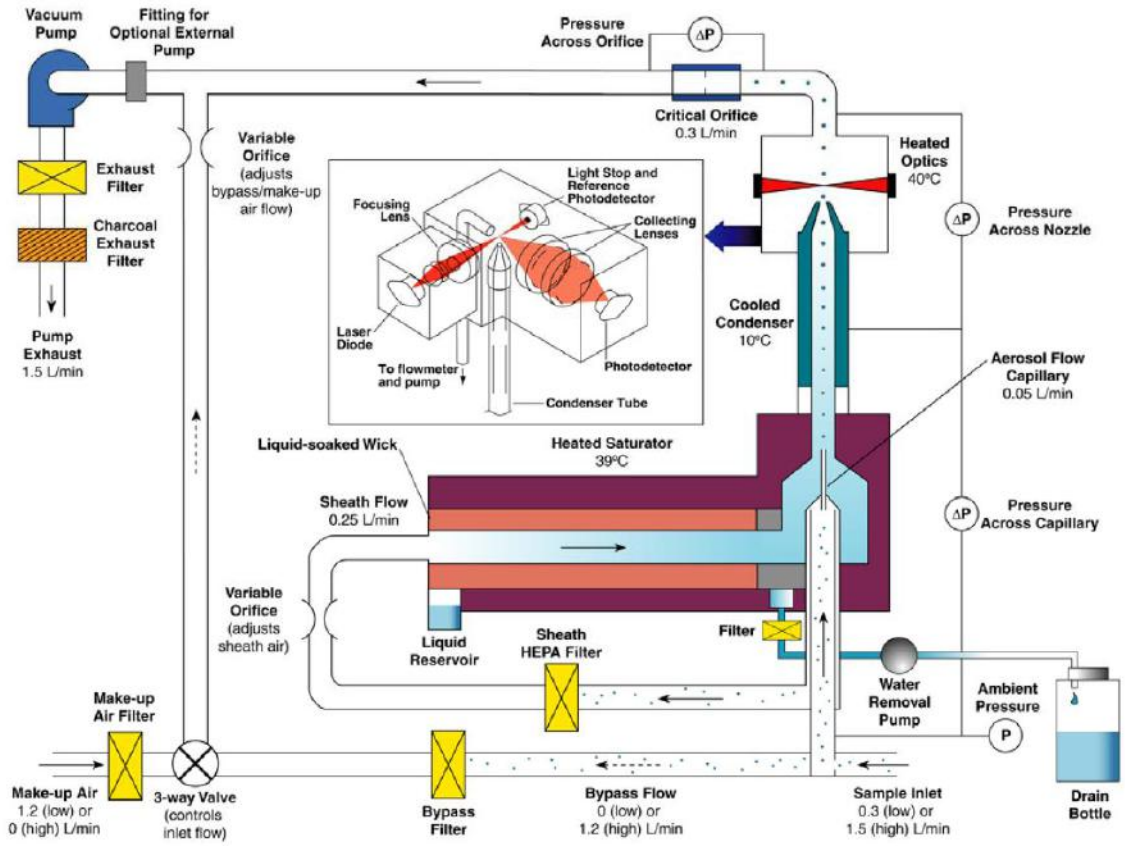

Figure 2.6 Schematic diagram of the UCPC model TSI 3776 (TSI, 2007).

The model 3783 EPC is one of the latest laminar flow water-based CPC (WCPC) because the sampled particles are grown to optically detectable diameters by water condensation (Figure 2.7). The size enhancement happens in a wetted and temperature controlled wick tube with an inner diameter of 4.77 mm. The default temperature settings for the conditioner and the growth tube are 20ºC and 60ºC, respectively. A supersaturation region, where the particle size enhancement takes place, is formed in the growth tube, as the mass diffusivity of water is faster than thermal diffusivity of air (Hakala et al., 2013).

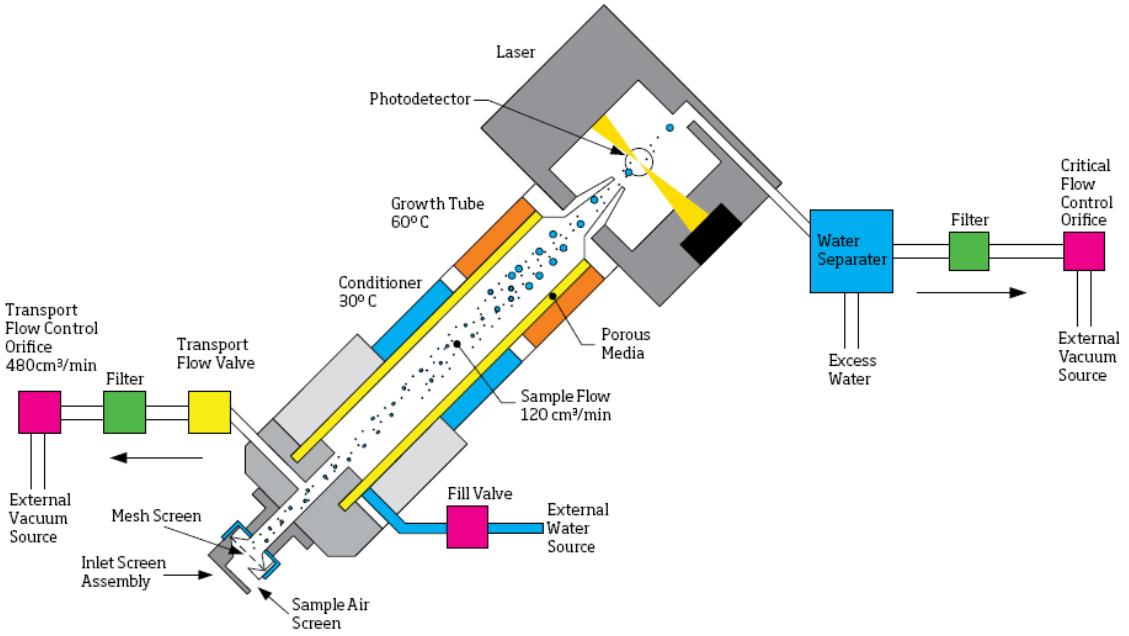

Figure 2.7 Schematic diagram of the EPC model TSI 3783 (TSI, 2010).

2.2.4. Particle number size distribution

During two intensive campaigns (July–August 2011 and January–February 2012) the particle number size distribution was measured continuously using a scanning mobility particle sizer (SMPS). This instrument was operated in the scanning mode of mobility diameters between 11 and 350 nm during the summer campaign and between 8 and 450 nm during the winter campaign. The sampling time resolution was set to 5 minutes. The SMPS system comprises a classifier unit (model TSI 3080) and a differential mobility analyzer (DMA, model TSI 3081) connected to a condensation particle counter (CPC, model TSI 3772). This instrument participates in the annual intercomparison workshop conducted within the Spanish environmental DMAs network (Red Española de DMAs Ambientales, REDMAAS, http://www.redmaas.com).

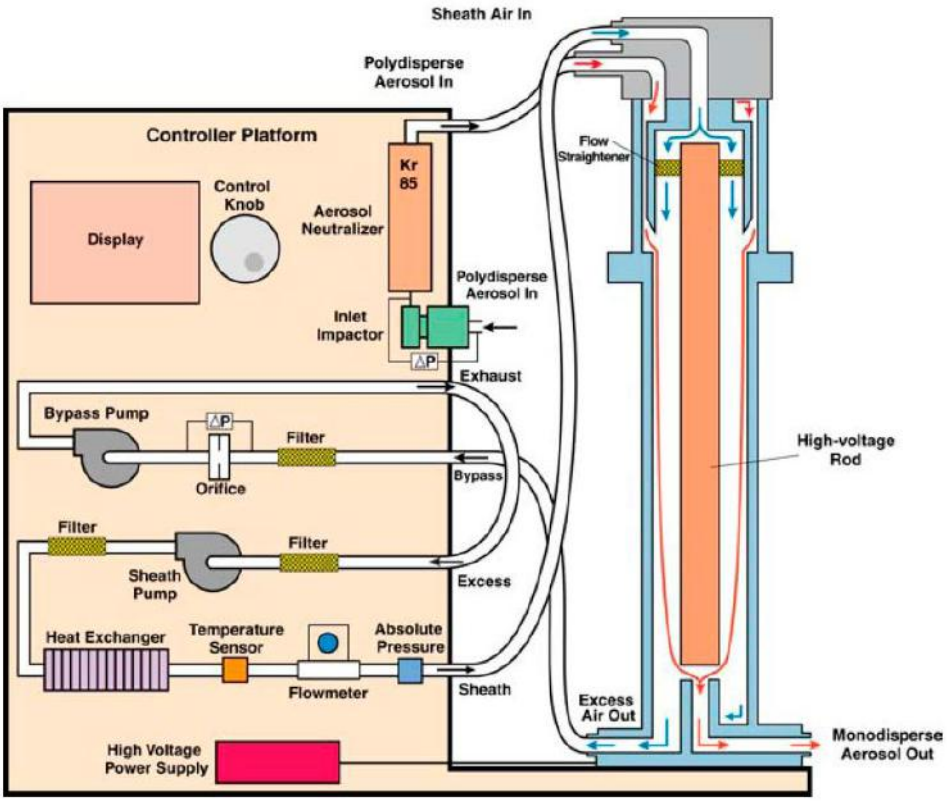

Figure 2.8 Schematic diagram of the DMA model TSI 3081 (TSI, 2009).

The sampled aerosol enters the system through the sampling inlet and is passed to a bipolar charger (neutralizer) which neutralizes the particles. The particles then enter the DMA where they are classified according to their electrical mobility, with only particles of a certain mobility (related to their size) exiting the DMA and passing through to the CPC which determines the particle concentration for that size range (Figure 2.8).

2.3. Measurements of aerosol optical properties

2.3.1. Aerosol absorption coefficient measurements

Measurements of absorption coefficient were carried out continuously using a multi-angle absorption photometer (MAAP) model Thermo 5012 set to 1 minute time resolution, operated in the heated sampling mode, and connected to a single PM_{10} inlet. In the MAAP instrument the aerosol optical absorption coefficient collected on a filter is determined by radiative transfer considerations which include multiple scattering effects and absorption enhancement due to reflections from the filter (Figure 2.9). The MAAP uses a complex inversion algorithm that is based on a radiation transport analysis of the aerosol layer and filter matrix system and thus incorporates the scattering effect of the aerosol into the analysis. Therefore, the MAAP measures the aerosol absorption coefficients directly and provides the cross-section absorption coefficient at 637 nm. However, it should be noted that even though the manufacturer specifies that the wavelength of the MAAP is 670 nm, the actual wavelength is 637 nm, as described by Müller et al. (2011a).

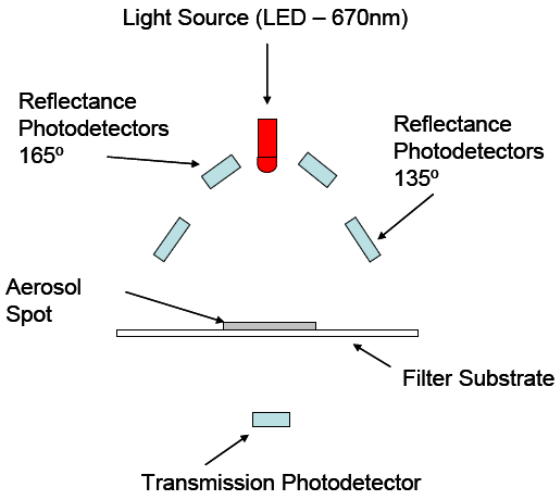

Figure 2.9 Schematic diagram of the MAAP detector block (Thermo, 2004).

$$BC = \frac{\text{abs. coefficient}}{\text{MAC}} \qquad \textbf{[Equation 2.1]}$$

As shown in Equation 2.1, equivalent BC mass concentrations (Petzold et al., 2013) provided by MAAP are calculated by the instrument software dividing the measured absorption coefficient σ_{ab} (λ) by 6.6 $m^2\ g^{-1}$, which is the mass absorption cross section (MAC) at 637 nm (Müller et al., 2011a). Nevertheless, during the development of this

thesis, the specific MAC for MSC was found to be 9.1 m^2 g^{-1} (Ripoll et al., 2014) and varied depending on the atmospheric episodes. MAAP is considered the reference instrument for BC measurements by ACTRIS.

Since 2014 aerosol absorption coefficients are also measured with an Aethalometer model AE33. This instrument allows for the continuous measurement of the attenuation of transmitted light at seven wavelengths (370, 470, 520, 590, 660, 880 and 950 nm), however data from this instrument is not used in this thesis.

2.3.2. Aerosol scattering coefficient measurements

The aerosol scattering (σ_{sp}) and hemispheric backscattering (σ_{bsp}) coefficients were continuously measured with a LED-based integrating nephelometer model ECOTECH Aurora 3000 (Figure 2.10) connected to a PM_{10} inlet. This instrument was modified and an external pump was incorporated to ensure that the flow was correct and not affected by the lower atmospheric pressure. Scattering depends on the wavelength of the incident light. The Aurora 3000 uses a light source emitting light at three different wavelengths (red 635 nm, green 525nm, and blue 450nm). The simultaneous measure of light scattering at three separate wavelengths allows for in-depth analysis of particles size, shape and/or composition: 450 nm interacts strongly with fine and ultrafine particles, 525 nm interacts strongly throughout the human range of visibility, and 635 nm interacts strongly with large particulate matter.

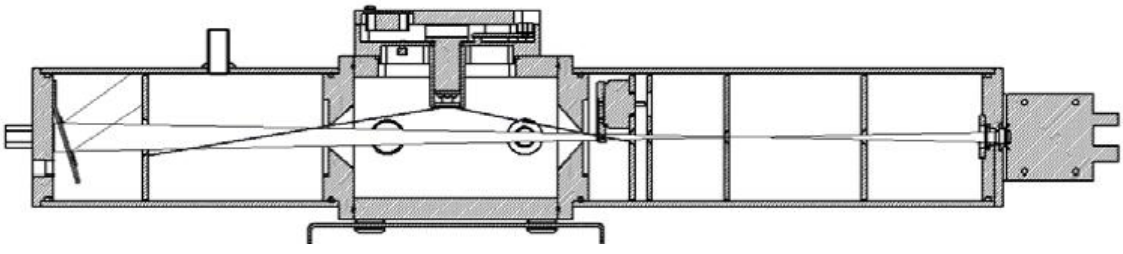

Figure 2.10 Schematic diagram of the light path layout of the nephelometer (Müller et al., 2011b).

The σ_{sp} and σ_{bsp} data were corrected for truncation errors, allowing scattering for 0–360º and backscattering for 90–270º to be reported, and for non-ideal (non-Lambertian) illumination function of the light source as described by Müller et al. (2011b). A full calibration of the nephelometer was performed four times per year by using CO_2 as span gas, while zero measurements and adjusts were performed once per week by using internally filtered particle free air.

2.4. Offline aerosol chemical composition and data analyses

2.4.1. Aerosol chemical composition analyses

The complete chemical analysis of the filters used for the mass concentrations determination was obtained following the procedures proposed by Querol et al. (2001a).

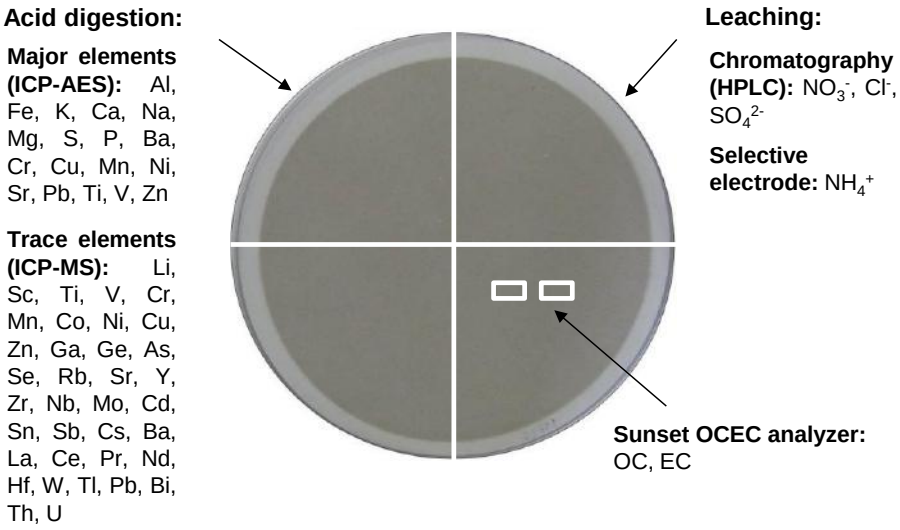

Figure 2.11 Schematic of the chemical analyses applied to the filters.

One-fourth of each filter was acid digested (1.25 mL HNO_3 and 2.5 mL HF) into a closed PFA vesicle at 90ºC for at least 8 hours. After cooling, the PFA vessels were opened and 1.25 mL $HClO_4$ was added. The acids were then completely evaporated by placing the PFA vessels on a heating plate at 230ºC. The remaining dry residue was dissolved with 1.25 mL HNO_3, diluted with ultrapure water (milliQ) to 25 mL, obtaining a solution of 5% HNO_3. This solution was used to determine and quantify major elements by using inductively coupled plasma atomic emission spectroscopy (ICP-AES, IRIS Advantage TJA Solutions, THERMO), and trace elements by using ICP mass spectrometry (ICP-MS, X Series II, THERMO) (Figure 2.11). About 10 mg of a reference material (NIST 1633b) were added to one-fourth of laboratory blank filters to check the accuracy of the analysis of the acidic digestions.

Another one-fourth of each filter was put in a PVC vessel and leached with 20 ml of ultrapure water to dissolve water soluble ions. The PVC vessel was placed in an ultrasound bath for ten minutes and then heated at 60ºC for 6 hours. After that, the leachate was filtered and analyzed to determine the content of SO_4^{2-}, NO_3^-, and Cl^- by

ion high-performance liquid chromatography (HPLC) using WATERS ICpakTM anion column with a WATERS 432 conductivity detector, and NH_4^+ concentrations with a selective electrode (MODEL 710 A+, THERMO Orion).

Two rectangular portions (1.5 cm^{-2}) of the remaining filter were used for the analysis of OC and EC by a Sunset OCEC analyzer using the EUSAAR 2 protocol (European Supersites for Atmospheric Aerosol Research; Cavalli et al. (2010)).

One blank filter was kept for each set of 10 filters and analyzed following the same procedures than the samples. Blank filter concentrations were subtracted from the samples concentrations to determine ambient concentrations.

The detection limit (DL) is widely accepted as a measure of the inherent detection capability of an instrument to measure the minimum analyte signal, amount or concentration. The DL was calculated as shown in Equation 2.2 (Escrig Vidal et al., 2009) propagating the estimates of the two uncertainties associated with the instruments employed for analysis (ICP-MS, ICP-AES, HPLC, Sunset, ion specific electrode) and the blank subtraction (IUPAC, 1995).

$$DL_j = \frac{3 \cdot \sqrt{\sigma_{0\,j}^2 + \sigma_{\mathrm{BLK}\,j}^2}}{V} \qquad \textbf{[Equation 2.2]}$$

where $\sigma_{0\,j}^2$ is the analytical error and $\sigma_{\mathrm{BKL\,j}}^2$ is the standard deviation of the blank filters that were analyzed with the samples. DL for the jth analyte is shown in Table B.1 of the Appendix.

The uncertainties of the chemical species analyzed were calculated using a similar methodology to that described by (Howarth and Thompson, 1976). In order to include all sources of uncertainty, the overall uncertainty is calculated by the Equation 2.3 (Escrig Vidal et al., 2009).

$$\sigma_{ij}^2 = \sqrt{\frac{\sigma_A^2}{V_i^2} + \left(\beta \cdot x_{ij}\right)^2} \qquad \textbf{[Equation 2.3]}$$

where σ_A is the analytical determination uncertainty, V_i is the air volume sampled, β is a coefficient estimated to be 0.15 which might account for the error in the flow rate and other additional sources of uncertainty, and x_{ij} is the concentration value of a species or compound for each sample. Average uncertainties estimated of each species are shown in Table B.2 of the Appendix.

2.4.2. Aerosol composition data analysis

The complete chemical mass balance was obtained calculating the following indirect determinations: (a) CO_3^{2-}, calculated from Ca as $CO_3^{2-}=1.5\times Ca$; (b) Al_2O_3, calculated from Al as $Al_2O_3=1.889\times Al$; and (c) SiO_2, calculated as $SiO_2=2.5\times Al_2O_3$ (Querol et al., 2001a). The organic matter (OM) was obtained by applying a factor of 2.2 to the OC concentrations following the suggestion from Takahama et al. (2011).

Overall, the aforementioned components accounted for 60–90% of the total PM mass. Most of the undetermined mass was attributed to water not eliminated during filter conditioning in the presence of hygroscopic species, but a contribution from sampling artifacts and from the use of factors to determine CO_3^{2-}, SiO_2, and OM cannot be discarded.

Aerosol chemical composition results allowed for the determination of the mineral matter (MM) as shown in Equation 2.4.

$$MM=CO_3^{2-}+SiO_2+Al_2O_3+Ca+Fe+K+nss\text{-}Na+Mg+Mn+Ti+P \quad \textbf{[Equation 2.4]}$$

where nss-Na is the non-sea-salt sodium.

The nss-Na was calculated as nss-Na = Al_2O_3x0.067 according to the composition of the mineral particles from the Sahara given by Moreno et al. (2006), and hence the remaining sodium was sea-salt sodium, ss-Na=Na - nss-Na.

Consequently, the sea salt (SS) determination was given by Equation 2.5.

$$SS=Cl^-+ss\text{-}Na \quad \textbf{[Equation 2.5]}$$

In order to identify the main common groups of trace elements in PM_{10}, a principal component analysis (PCA) was performed. This analysis identifies possible correlations between a number of different variables using orthogonal transformation. The resulting linear correlations (principal components) are interpreted as trace elements with a common origin. The PCA was done with the software STATISTICA v10.0, and the orthogonal transformation was applied using varimax normalized rotation (Thurston and Spengler, 1985), retaining principal components with eigenvalues greater than 1. The dataset used was comprised of the following PM_{10} constituents: Cl^-, NO_3^-, NH_4^+, SO_4^{2-}, Al_2O_3, Ca, K, Na, Mg, Fe, Li, Ti, V, Cr, Mn, Ni, Cu, Zn, As, Se, Sr, Cd, Sb, Pb, OC, and EC. All days with measurements of PM_{10} chemical analysis were included for this analysis, which totalled 390 cases.

2.5. Real-time aerosol chemical composition and data analyses

2.5.1. Aerosol chemical composition measurements

Measurements of real-time chemical composition of non-refractory submicron aerosol species (organic aerosol, nitrate, sulfate, ammonium and chloride) were carried out using an aerosol chemical speciation monitor (ACSM; Aerodyne Research Inc.). The ACSM is built upon the same technology as the aerosol mass spectrometer (AMS), however modifications in the ACSM design allow it to be smaller, less costly, and simpler to operate than the AMS (Ng et al., 2011b). The principal difference is that the ACSM does not measure particle size distribution. Nevertheless, it is capable of routine stable operation for long periods of time (months), and permit to investigate OA sources by applying source apportionment techniques to the organic mass spectra. The first time that an ACSM was tested under real ambient conditions was at MSY during the DAURE campaign.

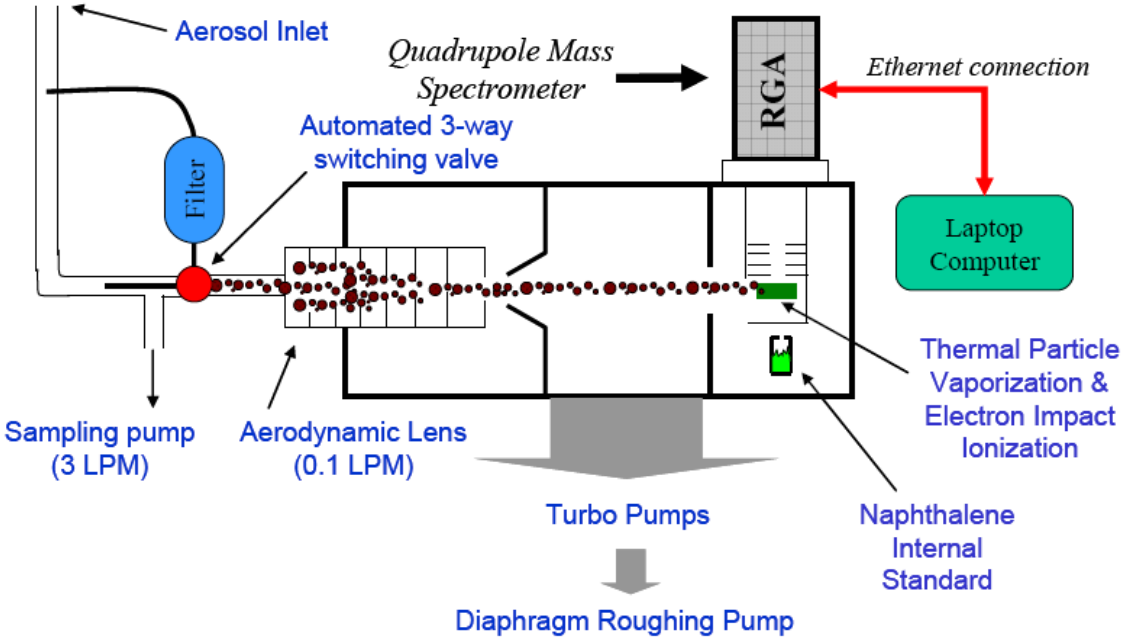

Figure 2.12 Schematic diagram of the ACSM instrument (Aerodyne Research, 2011).

The ACSM consists of a particle sampling inlet, three vacuum chambers and a residual gas analyzer mass spectrometer. An aerodynamic lens is used to sample and focus submicron particles (75-650 nm) into a narrow particle beam (Liu et al., 2007), with a flow of approximately 85 cc/min. The beam is transmitted into the final chamber, where particles are flash-vaporized on a hot oven (600 ºC) and subsequently detected

and chemically characterized with a 70 eV electron impact quadrupole mass spectrometer (Figure 2.12).

The mass concentration of the aforementioned species is determined from the collected aerosol mass spectra as the sum of the ion signals of a given species at each of its mass spectral fragments and its ionization efficiency (IE) (Canagaratna et al., 2007). Since calibration of IEs for all species is not feasible, the relative ionization efficiency (RIE) (compared to that of nitrate) is used (Jimenez et al., 2003). The mass calibration of the ACSM is based on determining the instrument response factor (RF) using ammonium nitrate aerosol. The instrument calibration was carried out following the methodology described by Ng et al. (2011b). Mono-disperse ammonium nitrate particles were delivered simultaneously into both the ACSM and a CPC. The mono-disperse aerosol was generated with an atomizer (TSI, Constant Output Atomizer model 3076), passed through a diffusion dryer and was size selected with a DMA (model TSI 3081 described in section 2.2.4) before arrive to the ACSM and the CPC (TSI 3772) (Figure 2.13).

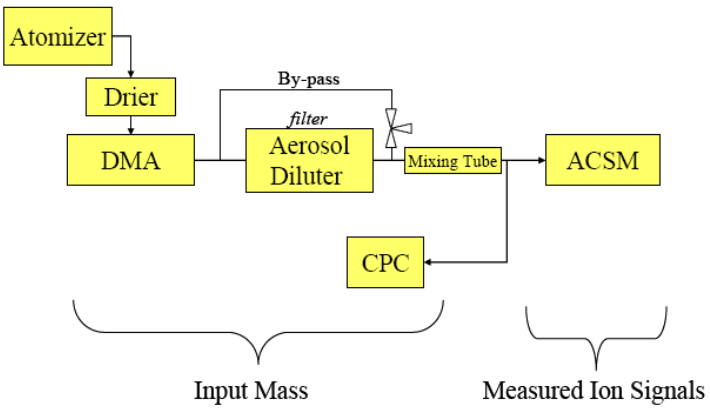

Figure 2.13 Schematic diagram of the ACSM calibration system (Aerodyne Research, 2011).

With the known particle size and number concentrations of the particles, the mass of particles can be calculated (Ng et al., 2011b). Therefore, RIE for ammonium is directly determined from the ammonium nitrate calibration. The sulfate RIE can be also determined directly by doing the aforementioned calibration exercise with ammonium sulfate mono-disperse aerosol.

2.5.2. ACSM data processing

The aerosol mass concentrations need to be corrected for the instrument performance limitations. This correction is based on the inlet pressure and N_2 signal.

Moreover, a correction for particle collection efficiency (CE) needs to be applied to the dataset. CE values can be less than 1 owing to (a) shape-related collection losses at the vaporizer from inefficient focusing of non-spherical particles, (b) particle losses at the vaporizer due to bouncing of solid particles before they are completely vaporized, and (c) particle losses in the aerodynamic inlet as a function of particle diameter (Canagaratna et al., 2007). Current ACSM systems use the identical aerodynamic lens and vaporizer design used in AMS systems so CE values are expected to be similar to those observed in AMS measurements (Ng et al., 2011b). The large database of AMS field results indicates that a CE value of 0.5 reproduces speciated AMS mass concentrations for ambient particles to within 25% of those measured by collocated instruments (Canagaratna et al., 2007). Nevertheless, Middlebrook et al. (2012) proposed an approach to calculate composition-dependent CE.

Comparison with co-located measurements is also used to further validate and correct the ACSM data. To this end, the sum of the ACSM species (= sulfate + nitrate + ammonium + OA + chloride) and the BC mass concentrations was compared with the co-located PM_1 and light scattering measurements. The comparison of ACSM plus BC concentrations versus PM_1 concentrations from the OPC and SMPS showed strong correlations (R^2=0.72 and R^2=0.87, respectively). These concentrations were also highly correlated with light scattering at 525 nm determined by the nephelometer (R^2=0.85). The offline measurements from the 24 h PM_1 filter samples were also used to validate individual ACSM species. For the first time, long-term series of PM_1 composition (187 samples) was compared with daily averaged ACSM species and all species showed strong correlations (R^2 between 0.77 and 0.96).

The ACSM data processing was carried out in collaboration with the Cooperative Institute for Research in Environmental Sciences (CIRES) at the University of Colorado Boulder, CO, USA, during a three-month stay. The internship was founded by the Spanish government (MINECO) and supervised by Prof. J. Jimenez and Dr. D. Day.

2.5.3. ACSM intercomparison study

Despite the fact that the ACSM is a relatively recent developed instrument, it is becoming a widely used instrument all around the world and especially in Europe due to the ACTRIS ACSMs network included in the frame of the WP21 (JRA2). This workpackage aims to enhance the capabilities of long-term measurements of aerosol chemistry at network stations, develop optimized and standardized techniques for the measurement of oxygenated volatile organic compounds, and perform mass closure experiments by combined measurements of organic carbon compounds in the gas and

particle phases. IDAEA-CSIC group, although not officially participating in the JRA2, also participated in its activities. Thus, the ACSM from IDAEA-CSIC group was sampling for one year at the MSY stations and also participated in the ACTRIS ACSM intercomparison exercise (Figure 2.14).

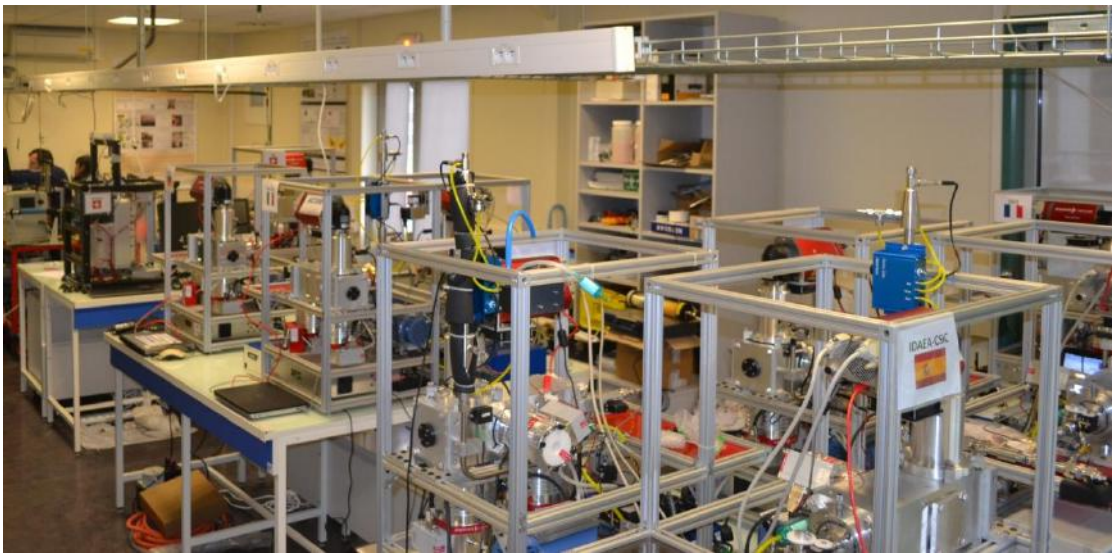

Figure 2.14 Picture of the SIRTA laboratory with the ACSM instruments operating in parallel.

The ACTRIS ACSM intercomparison campaign took place during three weeks in November and December 2013 at the SIRTA (Site Instrumental de Recherche par Télédétection Atmosphérique) station of the LSCE (Laboratoire des sciences du climat et l'environnement), in the region of Paris (France). In this intercomparison 15 individual aerosol mass spectrometers (13×Q-ACSM, 1×ToF-ACSM, 1×HR-ToF-AMS) employing the same experimental technique were operated in parallel under real ambient conditions for the first time. Results from this study are shown in two works. Part 1 reported the accuracy and precision of the instruments for all the measured species (Crenn et al., 2015), and part 2 focused on the intercomparison of organic components and the results from factor analysis source apportionment by positive matrix factorization (PMF) utilizing the multilinear engine 2 (ME-2) (Fröhlich et al., 2015). Good qualitative and quantitative agreement between all 15 aerosol mass spectrometers was achieved, and except for the organic contribution of *m/z* 44 to the total organics (f44), which varied by factors between 0.6 and 1.3 compared to the mean, the peaks in the organic mass spectra were similar among instruments.

2.5.4. Source apportionment of organic aerosol

The source apportionment of OA mass spectral data is usually investigated by applying two-dimensional bilinear models like PMF (Paatero and Tapper, 1994; Paatero, 1997) or chemical mass balance (CMB, Watson et al., 1997). PMF has successfully been used in numerous AMS source apportionment studies (Zhang et al., 2011). In both methods the organic *m*×*n* spectral matrix **X**, containing *m* organic mass spectra (rows) with *n* ion fragments each (columns), is factorized into two submatrices, the profiles **F** and time series **G**. **F** is a *p*×*n* and **G** a *m*×*p* matrix with *p* indicating the number of profiles (Equation 2.6). The residual *m*×*n* matrix **E** contains the fraction of **X** which is not explained by the current model solution and is minimized by the PMF algorithm.

$$X = GF + E \qquad \textbf{[Equation 2.6]}$$

In many cases, e.g., when two factors have similar time series (e.g., heating and cooking in the evening) or profiles (e.g., traffic and cooking, Mohr et al., 2009) PMF has difficulties separating these factors (e.g., Sun et al., 2010). With the ME-2 model this can be solved since it provides additional control over the rotational ambiguity (Paatero and Hopke, 2009). Here the solution space is explored by introducing a priori information (e.g., factor profiles) for some (not necessary all) of the factors *p*. The strength of this additional constraint is set by the so-called *a* value (Brown et al., 2012; Paatero and Hopke, 2009), which determines how much deviation from the constraint profile the model allows. It ranges from zero to one and can be understood as the relative fraction how much each *m/z* may individually deviate from the a priori profile (Canonaco et al., 2013). That way ME-2 covers the whole range of bilinear models: the traditional unconstrained PMF (no *a* value set), PMF with controlled rotations (in many cases this is simply denoted “ME-2”), and fully constrained PMF (with *a* = 0, a form of CMB). In the unconstrained PMF and constrained ME-2, the algorithm models the (entirely positive) profile and time series matrices **F** and **G** with a pre-set number of factors *p* by iteratively minimizing the quantity Q (Equation 2.7).

$$Q = \sum_{i=1}^{n}\sum_{j=1}^{m}\left(\frac{e_{ij}}{\sigma_{ij}}\right)^2 \qquad \textbf{[Equation 2.7]}$$

where e_{ij} represent the elements of the residual matrix **E** and σ_{ij} the measurement uncertainties for the *j* ion fragments in the *i* sample.

The source apportionment of the OA in the present study was investigated by the application of PMF and ME-2 to the organic spectra ACSM dataset. To this end, the custom software tool of source finder (SoFi) version 4.8 developed by Canonaco et al. (2013) and written in Igor Pro 6 (WaveMetrics, Inc., Lake Oswego, OR, USA) was used. This analysis was carried out separately for the summer period (14 Jul 11 – 24 Sep 11) and the winter period (10 Jan 12 – 7 Mar 12), and only m/z<=100 were used because: a) the signals of m/z>100 account for a minor fraction of the total organic mass (on average, 2 %), b) the m/z>100 have larger uncertainties, and c) the large interference of naphthalene signals (used for m/z calibration of the ACSM) at these m/z (e.g., m/z 127, 128, and 129) (Sun et al., 2012). The solution of ME-2 analysis selected for each season was based on several tests, with different number of factors and different a values, taking into account the correlations with external tracers (including nitrate, sulfate, BC and ozone), the daily patterns of each factor, and the residuals. The source apportionment was carried out in collaboration with the Paul Scherrer Institut (PSI), Switzerland.

2.6. Classification of atmospheric episodes

Additional tools based on meteorological maps and aerosol dispersion models were used to determine the transport pathways and classify the atmospheric episodes affecting the Montsec area.

2.6.1. Backward trajectories: Hysplit model

Backward trajectories were computed on each day of measurements from 12 a.m. for 120 hours using the hybrid single particle lagrangian integrated trajectory model (HYSPLIT; Draxler and Rolph, 2014; Rolph 2014; http://www.ready.noaa.gov/HYSPLIT_traj.php) from the NOAA Air Resources Laboratory. The backward trajectories were calculated for 3 different heights, 750, 1500, and 2500 m above ground level, using modeling vertical velocity. They were classified visually according to their predominant transport direction in: (1) Atlantic North (AN), (2) Atlantic North West (ANW), (3) Atlantic South West (ASW), (4) North African (NAF), (5) Mediterranean (MED), (6) European (EU), (7) Winter Regional (WREG, from October to March), and (8) Summer Regional (SREG, from April to September). Air mass origin sectors map and examples of backward trajectories for each sector are shown in Fig.S3 of the Appendix C1.

2.6.2. Boundary layer height

The planetary boundary layer (PBL) height was calculated using the meteorological global data assimilation system (GDAS1) model from the NOAA Air Resources Laboratory (http://www.ready.noaa.gov/READYamet.php), based on stability time series information. The limitations of PBL height estimate with this model needs to be considered when assessing its values. The GDAS1 model uses a 50 km resolution grid, since this horizontal resolution is not very good for mountain regions such as MSC (1000 m peak in just 20 kms, Figure 2.2), the estimate average terrain height from the model is around 580 m, whereas the real altitude of the site is 1570 m. Furthermore, the model gives only the PBL height every three hours and we assumed that the PBL height does not change during the next three hours after the datapoint.

2.6.3. Aerosol dispersion models

Daily NAAPS, SKIRON and BSC-DREAM8b maps were used to further asses the type of atmospheric episodes.

The NAAPS model produces aerosol maps from the Marine Meteorology Division of the Naval Research Laboratory (NRL, http://www.nrlmry.navy.mil/aerosol/index_shortcuts.html). These provide information on the total aerosol optical depth, sulfate surface concentration, dust surface concentration, and smoke surface concentration.

The SKIRON simulations produce also aerosol surface concentration maps (http://forecast.uoa.gr/dustindx.php; e.g. Kallos, 1997; Papadopoulos et al., 2001). These simulations provide information on total column loads and surface concentrations of dust, and in addition dry and wet deposition fluxes at a surface level.

The BSC-DREAM8b model from the Earth Sciences Division of the Barcelona Supercomputing Center (http://www.bsc.es/earth-sciences/mineral-dust-forecast-system/bsc-dream8b-forecast; Basart et al., 2012) predicts the atmospheric life cycle of the eroded desert dust. The current operational version is v2.0 which includes updates in the dry and wet deposition schemes as well as the inclusion of a "preferential source" mask in its emission scheme.

3

Articles included in this thesis

3.1. Author's contribution to the articles

- **Three years of aerosol mass, black carbon and particle number concentrations at Montsec (southern Pyrenees, 1570 m a.s.l.).**
  Joint effort with especially Jorge Pey. We organized the measurements of the aerosol parameters and performed the data analyses. I wrote the paper.
- **Joint analysis of continental and regional background environments in the western Mediterranean: PM_1 and PM_{10} concentrations and composition.**
  I conducted the measurements in the continental background environment and analysed the samples from this site. I conducted the data analysis of both sites and wrote the paper.
- **Long-term real-time chemical characterization of submicron aerosols at Montsec (Southern Pyrenees, 1570 m a.s.l.).**
  Joint effort with especially María Cruz Minguillón. We conducted the measurements, and I processed the data together with Jose L. Jimenez and Doug Day during a three-month stay in the University of Colorado at Boulder.
- **Climatology of aerosol optical properties and black carbon mass absorption cross section at a remote high-altitude site in the western Mediterranean Basin.**
  I was in charge of the measurements and data analyses together with Marco Pandolfi. I was involved in the writing of the paper.

3.2. Article 1: Three years of aerosol mass, black carbon and particle number concentrations at Montsec (southern Pyrenees, 1570 m a.s.l.)

Anna Ripoll[1,2], Jorge Pey[3], María Cruz Minguillón[1], Noemí Pérez[1], Marco Pandolfi[1], Xavier Querol[1], Andrés Alastuey[1]

[1]Institute of Environmental Assessment and Water Research (IDAEA-CSIC), Jordi Girona 18-26, 08034, Barcelona, Spain.

[2]Department of Astronomy and Meteorology, Faculty of Physics, University of Barcelona, Martí i Franquès 1, 08028, Barcelona, Spain.

[3]Aix-Marseille Université, CNRS, LCE FRE 3416, Marseille, 13331, France.

Atmos. Chem. Phys., 14, 4279-4295,

doi:10.5194/acp-14-4279-2014, 2014

Published: **30 April 2014**

Impact factor of Journal: **5.298**

Resum. En aquest article es presenten les mesures de massa de partícules (angl., particulate matter, PM), carboni negre (angl., black carbon, BC), i nombre de partícules (N) obtingudes durant el període 2010-2012 a l'estació de mesura dels aerosols del Montsec (MSC; 42º 3' N, 0º 44' E), situada a 1570 m sobre el nivell del mar, a la part sud dels Pirineus. Els resultats es comparen amb els obtinguts a altres estacions remotes del centre d'Europa, i amb els adquirits simultàniament a l'estació rural del Montseny (MSY). A més a més, s'interpreten les variacions anuals, estacionals, setmanals, i diàries d'aquests paràmetres, i se'n dedueixen els principals factors que les determinen.

Les concentracions de PM mesurades al MSC són comparables en magnitud a les d'altres estacions remotes del centre d'Europa, quan no es té en compte l'influencia de les intrusions africanes. Això fa que el terme fons continental sigui aplicable a l'estació del MSC. No obstant, les altes concentracions de N i les baixes concentracions de BC registrades al MSC ressalten la importància dels processos de formació de noves partícules i la menor influencia dels processos de combustió al sud d'Europa.

Tal i com s'ha mostrat en altres estudis de l'oest del Mediterrani, els paràmetres mesurats presenten una variació estacional amb concentracions altes a l'estiu i baixes a l'hivern. Tot i això, la fracció grollera del PM va presentar un patró més accentuat que la fracció fina (PM_1) i el BC. Això és degut a que la fracció grollera està més influenciada per les aportacions de la pols sahariana i de la resuspensió del sòl, les quals tenen una clara estacionalitat. Per contra, el PM_1 i el BC s'associen més a emissions antropogèniques, que tenen menys variacions estacionals però un patró setmanal més definit. Això es veu reflectit en les concentracions de PM_1 i BC, ja que mostren un mínim estadísticament significatiu el diumenge i el dilluns, corresponent a la disminució de l'activitat humana durant el cap de setmana. Això confirma que el MSC està situat a suficient distància de les emissions antropogèniques.

La combinació dels differents processos a nivell local, regional i continental dóna com a resultat una alta variabilitat dels cicles diaris d'aquests paràmetres, amb patrons poc definits a l'estiu però més clars a l'hivern, excepte pel N que mostra un cicle diari tot l'any, independentment de l'origen de la massa d'aire, amb un màxim al migdia.

Atmos. Chem. Phys., 14, 4279–4295, 2014
www.atmos-chem-phys.net/14/4279/2014/
doi:10.5194/acp-14-4279-2014
© Author(s) 2014. CC Attribution 3.0 License.

Atmospheric Chemistry and Physics Open Access

Three years of aerosol mass, black carbon and particle number concentrations at Montsec (southern Pyrenees, 1570 m a.s.l.)

A. Ripoll[1], J. Pey[1,*], M. C. Minguillón[1], N. Pérez[1], M. Pandolfi[1], X. Querol[1], and A. Alastuey[1]

[1]Institute of Environmental Assessment and Water Research (IDAEA-CSIC), Barcelona, 08034, Spain
[*]now at: Aix-Marseille Université, CNRS, LCE FRE 3416, Marseille, 13331, France

Correspondence to: A. Ripoll (anna.ripoll@idaea.csic.es)

Received: 30 July 2013 – Published in Atmos. Chem. Phys. Discuss.: 21 October 2013
Revised: 11 March 2014 – Accepted: 13 March 2014 – Published: 30 April 2014

Abstract. Time variation of mass particulate matter (PM_1 and PM_{1-10}), black carbon (BC) and number of particles (N_3: number of particles with an aerodynamic diameter higher than 3 nm, and N_{10}: higher than 10 nm) concentrations at the high-altitude site of Montsec (MSC) in the southern Pyrenees was interpreted for the period 2010–2012.

At MSC, PM_{10} (12 $\mu g\,m^{-3}$) and N_7 (2140 $\#\,cm^{-3}$) three-year arithmetic average concentrations were higher than those measured at other high-altitude sites in central Europe during the same period (PM_{10}: 3–9 $\mu g\,m^{-3}$ and N: 634–2070 $\#\,cm^{-3}$). By contrast, BC concentrations at MSC (0.2 $\mu g\,m^{-3}$) were equal to or even lower than those measured at these European sites (0.2–0.4 $\mu g\,m^{-3}$). These differences were attributed to the higher relevance of Saharan dust transport and to the higher importance of the biogenic precursor emissions and new particle formation (NPF) processes, and to the lower influence of anthropogenic emissions at MSC.

The different time variation of PM and BC concentrations compared with that of N suggests that these aerosol parameters were governed by diverse factors at MSC. Both PM and BC concentrations showed marked differences for different meteorological scenarios, with enhanced concentrations under North African air outbreaks (PM_{1-10}: 13 $\mu g\,m^{-3}$, PM_1: 8 $\mu g\,m^{-3}$ and BC: 0.3 $\mu g\,m^{-3}$) and low concentrations when Atlantic advections occurred (PM_{1-10}: 5 $\mu g\,m^{-3}$, PM_1: 4 $\mu g\,m^{-3}$ and BC: 0.1 $\mu g\,m^{-3}$). PM and BC concentrations increased in summer, with a secondary maximum in early spring, and were at their lowest in winter, due to the contrasting origin of the air masses in the warmer seasons (spring and summer) and in the colder seasons (autumn and winter). The maximum in the warmer seasons was attributed to long-range transport processes that mask the breezes and regional transport breaking the daily cycles of these pollutants. By contrast, PM and BC concentrations showed clear diurnal cycles, with maxima at midday in the colder seasons. A statistically significant weekly variation was also obtained for the BC concentrations, displaying a progressive increase from Tuesday to Saturday, followed by a significant decrease on Sunday and Monday.

N concentrations depended more on local meteorological variables such as temperature and solar radiation intensity than on the origin of the air mass. Therefore, arithmetic averages as a function of meteorological episodes showed the highest concentrations of N during summer regional episodes (N_3: 4461 $\#\,cm^{-3}$ and N_7: 3021 $\#\,cm^{-3}$) and the lowest concentrations during winter regional scenarios (N_3: 2496 $\#\,cm^{-3}$ and N_7: 1073 $\#\,cm^{-3}$). This dependence on temperature and solar radiation also accounted for the marked diurnal cycle of N concentrations throughout the year, with a peak at midday and for the absence of a weekly pattern.

Measurements carried out at MSC enabled us to characterize the tropospheric background aerosols in the western Mediterranean basin (WMB). Our results highlight the importance of the NPF processes in southern Europe, underline the high contribution of long-range dust transport with respect to central Europe and its prevalence in elevated layers, and reveal that MSC is much less affected by anthropogenic emissions than other high-altitude sites in central Europe.

Published by Copernicus Publications on behalf of the European Geosciences Union.

1 Introduction

Atmospheric aerosols have been extensively investigated because of their adverse effects on health (Pope III and Dockery, 2006), and because of their role in many atmospheric and climate processes, influencing the Earth's radiative balance (IPCC, 2007). Atmospheric particulate matter (PM) is associated with increasing mortality and morbidity in urban populations (WHO, 2013). Ambient concentrations of pollutants have therefore been measured in urban areas (Eeftens et al., 2012) and have been subject to regulation (Directive 2008/50/CE). Nonetheless, the effect of aerosols on climate is observed more clearly in the free troposphere (FT) than in the planetary boundary layer (PBL) because the FT is more representative of the global atmosphere (Laj et al., 2009). The reason for this is that the aerosol residence time is longer in the FT, i.e., several weeks (Kent et al., 1998). Consequently, in situ aerosol properties are measured at high-altitude mountain observatories (Asmi et al., 2013; Collaud Coen et al., 2013). Moreover, measurements at such sites enabled us to characterize background aerosols, source origins, particle formation mechanisms and long-range transport better without the interference of local pollution.

Although the number of studies based on surface aerosol measurement sites worldwide is considerable, most of them have been carried out in areas within the PBL because of air quality regulations and only a few concern high-elevation sites. Furthermore, the majority of these high-altitude studies have focused on greenhouse gases and aerosol radiative properties (Andrews et al., 2011; Zieger et al., 2012), whereas few studies deal with the seasonal, weekly and diurnal variation of parameters such as particle number concentration (N) and size distribution, black carbon (BC), and PM chemical composition, which are rising in importance (Asmi et al., 2011; Monks et al., 2009; Putaud et al., 2010).

Earlier studies at high-altitude sites in Europe were carried out inter alia in Switzerland (Jungfraujoch, 3578 m), France (Puy de Dôme, 1465 m), and Italy (Mt. Cimone, 2165 m). These studies showed a marked seasonal cycle for PM_{10} (Tositti et al., 2013), BC (Marinoni et al., 2008), and N (Collaud Coen et al., 2011; Venzac et al., 2009), with the lowest concentrations in winter and the highest in summer. The variation of these aerosol parameters is produced at two scales: (1) seasonal variation depending on the origin of the air mass and (2) daily variation controlled by PBL growth and mountain breeze transport. In contrast to central Europe, few studies on mountain aerosol have been carried out in the western Mediterranean basin (WMB).

The WMB is characterized by atmospheric dynamics that are atypical and complex because of its topography, the elevated emissions of anthropogenic pollutants, and the arrival of natural and anthropogenic aerosols as a result of long-range transport processes (Millan et al., 1997). All these characteristics prompted us to study the aerosol phenomenology. For this reason, a regional background aerosol monitoring station was installed at Montseny Natural Park (MSY, 720 m a.s.l.), 40 km north–northeast of Barcelona and 25 km from the Mediterranean coast, to study the regional-scale aerosols in the WMB (Pérez et al., 2008). However, the urban and industrial contributions to the regional background aerosol concentrations in the WMB have been found to be higher than those at other mountain sites in Europe (Pey et al., 2010b). Consequently, a remote aerosol measurement site was set up to gain further insight into the continental background aerosols. The site selected is in the Montsec mountain range, which is located at 1570 m a.s.l., in the southern Pyrenees, and removed from large urban and industrial areas.

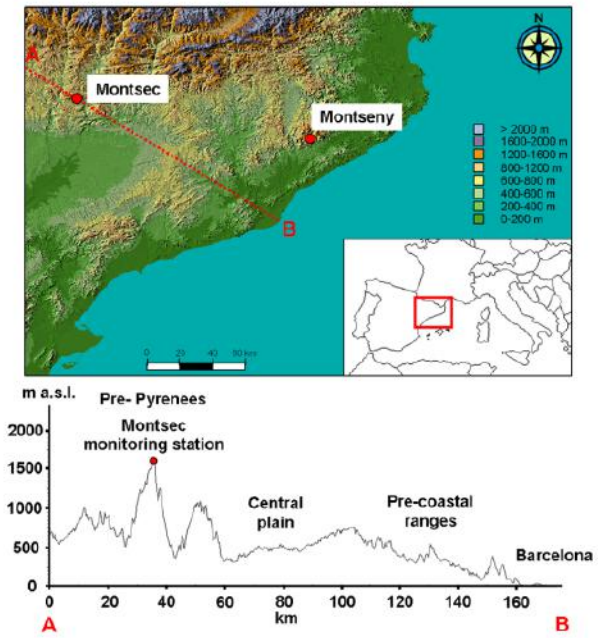

Fig. 1. Top: location of the two monitoring stations (Montsec and Montseny). Bottom: topography of the Montsec area following the red line.

In this study, the results of PM, BC and N measurements from a high-altitude site (Montsec) are presented and their variation is interpreted. Given the location of this site between the Atlantic and the Mediterranean, greater emphasis was placed on evaluating the influence of different meteorological scenarios on these parameters. The present study seeks to (1) evaluate the concentrations and evolution of PM, BC, and N at a remote site with no influence of local anthropogenic emission sources, (2) analyze the annual, seasonal, weekly, and daily variations in the concentration of continental background aerosols with respect to the MSY regional site, and (3) deduce the main factors influencing these variations.

2 Methodology

2.1 Monitoring sites

The Montsec site (MSC) is a high-altitude emplacement located in the northeast of the Iberian Peninsula. This station is placed at the Montsec Astronomical Observatory (Observatori Astronomic del Montsec, OAdM) facilities, supported by the Catalan Autonomous Government and owned by the *Consorci del Montsec* (CdM). This observatory is situated on the highest part of the Montsec d'Ares mountain, at an altitude of 1570 m a.s.l. (42°3′ N, 0° 44′ E), in a plain near to the edge of a 1000 m cliff to the south, with no wind obstructions present around. The Montsec mountain range has a west-to-east orientation and is located on the southern side of the Pyrenees, 50 km from the Axial Pyrenees to the north (Fig. 1). This region is sparsely populated and isolated from large urban and industrial agglomerations: 140 km from Barcelona to the southeast and 30 km from the largest city in the region (Balaguer, 15 769 inhabitants) to the south. Light pollution in the OAdM was found to be very low (Colomé et al., 2010), which could be an indicator of the very low anthropogenic impact at this site. The station is surrounded by forest (mainly pine and oak) and Cretaceous calcareous rock formations. There is a marked prevalence, especially in the colder seasons (autumn and winter), of Atlantic advections owing its latitudinal and longitudinal position, at mid-latitude in the Ferrel cell between the sub-polar lows belt and the subtropical highs belt, where westerly trade winds prevail. The atmospheric dynamics is governed by the typical Mediterranean climate, with long dry periods, sporadic but intense rains, and a prevalence of local and regional atmospheric air mass circulations.

Results were compared with those simultaneously obtained at the Montseny (MSY) station, a regional background site located in the Montseny Natural Park (41°19′ N, 02°21′ E, 720 m a.s.l.), 40 km north–northeast of the Barcelona urban area, and 25 km from the Mediterranean coast (Fig. 1). A detailed description of this site may be found in Pérez et al. (2008).

2.2 Sampling schedule and measurements

The MSC site consisted of a mobile laboratory equipped with aerosol monitoring instrumentation from January to August 2010. This was replaced by a permanent station in November 2010. The present paper provides results from January 2010 to December 2012. A detailed sampling schedule is shown in Fig. S1 in the Supplement. All the meteorological data were supplied by the Catalonian Meteorological Service from the Montsec d'Ares station, which has been in operation since 2007 (Tables S1, S2 and S3 and Fig. S2 in the Supplement) and which is also installed at the OAdM facilities. Real-time PM concentrations were continuously measured by an optical counter (GRIMM 1107). PM 30 min data were daily averaged and subsequently corrected by comparison with 24 h gravimetric mass measurements of PM_{10} collected every 4 days by a high-volume (hi-vol) sampler. The absorption coefficient was measured continuously using a Multi Angle Absorption Photometer (MAAP, model 5012, Thermo). Equivalent BC concentrations were calculated by the MAAP instrument software by dividing the measured absorption coefficient σ_{ab} (λ) by 6.6 $m^2\,g^{-1}$, which is the mass absorption cross section (MAC) at 637 nm (Müller et al., 2011; Petzold and Schönlinner, 2004). Absorption measurements were compared with elemental carbon (EC) determined by a SUNSET OCEC analyzer using the EUSAAR 2 protocol (Cavalli et al., 2010), in 24 h quartz filters collected with a hi-vol sampler. This comparison enabled us to determine the specific MAC for this site (9.1 $m^2\,g^{-1}$). Nevertheless, the instrument default MAC was used to calculate BC concentrations. Measurements of particle number (N) concentrations were carried out using a low-size detection (detects particles with an aerodynamic diameter (D_p) higher than 3 nm) condensation particle counter (TSI, CPC 3776) from March 2010 to August 2011, and an environmental ($D_p > 7$ nm) particle counter (TSI, EPC 3783) from December 2011 to December 2012 (Fig. S1 in the Supplement).

At MSY, concentrations of PM, BC and N were also measured from January 2010 to December 2012 (Fig. S1 in the Supplement) using a GRIMM (model 180), a MAAP (model 5012) and a CPC (model 3772, $D_p > 10$ nm), respectively. The comparison of N concentrations at both sites was limited by the different size ranges.

The mean values shown in the whole paper are arithmetical averages unless otherwise specified.

2.3 Classification of meteorological episodes

HYSPLIT (http://www.ready.noaa.gov/HYSPLIT_traj.php), BSC/DREAM8b (http://www.bsc.es/earth-sciences/mineral-dust-forecast-system/bsc-dream8b-forecast/north-africa-europe-and-middle-ea-0), SKIRON (http://forecast.uoa.gr/dustindx.php), and NAAPS (http://www.nrlmry.navy.mil/aerosol/index_shortcuts.html) models were used to determine the transport pathways and classify the atmospheric episodes affecting the MSC. 120 h backward trajectories (for 12 a.m. modeling vertical velocity and for 3 different heights, 750, 1500 and 2500 m.a.g.l) were computed on each day of measurements, and interpreted and classified visually according to their predominant transport direction in the (1) Atlantic North (AN), (2) Atlantic North West (ANW), (3) Atlantic South West (ASW), (4) North Africa (NAF), (5) Mediterranean (MED), (6) Europe (EU), (7) Winter Regional (WREG, from October to March), and (8) Summer Regional (SREG, from April to September) (Fig. S3 in the Supplement). Mineral matter (MM) determination was done for the same filters as EC determination using an inductively coupled plasma atomic emission spectroscopy (IPC-AES), in order to identify NAF

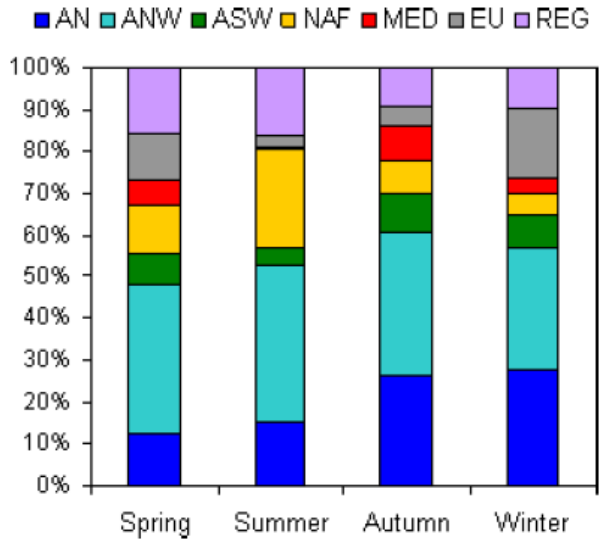

Fig. 2. Frequency of air mass origin as a function of season at Montsec.

episodes better. WREG and SREG are characterized by regional transport from the Iberian Peninsula but are divided owing to their seasonal differences. The global atmospheric circulation undergoes some seasonal oscillations, i.e., MSC is influenced by westerlies and northerlies in winter, whereas the prevailing winds come from the south in summer (Table S2 and Fig. S2 in the Supplement). As a result, clean oceanic Atlantic advections are more frequent in winter than in summer, whereas continental NAF air masses reach this region with a higher frequency in summer than in winter (Fig. 2).

Additionally, the boundary layer height was calculated using the HYSPLIT model from the NOAA Air Resources Laboratory (http://www.ready.noaa.gov/READYamet.php), using the information for stability time series. This was calculated every three hours during the whole period (Figs. S4 and S5 in the Supplement).

3 Results and discussion

3.1 PM, BC and *N* mean concentrations and comparison with high-altitude central European sites

The three-year average concentrations (5th, 50th, 95th percentiles) of PM measured at MSC reached 12 ($\mu g\,m^{-3}$) (2, 10, 27 $\mu g\,m^{-3}$), 8 $\mu g\,m^{-3}$ (2, 7, 18 $\mu g\,m^{-3}$) and 5 $\mu g\,m^{-3}$ (1, 4, 13 $\mu g\,m^{-3}$) for PM_{10}, $PM_{2.5}$ and PM_1, respectively. These concentrations were lower than the concentrations reported at nearby regional background stations, such as Els Torms and Cap de Creus, which are European Monitoring and Evaluation Programme (EMEP) sites, and Montseny

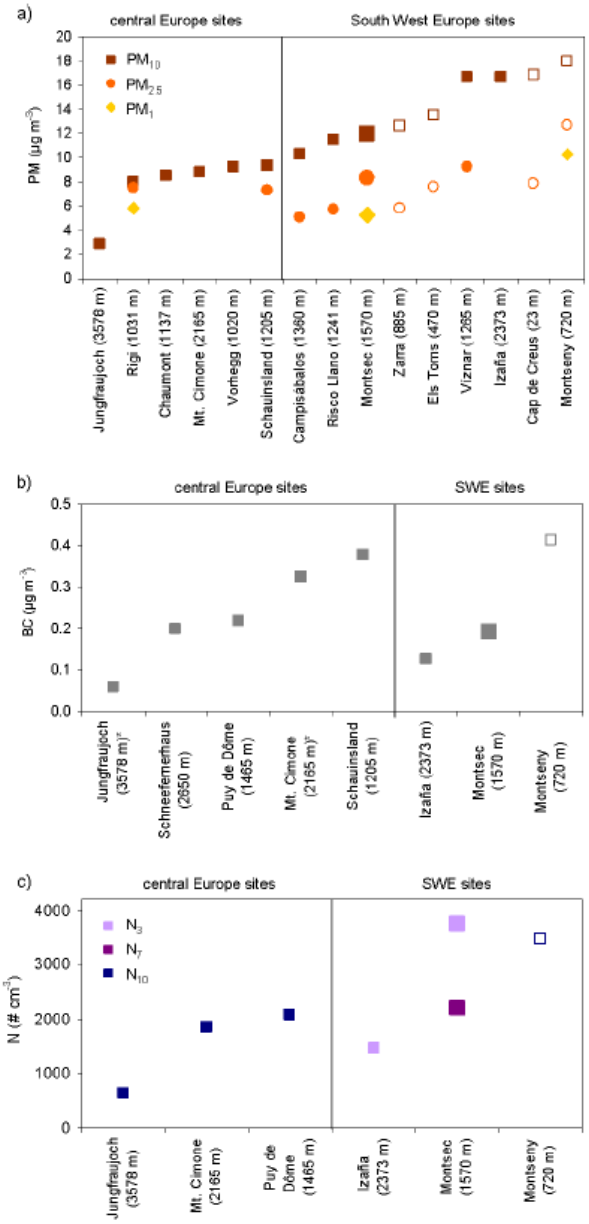

Fig. 3. Three-year (2010-2012) arithmetic average concentrations of **(a)** PM, **(b)** BC and **(c)** *N* compared with the data available in the ACTRIS Data Center web site. * Jungfraujoch and Mt. Cimone BC concentrations averaged from 2007 to 2009. Non-solid markers correspond to non-high-altitude sites.

(PM_{10}: 18 $\mu g\,m^{-3}$ (6, 17, 32 $\mu g\,m^{-3}$), $PM_{2.5}$: 13 $\mu g\,m^{-3}$ (4, 12, 24 $\mu g\,m^{-3}$), PM_1: 10 $\mu g\,m^{-3}$ (3, 9, 21 $\mu g\,m^{-3}$)) (Fig. 3a and Table S4 in the Supplement). Conversely, the mean PM at MSC were higher than those obtained at other high-altitude sites in central Europe, such as Jungfraujoch, Riji, Chaumont, Mt. Cimone, Vorhegg and Schauinsland (Fig. 3a

and Table S4 in the Supplement). The difference between the MSC and the nearby EMEP regional background sites could be due to the fact that the aforementioned sites are located at a lower altitude and are within the PBL. Higher concentrations at MSY were attributed to the fact that this regional site is closer to large urban agglomerations than MSC. Consequently, the anthropogenic influence is higher at MSY. The higher concentrations recorded at MSC with respect to those at other remote sites in central Europe may be due to the fact that these sites are located at higher altitudes (Jungfraujoch and Mt. Cimone), so that they are more affected by the FT conditions or/and are much less influenced by African dust outbreaks, which are a major natural source of PM in the Mediterranean basin (Pey et al., 2013; Querol et al., 2009).

The BC three-year average concentration at MSC was 0.2 $\mu g\,m^{-3}$ (0.02, 0.2, 0.5 $\mu g\,m^{-3}$), which was clearly lower than the concentrations found at MSY (0.4 $\mu g\,m^{-3}$ (0.1, 0.4, 0.8 $\mu g\,m^{-3}$)), and equal to or lower than the concentrations reported in central Europe at Schneefernerhaus, Puy de Dôme, Mt. Cimone and Schauinsland (Fig. 3b and Table S4 in the Supplement). These differences could be attributed to the influence of solid fuel use for power plants and domestic heating in central Europe (Gelencsér et al., 2007), and to the fact that these central Europe stations are located downwind from important BC sources such as densely populated areas. The higher PM_{10} / BC ratio found at MSC (63) with respect to that at other high-altitude European sites (25–49) corroborates the high influence of African dust in PM_{10} concentrations at MSC.

The three-year average concentration of N_7 at MSC reached 2140 $\#\,cm^{-3}$ (370, 1650, 5044 $\#\,cm^{-3}$), which was lower than the N_{10} average concentration found at MSY (3475 $\#\,cm^{-3}$ (1137, 3132, 6943 $\#\,cm^{-3}$)), probably due to the lower anthropogenic influence at MSC. On the other hand, the average N_7 concentration at MSC was slightly higher than the average N_{10} concentrations reported at Jungfraujoch, Mt. Cimone and Puy de Dôme (Fig. 3c and Table S4 in the Supplement). This difference can be partially due to the different size ranges of the instruments used and to the importance of biogenic particle precursors and NPF processes in southern Europe. This importance of biogenic compound emissions as a result of higher temperature (Seco et al., 2011), and the relevant role of the photochemical oxidation as a result of higher solar radiation in southern Europe (Cusack et al., 2013; Pey et al., 2008; Reche et al., 2011) is further confirmed by the higher N_3 concentrations (3716 $\#\,cm^{-3}$ (831, 3556, 7567 $\#\,cm^{-3}$)) with respect to the N_7 concentrations.

Thus, at MSC, concentrations of PM_{10} were higher than at high-altitude sites in central Europe because of the greater influence of the Saharan dust transport affecting the Mediterranean basin (Pey et al., 2013). The effect of these episodes on PM_{10} concentrations is discussed in the next section. Moreover, N concentrations were also higher at MSC, probably owing to greater temperature and solar radiation favoring biogenic particle precursor emissions and NPF processes. By contrast, concentrations of BC were lower because of the lower BC emissions reaching MSC.

3.2 Variation of PM, BC and N concentrations

3.2.1 Effects of meteorological episodes on aerosols

Backward trajectory calculations showed that air masses that reached MSC were mainly from the Atlantic sector (Atlantic North (AN): 20 %, Atlantic North West (ANW): 34 % and Atlantic South West (ASW): 7 %), whereas North African (NAF) episodes occurred for 13 % of the days. Air masses from Europe (EU) reached MSC for 9 % of the time; winter regional scenarios (WREG) prevailed for 5 % of the days, and summer regional (SREG) for 7 % of the time. Mediterranean (MED) air masses were detected very infrequently (< 4 %) and therefore conclusions on their characteristics will not be drawn in the present paper.

The PM_{1-10}, PM_1, BC and N median concentrations were determined for the different types of episodes at MSC and at MSY (Fig. 4). and at MSY (Fig. 4b). The meteorological episodes affected all aerosol parameters similarly at both sites. The highest coarse PM mean concentration was observed at MSC under NAF influence (13 $\mu g\,m^{-3}$), which is in agreement with what was measured at MSY (Fig. 4) (also 13 $\mu g\,m^{-3}$). Despite this similar average, calculation of the mass load from PM_{10} attributed to African dust (Pey et al., 2013) at MSC and MSY in the warmer seasons (Fig. S6 in the Supplement) showed that African dust plumes travel at various altitudes but that they present higher dust concentrations at upper layers. This is consistent with the highest concentrations of PM_{1-10} recorded during episodes of southerly winds (Fig. 5a). Furthermore, high concentrations of PM_{1-10} were also measured during SREG episodes at both sites, MSC (8 $\mu g\,m^{-3}$) and MSY (9 $\mu g\,m^{-3}$). The lowest concentrations of PM_{1-10} were associated with the Atlantic air masses (MSC: 5 $\mu g\,m^{-3}$, MSY: 6 $\mu g\,m^{-3}$), and with the WREG scenarios (MSC: 6 $\mu g\,m^{-3}$, MSY: 5 $\mu g\,m^{-3}$) (Fig. 4). Thus, the concentrations of PM_{1-10} were similar at both sites, probably as a consequence of a common origin of the coarse PM. The highest concentrations of fine PM at MSC were linked to air masses from central Europe (8 $\mu g\,m^{-3}$), North Africa (8 $\mu g\,m^{-3}$) and under SREG episodes (8 $\mu g\,m^{-3}$) (Fig. 4), which is consistent with what was found at MSY (13 $\mu g\,m^{-3}$ for EU and NAF, and 11 $\mu g\,m^{-3}$ for SREG) (Fig. 4). Low wind speeds were recorded at MSC during SREG episodes, and Fig. 5b shows how high PM_1 concentrations were associated with wind velocities lower than 10 $m\,s^{-1}$. Nevertheless, whereas the lowest PM_1 concentrations at MSC were recorded under the Atlantic advections (4 $\mu g\,m^{-3}$) and WREG scenarios (5 $\mu g\,m^{-3}$), results at MSY did not show a specific scenario with low PM_1 concentrations, owing to the

greater influence of anthropogenic emissions affecting this site.

BC concentrations at MSC varied concurrently with those of PM_1, with higher concentrations observed under NAF (0.3 $\mu g\,m^{-3}$), EU (0.3 $\mu g\,m^{-3}$) and SREG (0.3 $\mu g\,m^{-3}$) episodes, and lower concentrations under Atlantic advections (0.1 $\mu g\,m^{-3}$) and WREG scenarios (0.2 $\mu g\,m^{-3}$). BC concentrations at MSY were relatively high during EU (0.5 $\mu g\,m^{-3}$) and NAF (0.5 $\mu g\,m^{-3}$) episodes. The high BC concentrations observed during NAF episodes could be due to two reasons. The first reason is the possible occurrence of the simultaneous transport of African dust together with BC. The BC could be caused by wildfires in North Africa or in the Mediterranean basin (Cristofanelli et al., 2009) and/or by anthropogenic emissions from oil refineries in North Africa (Perrino et al., 2010; Rodríguez et al., 2011). A notable example of simultaneous transport of African dust and BC was recorded at MSC on 30 June 2012. Figure 6 shows how BC concentrations increased from late 29 to early 30 June at the same time as PM_{1-10}, and the NAAPS model reported high dust and smoke surface concentrations (Fig. S7 in the Supplement) at MSC. The second reason concerns the interference of some mineral matter constituents in the absorption measurements, which could lead to an increase in the absorption coefficient, as observed elsewhere (Vrekoussis et al., 2005). This was evident at MSC during episodes where the regional pollution was much lower compared with the African dust impact (the purest Saharan episodes). Figure 7 shows the absorption versus the elemental carbon (EC) concentrations determined by thermal–optical methods in 24 h filter samples as a function of the mineral matter concentration calculated by ICP-AES in the same filters. This shows that absorption and EC correlate strongly ($R^2 = 0.75$), except for the pure Saharan episodes highlighted in a yellow area and characterized by high concentrations of mineral matter, very low concentrations of EC, and abnormally high absorption. A good example was recorded on 28–29 June 2012 (Fig. 6), when hourly concentrations of PM_{1-10} increased up to 60 $\mu g\,m^{-3}$ or more, BC concentrations were about 0.4 $\mu g\,m^{-3}$, while the annual mean of BC at MSC was 0.2 $\mu g\,m^{-3}$, and the NAAPS model did not show any smoke surface concentrations affecting the Iberian Peninsula (Fig. S7 in the Supplement). Therefore, high concentrations of mineral dust may account for high absorption values (high BC artifact), which is more evident when EC concentration is low. This could also explain why high BC concentrations were associated with southerly winds (see Fig. 5c).

N concentrations at MSC underwent the largest variation for these different types of episodes (wide range of concentrations) (Fig. 4) compared with the other aerosol parameters. The higher mean N concentrations were reported under SREG (N_3: 4461 $\#\,cm^{-3}$ and N_7: 3021 $\#\,cm^{-3}$) and NAF (N_3: 3748 $\#\,cm^{-3}$ and N_7: 2388 $\#\,cm^{-3}$) episodes and under some Atlantic advections (ANW N_3: 4186 $\#\,cm^{-3}$ and N_7: 2440 $\#\,cm^{-3}$). By contrast, the lowest N concentrations were recorded under WREG (N_3: 2496 $\#\,cm^{-3}$ and N_7: 1073 $\#\,cm^{-3}$) scenarios. N concentrations at MSY showed a similar variation (Fig. 4), with high concentrations associated with SREG (4382 $\#\,cm^{-3}$), NAF (3712 $\#\,cm^{-3}$) and Atlantic episodes (ANW: 3568 $\#\,cm^{-3}$). However, low concentrations were not linked to a specific scenario. Thus, the highest N concentrations at both MSC and MSY were recorded in the warmer seasons (under SREG and NAF episodes) or when PM concentrations were low (Atlantic episodes). The high influence of enhanced photochemistry and biogenic compound emissions in the warmer seasons, and the higher frequency of NPF processes that occur during Atlantic advections, could account for this inter-episode variation.

Ternary plots including PM_1, PM_{1-10}, BC and N_3 concentrations at MSC and MSY (Fig. 8a, b) were elaborated to characterize the aerosol mixture during different episodes better. MSC mean was characterized by lower relative BC and PM_1, and higher relative PM_{1-10} and N, with respect to MSY mean. This reflected the lower anthropogenic influence and the higher relative mineral contribution at MSC. The low relative PM_1 and BC and the high N were more evident during Atlantic advections as a result of clean atmospheric conditions that favor NPF processes. Although PM_1, BC and N at MSC showed a similar distribution during the remaining episodes, PM_{1-10} increased from the EU episodes (with a composition similar to that of the MSY mean) to the NAF scenarios.

3.2.2 Seasonal variation of PM, BC and N

Figure 9 shows monthly averages of PM, BC and N concentrations measured at MSC for the study period (2010–2012), the monthly data availability, and the annual means. A significant seasonal variation was observed in all parameters, with maximum concentrations in summer and minimum in winter, which is typical of regional background environments in the WMB (Rodríguez et al., 2003).

The summer maximum is caused by a variety of factors: (1) the summer recirculation of air masses over the western Mediterranean (Millan et al., 1997), which hinders air mass renovation and therefore favors accumulation of pollutants; (2) the higher frequency of African dust episodes (Escudero et al., 2005) (Fig. 2) over eastern Spain; (3) the lower precipitation (Table S2 in the Supplement) that prevents atmospheric wet-scavenging processes; (4) the higher intensity of solar radiation, which increases the atmospheric photochemistry and therefore favors the formation of secondary organic and inorganic aerosols (Querol et al., 1999); (5) the higher temperature that increases biogenic compound emissions (Seco et al., 2011), which act as particles precursors; and (6) the increase in the PBL height, which favors the mixing of atmospheric pollutants at a regional scale (Figs. S4 and S5 in the Supplement).

A secondary maximum of PM and BC occurs in early spring. This secondary maximum was attributed to reasons

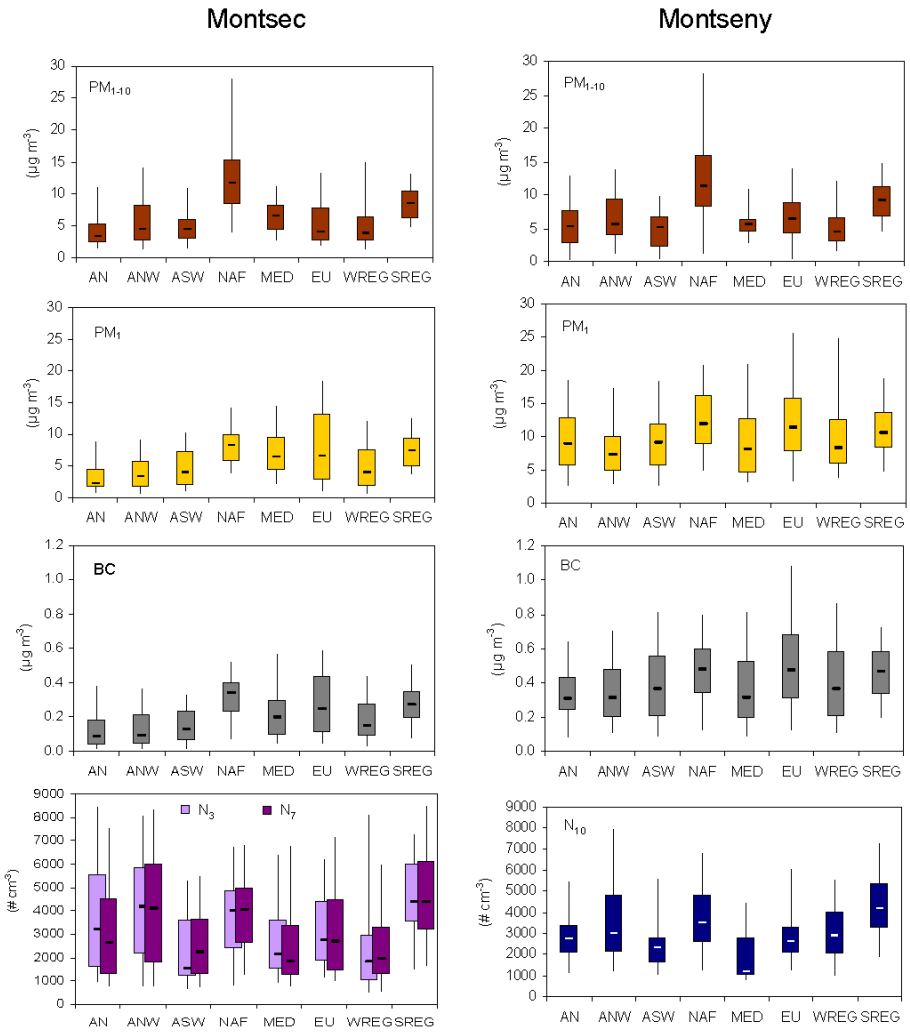

Fig. 4. Median (black line within the boxes) and percentiles (5-25-75-95, boxes and whiskers) of daily PM_{1-10}, PM_1, BC and *N* concentrations during the study period as a function of the air mass origin at Montsec and Montseny.

other than those leading to the summer maximum. In spring, MSC undergoes the lowest frequency of Atlantic advections (Fig. 2), severe anthropogenic pollution episodes affecting the whole region (Pey et al., 2010a), and a seasonal peak in African dust outbreaks (Pey et al., 2013). This secondary maximum is also shown in the ternary plots as a function of monthly means (Fig. S8 in the Supplement). A larger contribution of BC and relatively low coarse PM in February and March may be ascribed to a higher frequency of EU (Fig. 2) and regional polluting episodes. A similar behavior was observed at other mountain sites (Andrews et al., 2011).

In the colder seasons, the combination of (1) a higher frequency of occurrence and intensity of Atlantic advections (Fig. 2), (2) uncommon African dust transport (Fig. 2), and (3) a lower vertical development of the PBL, which leaves MSC in the FT on most days (Figs. S4 and S5 in the Supplement), accounts for the markedly reduced aerosol concentrations.

PM_{10} at MSC shows a more enhanced seasonal variation than PM_1 (Fig. 9a), with higher concentrations in the warmer seasons due to the lower precipitation in summer (Table S2 in the Supplement) and the higher impact of African and regional dust resuspension particles in this size fraction (Fig. 4). The seasonal behavior of BC concentrations (Fig. 9b) was very similar to that of PM, especially PM_1, which indicates that PM_1 and BC follow similar atmospheric dynamic processes at MSC. However, *N* concentrations (Fig. 9c) showed a different behavior, with a maximum in summer, probably due to the higher summer influence of regional emissions, higher photochemistry and enhanced

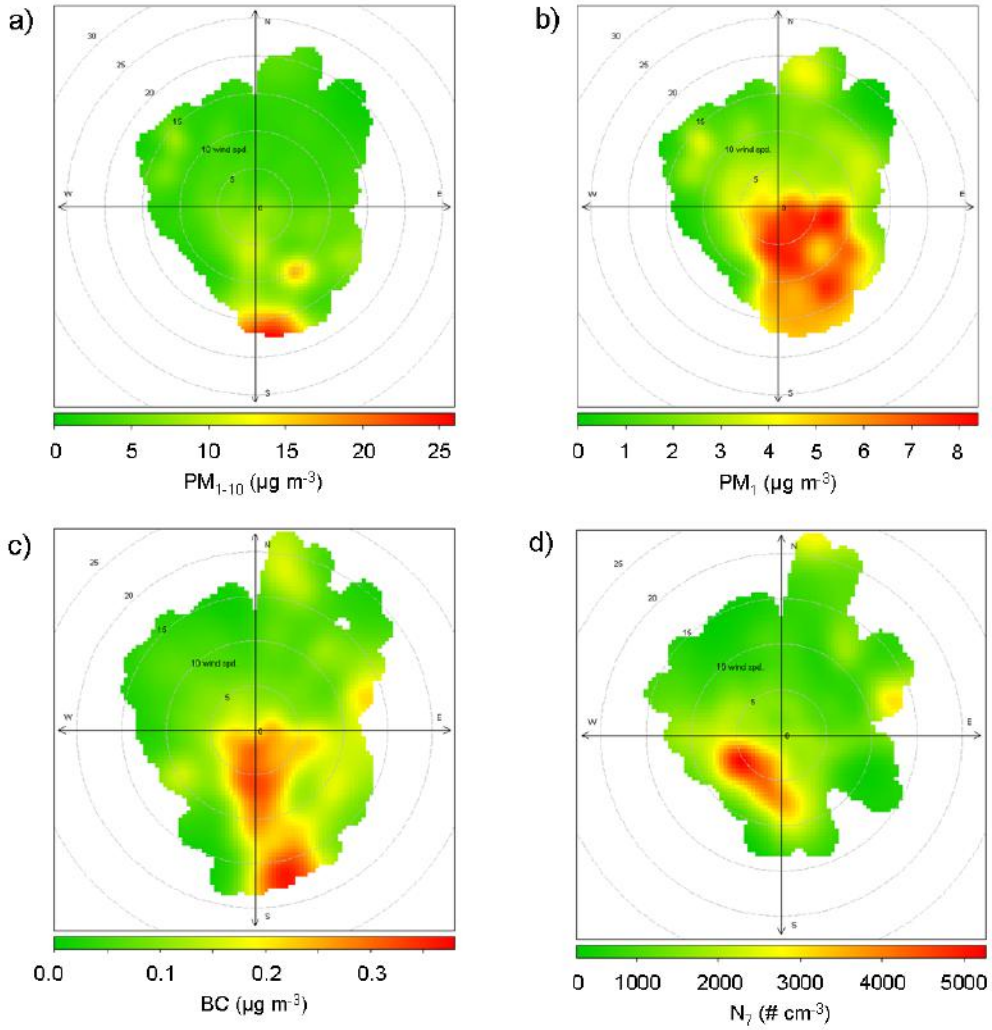

Fig. 5. Hourly concentrations of **(a)** PM_{1-10}, **(b)** PM_1, **(c)** BC, **(d)** N7 during the study period as a function of the wind speed and direction at Montsec.

biogenic emissions (Cusack et al., 2013). This behavior is also seen in Fig. S8 in the Supplement.

Figure 10 shows the monthly statistics of PM_{1-10}, PM_1, BC and N concentrations at MSC and MSY. The monthly median of PM_{1-10} and N concentrations is more similar between MSC and MSY than PM_1 and BC. Despite the differences in altitude, PM_{1-10} concentrations are similar at both sites throughout the year, probably as a consequence of a common origin of the PM_{1-10}. Earlier studies at MSY have shown that this coarse PM is mainly of natural origin (Pey et al., 2009). PM_1 and BC present a different variation for each site, with lower concentrations in winter at MSC and higher amplitude of the boxes and whiskers at MSY (Fig. 10) throughout the year. This is probably caused by the fact that MSY is considerably more influenced by winter anticyclonic pollution episodes (Pey et al., 2010a), and it is closer to the PM_1 and BC emission sources than MSC. Both stations have reported similar N concentrations despite the fact that MSC has a lower anthropogenic influence. The lack of correlation between PM_1 and N hourly concentrations observed at both sites ($R^2 = 0.0067$ ($n = 10636$) and $R^2 = 0.0615$ ($n = 11805$) at MSC and MSY, respectively) points to NPF processes occurring in situ, rather than to the transport of very fine particles together with PM_1 mass.

3.2.3 Weekly patterns of PM, BC and N

The weekly cycle of PM and BC concentrations at MSC (Figs. 11 and S9 in the Supplement) showed a minimum on Sunday and Monday, whereas N concentrations were slightly lower during Saturday and Sunday. Fine EC, crustal

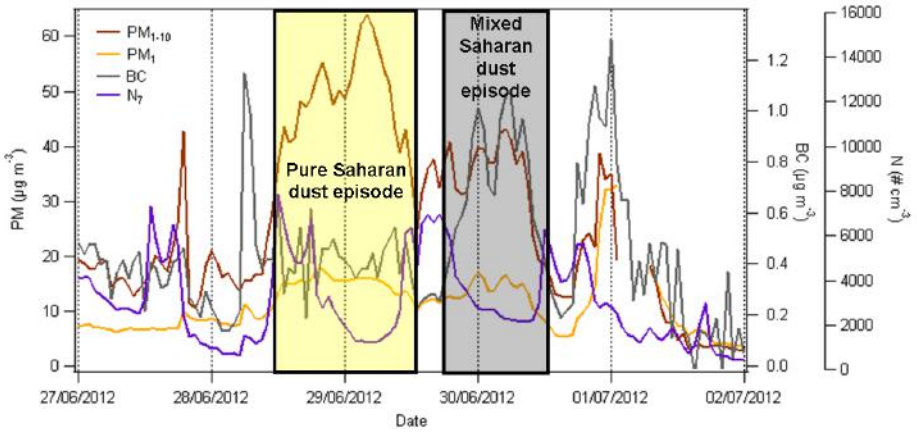

Fig. 6. Time series of PM_{1-10}, PM_1, BC and N concentrations under Saharan dust intrusion and wildfire episodes affecting the Montsec area.

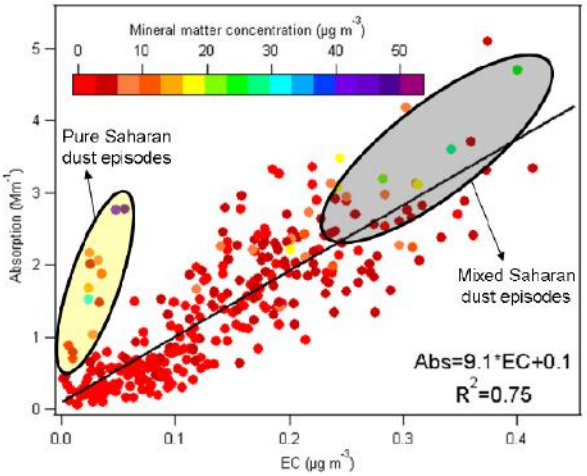

Fig. 7. Measured absorption versus PM_{10} elemental carbon (EC) concentration as a function of PM_{10} mineral matter concentration during the study period at Montsec. Data points correspond to daily values.

elements and coarse PM concentrations also showed a minimum on Sunday and Monday at remote sites in the United States (Murphy et al., 2008). However, BC and N concentrations at MSY (Fig. 11 and S9 in the Supplement) were the lowest on Saturday and Sunday, and PM concentrations did not show a clear weekly cycle. These different weekly patterns between MSC and MSY may be ascribed to the different distances from the anthropogenic emissions. This indicates that the reduced human activity at the weekend produces a delay of one day at MSC because of the distance from large industrial and urban agglomerations, whereas the delay is only of some hours at MSY (Moreno et al., 2011). Moreover, the fact that N concentrations were slightly lower at the weekend but not clearly defined as a weekly cycle corroborates the view that N concentrations at MSC are not only associated with anthropogenic emissions, but also with a local/regional non-anthropogenic origin.

Median concentrations of two groups, Tuesday–Saturday and Sunday–Monday, obtained from MSC were compared using the Kruskal–Wallis test (Barmet et al., 2009). A statistically significant difference (at a significance level of 5 %) between the two groups was observed only for BC ($p = 0.006$), with the lowest concentrations on Sunday–Monday compared with Tuesday–Saturday, whereas the difference was not statistically significant for PM_{1-10} ($p = 0.07$), PM_1 ($p = 0.16$) and N ($p = 0.5$). Comparison of Monday–Friday and Saturday–Sunday N concentrations at MSC showed no statistically significant differences ($p = 0.17$) either. Note that although the Kruskal–Wallis test may have some limitations in identifying weekly patterns (Daniel et al., 2012), in this study it is only used to assess the statistically significant differences between two groups.

3.2.4 Daily patterns of PM, BC and N

The diurnal cycle of PM (Fig. 12a) and BC (Fig. 12b) concentrations was less pronounced than that of N (Fig. 12c, d) concentrations at MSC, which demonstrates that the variation of these aerosol parameters depends on a variety of factors. The hourly variation of PM_{1-10} and PM_1 as well as that of BC was driven by mountain breezes and synoptic circulations, whereas that of N depended on the temperature and solar radiation cycle rather than on air mass origin.

In the warmer seasons PM_1, PM_{1-10} and BC (Fig. 12a, b) concentrations showed no clear diurnal patterns, which is consistent with the findings obtained for the aerosol particle composition at the Puy-de-Dôme station (Freney et al., 2011). Conversely, at MSY concentrations of PM, BC and N showed clear daily patterns throughout the year (Cusack

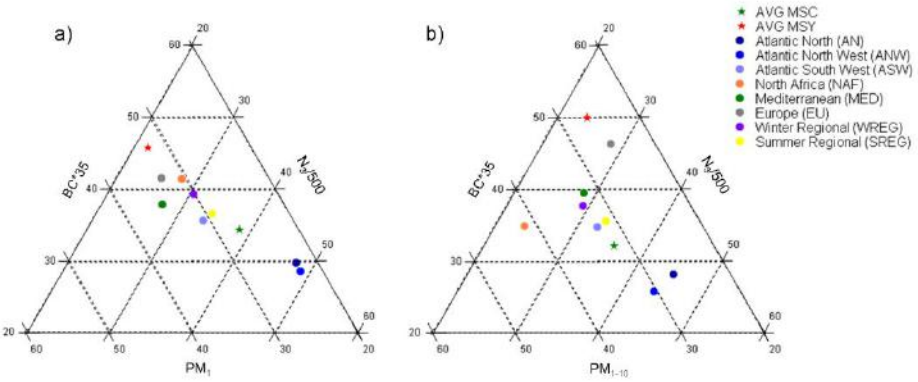

Fig. 8. Ternary plot of **(a)** PM_1, BC*35 and N3/500, and **(b)** PM_{1-10}, BC*35 and N3/500 average concentrations at Montsec and Montseny, and average concentrations as a function of air mass origin at Montsec during the study period.

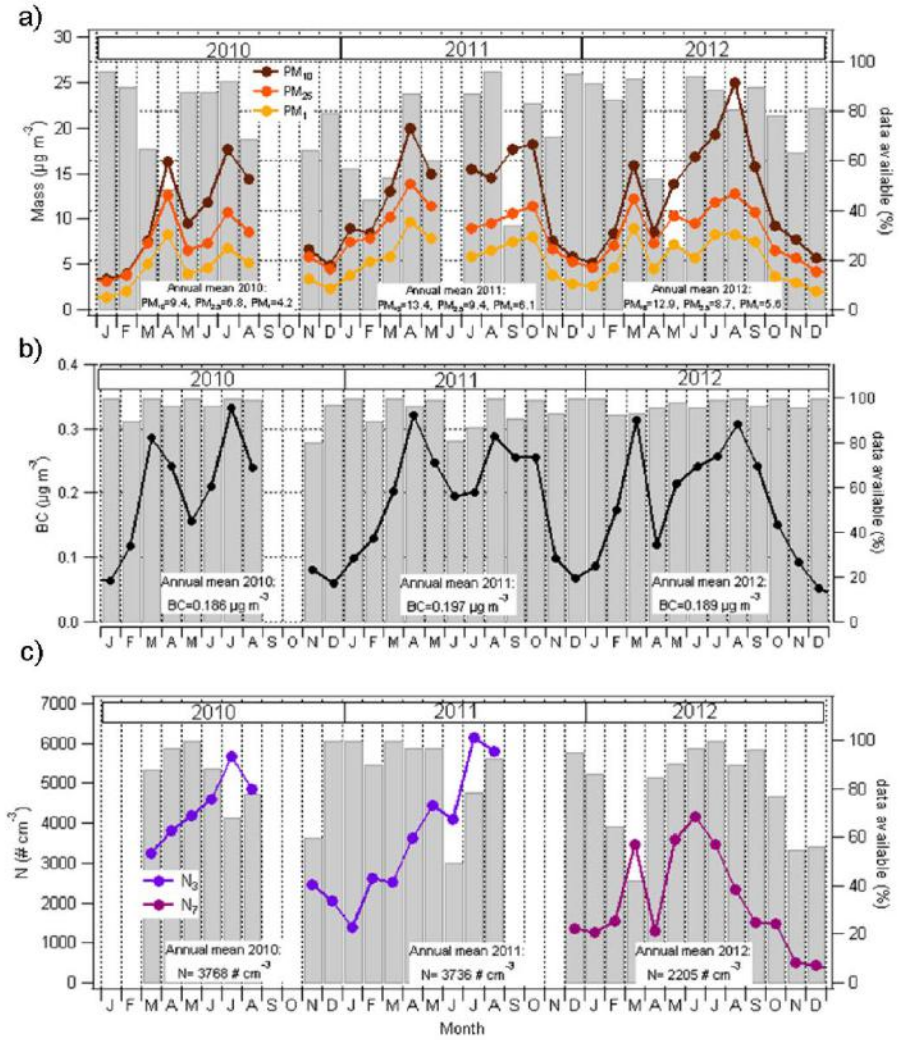

Fig. 9. Time series of monthly averaged **(a)** PM, **(b)** BC, and **(c)** *N* measured at Montsec.

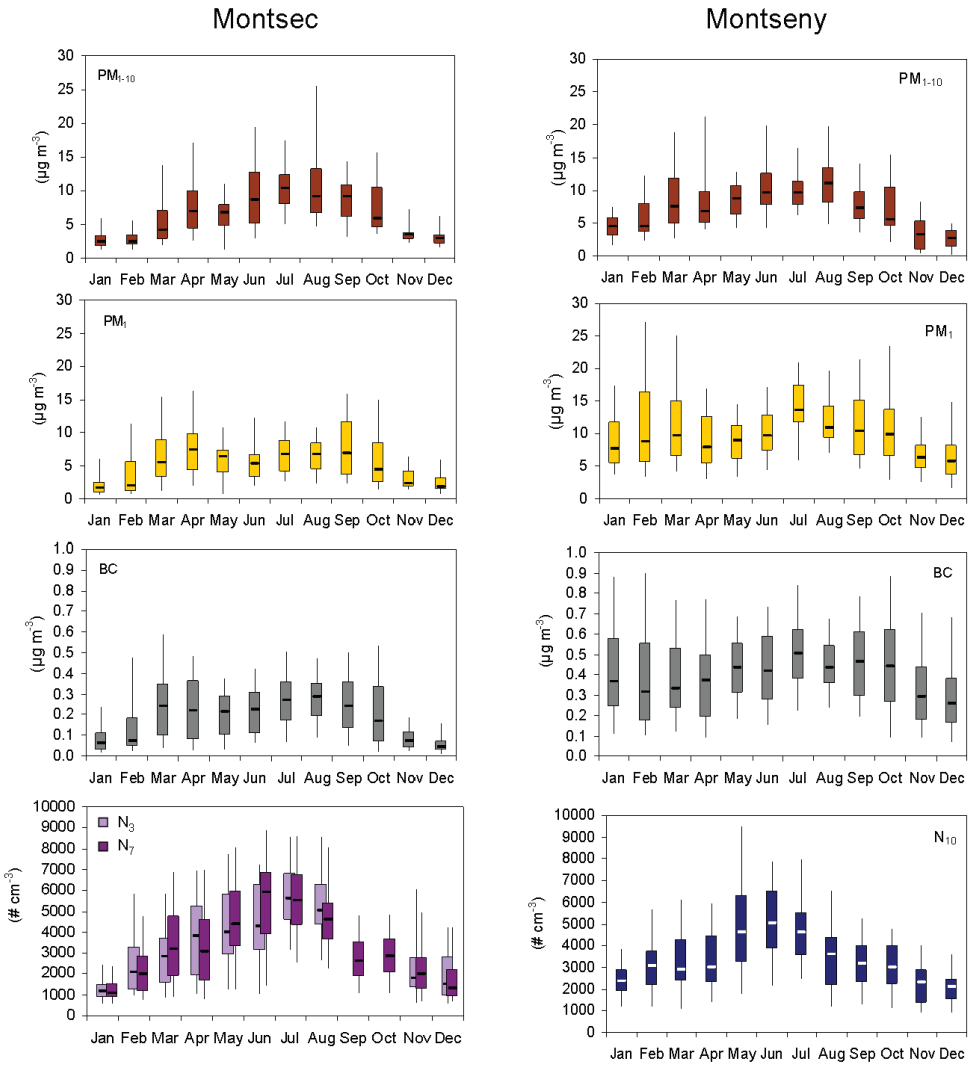

Fig. 10. Monthly median (black line within the boxes) and percentiles (5-25-75-95, boxes and whiskers) of daily PM_{1-10}, PM_1, BC and N concentrations during the study period at the Montsec and Montseny sites.

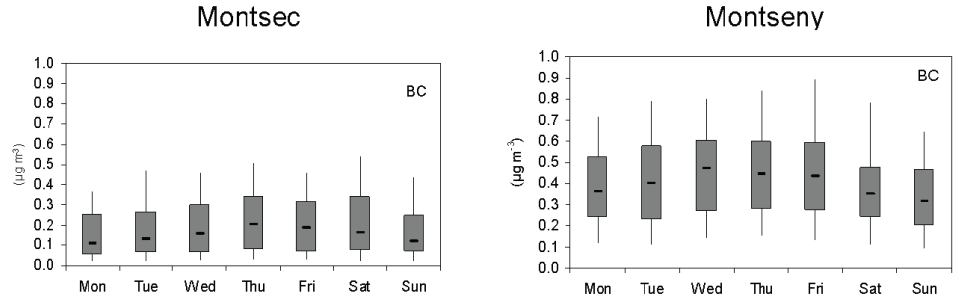

Fig. 11. Daily median (black line within the boxes) and percentiles (5-25-75-95, boxes and whiskers) of BC concentration during the study period at Montsec and Montseny.

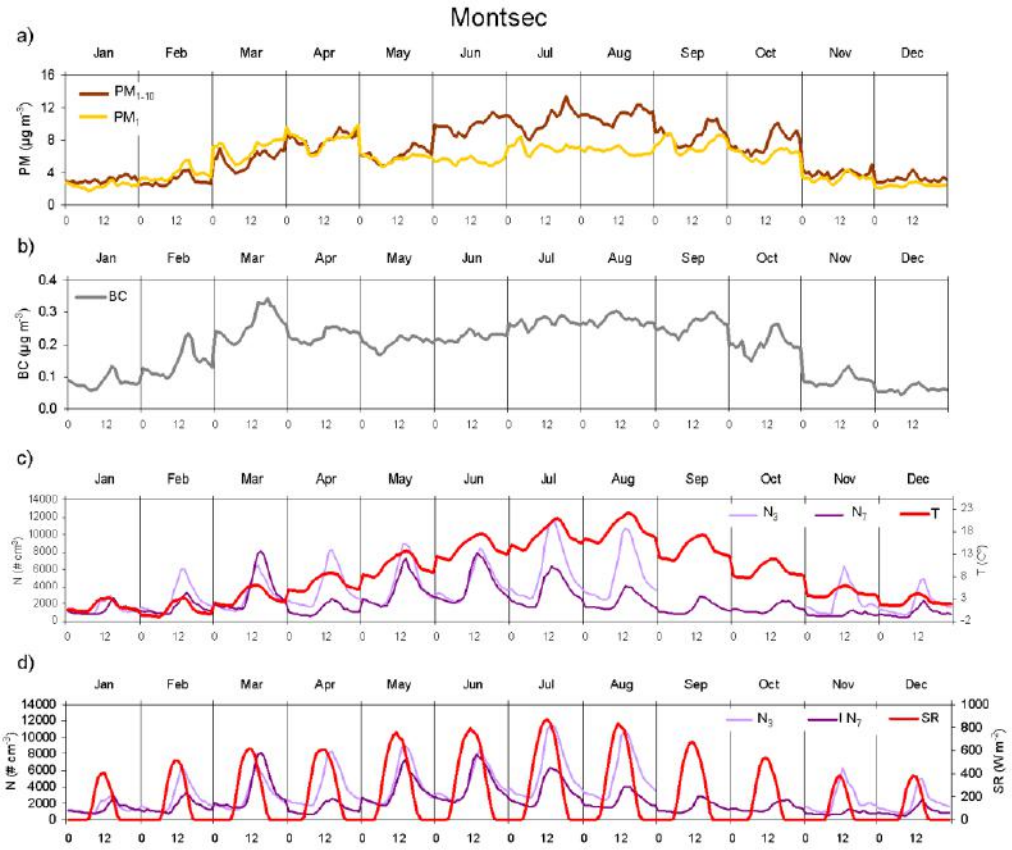

Fig. 12. Daily patterns of hourly **(a)** PM_1, PM_{1-10}, **(b)** BC, **(c)** N3, N7 and temperature, and **(d)** N3, N7 and solar radiation measurements averaged for each month during the study period at Montsec.

et al., 2013; Pérez et al., 2008) (Fig. S10 in the Supplement). The lack of a defined daily pattern in the warmer seasons at MSC could be due to the combination of different phenomena, i.e., (1) the highest frequency of Saharan dust intrusions from North Africa (Fig. 2) associated with high concentrations of PM_{1-10} and BC during the day; (2) the widespread occurrence of wildfires around the WMB; (3) the relatively high frequency of European polluted episodes in spring (Fig. 2), both scenarios being linked to high concentrations of PM_1 and BC during the day and at night; and (4) the summer recirculation over the WMB, which creates a continuous increase in the background concentrations of PM and BC. Such recirculation induced by an abrupt orography causes the formation of reserve strata at a relatively high altitude (Millan et al., 1997), which could be persistent at night, increasing nocturnal concentrations of PM and avoiding the definition of clear daily cycles. The occurrence of African dust outbreaks, which are more intense at higher altitude sites during specific episodes (Fig. S6 in the Supplement), could also interfere with the daily pattern of PM since PM concentrations could increase during these episodes regardless of the time of the day (see Fig. 6). Hence, the diurnal variation of PM and BC at MSC in the warmer seasons is dominated by the synoptic circulation, which masks the mountain breezes and the regional transport.

By contrast, in the colder seasons PM and BC concentrations showed the strongest diurnal variation, with a minimum at night and a maximum around 14:00–16:00 UTC. This behavior is probably because MSC is located most of the day within the FT in the colder seasons, whereas PBL air mass is usually only advected to the site during the central hours of the day (Figs. S4 and S5 in the Supplement). Moreover, thermal inversions are very frequent from 20:00 to 07:00 UTC. These situations prevent the transport of pollutants from the most populated areas towards high altitudes, especially at night. In the morning, mountain breezes develop, with an intensity sufficient to transport the pollutants from the adjacent valleys and plains to the top of the mountain arriving later in the afternoon. Similar phenomena have been observed at Jungfraujoch (Baltensperger et al., 1997), Mt. Cimone (Marinoni et al., 2008), Himalayas (Marinoni et al., 2010), and Puy-de-Dôme (Freney et al., 2011).

Mountain breezes therefore play an important role in determining the diurnal variation of PM and BC in the colder seasons at MSC. However, the long-range transport of atmospheric pollutants also accounts for the PM and BC in these seasons. The main difference is that the synoptic circulation in the colder seasons causes the transport of clean air masses from the Atlantic for about 70 % of the days (whereas this proportion reaches only 55 % in the warmer seasons). These air masses are associated with increased precipitation and intense winds (Table S3 and Fig. S2 in the Supplement), leading to low concentrations of PM pollutants (Fig. 4).

N concentrations had a markedly daily pattern throughout the year (Fig. 12c, d), with the highest concentrations between 12:00 and 16:00 UTC and the lowest at night and in the early morning. Although this increase in N concentrations takes place simultaneously with moderate southwesterlies (usually lower than 5 m s^{-1}) (Fig. 5d), it is not associated with transport, but with local/regional processes governing N variation (happening from 12:00 to 16:00 UTC mainly), since the daily pattern was independent of the synoptic conditions. This daily pattern is similar to that observed at other mountain sites such as Puy de Dôme (Venzac et al., 2009), where it was attributed to the height development of the PBL and to the higher frequency of new particle events at midday. In the present study, the diurnal cycle of N concentrations showed a very similar pattern to that of temperature and solar radiation intensity (Fig. 12c, d), since these parameters peak almost at the same time. Previous studies in the WMB found a dependency of monoterpenes biogenic emissions with temperature (Seco et al., 2011). Hence, the good correlation between temperature and N concentrations could be due to the condensation of the oxidation products of the biogenic volatile organic compounds (BVOCs), for example monoterpenes, onto small particles not detected by the CPC, leading to grown particles above the lower size detection of the CPC. Furthermore, the diurnal patterns of temperature, solar radiation and N concentrations seem to indicate a better correlation between temperature and N than between solar radiation and N. This could point to a higher importance of the BVOCs condensation processes than the NPF processes from photochemical oxidation (solar radiation) in N variation, which has been reported in recent studies (e.g., Paasonen et al., 2013). Despite the marked diurnal cycle throughout the year, the daily amplitude of N concentrations was lower in the colder seasons than in the warmer seasons. This difference is more evident for N_3 than for N_7 concentrations. At night (20:00–07:00 UTC), N_3 concentrations were more than 2100 # cm^{-3} in the warmer seasons, whereas they were about 1300 # cm^{-3} in the colder seasons. Moreover, during the day (08:00–19:00 UTC) the N_3 concentrations rose to 7000 # cm^{-3} in the warmer seasons, whereas they reached 2300 # cm^{-3} in the colder seasons. The daily ratios between day and night mean concentrations ranged from 2.4–2 in the colder seasons to 2.9–2.8 in the warmer seasons. This seasonal variation could be associated with the fact that MSC is frequently in the FT in the colder seasons, whereas in the warmer seasons it is more affected by the PBL air mass (Figs. S4, S5a and S5e in the Supplement), which increases N concentrations because biogenic emissions and photochemistry are enhanced by high temperature and high solar radiation intensity in the warmer seasons, favoring biogenic condensation and NPF processes, although other processes can not be discarded. The higher N_3 concentrations at midday with respect to the N_7 concentrations and the agreement of N_3 concentrations with the number size distribution data from an intensive campaign, which showed the typical banana profile (ongoing studies), further confirmed the relevant role of nucleation episodes and particles growth processes at MSC. The high background N concentrations in the warmer seasons could be ascribed to the recirculation transport that accumulates regional pollutants nearby, before transport by mountain breezes.

4 Conclusions

Aerosol parameters (PM, BC and N) and their variations were studied during 2010–2012 at a high-altitude site (Montsec) in the southern Pyrenees. Comparison of our data with those from other high-altitude sites in central Europe shows that Saharan dust transport is much more important at MSC. This is corroborated by the more elevated PM_{10} concentrations. The higher N concentrations at MSC are due to the higher importance of the biogenic precursor emissions and to the greater solar radiation that favors NPF processes. Conversely, BC concentrations are lower at MSC than at other sites in Europe, probably because of the lower BC emissions surrounding the site. The variations of PM and BC concentrations with respect to those of N demonstrated that these aerosol parameters are governed by various factors.

PM and BC show marked differences in mean concentrations for different meteorological episodes, the most polluted being the NAF air masses and the least polluted being the Atlantic advections. NAF air masses transport essentially Saharan dust, which increases PM, in addition to smoke particles from wildfires and/or anthropogenic emissions that enhance BC concentrations. In some cases it has been shown that mineral dust components interfere with absorption measurements, leading to increased BC concentrations. SREG and EU air masses were also identified as "polluted scenarios". Atlantic advections and WREG episodes lead to the lowest concentrations of PM and BC because of the cleansing effect of the Atlantic air masses and because of the longer time spent by MSC in the FT during WREG episodes.

Seasonal variation of PM and BC concentrations was also observed, with maximum concentrations in summer and minimum concentrations in winter. This was attributed to changes in the air mass origin from summer to winter, and to the different PBL height between seasons. However, PM_{10} concentrations showed more enhanced seasonal variation

than PM_1 and BC because coarse PM is more affected by NAF episodes and to a lesser degree by regional resuspension of dust. PM_1 and BC concentrations were more associated with an anthropogenic origin, which had a seasonal variation that was less marked, albeit a greater weekly influence. The reduced human activity at the weekend is reflected in the concentrations of PM_1 and BC with a delay of one day (minimum on Sunday and Monday), which confirms that MSC is located at a sufficient distance from anthropogenic emissions. Nevertheless, only BC concentrations showed a statistically significant weekly variation according to the Kruskal–Wallis test. Daily patterns of these parameters were also studied for each month. The hourly variations of PM and BC concentrations were driven by mountain breezes and synoptic circulations. However, the long-range transport masks the breezes and regional transport breaking the daily cycles in the warmer seasons, whereas the mountain breezes had a greater impact than the synoptic circulation in the colder seasons, which is reflected in clearer diurnal patterns.

N concentrations were less affected by the air mass pathway and depended more on meteorological variables such as temperature and solar radiation. Even so, under NAF and SREG episodes, *N* concentrations were also relatively high, because NAF episodes were more frequent in the warmer (18 %) than in the colder (7 %) seasons, and in these warm seasons the condensation and NPF processes could be enhanced because of the higher biogenic emissions and photochemistry. Furthermore, under the influence of the Atlantic advections, MSC yielded high concentrations of *N* because of the clean atmospheric conditions, which favor NPF processes as well. Seasonal variation of *N* concentrations showed a minimum in winter and a maximum in summer, which was attributed to the seasonal variation of the meteorological conditions and to the different PBL height between seasons. The undefined weekly pattern of *N* concentrations lent further support to the view that *N* concentrations are more associated with a local/regional non-anthropogenic origin than with an anthropogenic origin. In addition, the *N* diurnal pattern proved to be independent of the air mass origin and followed the temperature and solar radiation cycle. Despite the daily cycle throughout the year, the daily amplitude and the background *N* concentrations were higher in the warmer than in the colder seasons. This seasonal variation was related to different PBL height between seasons and to the increased emission intensity within the PBL in the warmer seasons.

The results obtained at MSC allowed us to characterize the tropospheric background aerosols in the WMB. They are representative of a wide area and could be of interest in the investigation of the radiative balance of aerosols in southwestern Europe. These results (1) confirm a lower regional anthropogenic influence at MSC than at MSY; (2) highlight the relevant role of nucleation episodes and particle growth processes in southwestern Europe as a result of higher solar radiation intensity (and thus photochemistry) and higher temperature (and thus biogenic precursor emissions); (3) reveal that MSC is much less affected by anthropogenic emissions than other high-altitude sites in central Europe; and 4) underline the contribution of long-range transport, especially African dust in elevated layers. All these processes could alter optical properties of aerosols and could therefore exert a significant influence on the radiative forcing. For this reason, aerosol chemical composition and scattering properties were also measured at this site. The results obtained will be discussed in forthcoming publications.

Supplementary material related to this article is available online at http://www.atmos-chem-phys.net/14/4279/2014/acp-14-4279-2014-supplement.pdf.

Acknowledgements. This study was supported by the Ministry of Economy and Competitiveness and FEDER funds under the PRISMA (CGL2012-39623-C02-0), and CARIATI (CGL2008-06294/CLI) projects, and by the Generalitat de Catalunya (AGAUR 2009 SGR8 and DGQA). The research received funding from European Union Seventh Framework Programme (FP7/ 2007-2013) ACTRIS under grant agreement no. 262254. The authors would like to extend their gratitude to the personnel form the OAdM. We would also like to express our gratitude to METEOCAT for the meteorological data, to ACTRIS Data Center for the data from the high-altitude central Europe sites, to the Laboratory of Atmospheric Chemistry at the Paul Scherrer Institute for providing the Jungfraujoch BC and *N* data, the International Foundation High Altitude Research Stations Jungfraujoch and Gornergrat (HFSJG), and the support by MeteoSwiss within the Swiss program of the WMO Global Atmosphere Watch (GAW), to the NABEL (FOEN/Empa) for providing the PM data from the Swiss sites, to the background monitoring network of Umweltbundesamt, Vienna, for providing the Vorhegg PM10 data, to the OPGC (Observatoire de Physique du Globe de Clermont-Ferrand) for providing the Puy de Dôme BC and *N* data, and to the NOAA Air Resources Laboratory (ARL) for the provision of the HYSPLIT transport and dispersion model, and the boundary layer height calculation used in this publication. M. C. Minguillón and M. Pandolfi were funded by the JAE-Doc CSIC program, co-funded by the European Social Fund (ESF).

Edited by: V.-M. Kerminen

References

Andrews, E., Ogren, J. A., Bonasoni, P., Marinoni, A., Cuevas, E., Rodríguez, S., Sun, J. Y., Jaffe, D. A., Fischer, E. V., Baltensperger, U., Weingartner, E., Collaud Coen, M., Sharma, S., Macdonald, A. M., Leaitch, W. R., Lin, N.-H., Laj, P., Arsov, T., Kalapov, I., Jefferson, A., and Sheridan, P.: Climatology of aerosol radiative properties in the free troposphere, Atmos. Res., 102, 365–393, doi:10.1016/j.atmosres.2011.08.017, 2011.

Asmi, A., Wiedensohler, A., Laj, P., Fjaeraa, A.-M., Sellegri, K., Birmili, W., Weingartner, E., Baltensperger, U., Zdimal, V.,

Zikova, N., Putaud, J.-P., Marinoni, A., Tunved, P., Hansson, H.-C., Fiebig, M., Kivekäs, N., Lihavainen, H., Asmi, E., Ulevicius, V., Aalto, P. P., Swietlicki, E., Kristensson, A., Mihalopoulos, N., Kalivitis, N., Kalapov, I., Kiss, G., De Leeuw, G., Henzing, B., Harrison, R. M., Beddows, D., O'Dowd, C., Jennings, S. G., Flentje, H., Weinhold, K., Meinhardt, F., Ries, L., and Kulmala, M.: Number size distributions and seasonality of submicron particles in Europe 2008–2009, Atmos. Chem. Phys., 11, 5505–5538, doi:10.5194/acp-11-5505-2011, 2011.

Asmi, A., Collaud Coen, M., Ogren, J. A., Andrews, E., Sheridan, P., Jefferson, A., Weingartner, E., Baltensperger, U., Bukowiecki, N., Lihavainen, H., Kivekäs, N., Asmi, E., Aalto, P. P., Kulmala, M., Wiedensohler, A., Birmili, W., Hamed, A., O'Dowd, C., G Jennings, S., Weller, R., Flentje, H., Fjaeraa, A. M., Fiebig, M., Myhre, C. L., Hallar, A. G., Swietlicki, E., Kristensson, A., and Laj, P.: Aerosol decadal trends – Part 2: In-situ aerosol particle number concentrations at GAW and ACTRIS stations, Atmos. Chem. Phys., 13, 895–916, doi:10.5194/acp-13-895-2013, 2013.

Baltensperger, U., Gfiggeler, H. W., Jost, D. T., Lugauer, M., Schwikowski, M. and Weingartner, E.: Aerosol climatology at the high-alpine site Jungfraujoch, Switzerland, J. Geophys. Res., 102, 19707–19715, 1997.

Barmet, P., Kuster, T., Muhlbauer, A., and Lohmann, U.: Weekly cycle in particulate matter versus weekly cycle in precipitation over Switzerland, J. Geophys. Res., 114, D05206, doi:10.1029/2008JD011192, 2009.

Cavalli, F., Viana, M., Yttri, K. E., Genberg, J., and Putaud, J. P.: Toward a standardised thermal-optical protocol for measuring atmospheric organic and elemental carbon: the EUSAAR protocol, Atmos. Meas. Tech., 3, 79–89, doi:10.5194/amt-3-79-2010, 2010.

Collaud Coen, M., Weingartner, E., Furger, M., Nyeki, S., Prévôt, A. S. H., Steinbacher, M. and Baltensperger, U.: Aerosol climatology and planetary boundary influence at the Jungfraujoch analyzed by synoptic weather types, Atmos. Chem. Phys., 11, 5931–5944, doi:10.5194/acp-11-5931-2011, 2011.

Collaud Coen, M., Andrews, E., Asmi, A., Baltensperger, U., Bukowiecki, N., Day, D., Fiebig, M., Fjaeraa, A. M., Flentje, H., Hyvärinen, A., Jefferson, A., Jennings, S. G., Kouvarakis, G., Lihavainen, H., Lund Myhre, C., Malm, W. C., Mihapopoulos, N., Molenar, J. V., O'Dowd, C., Ogren, J. A., Schichtel, B. A., Sheridan, P., Virkkula, A., Weingartner, E., Weller, R. and Laj, P.: Aerosol decadal trends – Part 1: In-situ optical measurements at GAW and IMPROVE stations, Atmos. Chem. Phys., 13, 869–894, doi:10.5194/acp-13-869-2013, 2013.

Colomé, J., Ribas, I., Francisco, X., Casteels, K., Fernández, D., Isern, J., Palau, X., and Torra, J.: The OAdM Robotic Observatory, Advances in Astronomy, 2010, 1–8, doi:10.1155/2010/183016, 2010.

Cristofanelli, P., Marinoni, A., Arduini, J., Bonaf, U., Calzolari, F., Colombo, T., Decesari, S., Duchi, R., Facchini, M. C., Fierli, F., Finessi, E., Maione, M., Chiari, M., Calzolai, G., Messina, P., Orlandi, E., Roccato, F., and Bonasoni, P.: Significant variations of trace gas composition and aerosol properties at Mt. Cimone during air mass transport from North Africa – contributions from wildfire emissions and mineral dust, Atmos. Chem. Phys., 9, 4603–4619, doi:10.5194/acp-9-4603-2009, 2009.

Cusack, M., Pérez, N., Pey, J., Wiedensohler, A., Alastuey, A., and Querol, X.: Variability of sub-micrometer particle number size distributions and concentrations in the Western Mediterranean regional background, Tellus B, 65, 1–19, 2013.

Daniel, J. S., Portmann, R. W., Solomon, S., and Murphy, D. M.: Identifying weekly cycles in meteorological variables: The importance of an appropriate statistical analysis, J. Geophys. Res., 117, D13203, doi:10.1029/2012JD017574, 2012.

Directive 2008/50/EC of the European Parliament and of the Council of 21 May 2008 on ambient air quality and cleaner air for Europe (OJ L 152, 11 June 2008, 1–44, http://eur-lx.europa.eu/LexUriServ/LexUriServ.do?uri$=$OJ:L:2008:152:0001:0044:EN:PDF

Eeftens, M., Tsai, M.-Y., Ampe, C., Anwander, B., Beelen, R., Bellander, T., Cesaroni, G., Cirach, M., Cyrys, J., De Hoogh, K., De Nazelle, A., De Vocht, F., Declercq, C., Dėdelė, A., Eriksen, K., Galassi, C., Gražulevičienė, R., Grivas, G., Heinrich, J., Hoffmann, B., Iakovides, M., Ineichen, A., Katsouyanni, K., Korek, M., Krämer, U., Kuhlbusch, T., Lanki, T., Madsen, C., Meliefste, K., Mölter, A., Mosler, G., Nieuwenhuijsen, M., Oldenwening, M., Pennanen, A., Probst-Hensch, N., Quass, U., Raaschou-Nielsen, O., Ranzi, A., Stephanou, E., Sugiri, D., Udvardy, O., Vaskövi, É., Weinmayr, G., Brunekreef, B., and Hoek, G.: Spatial variation of $PM_{2.5}$, PM_{10}, $PM_{2.5}$ absorbance and PM coarse concentrations between and within 20 European study areas and the relationship with NO2 – Results of the ESCAPE project, Atmos. Environ., 62, 303–317, doi:10.1016/j.atmosenv.2012.08.038, 2012.

Escudero, M., Castillo, S., Querol, X., Avila, A., Alarco, M., Alastuey, A., Cuevas, E., and Rodríguez, S.: Wet and dry African dust episodes over eastern Spain, J. Geophys. Res., 110, D18S08, doi:10.1029/2004JD004731, 2005.

Freney, E. J., Sellegri, K., Canonaco, F., Boulon, J., Hervo, M., Weigel, R., Pichon, J. M., Colomb, A., Prévôt, A. S. H., and Laj, P.: Seasonal variations in aerosol particle composition at the puy-de-Dôme research station in France, Atmos. Chem. Phys., 11, 13047–13059, doi:10.5194/acp-11-13047-2011, 2011.

Gelencsér, A., May, B., Simpson, D., Sánchez-Ochoa, A., Kasper-Giebl, A., Puxbaum, H., Caseiro, A., Pio, C. and Legrand, M.: Source apportionment of $PM_{2.5}$ organic aerosol over Europe: Primary/secondary, natural/anthropogenic, and fossil/biogenic origin, J. Geophys. Res., 112, D23S04, doi:10.1029/2006JD008094, 2007.

IPCC 2007 in: Climate Change 2007: The Physical Science Basis (Contribution of Working Group I to the Fourth Assessment Report of the Intergovernmental Panel on Climate Change) edited by: Solomon, S., Qin, D. Manning, M., Chen, Z., Marquis, M., Averyt, K. B., Tignor, M., and Miller, H. L., Cambridge Univ. Press, New York, USA, 131–217, 2007.

Kent, G. S., Trepte, C. R., and Lucker, P. L.: Long-term stratospheric aerosol and gas experiment I and II measurements of upper tropospheric aerosol extinction, J. Geophys. Res., 103, 28863, doi:10.1029/98JD02583, 1998.

Laj, P., Klausen, J., Bilde, M., Plaß-Duelmer, C., Pappalardo, G., Clerbaux, C., Baltensperger, U., Hjorth, J., Simpson, D., Reimann, S., Coheur, P.-F., Richter, A., De Mazière, M., Rudich, Y., McFiggans, G., Torseth, K., Wiedensohler, A., Morin, S., Schulz, M., Allan, J. D., Attié, J.-L., Barnes, I., Birmili, W., Cammas, J. P., Dommen, J., Dorn, H.-P., Fowler, D., Fuzzi, S., Glasius, M., Granier, C., Hermann, M., Isaksen, I. S. A., Kinne, S., Koren, I., Madonna, F., Maione, M., Massling, A., Moehler, O.,

Mona, L., Monks, P. S., Müller, D., Müller, T., Orphal, J., Peuch, V.-H., Stratmann, F., Tanré, D., Tyndall, G., Abo Riziq, A., Van Roozendael, M., Villani, P., Wehner, B., Wex, H., and Zardini, A. A.: Measuring atmospheric composition change, Atmos. Environ., 43, 5351–5414, doi:10.1016/j.atmosenv.2009.08.020, 2009.

Marinoni, A., Cristofanelli, P., Calzolari, F., Roccato, F., Bonafè, U., and Bonasoni, P.: Continuous measurements of aerosol physical parameters at the Mt. Cimone GAW Station (2165 m asl, Italy), Sci. Total Environ., 391, 241–51, doi:10.1016/j.scitotenv.2007.10.004, 2008.

Marinoni, A., Cristofanelli, P., Laj, P., Duchi, R., Calzolari, F., Decesari, S., Sellegri, K., Vuillermoz, E., Verza, G. P., Villani, P., and Bonasoni, P.: Aerosol mass and black carbon concentrations, a two year record at NCO-P (5079 m, Southern Himalayas), Atmos. Chem. Phys., 10, 8551–8562, doi:10.5194/acp-10-8551-2010, 2010.

Millan, M. M., Salvador, R., Mantilla, E., and Kallos, G.: Photooxidant dynamics in the Mediterranean basin in summer: Results from European research projects, J. Geophys. Res., 102, 8811–8823, 1997.

Monks, P. S., Granier, C., Fuzzi, S., Stohl, A., Williams, M. L., Akimoto, H., Amann, M., Baklanov, A., Baltensperger, U., Bey, I., Blake, N., Blake, R. S., Carslaw, K., Cooper, O. R., Dentener, F., Fowler, D., Fragkou, E., Frost, G. J., Generoso, S., Ginoux, P., Grewe, V., Guenther, A., Hansson, H. C., Henne, S., Hjorth, J., Hofzumahaus, A., Huntrieser, H., Isaksen, I. S. A., Jenkin, M. E., Kaiser, J., Kanakidou, M., Klimont, Z., Kulmala, M., Laj, P., Lawrence, M. G., Lee, J. D., Liousse, C., Maione, M., McFiggans, G., Metzger, A., Mieville, A., Moussiopoulos, N., Orlando, J. J., O'Dowd, C. D., Palmer, P. I., Parrish, D. D., Petzold, A., Platt, U., Pöschl, U., Prévôt, A. S. H., Reeves, C. E., Reimann, S., Rudich, Y., Sellegri, K., Steinbrecher, R., Simpson, D., Ten Brink, H., Theloke, J., Van der Werf, G. R., Vautard, R., Vestreng, V., Vlachokostas, C. and Von Glasow, R.: Atmospheric composition change – global and regional air quality, Atmos. Environ., 43, 5268–5350, doi:10.1016/j.atmosenv.2009.08.021, 2009.

Moreno, T., Querol, X., Alastuey, A., Reche, C., Cusack, M., Amato, F., Pandolfi, M., Pey, J., Richard, A., Prévôt, A. S. H., Furger, M., and Gibbons, W.: Variations in time and space of trace metal aerosol concentrations in urban areas and their surroundings, Atmos. Chem. Phys., 11, 9415–9430, doi:10.5194/acp-11-9415-2011, 2011.

Müller, T., Henzing, J. S., De Leeuw, G., Wiedensohler, A., Alastuey, A., Angelov, H., Bizjak, M., Collaud Coen, M., Engström, J. E., Gruening, C., Hillamo, R., Hoffer, A., Imre, K., Ivanow, P., Jennings, G., Sun, J. Y., Kalivitis, N., Karlsson, H., Komppula, M., Laj, P., Li, S.-M., Lunder, C., Marinoni, A., Martins dos Santos, S., Moerman, M., Nowak, A., Ogren, J. A., Petzold, A., Pichon, J. M., Rodriquez, S., Sharma, S., Sheridan, P. J., Teinilä, K., Tuch, T., Viana, M., Virkkula, A., Weingartner, E., Wilhelm, R., and Wang, Y. Q.: Characterization and intercomparison of aerosol absorption photometers: result of two intercomparison workshops, Atmos. Meas. Tech., 4, 245–268, doi:10.5194/amt-4-245-2011, 2011.

Murphy, D. M., Capps, S. L., Daniel, J. S., Frost, G. J., and White, W. H.: Weekly patterns of aerosol in the United States, Atmos. Chem. Phys., 8, 2729–2739, doi:10.5194/acp-8-2729-2008, 2008.

Paasonen, P., Asmi, A., Petäjä, T., Kajos, M. K., Äijälä, M., Junninen, H., Holst, T., Abbatt, J. P. D., Arneth, A., Birmili, W., Denier van der Gon, H., Hamed, A., Hoffer, A., Laakso, L., Laaksonen, A., Leaitch, W. R., Plass-Dülmer, C., Pryor, S. C., Räisänen, P., Swietlicki, E., Wiedensohler, A., Worsnop D.R., Kerminen, V.-M., and Kulmala, M.: Warming-induced increase in aerosol number concentration likely to moderate climate change. Nat. Geosci., 6, 438–442. doi:10.1038/ngeo1800, 2013.

Pérez, N., Pey, J., Castillo, S., Viana, M., Alastuey, A and Querol, X.: Interpretation of the variability of levels of regional background aerosols in the Western Mediterranean., Sci. total environ., 407, 527–540, doi:10.1016/j.scitotenv.2008.09.006, 2008.

Perrino, C., Canepari, S., Pappalardo, S. and Marconi, E.: Time-resolved measurements of water-soluble ions and elements in atmospheric particulate matter for the characterization of local and long-range transport events, Chemosphere, 80, 1291–300, doi:10.1016/j.chemosphere.2010.06.050, 2010.

Petzold, A. and Schönlinner, M.: Multi-angle absorption photometry – a new method for the measurement of aerosol light absorption and atmospheric black carbon, J. Aerosol Sci., 35, 421–441, doi:10.1016/j.jaerosci.2003.09.005, 2004.

Pey, J., Rodríguez, S., Querol, X., Alastuey, A., Moreno, T., Putaud, J. P., and Van Dingenen, R.: Variations of urban aerosols in the western Mediterranean, Atmos. Environ., 42, 9052–9062, doi:10.1016/j.atmosenv.2008.09.049, 2008.

Pey, J., Pérez, N., Castillo, S., Viana, M., Moreno, T., Pandolfi, M., López-Sebastián, J. M., Alastuey, A., and Querol, X.: Geochemistry of regional background aerosols in the Western Mediterranean, Atmos. Res., 94, 422–435, doi:10.1016/j.atmosres.2009.07.001, 2009.

Pey, J., Pérez, N., Querol, X., Alastuey, A., Cusack, M., and Reche, C.: Intense winter atmospheric pollution episodes affecting the Western Mediterranean., Sci. total environ., 408, 1951–1959, doi:10.1016/j.scitotenv.2010.01.052, 2010a.

Pey, J., Querol, X., and Alastuey, A.: Discriminating the regional and urban contributions in the North-Western Mediterranean: PM levels and composition, Atmos. Environ., 44, 1587–1596, doi:10.1016/j.atmosenv.2010.02.005, 2010b.

Pey, J., Querol, X., Alastuey, A., Forastiere, F., and Stafoggia, M.: African dust outbreaks over the Mediterranean Basin during 2001–2011: PM_{10} concentrations, phenomenology and trends, and its relation with synoptic and mesoscale meteorology, Atmos. Chem. Phys., 13, 1395–1410, doi:10.5194/acp-13-1395-2013, 2013.

Pope III, C. A. and Dockery, D. W.: Health effects of fine particulate air pollution: Lines that connect, J. Air Waste Manage., 56, 709–742, 2006.

Putaud, J. P., Van Dingenen, R., Alastuey, A., Bauer, H., Birmili, W., Cyrys, J., Flentje, H., Fuzzi, S., Gehrig, R., Hansson, H. C., Harrison, R. M., Herrmann, H., Hitzenberger, R., Hüglin, C., Jones, A. M., Kasper-Giebl, A., Kiss, G., Kousa, A., Kuhlbusch, T. A. J., Löschau, G., Maenhaut, W., Molnar, A., Moreno, T., Pekkanen, J., Perrino, C., Pitz, M., Puxbaum, H., Querol, X., Rodriguez, S., Salma, I., Schwarz, J., Smolik, J., Schneider, J., Spindler, G., Ten Brink, H., Tursic, J., Viana, M., Wiedensohler, A. and Raes, F.: A European aerosol phenomenology - 3: Physical and chemical characteristics of particulate matter from 60 rural, urban, and kerbside sites across Europe, Atmos. Environ., 44, 1308–1320, 2010.

Querol, X., Alastuey, A., Lopez-soler, A., Plana, F., and Puicercus, J. A.: Daily evolution of sulphate aerosols in a rural area, northeastern Spain – elucidation of an atmospheric reservoir effect, Environ. Pollut., 105, 1999.

Querol, X., Alastuey, A., Pey, J., Cusack, M., Pérez, N., Mihalopoulos, N., Theodosi, C., Gerasopoulos, E., Kubilay, N., and Koçak, M.: Variability in regional background aerosols within the Mediterranean, Atmos. Chem. Phys., 9, 4575–4591, doi:10.5194/acp-9-4575-2009, 2009.

Reche, C., Viana, M., Moreno, T., Querol, X., Alastuey, A., Pey, J., Pandolfi, M., Prévôt, A., Mohr, C., Richard, A., Artiñano, B., Gomez-Moreno, F. J., and Cots, N.: Peculiarities in atmospheric particle number and size-resolved speciation in an urban area in the western Mediterranean: Results from the DAURE campaign, Atmos. Environ., 45, 5282–5293, doi:10.1016/j.atmosenv.2011.06.059, 2011.

Rodríguez, S., Querol, X., Alastuey, A., Viana, M.-M., and Mantilla, E.: Events affecting levels and seasonal evolution of airborne particulate matter concentrations in the Western Mediterranean., Environ. Sci. Technol., 37, 216–222, 2003.

Rodríguez, S., Alastuey, A., Alonso-Pérez, S., Querol, X., Cuevas, E., Abreu-Afonso, J., Viana, M., Pérez, N., Pandolfi, M., and De la Rosa, J.: Transport of desert dust mixed with North African industrial pollutants in the subtropical Saharan Air Layer, Atmos. Chem. Phys., 11, 6663–6685, doi:10.5194/acp-11-6663-2011, 2011.

Seco, R., Peñuelas, J., Filella, I., Llusià, J., Molowny-Horas, R., Schallhart, S., Metzger, A., Müller, M., and Hansel, A.: Contrasting winter and summer VOC mixing ratios at a forest site in the Western Mediterranean Basin: the effect of local biogenic emissions, Atmos. Chem. Phys., 11, 13161–13179, doi:10.5194/acp-11-13161-2011, 2011.

Tositti, L., Riccio, A., Sandrini, S., Brattich, E., Baldacci, D., Parmeggiani, S., Cristofanelli, P. and Bonasoni, P.: Short-term climatology of PM_{10} at a high altitude background station in southern Europe, Atmos. Environ., 65, 142–152, doi:10.1016/j.atmosenv.2012.10.051, 2013.

Venzac, H., Sellegri, K., Villani, P., Picard, D. and Laj, P.: Seasonal variation of aerosol size distributions in the free troposphere and residual layer at the puy de Dôme station, France, Atmos. Chem. Phys., 9, 1465–1478, doi:10.5194/acp-9-1465-2009, 2009.

Vrekoussis, M., Liakakou, E., Koçak, M., Kubilay, N., Oikonomou, K., Sciare, J., and Mihalopoulos, N.: Seasonal variability of optical properties of aerosols in the Eastern Mediterranean, Atmos. Environ., 39, 7083–7094, doi:10.1016/j.atmosenv.2005.08.011, 2005.

WHO 2013: Review of evidence on health aspects of air pollution – REVIHAAP. First Results. WHO's Regional Office for Europe, Copenhaguen, 28 pp., http://www.euro.who.int/__data/assets/pdf_file/0020/182432/e96762-final.pdf, 2013.

Zieger, P., Kienast-Sjögren, E., Starace, M., von Bismarck, J., Bukowiecki, N., Baltensperger, U., Wienhold, F. G., Peter, T., Ruhtz, T., Collaud Coen, M., Vuilleumier, L., Maier, O., Emili, E., Popp, C., and Weingartner, E.: Spatial variation of aerosol optical properties around the high-alpine site Jungfraujoch (3580 m a.s.l.), Atmos. Chem. Phys., 12, 7231–7249, doi:10.5194/acp-12-7231-2012, 2012.

Supplementary material related to "Three years of aerosol mass, black carbon and particle number concentrations at Montsec (southern Pyrenees, 1570 m a.s.l.)"

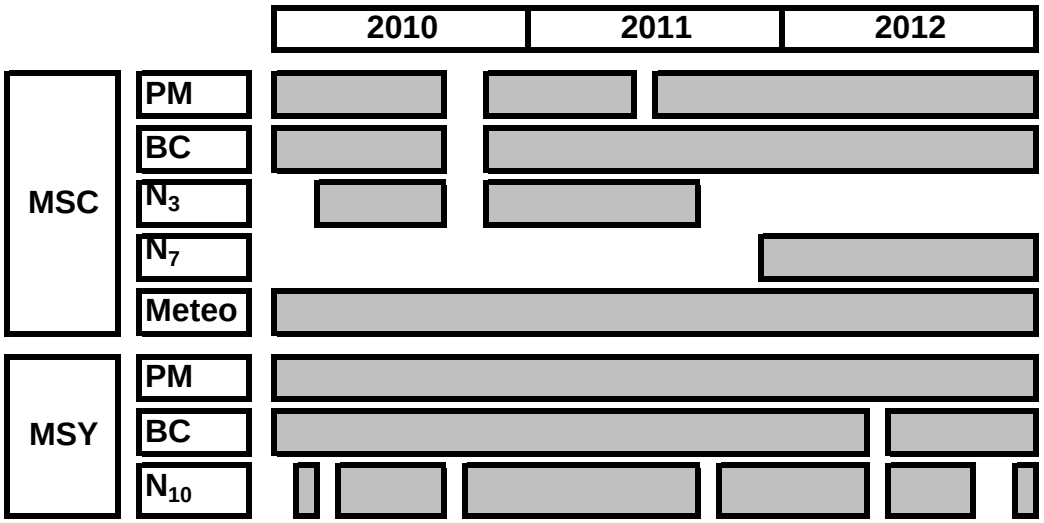

Fig. S1. Data schedule at Montsec (MSC) and Montseny (MSY).

Table S1. Arithmetic annual average of meteorological parameters at Montsec

Montsec d'Ares	T (ºC)	Tmax (ºC)	Tmin (ºC)	RH (%)	TotalPP* (mm)	WS** (m s^{-1})	WD** (degrees)	P (hPa)	SR (W m^{-2})
2007	8.6	28.3	-8.9	62	506	4.7	-	-	-
2008	7.9	27.2	-10.1	70	1186	4.3	-	-	-
2009	9	27.6	-9.8	66	639	5.8	297	843	-
2010	7.4	28.5	-12.4	69	755	4.4	293	846	189
2011	9.4	29.7	-9.9	65	597	4.3	247	852	198
2012	8.9	30.4	-13.5	59	640	4.9	312	851	203

*Annual accumulated precipitation

**Vector annual average

Table S2. Arithmetic seasonal average of meteorological parameters at Montsec during the study

Montsec d'Ares	T (ºC)	Tmax (ºC)	Tmin (ºC)	RH (%)	TotalPP* (mm)	WS** (m s^{-1})	WD** (degrees)	P (hPa)	SR (W m^{-2})
Spring	9.0	24.2	-3.7	69	215	4.4	218	850	242
Summer	17.2	30.4	3.5	57	57	3.8	203	854	288
Autumn	6.1	22.9	-8.6	72	119	4.9	319	848	121
Winter	1.7	15.4	-13.5	61	108	5.3	359	848	129

*Seasonal accumulated precipitation

**Vector seasonal average

Table S3. Arithmetic average of meteorological parameters at Montsec as a function of air mass origin.

Montsec d'Ares	T (ºC)	Tmax (ºC)	Tmin (ºC)	RH (%)	TotalPP* (mm)	WS** (m s^{-1})	WD** (degrees)	P (hPa)	SR (W m^{-2})
AN	5.4	25.5	-11.1	57	31	4.7	16	850	190
ANW	9.1	28.1	-8.4	66	68	4.7	291	850	208
ASW	8.0	24.3	-5.0	77	90	4.6	233	847	133
NAF	14.4	30.4	-1.9	63	92	4.6	178	852	232
MED	7.4	20.3	-3.4	71	35	4.0	134	851	161
EU	3.7	22.1	-13.5	58	9	4.7	30	849	194
WREG	4.3	20.2	-5.8	78	24	4.3	295	848	111
SREG	14.9	27.4	0.4	66	66	4.0	189	852	249

*Accumulated precipitation

**Vector average

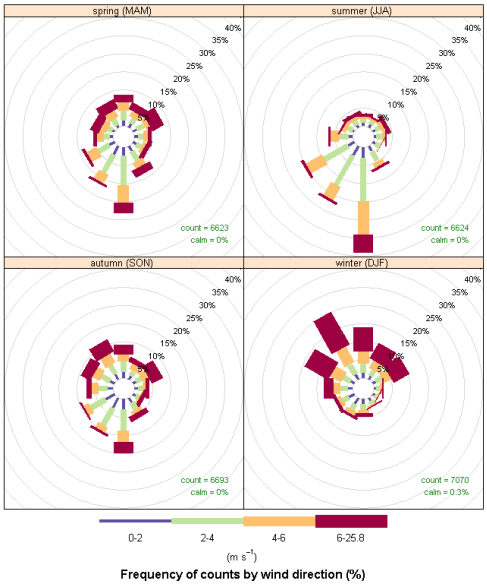

Fig. S2. Seasonal wind rose frequency for the study period at Montsec.

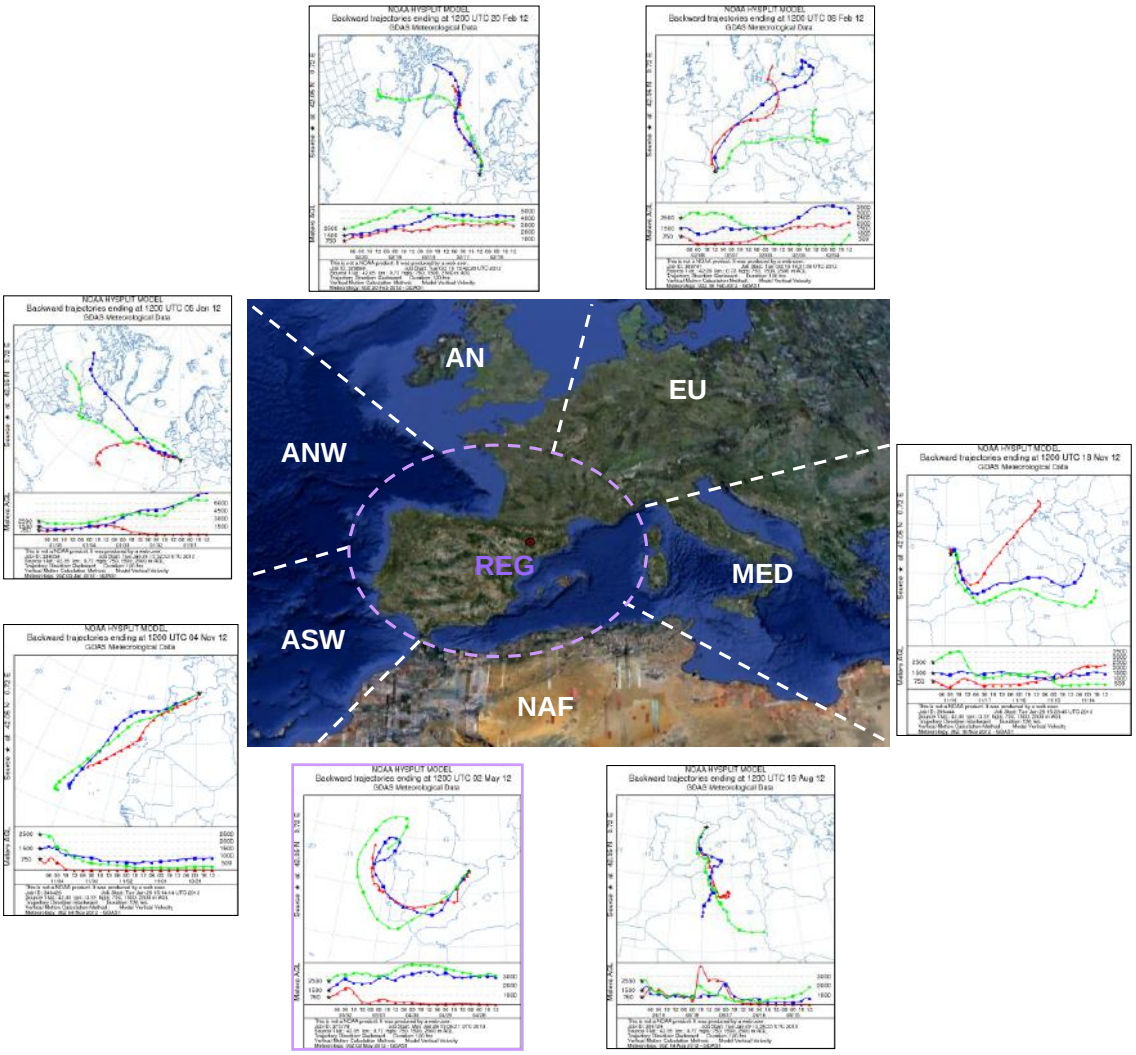

Fig. S3. Air mass origin sectors map and examples of backward trajectories for each sector according to their predominant transport direction.

Table S4. Three-year (2010-2012) arithmetic averages concentrations of PM, BC and N at different high altitude and rural stations in Europe.

		PM_{10} ($\mu g\ m^{-3}$)	$PM_{2.5}$ ($\mu g\ m^{-3}$)	PM_1 ($\mu g\ m^{-3}$)	BC ($\mu g\ m^{-3}$)	N_{10} (# cm^{-3})	N_7 (# cm^{-3})	N_3 (# cm^{-3})
Switzerland	Jungfraujoch (3578 m)	2.9	-	-	0.06*	634	-	-
	Rigi (1030 m)	8.0	7.5	5.8	-	-	-	-
	Chaumont (1137 m)	8.6	-	-	-	-	-	-
Italy	Mt. Cimone (2165 m)	8.8	-	-	0.33*	1847	-	-
Austria	Vorhegg (1020 m)	9.3	-	-	-	-	-	-
Germany	Schauinsland (1205 m)	9.3	7.3	-	0.38	-	-	-
	Schneefernerhaus (2650 m)	-	-	-	0.20	-	-	-
France	Puy de Dôme (1465 m)	-	-	-	0.22	2070	-	-
Spain	Campisábalos (1360 m)	10.3	5.1	-	-	-	-	-
	Risco Llano (1241 m)	11.5	5.8	-	-	-	-	-
	Montsec (1570 m)	11.9	8.2	5.3	0.19	-	2140	3716
	Zarra (885 m)	12.6	5.8	-	-	-	-	-
	Els Toms (470 m)	13.5	7.6	-	-	-	-	-
	Víznar (1265 m)	16.6	9.2	-	-	-	-	-
	Izaña (2373 m)	16.6	-	-	0.13	-	-	1467
	Cap de Creus (23 m)	16.8	7.9	-	-	-	-	-
	Montseny (720 m)	18.0	12.7	10.3	0.41	3475	-	-

Data from the ACTRIS Data Center web site.

* Jungfraujoch and Mt.Cimone BC concentrations averaged from 2007 to 2009.

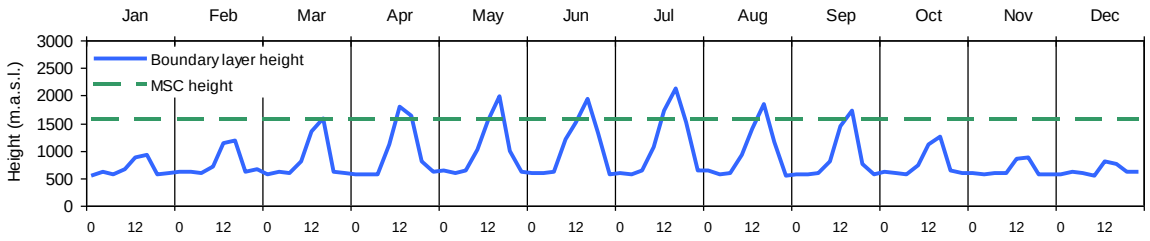

Fig. S4. Diurnal variation of the boundary layer height (computed with HYSPLIT model) averaged for each month during the study period at Montsec.

a)

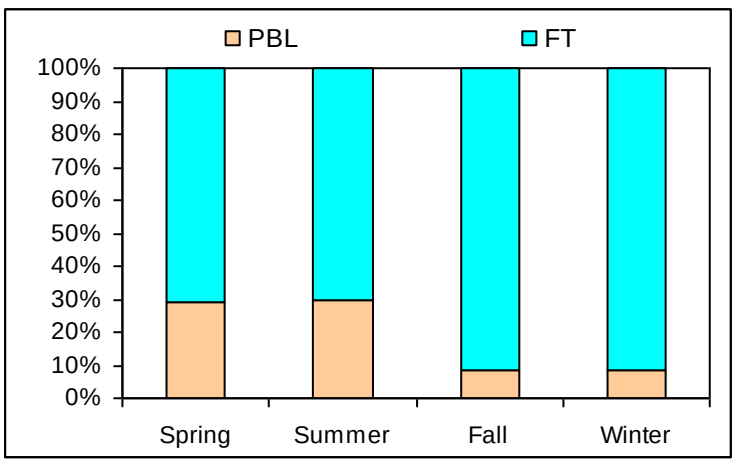

b)

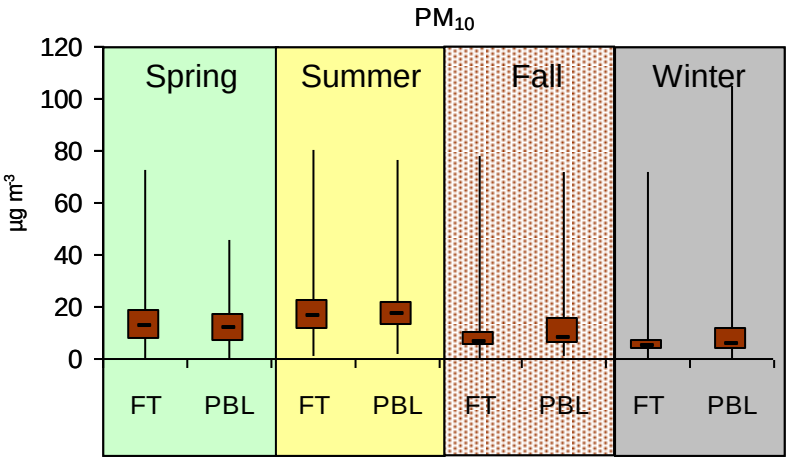
PM10
120
100
80
60
40
20
0
µg m-3
Spring
Summer
Fall
Winter
FT
PBL
FT
PBL
FT
PBL
FT
PBL

c)

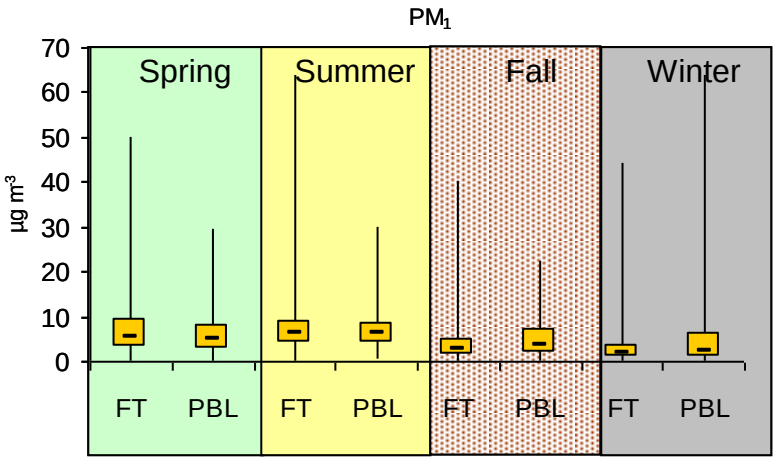
PM1
70
60
50
40
30
20
10
0
µg m-3
Spring
Summer
Fall
Winter
FT
PBL
FT
PBL
FT
PBL
FT
PBL

d)

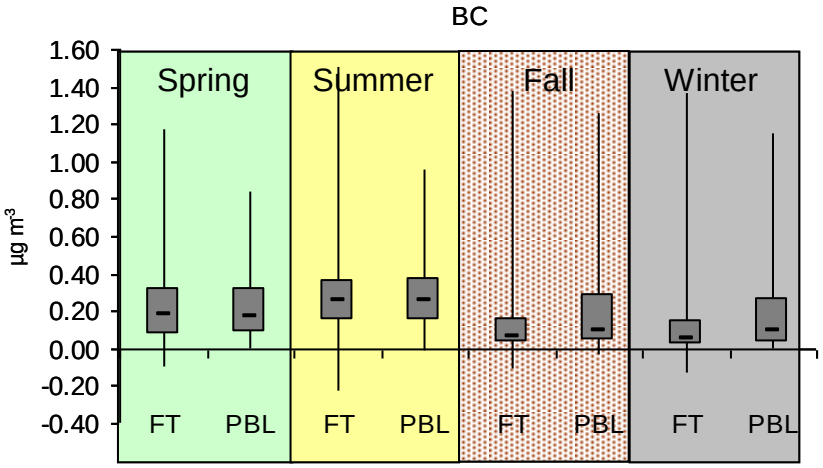
BC
1.60
1.40
1.20
1.00
0.80
0.60
0.40
0.20
0.00
-0.20
-0.40
µg m-3
Spring
Summer
Fall
Winter
FT
PBL
FT
PBL
FT
PBL
FT
PBL

e)

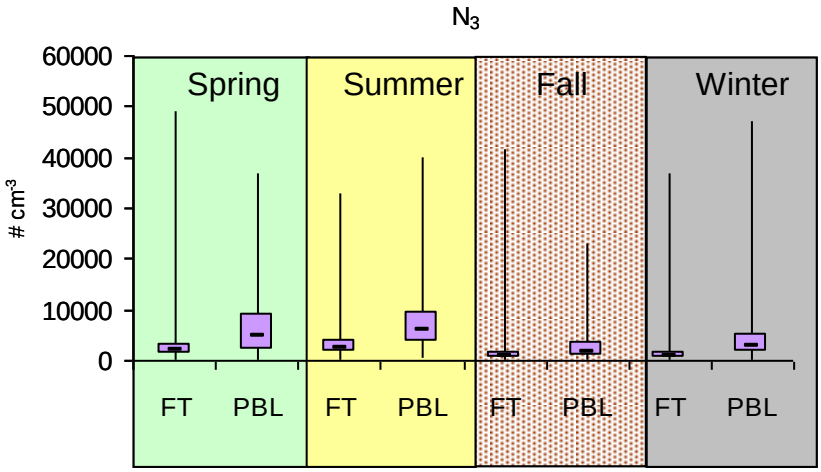

Fig. S5. (a) Percentage of time that Montsec is within or outside the PBL as a function of season. FT indicates that Montsec was in the free troposphere; PBL indicates that Montsec was within the planetary boundary layer. (b-e) Median (black line within the boxes) and percentiles (5-25-75-95, boxes and whiskers) of BC, PM_{10}, PM_1 and N_3 concentrations during the study period as a function of the season and the PBL height.

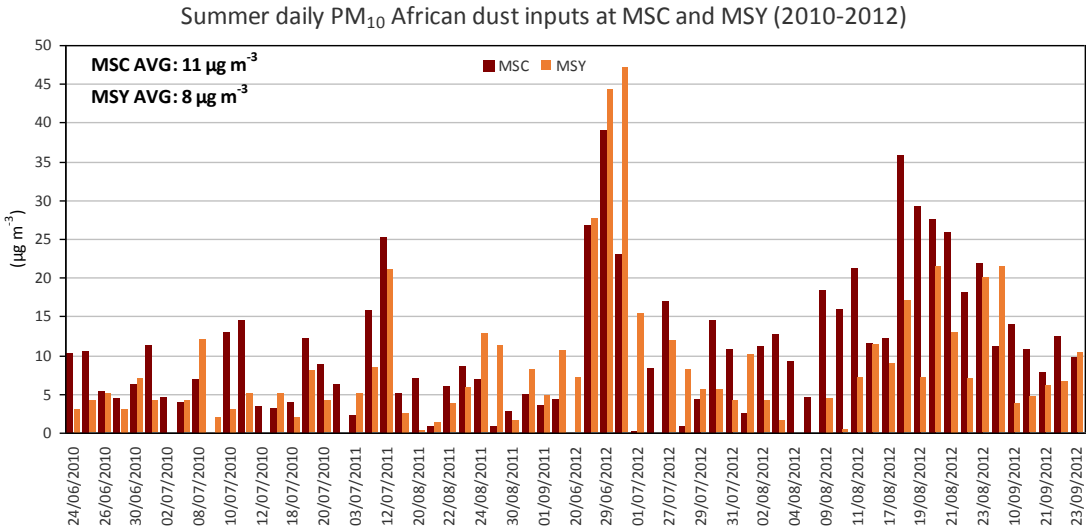

Fig. S6. Mass load from PM_{10} attributed to African dust in the warmer seasons and the three-year average at Montsec and Montseny.

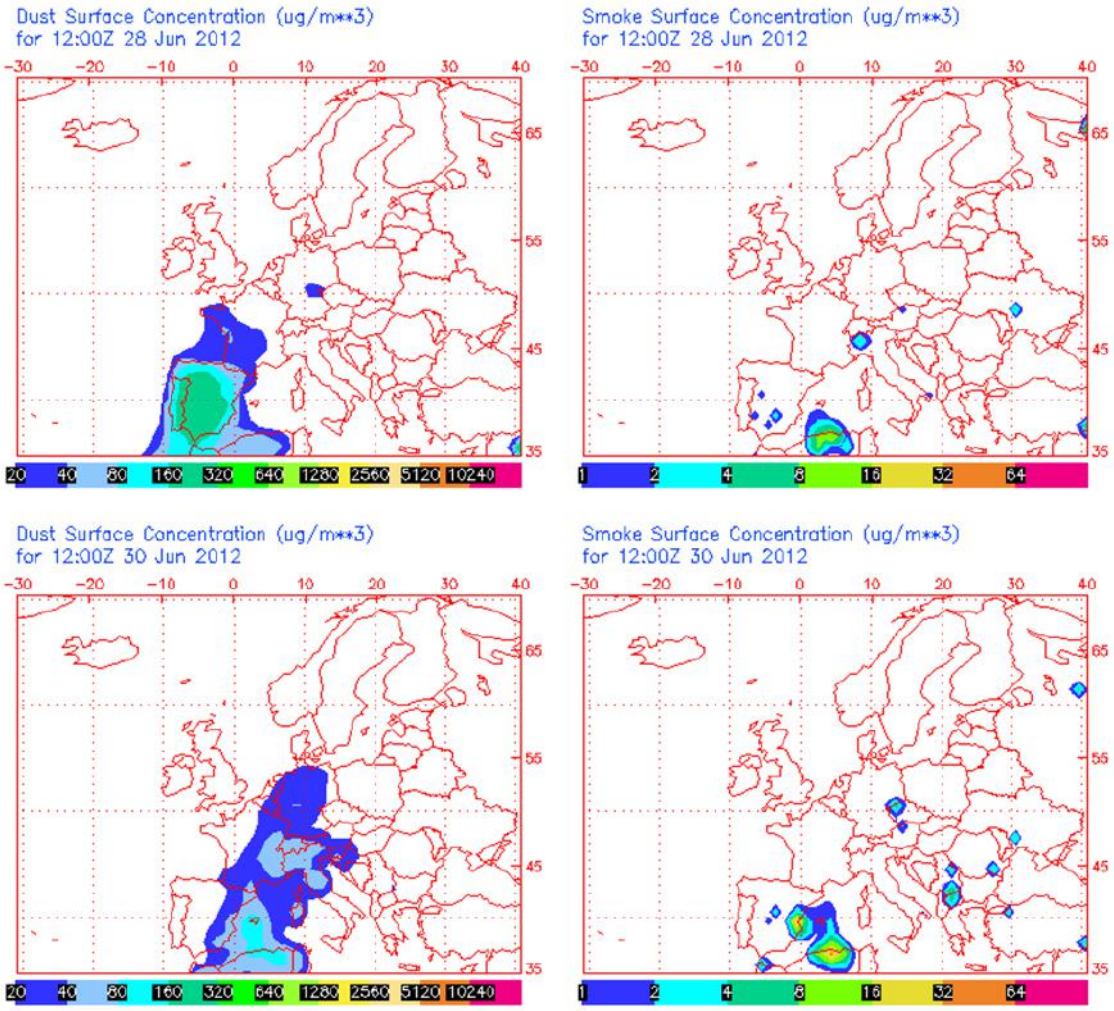

Fig. S7. Dust and smoke surface concentration from the NAAPS model under Saharan dust intrusion and wildfire episode affecting Montsec area.

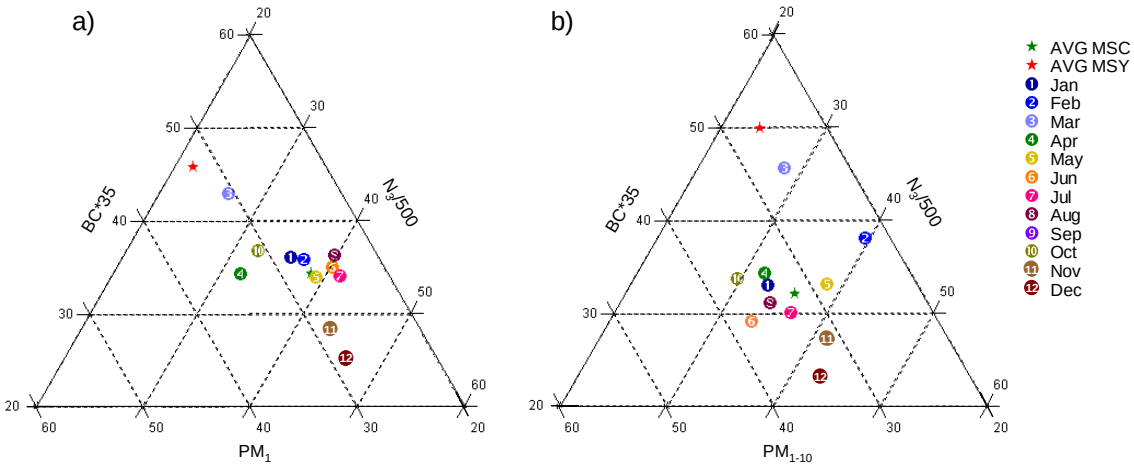

Fig. S8. Ternary Plot of (a) PM_1, BC*35 and N/500, and (b) PM_{1-10}, BC*35 and N/500 average and monthly averages concentrations at Montsec during the study period.

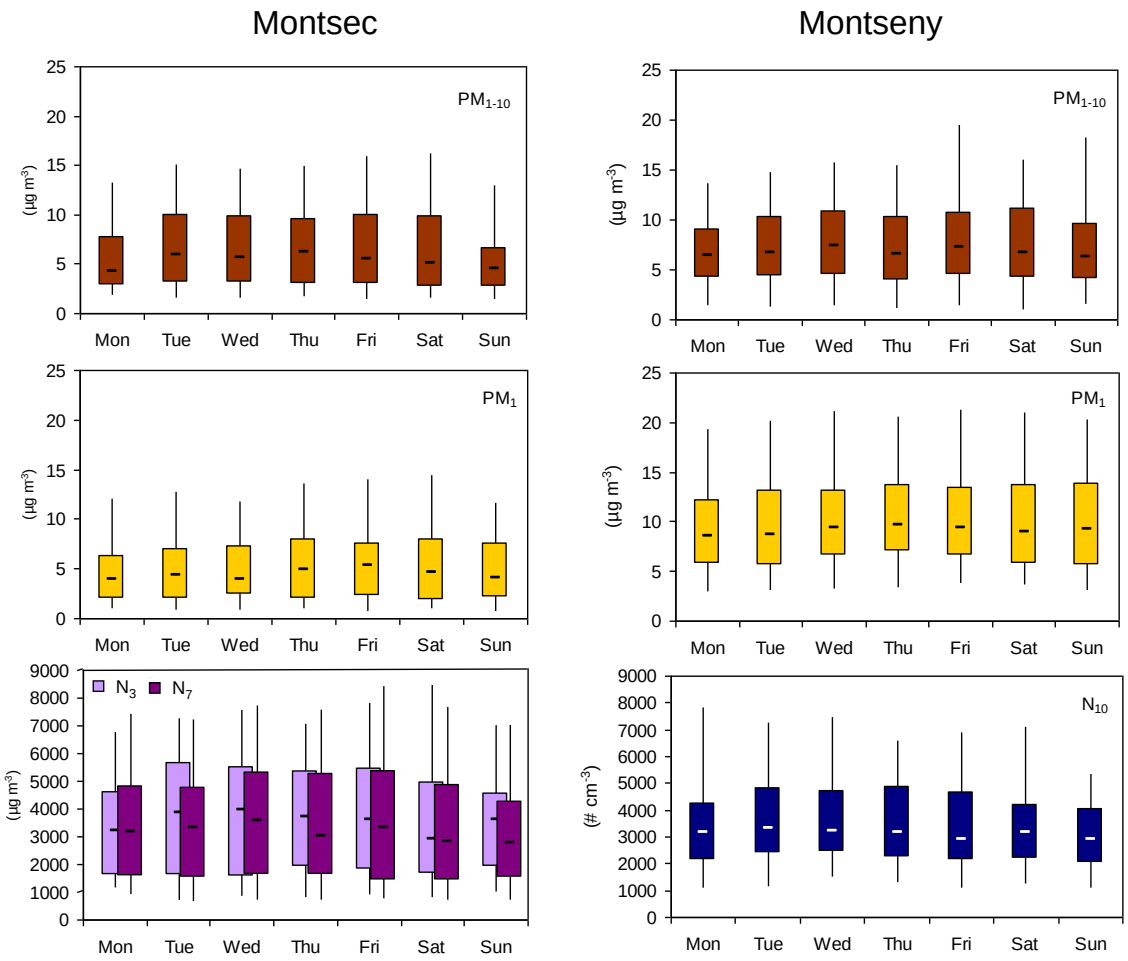

Fig. S9. Daily median (black line within the boxes) and percentiles (5-25-75-95, boxes and whiskers) of PM_{1-10}, PM_1 and N concentration during the study period at Montsec and Montseny.

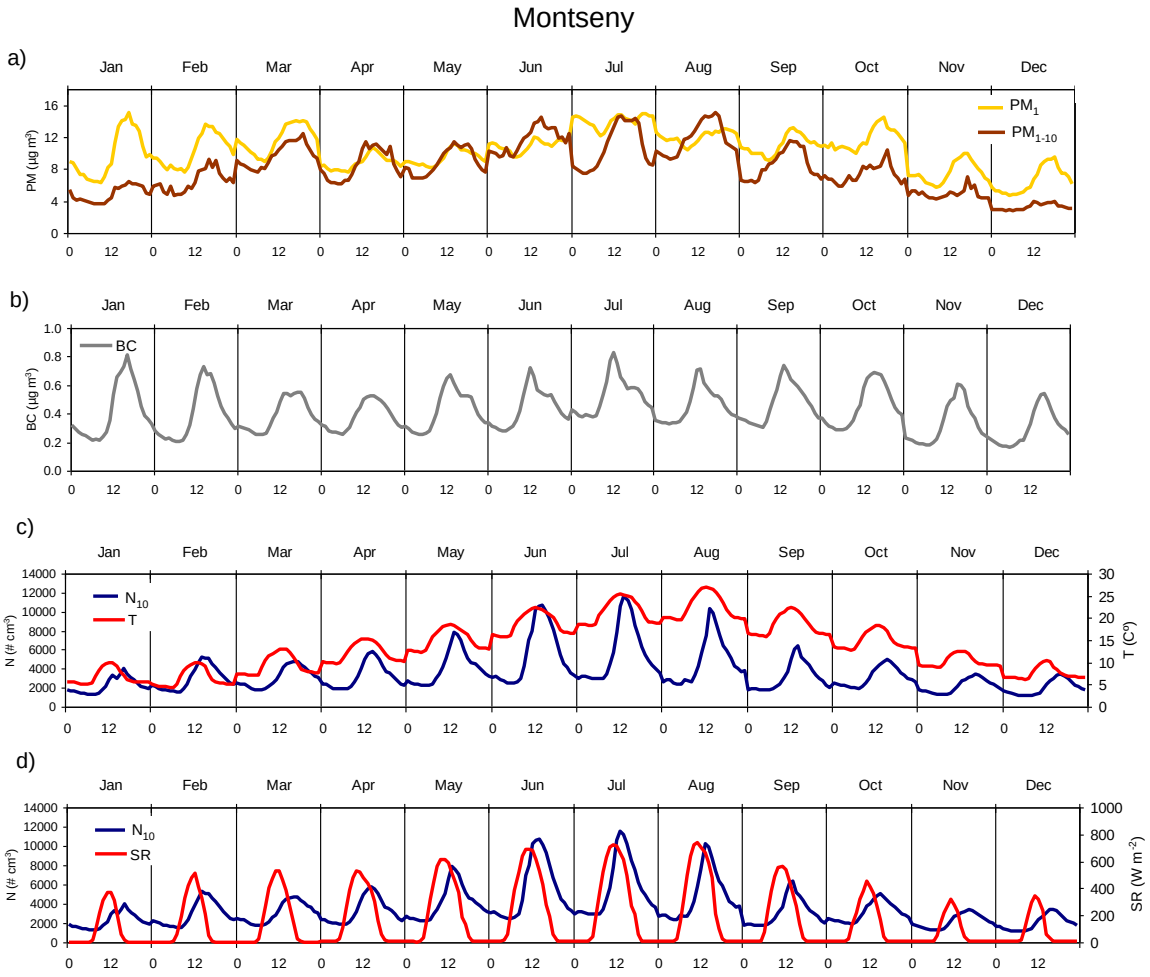

Fig. S10. Daily patterns of hourly (a) PM_1, $PM_{1\text{-}10}$, (b) BC, (c) N_{10} and temperature, and (d) N_3, N_7 and solar radiation (c) N measurements averaged for each month during the study period at Montseny.

3.3. Article 2: Joint analysis of continental and regional background environments in the western Mediterranean: PM_1 and PM_{10} concentrations and composition

Anna Ripoll[1,2], María Cruz Minguillón[1], Jorge Pey[3], Noemí Pérez[1], Xavier Querol[1], Andrés Alastuey[1]

[1]Institute of Environmental Assessment and Water Research (IDAEA-CSIC), Jordi Girona 18-26, 08034, Barcelona, Spain.

[2]Department of Astronomy and Meteorology, Faculty of Physics, University of Barcelona, Martí i Franquès 1, 08028, Barcelona, Spain.

[3]Aix-Marseille Université, CNRS, LCE FRE 3416, Marseille, 13331, France.

Atmos. Chem. Phys., 15, 1129-1145,
doi:10.5194/acp-15-1129-2015, 2015

Published: **30 January 2015**

Impact factor of Journal: **5.298**

Resum. En aquest article s'estudia de forma conjunta la composició química completa de les partícules atmosfèriques (angl., particulate matter, PM_1 i PM_{10}) d'un lloc representatiu del fons continental (Montsec, MSC, 1570 m s.n.m.) i d'un representatiu del fons regional (Montseny, MSY, 720 m s.n.m.) de l'oest del Mediterrani durant un període relativament llarg (gener 2010-març 2013).

Les diferències entre les concentracions mitjanes obtingudes al MSC i al MSY van ser atribuïdes a la diferent altitud, distància a les fonts antropogèniques, i influencia dels episodis atmosfèrics. Tots aquests factors van fer que les concentracions d'aerosols fossin 1.1 µg m^{-3} pel PM_1 i 4.0 µg m^{-3} pel PM_{10} més altes al fons regional que al fons continental. L'increment del PM_1 es va atribuir a les majors concentracions de sulfat, carboni elemental, matèria orgànica i alguns elements traces (V, Ni, Cu, Zn i Pb) trobades al fons regional, mentre que l'increment de PM_{10} es va associà a les concentracions més elevades de matèria orgànica, sulfat, nitrat i sal marina.

La mesura simultània de la composició química dels aerosols al MSC i al MSY va permetre demostrar, per primera vegada en la zona d'estudi, que l'impacte de les masses d'aire procedents d'Àfrica i d'Europa és molt sovint major a les parts altes de la troposfera que a les parts baixes. Això es va veure reflectit en les majors concentracions mitjanes de PM_{1-10} de matèria mineral al MSC (14 µg m^{-3}) respecte al MSY (8 µg m^{-3}) durant les intrusions de pols sahariana. Quan la zona d'estudi es veu afectada per episodis europeus, les concentracions de PM_1, carboni negre (angl., black carbon, BC), nitrat, matèria orgànica, i elements traça relacionats amb les emissions industrials i del trànsit rodat experimenten un increment que normalment és més evident al fons continental que al regional. Per altra banda, durant els episodis anticiclònics de l'hivern, el MSY es veu molt més afectat ja que el MSC acostuma a trobar-se a la troposfera lliure durant aquests episodis.

La majoria dels components químics van mostrar una clara variació estacional, amb els valors més alts a l'estiu i els més baixos a l'hivern, excepte el nitrat, tal i com s'ha vist en altres estudis sobre l'oest del Mediterrani. Les majors concentracions de nitrat a l'hivern que a l'estiu es van atribuir a l'alta volatilitat del nitrat amònic quan la humitat és baixa i la temperatura és relativament alta. Els valors màxims registrats per la resta de components químics durant l'estiu van ser causats per la combinació dels següents factors: 1) l'augment de l'altura de la capa de barreja; 2) la major intensitat dels processos de convecció; 3) la recirculació de masses d'aire, que indueix l'acumulació de contaminants a aquesta regió; 4) la intensitat més elevada de la radiació solar; 5) la major temperatura; 6) la disminució de la precipitació; i 7) la major freqüència d'intrusions saharianes.

Atmos. Chem. Phys., 15, 1129–1145, 2015
www.atmos-chem-phys.net/15/1129/2015/
doi:10.5194/acp-15-1129-2015
© Author(s) 2015. CC Attribution 3.0 License.

Atmospheric Chemistry and Physics
Open Access

Joint analysis of continental and regional background environments in the western Mediterranean: PM_1 and PM_{10} concentrations and composition

A. Ripoll[1,2], M. C. Minguillón[1], J. Pey[1,*], N. Pérez[1], X. Querol[1], and A. Alastuey[1]

[1]Institute of Environmental Assessment and Water Research (IDAEA-CSIC), Jordi Girona 18–26, 08034, Barcelona, Spain
[2]Department of Astronomy and Meteorology, Faculty of Physics, University of Barcelona, Martí i Franquès 1, 08028, Barcelona, Spain
[*]now at: Aix-Marseille Université, CNRS, LCE FRE 3416, Marseille, 13331, France

Correspondence to: A. Ripoll (anna.ripoll@idaea.csic.es)

Received: 26 March 2014 – Published in Atmos. Chem. Phys. Discuss.: 18 June 2014
Revised: 25 November 2014 – Accepted: 22 December 2014 – Published: 30 January 2015

Abstract. The complete chemical composition of atmospheric particulate matter (PM_1 and PM_{10}) from a continental (Montsec, MSC, 1570 m a.s.l.) and a regional (Montseny, MSY, 720 m a.s.l) background site in the western Mediterranean Basin (WMB) were jointly studied for the first time over a relatively long-term period (January 2010–March 2013).

Differences in average PM_X concentration and composition between both sites were attributed to distance to anthropogenic sources, altitude, and different influence of atmospheric episodes. All these factors result in a continental-to-regional background increase of 4.0 $\mu g\,m^{-3}$ for PM_{10} and 1.1 $\mu g\,m^{-3}$ for PM_1 in the WMB. This increase is mainly constituted by organic matter, sulfate, nitrate, and sea salt. However, higher mineral matter concentrations were measured at the continental background site owing to the higher influence of long-range transport of dust and dust resuspension.

Seasonal variations of aerosol chemical components were attributed to evolution of the planetary boundary layer (PBL) height throughout the year, variations in the air mass origin, and differences in meteorology. During warmer months, weak pressure gradients and elevated insolation generate recirculation of air masses and enhance the development of the PBL, causing the aging of aerosols and incrementing pollutant concentrations over a large area in the WMB, including the continental background. This is reflected in a more similar relative composition and absolute concentrations of continental and regional background aerosols. Nevertheless, during colder months the thermal inversions and the lower vertical development of the PBL leave MSC in the free troposphere most of the time, whereas MSY is more influenced by regional pollutants accumulated under winter anticyclonic conditions. This results in much lower concentrations of PM_X components at the continental background site with respect to those at the regional background site.

The influence of certain atmospheric episodes caused different impacts at regional and continental scales. When long-range transport from central and eastern Europe and from north Africa occurs, the continental background site is frequently more influenced, thus indicating a preferential transport of pollutants at high altitude layers. Conversely, the regional background site was more influenced by regional processes.

Continental and regional aerosol chemical composition from the WMB revealed (a) high relevance of African dust transport and regional dust resuspension; (b) low biomass burning contribution; (c) high organic matter contribution; (d) low summer nitrate concentrations; and (e) high aerosol homogenization in summer.

Published by Copernicus Publications on behalf of the European Geosciences Union.

1 Introduction

The influence of atmospheric particulate matter (PM) on the Earth's radiative budget generates a strong scientific interest because of its effect on climate. Atmospheric PM interacts with the Earth's climate system by scattering and absorbing solar radiation (direct climate forcing effect), and by acting as cloud condensation nuclei (indirect climate forcing effect) (IPCC, 2013). Aerosols also have adverse effects on air quality (Directive 2008/50/EC) and human health (WHO, 2013), as well as on ecosystems (e.g. Burkhardt and Pariyar, 2014). The size distribution of aerosol chemical components is a key factor in modulating these effects, and it provides valuable information on the aerosol origins and sources. Aerosol chemical composition measurements carried out at complex sites such as urban areas constrain the assessment of the origin of regional and long-range-transported aerosols, as local sources prevail. For this reason, measurements performed at a sufficient distance from large emission sources are needed to determine background conditions and to evaluate air mass transport effects. Furthermore, an improved understanding of synoptic and mesoscale meteorological effects is necessary to develop a better predictive capability of air quality and climate models.

Although there is not a well-established definition, continental background environments can be described as representative of the air quality of a wide area of hundreds of kilometers, as proposed by Laj et al. (2009), with the absence of local emissions. However, aerosols found in this type of environments are not purely natural; the presence of some pollutants in these sites indicates that they are affected by long-range transport of anthropogenic emissions, since generally they are isolated from large polluted areas (> 50 km) (Putaud et al., 2010). For this reason, these environments are also classified as remote sites. In many cases the monitoring sites chosen to represent this type of environments are located in mountaintops over 1000 m a.s.l.; therefore they are also called high-altitude sites (Nyeki et al., 1998) or free troposphere (FT) environments (Andrews et al., 2011). The areas located at sufficient distance from large anthropogenic sources but frequently within the planetary boundary (PBL) are classified as regional background environments (Putaud et al., 2010). These environments are representative of the air quality of a less extensive area, and they are more influenced by regional transport of polluted air masses than continental background environments.

Aerosol chemical characterization has been performed at many locations across Europe, providing information on PM_{10} and $PM_{2.5}$ chemical composition from different types of environments (e.g. Putaud et al., 2010), improving the knowledge on the variation and trends of PM composition (e.g. Cusack et al., 2012) and increasing the understanding of PM sources (Belis et al., 2013). Nevertheless, the PM_1 fraction remains relatively understudied, especially outside urban areas. Most studies focusing on PM_1 have been carried out within the PBL, whereas measurements at continental background sites in Europe are scarce and were mostly taken in short-term measurement campaigns (e.g. Carbone et al., 2010; Marenco et al., 2006). The study of PM_1 chemical composition at continental background sites may be necessary to assess the contribution of regional and long-range transport, since it is in the PM_1 fraction where most of the anthropogenic constituents are concentrated (Minguillón et al., 2012; Pérez et al., 2008b).

Among the few long-term European studies at continental background environments, Cozic et al. (2008) investigated the chemical composition of coarse and PM_1 aerosols for 7 years at the high Alpine site of Jungfraujoch (Switzerland). Bourcier et al. (2012) studied PM_{10} and PM_1 water-soluble inorganic components over 1 year at the high-altitude site of Puy de Dôme (France). Recently, Carbone et al. (2014) performed a study on long-term measurements of chemical composition in the continental background environment of southern Europe/northern Mediterranean. This study was focused on nocturnal PM_1 chemical composition for 3 years at the high mountain station of Mt. Cimone (Italy).

The Mediterranean region is characterized by particular atmospheric dynamics strongly influenced by its topography (Jorba et al., 2013; Millan et al., 1997). Over this region, elevated emissions of anthropogenic pollutants occur, arrival of natural and anthropogenic aerosols as a result of long-range transport from Africa and Europe is frequent (Pey et al., 2010, 2013b; Ripoll et al., 2014), and accumulation and recirculation processes are recurrently observed (Rodríguez et al., 2002).

For these reasons, results of PM_{10} and PM_1 chemical characterization from Montsec (MSC) and Montseny (MSY) Global Atmosphere Watch (GAW) stations for the period of January 2010–March 2013 are presented in this study. MSC is representative of the continental background conditions of the western Mediterranean Basin (WMB) (Ripoll et al. 2014). This station is located in the FT most of the time due to its elevation (1570 m a.s.l.); although during the warmer months that isolation is broken as a result of vertical mixing and mountain breeze regimes (Ripoll et al. 2014). MSY is a regional background observatory located in the WMB (720 m a.s.l.) in operation since 2002 (Cusack et al., 2012; Pérez et al., 2008a), and it is influenced by regional anthropogenic emissions in specific scenarios (Pérez et al., 2008a; Pey et al., 2010). The record of a relatively long series of PM_{10} and PM_1 concentrations and complete chemical composition at two different WMB environments has allowed for the investigation of temporal and spatial aerosol variations in the WMB with a focus on regional and long-range transport processes. Daily and seasonal patterns of PM_{10} and PM_1 concentrations, as well as their major components and trace elements at MSC and MSY, were investigated. Greater emphasis was placed on the evaluation of the influence of different meteorological scenarios, with a focus on the partitioning of the chemical components into different size fractions in

order to discriminate natural and anthropogenic impacts affecting PM_{10} and PM_1. To the authors' knowledge, no similar studies exist in the literature that compare continental and regional background environments and their seasonal variation.

2 Methodology

2.1 Monitoring sites and sampling schedule

The continental background site was set up in the Montsec (MSC) mountain range, located in the NE of the Iberian Peninsula (42°3′ N, 0°44′ E, 1570 m a.s.l.). This station is situated 50 km to the S of the Axial Pyrenees and 140 km to the NW of Barcelona (Fig. S1). A detailed description of this site can be found in Ripoll et al. (2014).

Results from MSC were jointly studied with those simultaneously obtained at the Montseny (MSY) station, a regional background observatory located in the Montseny Natural Park (41°19′ N, 2°21′ E, 720 m a.s.l.), 40 km to the N-NE of the Barcelona urban area, and 25 km from the Mediterranean coast (Fig. S1) (Pérez et al., 2008a).

At the MSC site, 24 h samples of PM_{10} and PM_1 were collected every 4 days on 150 mm quartz micro-fiber filters (Pallflex QAT) using high-volume samplers (30 $m^3 h^{-1}$, MCV CAV-A/MSb) equipped with MCV PM_{10} and PM_1 cut-off inlets. PM_{10} and PM_1 sampling began in November 2009 and in March 2011, respectively. In this work we study the results from January 2010 (March 2011 for PM_1) to March 2013. In addition to the routine measurements, five intensive campaigns (daily sampling) were performed during March–April 2011, July–August 2011, January–February 2012, June–July 2012, and January–February 2013. Overall, 391 and 235 samples of PM_{10} and PM_1, respectively, were collected throughout the study period, and PM_{1-10} concentrations were calculated by the difference of simultaneous PM_1 and PM_{10} daily samples (190 days).

At the MSY site, 24 h samples of PM_{10} and PM_1 were also collected from January 2010 to March 2013 using high-volume samplers (30 $m^3 h^{-1}$, DIGITEL-DH80) equipped with PM_{10} and PM_1 cut-off inlet (also DIGITEL). A total of 351 and 335 samples of PM_{10} and PM_1, respectively, were collected during the study period, and PM_{1-10} samples were calculated for 147 days. In most cases, sampling days were coincident at MSC and at MSY.

2.2 Chemical characterization

PM mass concentrations were determined by standard gravimetric procedures, and complete chemical analysis for all filters was performed following the procedures proposed by Querol et al. (2001).

Acid digestion ($HF:HNO_3:HClO_4$) of one-fourth of each filter was carried out to determine and quantify major and trace elements by inductively coupled plasma mass spectrometry (ICP-MS, X Series II, THERMO) and atomic emission spectroscopy (ICP-AES, IRIS Advantage TJA Solutions, THERMO). A few milligrams of the reference material NIST 1633b were added to one-fourth of laboratory blank filters to check the accuracy of the analysis of the acidic digestions. One 1/4 of each filter was leached with ultrapure water (miliQ) to determine the content of Cl^-, SO_4^{2-}, and NO_3^- by ion high-performance liquid chromatography (HPLC) using a WATERS ICpakTM anion column with a WATERS 432 conductivity detector, and NH_4^+ concentrations with a selective electrode (MODEL 710 A+, THERMO Orion). A rectangular portion (1.5 cm^{-2}) of the remaining filter was used for the analysis of organic carbon (OC) and elemental carbon (EC) by a Sunset OCEC analyzer using the EUSAAR 2 protocol (European Supersites for Atmospheric Aerosol Research; Cavalli et al., 2010). Moreover, one blank filter was kept for each set of 10 filters. Blank concentrations were subtracted from the total concentration measured for each sample, thus giving ambient concentrations. To complete mass balances, the following indirect determinations were obtained: (a) CO_3^{2-}, calculated from Ca as $CO_3^{2-} = 1.5 \times Ca$; (b) Al_2O_3, calculated from Al as $Al_2O_3 = 1.889 \times Al$; (c) SiO_2, calculated as $SiO_2 = 2.5 \times Al_2O_3$; and (d) organic matter (OM) obtained by applying a factor of 2.2 to the OC concentrations for MSC samples and a factor of 2.1 for MSY samples, following the suggestion from Takahama et al. (2011). By following these procedures we were able to determine and quantify the concentrations of major components (OC, EC, SiO_2, CO_3^{2-}, Al_2O_3, Ca, Al, Na, Mg, Fe, K, NO_3^-, SO_4^{2-}, NH_4^+, and Cl^-) and trace elements (Li, P, Ti, V, Cr, Mn, Co, Ni, Cu, Zn, As, Se, Rb, Sr, Cd, Sn, Sb, Ba, La, Pb, among others). Overall, the aforementioned components accounted for 60–90 % of the total PM mass. Most of the undetermined mass was attributed to water not eliminated during filter conditioning in the presence of hygroscopic species, but a contribution from sampling artifacts and from the use of factors to determine CO_3^{2-}, SiO_2, and OM cannot be discarded.

At MSC the mineral matter (MM) determination was calculated as

$$MM = CO_3^{2-} + SiO_2 + Al_2O_3 + Ca + Fe + K + nss\text{-}Na + Mg + Mn + Ti + P, \quad (1)$$

where nss-Na is the non-sea-salt sodium; it was calculated as $nss\text{-}Na = Al_2O_3 \times 0.067$ according to the composition of the mineral particles from the Sahara given by Moreno et al. (2006), and hence the remaining sodium was sea-salt sodium ($ss\text{-}Na = Na - nss\text{-}Na$).

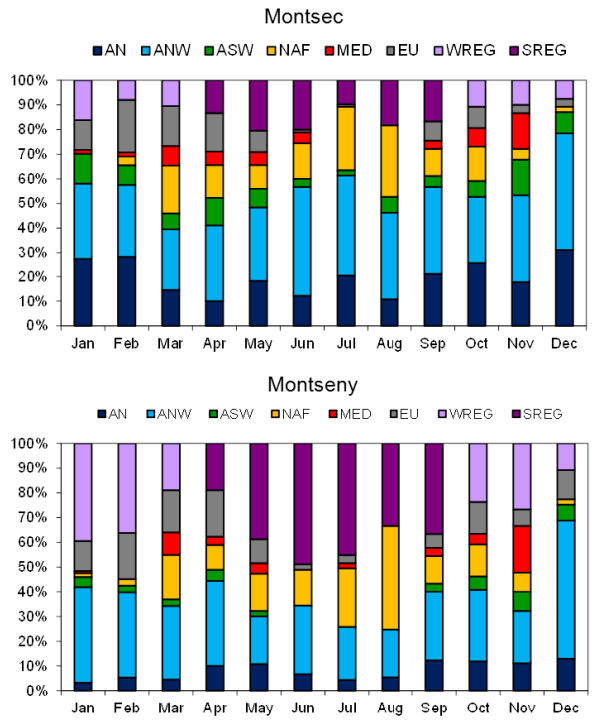

Figure 1. Average frequency of air mass origin at Montsec and Montseny for the different months based on daily calculations between January 2010 and March 2013.

Consequently, the sea salt (SS) determination at MSC was given by

$$SS = Cl^- + ss\text{-}Na. \quad (2)$$

At MSY, Na concentrations were entirely attributed to SS, given that it is located closer to the sea and in agreement with Pey et al. (2009).

2.3 Principal component analysis

Principal component analysis (PCA) was performed using the software STATISTICA v10.0. The orthogonal transformation method with varimax rotation (Thurston and Spengler, 1985) was employed, retaining principal components with eigenvalues greater than 1. The data set used for PCA was comprised of the following PM_{10} constituents: Cl^-, NO_3^-, NH_4^+, SO_4^{2-}, Al_2O_3, Ca, K, Na, Mg, Fe, Li, Ti, V, Cr, Mn, Ni, Cu, Zn, As, Se, Sr, Cd, Sb, Pb, OC, and EC. All days with measurements of PM_{10} chemical analysis were included for PCA analysis, which totalled 390 cases from MSC and 351 cases from MSY. A typical robust PCA analysis requires at least a data set with 100 cases. This technique allowed for the identification of main common groups of trace elements in PM_{10} at the continental and regional background sites.

2.4 Classification of atmospheric episodes

The classification of the atmospheric episodes affecting the MSC and MSY sites on each day of the sampling period was performed following the procedure described by Ripoll et al. (2014), and the different air mass transport pathways determined were (1) Atlantic north (AN), (2) Atlantic northwest (ANW), (3) Atlantic southwest (ASW), (4) north Africa (NAF), (5) Mediterranean (MED), (6) Europe (EU), (7) winter regional (WREG, from November to April), and (8) summer regional (SREG, from May to October) (Fig. 1).

Additionally, the boundary layer height was calculated at the MSC and MSY sites using the READY (Real-time Environmental Applications and Display sYstem) model from the NOAA Air Resources Laboratory (http://www.ready.noaa.gov/READYamet.php), which is based in meteorological conditions defining Pasquill stability classes, and uses a resolution grid of 50 km. This was calculated every 3 hours during the whole period (Fig. S2). Despite the limited suitability of this type of model for mountainous terrains, the differences found throughout the year and among different atmospheric scenarios can be considered as a good approximation of the actual PBL variations.

3 Results and discussion

3.1 Continental vs. regional background PM concentrations in the western Mediterranean

PM_{10} and PM_1 average concentrations (±SD) measured at MSC continental background site reached $11.5 \pm 9.3\ \mu g\ m^{-3}$ and $7.1 \pm 3.9\ \mu g\ m^{-3}$, respectively, whereas at MSY regional background site these concentrations were $15.5 \pm 7.9\ \mu g\ m^{-3}$ and $8.2 \pm 4.1\ \mu g\ m^{-3}$ (Table S1). Thus, the continental-to-regional background increase is estimated to be $4.0\ \mu g\ m^{-3}$ for PM_{10} and $1.1\ \mu g\ m^{-3}$ for PM_1 in the WMB. This increase is caused by differences of (a) altitude, (b) distance to anthropogenic sources, and (c) impact of atmospheric episodes. The contribution of different aerosol chemical components to this increment will be discussed in Sect. 3.2.

A significant seasonal variation of PM_{10} and PM_1 mass concentrations was observed at both sites, with maximum values in summer and minimum values in winter (Fig. 2). Comparable seasonal patterns for PM_X concentrations were described for MSC (Ripoll et al., 2014) and for other regional and continental background sites in southern Europe (e.g. Cozic et al., 2008; Querol et al., 1998; Rodríguez et al., 2003; Tositti et al., 2013). In those studies the seasonal pattern was attributed to changes in the air mass origin from summer to winter, and to the different PBL height between seasons. Moreover, at both MSC and MSY a secondary maximum of PM_{10} and PM_1 concentrations was observed in early spring (Fig. 2).

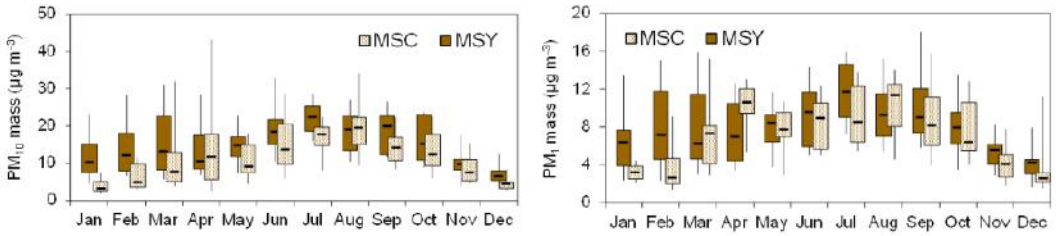

Figure 2. Monthly median (black line within the boxes) and percentiles (5–25–75–95, boxes and whiskers) of daily PM_{10} and PM_1 mass concentrations at Montsec (MSC) and Montseny (MSY) based on daily measurements between January 2010 and March 2013.

PM_{10} concentrations showed a stronger seasonal pattern than PM_1 concentrations at both sites (Fig. 2). This is attributed to the higher impact of resuspended and long-range-transported dust on the PM_{10} fraction, both enhanced in summer (see Sect. 3.3), and to the prevalence of the anthropogenic constituents in PM_1, whose emissions occur throughout the year.

Comparison of these results with those from other continental background sites in central Europe, such as Puy de Dôme at 1465 m a.s.l. in France (Bourcier et al., 2012) and Jungfraujoch at 3454 m a.s.l. in Switzerland (Cozic et al., 2008), shows that PM_{10} and PM_1 concentrations were higher at the continental background site in the WMB (Fig. S3 and Table S1). Such higher PM_{10} and PM_1 concentrations at MSC are related to the increasing role of Saharan dust particles over this area, as discussed in Sect. 3.3 and in agreement with Ripoll et al. (2014), and to the more polluted atmosphere in summer as a result of the air mass recirculation over the WMB (Millan et al., 1997). By contrast, PM_{10} concentrations at the regional background site in the WMB were lower than those at the rural sites in Switzerland (Gianini et al., 2012) (Fig. S3 and Table S1), probably because of the specific Alpine location of these sites which hinders pollution dispersion.

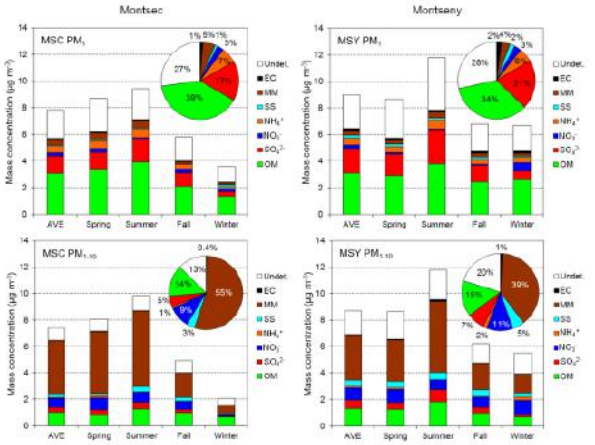

Figure 3. Average concentrations of aerosol major components in PM_1 and PM_{1-10} fractions at Montsec and Montseny for the whole period (AVE) and for different seasons based on daily measurements between January 2010 and March 2013. Pie charts represent the average relative contribution of aerosol major components to total mass for each fraction.

3.2 Continental vs. regional background aerosol chemical composition in the western Mediterranean

3.2.1 Average aerosol chemical composition

PM_1 was mainly composed of OM at both sites (39 % at MSC and 34 % at MSY), followed by sulfate (17 and 21 %), ammonium (7 and 6 %), MM (5 and 4 %), nitrate (3 %), SS (1 and 2 %), and EC (1 and 2 %) (Fig. 3 and Table S1). The undetermined mass accounted for 27 and 28 %. The PM_{1-0} fraction mainly differed in the contribution of MM (55 % at MSC and 39 % at MSY), whereas the other components contributed similarly: OM (14 and 15 %), nitrate (9 and 11 %), sulfate (5 and 7 %), SS (3 and 5 %), ammonium (1 and 2 %), and EC (0.4 and 1 %). The undetermined mass was 20 % at MSY and 13 % at MSC. The closer compositional similarities for PM_1 fraction point to the suitability of using PM_1 as an indicator of regional anthropogenic pollution in Europe, and reflect the wider spatial representativeness of the fine PM.

Overall, average absolute concentrations of chemical components were more similar between MSC and MSY for PM_1 than for the PM_{10} (Fig. 3 and Table S1). The PM_1 continental-to-regional background increase of 1.1 µg m^{-3} is attributed to the higher concentrations of PM_1 sulfate, EC, OM, and some anthropogenic trace elements (V, Ni, Cu, Zn, and Pb) at the regional background site. The increase of 4.0 µg m^{-3} of PM_{10} at MSY with respect to MSC is attributed to higher concentrations of OM, sulfate, nitrate, and SS. These differences confirm that MSC is located at a sufficient altitude and distance from large urban/industrial agglomerations to avoid direct anthropogenic influence and to be considered a continental background site of the WMB. This also confirms that MSY is more affected by the marine aerosols as it is located closer to the coast. Nevertheless, MM and MM-related elements' (Ti, Mn, Li, and Sr) PM_{10} concen-

trations were higher at the continental background site than at the regional background site, probably due to the prevalence of long-range dust transport at higher altitude layers (Sicard et al., 2011), and to the higher dust resuspension at MSC.

In order to provide a global picture of the origin and variability of trace elements in the study region, a principal component analysis (PCA) was performed. This exploration permitted the identification of three main common groups of trace elements in PM_{10} at the continental and regional background sites. Ordered by their contribution to the total mass of trace elements in PM_{10}, these groups were mineral, industrial and road traffic, and fuel-oil-combustion-related elements (Tables S2 and S3).

In the mineral group typical crustal elements (Ti, Mn, Li, and Sr) were included; furthermore, V, Cr, Co, Ni, and As were also partially associated with this factor since these elements, usually attributed to anthropogenic sources, are also found in clay mineral assemblages. The group for which high loading factors were obtained for Cu, Zn, As, Cd, Pb, Sb, and Sn was associated with industrial and road traffic sources, based on previous studies which identified (a) Pb, Zn, Mn, and Cd as tracers of the influence of industrial activities located in the surroundings of Barcelona, such as smelters and cement kilns, and (b) Cu, Sn, and Sb as tracers of non-exhaust vehicle emissions (Amato et al., 2009). These sources could not be split by the PCA probably because these emissions are mixed during their transportation from industrial and urban areas to MSY and MSC. The fuel oil combustion group was better identified at MSY than at MSC, and it was traced by V and Ni. These elements are typical markers of fuel oil combustion, strongly influenced by shipping emissions in the study region (Minguillón et al., 2014; Pey et al., 2013a).

Figures S3 and S4 and Table S1 show average concentrations of chemical components in PM_{10} at the continental background site of Puy de Dôme (Bourcier et al., 2012) and at the rural stations of Payerne and Magadino (Gianini et al., 2012). Nitrate and ammonium PM_{10} concentrations at MSC were slightly higher than those observed at Puy de Dôme, whereas the concentrations registered at MSY were lower than those measured at Payerne and Magadino. The similar sulfate concentrations across Europe in both continental and regional background areas corroborate that this component can remain in the atmosphere for a long time, homogenizing sulfate concentrations in Europe. Average PM_{10} concentrations of EC and OM in the WMB were lower than those measured at Payerne and Magadino, probably due to the higher influence of biomass burning in central Europe. This is confirmed by the higher concentrations of the well-known biomass burning tracer potassium (Pio et al., 2008) registered at the Swiss stations, most of it water soluble (Gianini et al., 2012). Mineral major (Al + Ca + Mg) and trace (Ti, Sr, La or Ce) elements at MSC and MSY were recorded in concentrations twice as high as those at Payerne and Magadino, indicating the higher influence of Saharan dust transport and regional dust resuspension in the Mediterranean area. As expected, a higher influence of SS particles was observed at MSC and MSY than at Payerne and Magadino owing to their closer location to the Mediterranean Sea. Conversely, the highest concentrations of typical anthropogenic trace elements – such as Ni, Cu, Zn, As, Cd, Sb, and Pb – were recorded at the Swiss stations, with the exception of V, which was higher at the Spanish sites. This can be partially attributed to a greater influence of emissions from fuel oil combustion, mostly from shipping emissions in the Mediterranean region (Pey et al., 2009).

3.2.2 Partitioning of major and trace components in PM_1 and PM_{1-10}

In the WMB region nitrate showed a prevalent coarse-grain size distribution (Figs. 3 and S5). PM_{1-10} nitrate compounds were partially associated with mineral dust and sea salt particles, since nitric acid and/or some other nitrogen compounds can react with these particles (Wall et al., 1988; Zhuang et al., 1999a). The resulting coarse sodium or calcium nitrate particles are much more stable than ammonium nitrate at high temperature and low humidity (Zhuang et al., 1999b).

As expected, sulfate was mainly fine at both sites (Figs. 3 and S5) and hence attributed to the presence of ammonium sulfate as deduced by the good ionic balance fitting between sulfate and ammonium ($R^2 = 0.899$). Nevertheless, PM_{1-10} sulfate was also detected at MSC and MSY, and it was partially attributed to mineral dust and sea salt particles, and partially attributed to the reaction product between sulfuric acid and/or sulfur dioxide (SO_2) and these natural particles (Wall et al., 1988; Zhuang et al., 1999a).

Ammonium showed a prevalent fine-grain size distribution at the continental and regional background sites (Figs. 3 and S5). Fine ammonium was attributed to the presence of both ammonium nitrate and ammonium sulfate. PM_{1-10} ammonium is most likely in $PM_{1-2.5}$ fraction, according to Querol et al. (2009).

OM was mainly fine at both sites (Figs. 3 and S5). A high number of studies have demonstrated the dominant secondary origin of the fine OM (Jimenez et al., 2009). In the study area, previous works found that secondary organic aerosol (SOA) accounted for 91 and 55 % of the OM at MSY and at the city of Barcelona, respectively (Minguillón et al., 2011; Mohr et al., 2012). Therefore, fine OM at MSC is expected to be dominated by SOA, even more than at MSY given its remote settlement. Furthermore, the presence of OM in PM_{1-10}, especially in spring and summer, suggests the impact of primary bioaerosols (Pöschl et al., 2010).

Although EC was mainly fine at both sites (Figs. 3 and S5), PM_{1-10} EC was also detected, suggesting a partial association between EC and MM by means of adsorption of anthropogenic pollutants onto dust.

As expected, most of the MM species and the mineral trace elements were encountered in the PM_{1-10} fraction, while

the concentrations in PM_1 were clearly lower at both sites (Figs. 3 and S6 and Table S1). Contrary to the rest of MM species, K was also abundant in PM_1 fraction and its concentrations were slightly higher at MSY than those at MSC (Figs. S6 and S7c). This indicates an additional source origin other than mineral (generally as K-feldspar and illite, a K-bearing clay mineral), such as biomass burning, especially over the regional background. The winter DAURE campaign (Determination of the sources of atmospheric Aerosols in Urban and Rural Environments in the western Mediterranean) performed in March 2009 revealed that biomass burning emissions accounted for 33 % of EC and 22 % of OM at MSY (Minguillón et al., 2011). Nevertheless, these contributions are much lower than those obtained at other European regions (Pio et al., 2011).

SS components were found mainly in the PM_{1-10} fraction at both sites (Figs. 3 and S5) as we expected. In the continental background, the lower variation of SS concentrations as a function of atmospheric episodes reflects the minor impact of marine aerosols in this continental background area.

Most of the trace elements showed a prevalent fine-grain size distribution at MSC and MSY (Fig. S8), especially the ones included in the industrial and road traffic group and in the fuel oil combustion group. V, Cr, Co, Ni, and As were also found in the PM_{1-10} fraction because these elements are also present in clay mineral assemblages.

3.3 Atmospheric episodes affecting continental and regional background aerosol chemical composition in the western Mediterranean

The WMB is affected by peculiar atmospheric episodes which influence aerosol chemical composition. At the MSC site, a higher frequency of Atlantic advections was detected, whereas the MSY site was more influenced by regional episodes (Fig. 1). However, the seasonal distribution of the main atmospheric episodes throughout the year is very similar at both sites. The NAF episodes were more frequent from March to October (17 and 18 % of the days, at MSC and MSY, respectively), and very often they alternated with the SREG scenarios (12 and 27 % of the days) or both episodes occurred simultaneously, when the NAF air masses travel at high altitudes and the stagnation of air masses prevails at surface levels (Escudero et al., 2005). The WREG scenarios were detected from October to March (11 and 27 % of the days), as were the EU episodes (11 and 13 % of the days). Air masses from the Atlantic (AN, ANW, and ASW) affected the WMB throughout the year (62 and 41 % of the days). Conversely, the MED episodes were detected sporadically (4 % of the days at both sites), and therefore conclusions on their characteristics will not be drawn in the present study. Moreover, the WMB is affected by sporadic large wildfire events, especially during summer (Cristofanelli et al., 2009).

3.3.1 North African episodes (NAF)

The non-NAF-to-NAF increase in PM_1 concentrations is estimated to be 2.9 $\mu g\,m^{-3}$ and 4.6 $\mu g\,m^{-3}$ at MSC and MSY, respectively, whereas this increase in PM_{1-10} concentrations is estimated to be 14.3 $\mu g\,m^{-3}$ and 7 $\mu g\,m^{-3}$ (Figs. 4 and 5). The PM_1 non-NAF-to-NAF increase was attributed to the increment of PM_1 MM, sulfate, nitrate, ammonium, OM, and EC (Figs. S5 and S6). In relative contribution the highest difference in PM_1 concentrations was recorded for MM at MSC (Fig. 4), thus evidencing that NAF episodes also affect the fine fraction.

On the other hand, the higher concentrations of PM_{1-10} MM under NAF episodes accounted for the non-NAF-to-NAF increase of PM_{1-10} concentrations. Additionally, average concentrations of trace elements from the mineral group were higher at the continental background site than at the regional background site under NAF episodes (Fig. S6). Concentrations of nitrate and sulfate were high during NAF episodes at both sites when compared with the average (Figs. S5 and S7b). At MSY concentrations of coarse ammonium and EC also increased.

The higher impact of NAF scenarios on the continental than on the regional background aerosols in the WMB confirms that African dust travels preferentially at high altitudes. The concurrent increase of secondary pollutants (nitrate and sulfate) at MSC demonstrates that dust arrives together with industrial pollutants, as shown at the Canary Islands by Rodríguez et al. (2011). The relatively high concentrations of secondary pollutants and EC during NAF at MSY in PM_1 and PM_{1-10} can be related to the interaction of dust with anthropogenic pollutants. During NAF episodes a compression of the PBL is observed at regional scale (Alastuey et al., 2005; Pandolfi et al., 2013) (Fig. S9), and a dominance of southern winds during the whole day breaks the regular sea breeze circulation (Jorba et al., 2013). These processes enhance the concentration of regional pollutants in the lowest part of the troposphere and inhibit the sea breeze "clean-up" effect.

The net contribution of African dust to the PM_{10} concentrations was estimated to be 16 % at MSC and 11 % at MSY. This is in agreement with results presented by Pey et al. (2013b).

An example of the impact of NAF episodes on the continental and regional background aerosols was recorded on 26 March 2011 (Fig. 5b). Backward trajectory for this day clearly showed a North African air mass origin (Fig. S10), and the Navy Aerosol Analysis and Prediction System (NAAPS) indicated high dust surface concentrations over the Iberian Peninsula (Fig. S11). During this episode, dust transport more strongly affected MSC than MSY, with PM_{10} MM concentration reaching 16 $\mu g\,m^{-3}$ at MSC (more than 5 times higher than the annual average) and 9 $\mu g\,m^{-3}$ at MSY (about 3 times higher than the annual average). At MSC, concentrations of MM increased simultaneously with those of sulfate

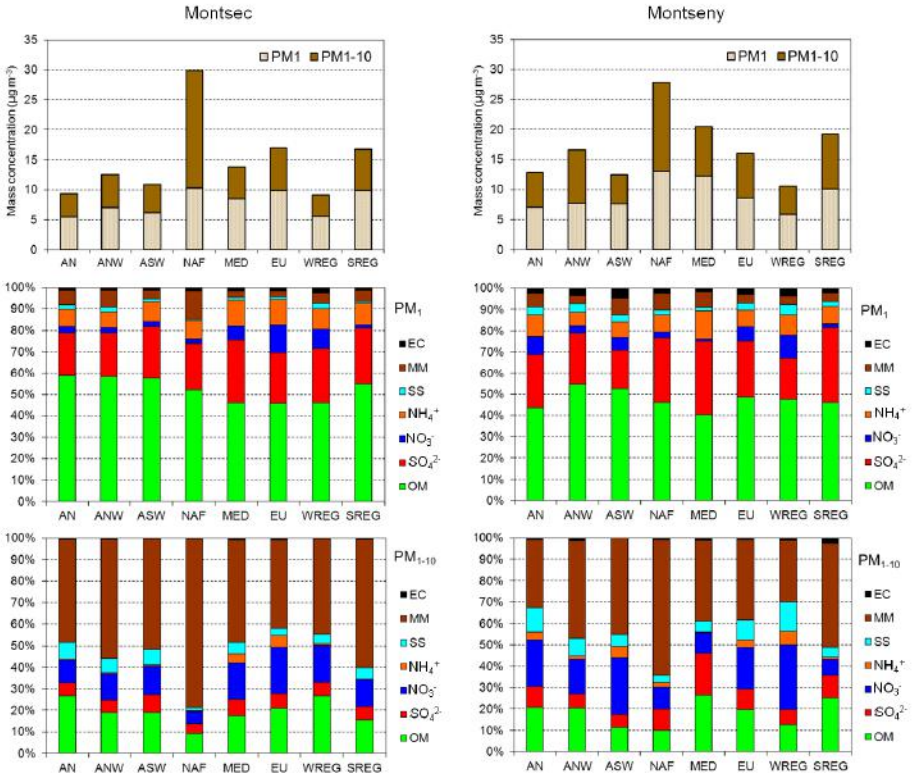

Figure 4. Average concentrations of PM_1 and PM_{1-10} mass and relative contribution of aerosol major components in PM_1 and PM_{1-10} fractions for different meteorological episodes at Montsec and Montseny based on daily measurements between January 2010 and March 2013.

(2 times higher than the annual average), nitrate (3 times), and other anthropogenic elements, such as Sb and EC, reflecting that dust is transported together with these pollutants. The increments of absolute concentrations of nitrate, sulfate, Sb, and EC were higher at MSY than MSC, probably due to the aforementioned effect of both the PBL compression and the breeze.

3.3.2 Summer regional episodes (SREG)

The importance of the SREG scenarios in the WMB has been studied in a number of works (e.g. Escudero et al., 2005; Gangoiti et al., 2001; Millan et al., 1997; Rodríguez et al., 2002). These episodes take place under a weak barometric gradient and a lack of advections in summer, which causes the recirculation of air masses over the WMB. Generally, these situations last for several days, favoring the accumulation of pollutants at regional scale, increasing the magnitude of convection and aging processes, and enhancing the dust resuspension and the formation of secondary organic and inorganic aerosols. For these reasons, under SREG episodes high concentrations of PM_1 and PM_{1-10} were measured at the regional background site (Fig. 4). The PM_1 increase was attributed to higher concentrations of PM_1 sulfate, OM, EC, and trace elements of industrial and road traffic group, and the PM_{1-10} increase was attributed to higher concentrations of PM_{1-10} MM, OM, and EC (Figs. S5, S6 and S8).

In spite of the high altitude of MSC, the continental background site was also affected by this type of episodes due to a higher development of the PBL over the continental areas (Fig. S9), which favors the transport of anthropogenic pollutants towards high-altitude sites such as MSC and enhances the dust resuspension (Figs. 4, S5, S6 and S8).

High concentrations of elements such as Ca, Mg, Sr, and Mn during SREG scenarios (Fig. S6) confirm the local/regional origin of these dust particles at both sites. However, the ratio of concentrations of these specific elements with respect to Al during SREG scenarios was higher at MSC compared to MSY, probably because of the calcareous (richer in Ca, Mg, Sr, and Mn) nature of the Montsec Range as opposed to the slate and granitic composition (richer in Al) of the Montseny Range.

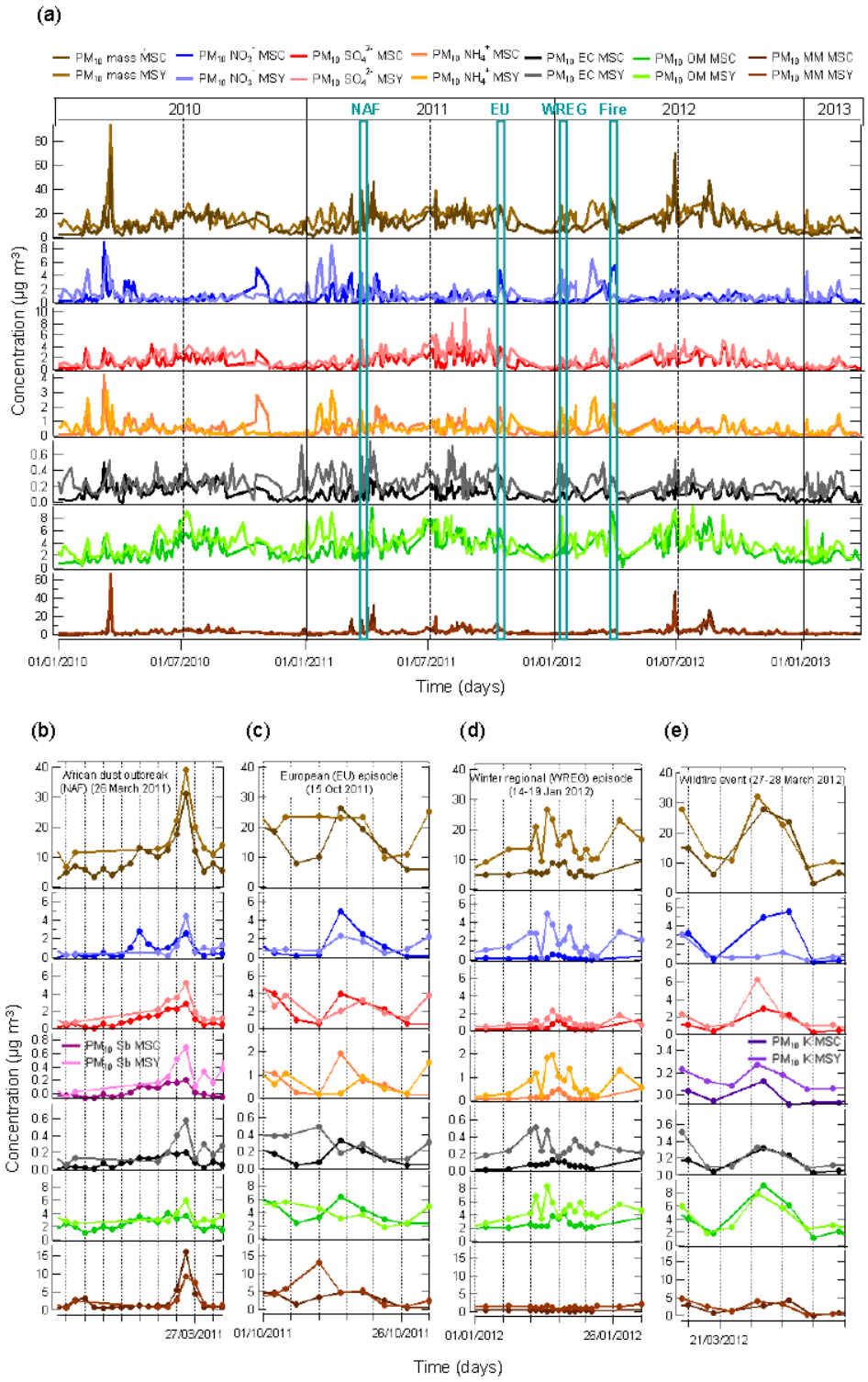

Figure 5. (a) Time series of daily PM_{10} mass and major PM_{10} chemical components concentrations at Montsec (MSC) and Montseny (MSY) between January 2010 and March 2013. Green bands indicate four examples of different episodes affecting the study area. Zoom of the four selected meteorological episodes – (b) African dust outbreak, (c) European episode, (d) winter regional episode, and (e) wildfire event – with daily PM_{10} mass and PM_{10} chemical components concentrations.

3.3.3 Winter regional episodes (WREG)

The WREG episodes affecting the WMB have been described by Pey et al. (2010) as winter anticyclonic episodes (WAEs), based on a comparison between urban and regional background sites. In the present study the WREG episodes showed low concentrations of PM_1 and PM_{1-10} on average (Fig. 4), but the chemical composition revealed the higher relative contribution of anthropogenic sources and the lower relative proportion of natural emissions, with high concentrations of PM_1 nitrate, ammonium, OM, and EC and the lowest concentrations of PM_{1-10} OM and MM, especially at MSY (Figs. S5, S6 and S7a).

The impact of these episodes on the continental and regional background aerosols can be explained by the persistence of anticyclonic conditions in the WMB. During these situations the stagnation of air masses occurs, which increases the pollution around the emission sources (mainly urban and industrial areas); therefore regional and continental background areas are presumably free of this anthropogenic pollution. However, the meteorological conditions (sunny days and thermal inversion) together with the topography of the WMB (very mountainous) may develop mountain breezes. In this case, the anthropogenic pollution accumulated over the adjacent valleys reaches regional background sites and rarely continental background areas as intense pollution episodes.

Figure 5d shows an example of a WREG episode affecting the WMB during the period 14–19 January 2012. Backward trajectory of air masses for these days corroborates a WREG situation (Fig. S10). During this episode PM_{10} nitrate, ammonium, EC, and OM concentrations at the regional background site increased from 0.2 $\mu g\,m^{-3}$, 0.2 $\mu g\,m^{-3}$, 0.2 $\mu g\,m^{-3}$, and 3.4 $\mu g\,m^{-3}$ on 13 January to 1.3–5.0 $\mu g\,m^{-3}$, 0.6–1.9 $\mu g\,m^{-3}$, 0.2–0.5 $\mu g\,m^{-3}$, and 3.7–8.4 $\mu g\,m^{-3}$ between 14 and19 January 2012, respectively. Simultaneously, the continental background site was almost unaffected by such polluted air masses since nitrate, ammonium, EC, and OM concentrations in PM_{10} remained 0.1–0.6 $\mu g\,m^{-3}$, 0.1–0.5 $\mu g\,m^{-3}$, 0.05–0.13 $\mu g\,m^{-3}$, and 2.3–4.2 $\mu g\,m^{-3}$, respectively.

3.3.4 European episodes (EU)

During EU episodes air masses from central and eastern Europe are transported towards the WMB, crossing the whole continent. This type of episode is associated with cold meteorological conditions and polluted air masses (Pey et al., 2010). For this reason, under EU episodes high concentrations of PM_1 and PM_{1-10} were measured at both sites (Fig. 4). This increase was attributed to higher concentrations of nitrate, ammonium, OM, EC, and trace elements of industrial and road traffic group at both fractions PM_1 and PM_{1-10}, especially at MSC (Figs. S5 and S8).

The higher impact of EU scenarios on the continental background aerosols than on the regional background aerosols confirms that the transport of pollutants occurs preferentially at high altitude layers (915–1930 m), as observed by Sicard et al. (2011).

An example of the impact of EU episodes on the continental and regional background aerosols was recorded on 15 October 2011 (Fig. 5c). During this episode the air mass remained 3 days over central Europe before reaching the WMB, as shown by the backward trajectory (Fig. S4). Under these meteorological conditions PM_{10} nitrate, sulfate, ammonium, EC, and OM daily concentration at MSC reached 5 $\mu g\,m^{-3}$ (6 times higher than the annual average), 4 $\mu g\,m^{-3}$ (about 3 times higher than the annual average), 2 $\mu g\,m^{-3}$ (more than 4 times higher than the annual average), 0.3 $\mu g\,m^{-3}$ (almost 3 times higher than the annual average), and 6.4 $\mu g\,m^{-3}$ (about 2 times higher than the annual average), respectively. Simultaneously, the regional background site was less affected by this episode as PM_{10} nitrate, sulfate, ammonium, EC, and OM concentrations at MSY were 2.3 $\mu g\,m^{-3}$ (1 $\mu g\,m^{-3}$ higher than the annual average), 2.0 $\mu g\,m^{-3}$, 0.2 $\mu g\,m^{-3}$, 0.2 $\mu g\,m^{-3}$, and 3.2 $\mu g\,m^{-3}$, respectively.

3.3.5 Atlantic advections (AN, ANW, ASW)

The WMB is strongly affected by oceanic air masses owing to the large influence of Atlantic winds over this region, which is favored by the displacement of the Azores High westwards or southwards, allowing the movement of depression systems towards the Mediterranean (Lopez-Bustins et al., 2008). This type of episodes is associated with increased precipitation and intense winds, which favor the atmospheric wet-scavenging processes, leading to the renovation of the regional aged air masses.

These meteorological conditions explain why low PM_1 and PM_{1-10} concentrations were measured under Atlantic advections at both sites (Fig. 4) and for most of the aerosol chemical components (Figs. S5, S6, and S8).

3.3.6 Wildfire events

Although biomass burning is not a major source in the WMB, some contribution of biomass burning is observed and partially attributed to wildfires. Therefore, high concentrations of PM_1 OM and EC during NAF and SREG episodes (Fig. S5) were partially attributed to a higher frequency of wildfires, since these episodes very often occur simultaneously.

Figure 5e illustrates the impact of a wildfire on continental and regional background aerosols in the WMB. This event took place in eastern Europe on 27–28 March 2012, as shown by the NAAPS model with high smoke surface concentrations over SE Europe (Fig. S11). Backward trajectory for these days clearly showed a transport of air masses

from SE Europe towards the WMB (Fig. S10). During this episode, daily PM_{10} OM and EC concentration at MSY reached 7.9 $\mu g\,m^{-3}$ (almost 2 times higher than the annual average) and 0.3 $\mu g\,m^{-3}$ (1.5 times higher than the annual average), respectively, and at MSC it was 9.1 $\mu g\,m^{-3}$ (almost 3 times higher than the annual average) and 0.3 $\mu g\,m^{-3}$ (3 times higher than the annual average). Moreover, K concentrations in PM_{10} at MSY reached 0.27 $\mu g\,m^{-3}$ (2 times higher than the annual average), with a prevalent fine partitioning ($PM_1/PM_{10} = 0.55$), instead of its main coarse occurrence ($PM_1/PM_{10} = 0.28$) during NAF episodes, which confirms the biomass burning origin.

3.4 Seasonal variation of continental and regional background aerosol chemical composition in the western Mediterranean

In addition to the atmospheric episodes discussed above, the aerosols in the WMB are also affected by the different evolution of the PBL height and differences in the meteorological parameters throughout the year. In the warmer months (April–September) the development of the PBL at MSC is much more relevant than that at MSY (Figs. S2 and S9), owing to the higher convection at the continental background sites (Rodríguez et al., 2002) and to the greater cooling effect from the sea breeze at the regional background sites. On the other hand, in the colder months (October–March) the lower vertical development of the PBL at the inland sites leaves MSC in the FT on most days, whereas the regional background site is located most of the day within the PBL (Fig. S2).

Nitrate concentrations decreased in summer at both sites, especially in PM_1 (Fig. 6) (2 and 3 times lower than the winter concentrations at MSC and MSY, respectively). This decrease was attributed to the high volatility of ammonium nitrate (Pey et al., 2009) at low humidity and high temperature (Zhuang et al., 1999b). During the colder months higher nitrate concentrations are associated with WREG episodes at MSY and with EU episodes at MSC, with the exception of the November-to-January period, when MSC is mostly within the FT and therefore low nitrate concentrations were registered.

Sulfate showed similar seasonal variations at both sites and relatively similar absolute concentrations, with the highest values during the warmer months (3 and 2 times higher than the winter concentrations at MSC and MSY, respectively) (Fig. 6). The squared Pearson correlation coefficient between the daily sulfate concentrations at MSC and MSY was 0.71. This similarity reflects the high stability of sulfate and its longer residence time in the atmosphere, resulting in a homogeneous sulfate concentration in the WMB. The summer maximum was likely due to the higher photochemistry in the atmosphere that enhances the SO_2 oxidation (6 $\%\,h^{-1}$ in summer vs. $< 1\,\%\,h^{-1}$ in winter; Querol et al., 1999) and to the accumulation of pollutants over the WMB as a result of the SREG and NAF episodes. Additionally, regional background sulfate aerosols in summer could be affected by the transport of shipping emissions from the Mediterranean to the continental areas, due to the more intense sea breeze circulation at MSY. The lower concentrations during the colder months were attributed to the lower rate of SO_2 oxidation (Querol et al., 1999), and at MSC to the FT conditions.

Ammonium concentration did not follow a clear seasonal pattern (Fig. 6) due to its association with both sulfate and nitrate.

Organic matter concentrations followed a similar seasonal variation at both sites, with the highest values during the warmer months (1.8 and 1.5 times higher than the winter concentrations at MSC and MSY, respectively) (Fig. 6). The summer maximum was due to (1) the higher temperature and photochemistry in the atmosphere that enhances the formation of SOA; (2) the accumulation of pollutants over the WMB owing to the occurrence of SREG and NAF episodes; (3) the greater biogenic emissions from vegetation (Seco et al., 2011); and (4) the higher frequency of wildfires. Furthermore, at MSY a secondary maximum of OM concentrations occurred in October–March, linked to the occurrence of WREG episodes. The continental background site was less affected by this type of episodes, since MSC is mostly within the FT in winter.

Elemental carbon showed high concentrations in the warmer months at MSC and a less marked seasonal variation at MSY (Fig. 6). The smoother seasonal variation at MSY reflects the regional anthropogenic influence on the levels of this component, since anthropogenic emissions occur throughout the year. The higher summer EC concentrations at both sites (more elevated at MSY) were attributed to the impact of the SREG and NAF episodes, and to the higher occurrence of wildfires. Additionally, at MSY high concentrations of EC in summer may be caused by the greater transport of shipping emissions. The increase of EC during the colder months was not registered simultaneously at both environments (Fig. 6) because at the regional background site it was attributed to the impact of WREG episodes, whereas at the continental background site it was associated with EU episodes.

Mineral matter concentrations and mineral trace elements in the WMB are driven by the local and regional dust resuspension and by the contribution of African dust outbreaks, both enhanced in the warmer months. Consequently, the highest values were measured in summer and the lowest in winter, with sporadic high concentrations in March–April (Figs. 6 and 7).

Trace elements concentrations of the industrial and road traffic group showed low variations, especially at MSY (Fig. 7), since anthropogenic emissions occur throughout the year. Fuel oil combustion elements showed a marked seasonal pattern at both sites, with the highest values in summer (Fig. 7) due to the higher shipping emissions and the more

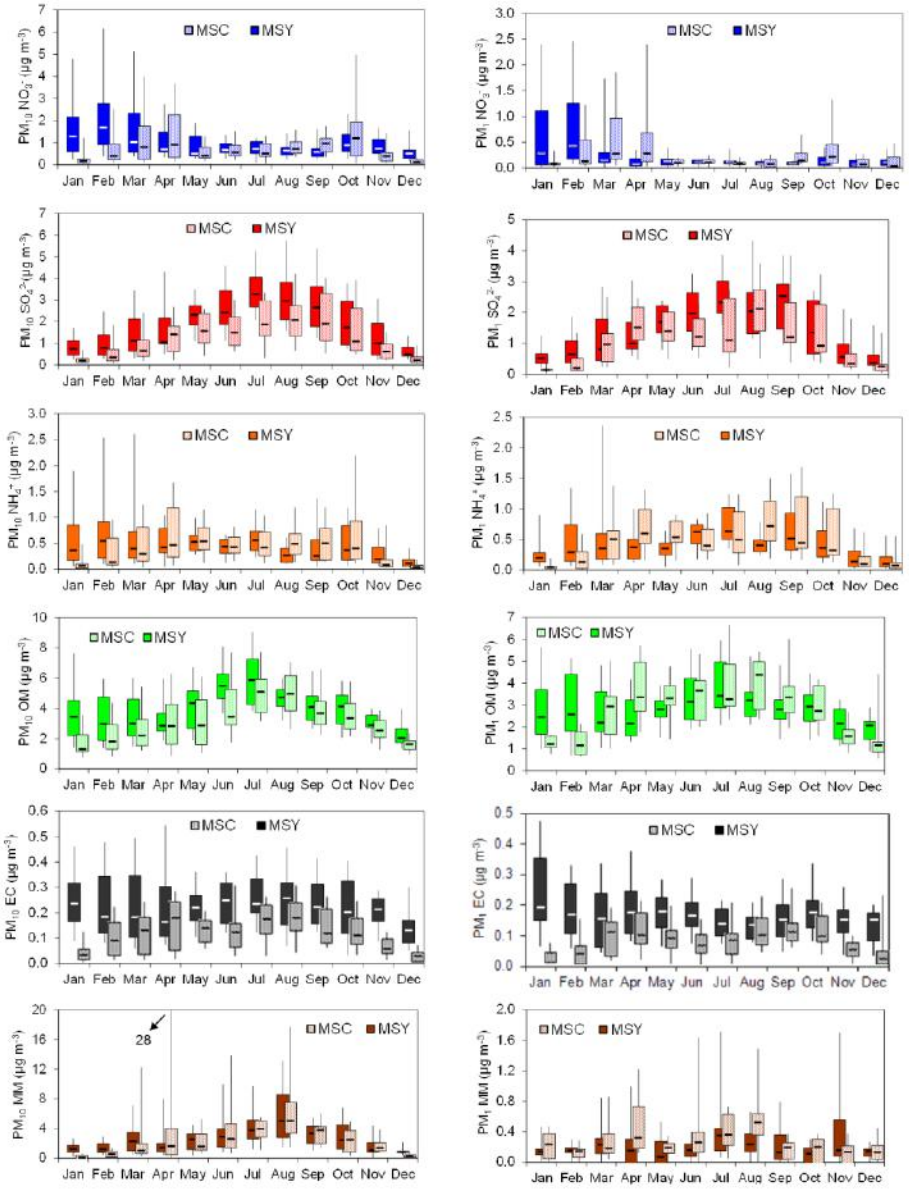

Figure 6. Monthly median (black line within the boxes) and percentiles (5–25–75–95, boxes and whiskers) of major PM_{10} and PM_1 chemical components concentrations at Montsec (MSC) and Montseny (MSY) based on daily measurements between January 2010 and March 2013.

frequent and intense sea breeze circulation, which enhances the transport of air masses from the Mediterranean Sea.

4 Conclusions

Aerosol chemical characterization (PM_1, PM_{1-10}, and PM_{10}) and its time variation were studied during January 2010–March 2013 simultaneously at a continental (Montsec, MSC) and a regional (Montseny, MSY) background site in the western Mediterranean Basin.

In this particular region of the WMB, the continental-to-regional background increase was estimated to be 4.0 $\mu g\,m^{-3}$ for PM_{10} and 1.1 $\mu g\,m^{-3}$ for PM_1. Relative chemical composition and absolute concentrations of PM_X showed very similar values at both environments, especially in PM_1, in spite of their altitudinal and longitudinal differences. The similarities are more pronounced in the warmer months, when recirculation processes at a regional scale are recurrent in the WMB,

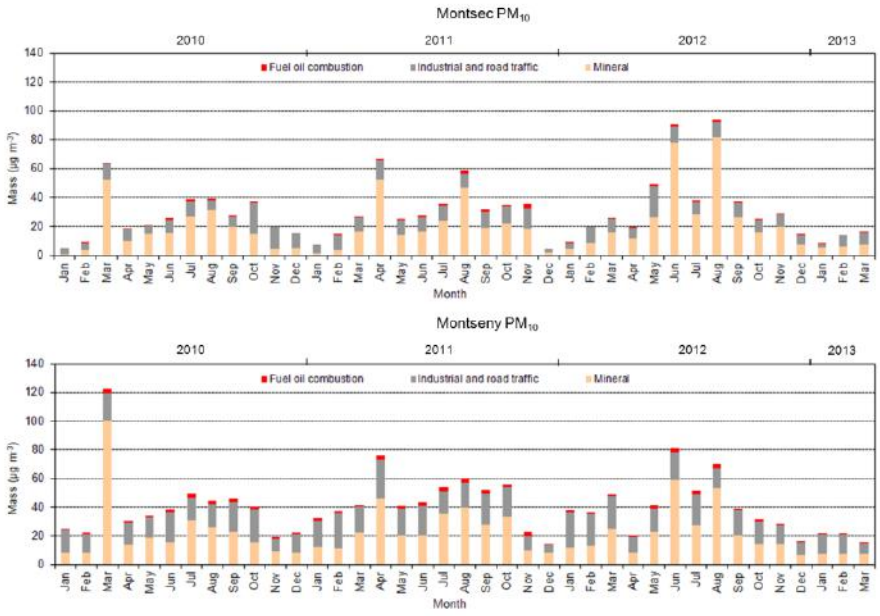

Figure 7. Monthly average concentrations of trace element groups at Montsec and Montseny based on daily measurements of PM_{10} between January 2010 and March 2013.

and a strong development of the PBL occurs over continental areas, favoring the transport of anthropogenic pollutants towards remote sites such as MSC. These processes cause a homogenization of PM_1 concentration and composition throughout the region, allowing us to consider PM_1 as a more suitable indicator of anthropogenic impact than PM_{10}. Moreover, the higher temperature and solar radiation in the warmer months augment atmospheric photochemistry, promoting the formation of secondary inorganic and organic aerosols, and thus incrementing markedly the concentration of certain components such as sulfate and OM. Additionally, sea breeze circulation is enhanced, favoring the transport of shipping emissions from the Mediterranean to the continental areas and thereby increasing the concentrations of sulfate, EC, and fuel-oil-combustion-related trace elements, especially at the regional background since it is located closer to the coast. Furthermore, the occurrence of wildfires across the WMB increases in summer, which contributes to an extra increment of the OM and EC concentrations. Conversely, nitrate is not abundant in summer due to the high volatility of ammonium nitrate at high temperatures and low humidity. In the colder months the lower vertical development of the PBL leaves MSC in the FT on most days, whereas MSY is frequently located within the PBL due to its lower elevation. As a result, very low concentrations of all chemical components are recorded at MSC in winter, while MSY is regularly affected by nearby polluted air masses, which enhanced the concentrations of PM_X components.

The seasonal variation of major and trace PM_X components was also governed by changes in the air mass origin from summer to winter. Whereas southern flows and regional recirculation episodes are more frequent in summer, Atlantic advections and northeastern winds from mainland Europe are more common in winter. As a result, African dust outbreaks and regional dust resuspension increase MM concentrations over the WMB in the warmer months. This MM increase affects both PM_1 and PM_{1-10}, and it is frequently more pronounced at MSC, since long-range transport of dust occurs preferentially at high altitude layers and dust resuspension is enhanced by the drier surface and higher convection at this site. During NAF episodes concentrations of nitrate and sulfate also increase, demonstrating that dust arrives together with industrial pollutants. Moreover, a compression of the PBL and a change in the wind regime towards a permanent southern flow increase the concentrations of regional pollutants (sulfate, EC, and industrial and traffic tracers) in the lowest part of the troposphere. Regional recirculation of air masses (SREG episodes) also accounts for the accumulation of airborne particulates, increasing the concentrations of sulfate, OM, EC, industrial, traffic, and fuel oil combustion tracers at both continental and regional background environments.

In the colder months, the predominance of clean Atlantic advections prevents the accumulation of regional pollution and consequently reduces the concentration of all chemical components at both sites. However, the sporadic transport of polluted air masses from central and eastern Europe towards

the WMB increases the concentrations of nitrate, OM, EC, and industrial and traffic-related trace elements. The impact of these polluted air masses on the concentrations of PM_X components is usually higher in the continental background, since this transport from Europe occurs preferentially at high altitude layers. Occasionally, intense peaks of nitrate, OM, and EC are measured at the regional background site during the winter anticyclonic episodes (WREG). These stagnant situations cause the accumulation of pollutants around the emission sources (such as the Barcelona metropolitan area), and pollutants can be transported towards relatively nearby areas under favorable conditions. The distance from MSC to large anthropogenic sources and its altitude are restricting factors for the occurrence of this process.

Finally, the comparison of these results with those from other continental and regional background sites in central Europe shows that African dust transport and regional dust resuspension are much more important in the western Mediterranean area. The net contribution of African dust to the PM_{10} concentrations was estimated to be 16 % at MSC and 11 % at MSY. This is reflected in more elevated concentrations of mineral elements across the Mediterranean, with the only exception being potassium, higher in central Europe due to the contribution of biomass burning emissions. The surprising similar sulfate concentrations across Europe in both continental and regional background environments are probably linked to the long residence time of sulfate aerosols in the atmosphere. However, nitrate and ammonium showed different concentrations as a function of site, and nitrate maximum concentration was observed in winter in the WMB, whereas in the central Europe continental environments it was measured in summer. Moreover, the highest concentrations of typical anthropogenic trace elements were recorded at some European rural environments, with the exception of V, which was higher in the Mediterranean area due to the greater influence of shipping emissions.

The concurrent monitoring of aerosol properties in continental and regional background sites in the WMB provides a complete picture of the aerosol phenomenology of this region. In view of the relatively high concentrations of atmospheric aerosols from a variety of natural and anthropogenic sources, and taking into account the importance of atmospheric processes, the simultaneous characterization of atmospheric aerosols at continental and regional background sites provides valuable information to policy makers and air quality and climate models.

The Supplement related to this article is available online at doi:10.5194/acp-15-1129-2015-supplement.

Acknowledgements. This study was supported by the Ministry of Economy and Competitiveness and FEDER funds under the PRISMA (CGL2012-39623-C02-1) and CARIATI (CGL2008-06294/CLI) projects, and by the Generalitat de Catalunya (AGAUR 2009 SGR8 and the DGQA). The research received funding from the European Union Seventh Framework Programme (FP7/ 2007-2013) ACTRIS under grant agreement no. 262254. The authors would like to extend their gratitude to the personnel from the COU and the OAdM. We would also like to express our gratitude to the NOAA Air Resources Laboratory (ARL) for the provision of the HYSPLIT transport and dispersion model, and boundary layer height calculation, used in this publication.

Edited by: P. Formenti

References

Alastuey, A., Querol, X., Castillo, S., Escudero, M., Avila, A., Cuevas, E., Torres, C., Romero, P., Exposito, F., and Garcia, O.: Characterisation of TSP and $PM_{2.5}$ at Izaña and Sta. Cruz de Tenerife (Canary Islands, Spain) during a Saharan Dust Episode (July 2002), Atmos. Environ., 39, 4715–4728, doi:10.1016/j.atmosenv.2005.04.018, 2005.

Amato, F., Pandolfi, M., Escrig, A., Querol, X., Alastuey, A., Pey, J., Perez, N., and Hopke, P. K.: Quantifying road dust resuspension in urban environment by Multilinear Engine: a comparison with PMF2, Atmos. Environ., 43, 2770–2780, doi:10.1016/j.atmosenv.2009.02.039, 2009.

Andrews, E., Ogren, J. A., Bonasoni, P., Marinoni, A., Cuevas, E., Rodríguez, S., Sun, J. Y., Jaffe, D. A., Fischer, E. V., Baltensperger, U., Weingartner, E., Coen, M. C., Sharma, S., Macdonald, A. M., Leaitch, W. R., Lin, N.-H., Laj, P., Arsov, T., Kalapov, I., Jefferson, A., and Sheridan, P.: Climatology of aerosol radiative properties in the free troposphere, Atmos. Res., 102, 365–393, doi:10.1016/j.atmosres.2011.08.017, 2011.

Belis, C. A., Karagulian, F., Larsen, B. R., and Hopke, P. K.: Critical review and meta-analysis of ambient particulate matter source apportionment using receptor models in Europe, Atmos. Environ., 69, 94–108, doi:10.1016/j.atmosenv.2012.11.009, 2013.

Bourcier, L., Sellegri, K., Chausse, P., Pichon, J. M., and Laj, P.: Seasonal variation of water-soluble inorganic components in aerosol size-segregated at the puy de Dôme station (1465 m a.s.l.), France, J. Atmos. Chem., 69, 47–66, doi:10.1007/s10874-012-9229-2, 2012.

Burkhardt, J. and Pariyar, S.: Particulate pollutants are capable to "degrade" epicuticular waxes and to decrease the drought tolerance of Scots pine (*Pinus sylvestris* L.), Environ. Pollut., 184, 659–67, doi:10.1016/j.envpol.2013.04.041, 2014.

Carbone, C., Decesari, S., Mircea, M., Giulianelli, L., Finessi, E., Rinaldi, M., Fuzzi, S., Marinoni, a., Duchi, R., Perrino, C., Sargolini, T., Vardè, M., Sprovieri, F., Gobbi, G. P., Angelini, F., and Facchini, M. C.: Size-resolved aerosol chemical composition over the Italian Peninsula during typical summer and winter conditions, Atmos. Environ., 44, 5269–5278, doi:10.1016/j.atmosenv.2010.08.008, 2010.

Carbone, C., Decesari, S., Paglione, M., Giulianelli, L., Rinaldi, M., Marinoni, A., Cristofanelli, P., Didiodato, A., Bonasoni, P.,

Fuzzi, S., and Facchini, M. C.: 3-year chemical composition of free tropospheric PM_1 at the Mt. Cimone GAW global station – South Europe – 2165 m a.s.l., Atmos. Environ., 87, 218–227, doi:10.1016/j.atmosenv.2014.01.048, 2014.

Cavalli, F., Viana, M., Yttri, K. E., Genberg, J., and Putaud, J.-P.: Toward a standardised thermal-optical protocol for measuring atmospheric organic and elemental carbon: the EUSAAR protocol, Atmos. Meas. Tech., 3, 79–89, doi:10.5194/amt-3-79-2010, 2010.

Cozic, J., Verheggen, B., Weingartner, E., Crosier, J., Bower, K. N., Flynn, M., Coe, H., Henning, S., Steinbacher, M., Henne, S., Collaud Coen, M., Petzold, A., and Baltensperger, U.: Chemical composition of free tropospheric aerosol for PM1 and coarse mode at the high alpine site Jungfraujoch, Atmos. Chem. Phys., 8, 407–423, doi:10.5194/acp-8-407-2008, 2008.

Cristofanelli, P., Marinoni, A., Arduini, J., Bonafè, U., Calzolari, F., Colombo, T., Decesari, S., Duchi, R., Facchini, M. C., Fierli, F., Finessi, E., Maione, M., Chiari, M., Calzolai, G., Messina, P., Orlandi, E., Roccato, F., and Bonasoni, P.: Significant variations of trace gas composition and aerosol properties at Mt. Cimone during air mass transport from North Africa – contributions from wildfire emissions and mineral dust, Atmos. Chem. Phys., 9, 4603–4619, doi:10.5194/acp-9-4603-2009, 2009.

Cusack, M., Alastuey, A., Pérez, N., Pey, J., and Querol, X.: Trends of particulate matter ($PM_{2.5}$) and chemical composition at a regional background site in the Western Mediterranean over the last nine years (2002–2010), Atmos. Chem. Phys., 12, 8341–8357, doi:10.5194/acp-12-8341-2012, 2012.

Cusack, M., Pérez, N., Pey, J., Wiedensohler, A., Alastuey, A., and Querol, X.: Variability of sub-micrometer particle number size distributions and concentrations in the Western Mediterranean regional background, Tellus B, 65, 1–19, doi:10.3402/tellusb.v65i0.19243, 2013.

EC: Directive 2008/50/EC of the European Parliament and of the Council of 21 May 2008 on Ambient Air Quality and Cleaner Air for Europe (OJ L 152, 11.6.2008, pp. 1–44), available at: http://eur-lex.europa.eu/homepage.html (last access: 16 June 2014), 2008.

Escudero, M., Castillo, S., Querol, X., Avila, A., Alarco, M., Alastuey, A., Cuevas, E. and Rodríguez, S.: Wet and dry African dust episodes over eastern Spain, J. Geophys. Res., 110, D18S08, doi:10.1029/2004JD004731, 2005.

Gangoiti, G., Millan, M. M., Salvador, R. and Mantilla, E.: Long-range transport and re-circulation of pollutants in the western Mediterranean during the project Regional Cycles of Air Pollution in the West-Central Mediterranean Area, Atmos. Environ., 35, 6267–6276, doi:10.1016/S1352-2310(01)00440-X, 2001.

Gianini, M. F. D., Gehrig, R., Fischer, A., Ulrich, A., Wichser, A., and Hueglin, C.: Chemical composition of PM_{10} in Switzerland: an analysis for 2008/2009 and changes since 1998/1999, Atmos. Environ., 54, 97–106, doi:10.1016/j.atmosenv.2012.02.037, 2012.

IPCC 2013: Climate Change 2013: The Physical Science Basis (Contribution of Working Group I to the Fifth Assessment Report of the Intergovernmental Panel on Climate Change), edited by: Stocker, T. F., Qin, D., Plattner, G. K., Tignor, M. M. B., Allen, S. K., Boschung, J., Nauels, A., Xia, Y., Bex, V., and Midgley, P. M., Cambridge Univ. Press, UK and New York, USA, 2013.

Jimenez, J. L., Canagaratna, M. R., Donahue, N. M., Prevot, A. S. H., Zhang, Q., Kroll, J. H., DeCarlo, P. F., Allan, J. D., Coe, H., Ng, N. L., Aiken, A. C., Docherty, K. S., Ulbrich, I. M., Grieshop, A. P., Robinson, A. L., Duplissy, J., Smith, J. D., Wilson, K. R., Lanz, V. A., Hueglin, C., Sun, Y. L., Tian, J., Laaksonen, A., Raatikainen, T., Rautiainen, J., Vaattovaara, P., Ehn, M., Kulmala, M., Tomlinson, J. M., Collins, D. R., Cubison, M. J., Dunlea, E. J., Huffman, J. A., Onasch, T. B., Alfarra, M. R., Williams, P. I., Bower, K., Kondo, Y., Schneider, J., Drewnick, F., Borrmann, S., Weimer, S., Demerjian, K., Salcedo, D., Cottrell, L., Griffin, R., Takami, A., Miyoshi, T., Hatakeyama, S., Shimono, A., Sun, J. Y., Zhang, Y. M., Dzepina, K., Kimmel, J. R., Sueper, D., Jayne, J. T., Herndon, S. C., Trimborn, A. M., Williams, L. R., Wood, E. C., Middlebrook, A. M., Kolb, C. E., Baltensperger, U., and Worsnop, D. R.: Evolution of organic aerosols in the atmosphere, Science, 326, 1525–1529, doi:10.1126/science.1180353, 2009.

Jorba, O., Pandolfi, M., Spada, M., Baldasano, J. M., Pey, J., Alastuey, A., Arnold, D., Sicard, M., Artiñano, B., Revuelta, M. A., and Querol, X.: Overview of the meteorology and transport patterns during the DAURE field campaign and their impact to PM observations, Atmos. Environ., 77, 607–620, doi:10.1016/j.atmosenv.2013.05.040, 2013.

Laj, P., Klausen, J., Bilde, M., Plaß-Duelmer, C., Pappalardo, G., Clerbaux, C., Baltensperger, U., Hjorth, J., Simpson, D., Reimann, S., Coheur, P.-F., Richter, A., De Mazière, M., Rudich, Y., McFiggans, G., Torseth, K., Wiedensohler, A., Morin, S., Schulz, M., Allan, J. D., Attié, J.-L., Barnes, I., Birmili, W., Cammas, J. P., Dommen, J., Dorn, H.-P., Fowler, D., Fuzzi, S., Glasius, M., Granier, C., Hermann, M., Isaksen, I. S. A., Kinne, S., Koren, I., Madonna, F., Maione, M., Massling, A., Moehler, O., Mona, L., Monks, P. S., Müller, D., Müller, T., Orphal, J., Peuch, V.-H., Stratmann, F., Tanré, D., Tyndall, G., Abo Riziq, A., Van Roozendael, M., Villani, P., Wehner, B., Wex, H., and Zardini, A. A.: Measuring atmospheric composition change, Atmos. Environ., 43, 5351–5414, doi:10.1016/j.atmosenv.2009.08.020, 2009.

Lopez-Bustins, J.-A., Martin-Vide, J. and Sanchez-Lorenzo, A.: Iberia winter rainfall trends based upon changes in teleconnection and circulation patterns, Glob. Planet. Change, 63, 171–176, doi:10.1016/j.gloplacha.2007.09.002, 2008.

Marenco, F., Bonasoni, P., Calzolari, F., Ceriani, M., Chiari, M., Cristofanelli, P., D'Alessandro, A., Fermo, P., Lucarelli, F., Mazzei, F., Nava, S., Piazzalunga, A., Prati, P., Valli, G., and Vecchi, R.: Characterization of atmospheric aerosols at Monte Cimone, Italy, during summer 2004: source apportionment and transport mechanisms, J. Geophys. Res., 111, D24202, doi:10.1029/2006JD007145, 2006.

Millan, M. M., Salvador, R., Mantilla, E., and Kallos, G.: Photooxidant dynamics in the Mediterranean basin in summer: results from European research projects, J. Geophys. Res., 102, 8811–8823, 1997.

Minguillón, M. C., Cirach, M., Hoek, G., Brunekreef, B., Tsai, M., de Hoogh, K., Jedynska, A., Kooter, I. M., Nieuwenhuijsen, M. and Querol, X.: Spatial variability of trace elements and sources for improved exposure assessment in Barcelona, Atmos. Environ., 89, 268–281, doi:10.1016/j.atmosenv.2014.02.047, 2014.

Minguillón, M. C., Perron, N., Querol, X., Szidat, S., Fahrni, S. M., Alastuey, A., Jimenez, J. L., Mohr, C., Ortega, A. M., Day, D. A.,

Lanz, V. A., Wacker, L., Reche, C., Cusack, M., Amato, F., Kiss, G., Hoffer, A., Decesari, S., Moretti, F., Hillamo, R., Teinilä, K., Seco, R., Peñuelas, J., Metzger, A., Schallhart, S., Müller, M., Hansel, A., Burkhart, J. F., Baltensperger, U., and Prévôt, A. S. H.: Fossil versus contemporary sources of fine elemental and organic carbonaceous particulate matter during the DAURE campaign in Northeast Spain, Atmos. Chem. Phys., 11, 12067–12084, doi:10.5194/acp-11-12067-2011, 2011.

Minguillón, M. C., Querol, X., Baltensperger, U., and Prévôt, A. S. H.: Fine and coarse PM composition and sources in rural and urban sites in Switzerland: local or regional pollution?, Sci. Total Environ., 427–428, 191–202, doi:10.1016/j.scitotenv.2012.04.030, 2012.

Mohr, C., DeCarlo, P. F., Heringa, M. F., Chirico, R., Slowik, J. G., Richter, R., Reche, C., Alastuey, A., Querol, X., Seco, R., Peñuelas, J., Jiménez, J. L., Crippa, M., Zimmermann, R., Baltensperger, U., and Prévôt, A. S. H.: Identification and quantification of organic aerosol from cooking and other sources in Barcelona using aerosol mass spectrometer data, Atmos. Chem. Phys., 12, 1649–1665, doi:10.5194/acp-12-1649-2012, 2012.

Moreno, T., Querol, X., Castillo, S., Alastuey, A., Cuevas, E., Herrmann, L., Mounkaila, M., Elvira, J., and Gibbons, W.: Geochemical variations in aeolian mineral particles from the Sahara-Sahel Dust Corridor, Chemosphere, 65, 261–70, doi:10.1016/j.chemosphere.2006.02.052, 2006.

Nyeki, S., Baltensperger, U., Colbeck, I., Jost, D. T., Weingartner, E., and Gäggeler, H. W.: The Jungfraujoch high-alpine research station (3454 m) as a background clean continental site for the measurement of aerosol parameters, J. Geophys. Res., 103, 6097–6107, 1998.

Pandolfi, M., Martucci, G., Querol, X., Alastuey, A., Wilsenack, F., Frey, S., O'Dowd, C. D., and Dall'Osto, M.: Continuous atmospheric boundary layer observations in the coastal urban area of Barcelona during SAPUSS, Atmos. Chem. Phys., 13, 4983–4996, doi:10.5194/acp-13-4983-2013, 2013.

Pérez, N., Pey, J., Castillo, S., Viana, M., Alastuey, A., and Querol, X.: Interpretation of the variability of levels of regional background aerosols in the Western Mediterranean., Sci. Total Environ., 407, 527–40, doi:10.1016/j.scitotenv.2008.09.006, 2008a.

Pérez, N., Pey, J., Querol, X., Alastuey, A., López, J. M., and Viana, M.: Partitioning of major and trace components in PM_{10}–PM2.5–PM_1 at an urban site in Southern Europe, Atmos. Environ., 42, 1677–1691, doi:10.1016/j.atmosenv.2007.11.034, 2008b.

Pey, J., Pérez, N., Castillo, S., Viana, M., Moreno, T., Pandolfi, M., López-Sebastián, J. M., Alastuey, A., and Querol, X.: Geochemistry of regional background aerosols in the Western Mediterranean, Atmos. Res., 94, 422–435, doi:10.1016/j.atmosres.2009.07.001, 2009.

Pey, J., Pérez, N., Querol, X., Alastuey, A., Cusack, M., and Reche, C.: Intense winter atmospheric pollution episodes affecting the Western Mediterranean., Sci. Total Environ., 408, 1951–1959, doi:10.1016/j.scitotenv.2010.01.052, 2010.

Pey, J., Pérez, N., Cortés, J., Alastuey, A., and Querol, X.: Chemical fingerprint and impact of shipping emissions over a western Mediterranean metropolis: Primary and aged contributions, Sci. Total Environ., 497–507, doi:10.1016/j.scitotenv.2013.06.061, 2013a.

Pey, J., Querol, X., Alastuey, A., Forastiere, F., and Stafoggia, M.: African dust outbreaks over the Mediterranean Basin during 2001–2011: PM_{10} concentrations, phenomenology and trends, and its relation with synoptic and mesoscale meteorology, Atmos. Chem. Phys., 13, 1395–1410, doi:10.5194/acp-13-1395-2013, 2013b.

Pio, C. A., Legrand, M., Alves, C. A., Oliveira, T., Afonso, J., Caseiro, A., Puxbaum, H., Sanchez-Ochoa, A., and Gelencsér, A.: Chemical composition of atmospheric aerosols during the 2003 summer intense forest fire period, Atmos. Environ., 42, 7530–7543, doi:10.1016/j.atmosenv.2008.05.032, 2008.

Pio, C., Cerqueira, M., Harrison, R. M., Nunes, T., Mirante, F., Alves, C., Oliveira, C., Sanchez de la Campa, A., Artíñano, B., and Matos, M.: OC/EC ratio observations in Europe: Re-thinking the approach for apportionment between primary and secondary organic carbon, Atmos. Environ., 45, 6121–6132, doi:10.1016/j.atmosenv.2011.08.045, 2011.

Pöschl, U., Martin, S. T., Sinha, B., Chen, Q., Gunthe, S. S., Huffman, J. A., Borrmann, S., Farmer, D. K., Garland, R. M., Helas, G., Jimenez, J. L., King, S. M., Manzi, A., Mikhailov, E., Pauliquevis, T., Petters, M. D., Prenni, A. J., Roldin, P., Rose, D., Schneider, J., Su, H., Zorn, S. R., Artaxo, P., and Andreae, M. O.: Rainforest aerosols as biogenic nuclei of clouds and precipitation in the Amazon, Science, 329, 1513–6, doi:10.1126/science.1191056, 2010.

Putaud, J. P., Van Dingenen, R., Alastuey, A., Bauer, H., Birmili, W., Cyrys, J., Flentje, H., Fuzzi, S., Gehrig, R., Hansson, H. C., Harrison, R. M., Herrmann, H., Hitzenberger, R., Hüglin, C., Jones, A. M., Kasper-Giebl, A., Kiss, G., Kousa, A., Kuhlbusch, T. A. J., Löschau, G., Maenhaut, W., Molnar, A., Moreno, T., Pekkanen, J., Perrino, C., Pitz, M., Puxbaum, H., Querol, X., Rodríguez, S., Salma, I., Schwarz, J., Smolik, J., Schneider, J., Spindler, G., ten Brink, H., Tursic, J., Viana, M., Wiedensohler, A., and Raes, F.: A European aerosol phenomenology – 3: Physical and chemical characteristics of particulate matter from 60 rural, urban, and kerbside sites across Europe, Atmos. Environ., 44, 1308–1320, doi:10.1016/j.atmosenv.2009.12.011, 2010.

Querol, X., Alastuey, A. S., Puicercus, J. A., Mantilla, E., Miro, J. V, Lopez-soler, A., Plana, F., and Artiñano, B.: Seasonal evolution of suspended particles around a large coal-fired power station: chemical characterization, 32, 719–731, 1998.

Querol, X., Alastuey, A., Lopez-soler, A., Plana, F., and Puicercus, J. A.: Daily evolution of sulphate aerosols in a rural area, northeastern Spain – elucidation of an atmospheric reservoir effect, Environ. Pollut., 105, 397–407, doi:10.1016/S0269-7491(99)00037-8, 1999.

Querol, X., Alastuey, A., Rodríguez, S., Plana, F., Mantilla, E., and Ruiz, C. R.: Monitoring of PM_{10} and $PM_{2.5}$ around primary particulate anthropogenic emission sources, Atmos. Environ., 35, 845–858, doi:10.1016/S1352-2310(00)00387-3, 2001.

Querol, X., Viana, M., Alastuey, A., Amato, F., Moreno, T., Castillo, S., Pey, J., de la Rosa, J., Sánchez de la Campa, A., Artíñano, B., Salvador, P., García Dos Santos, S., Fernández-Patier, R., Moreno-Grau, S., Negral, L., Minguillón, M. C., Monfort, E., Gil, J. I., Inza, A., Ortega, L. A., Santamaría, J. M., and Zabalza, J.: Source origin of trace elements in PM from regional background, urban and industrial sites of Spain, Atmos. Environ., 41, 7219–7231, doi:10.1016/j.atmosenv.2007.05.022, 2007.

Querol, X., Alastuey, A., Pey, J., Cusack, M., Pérez, N., Mihalopoulos, N., Theodosi, C., Gerasopoulos, E., Kubilay, N., and Koçak, M.: Variability in regional background aerosols within the Mediterranean, Atmos. Chem. Phys., 9, 4575–4591, doi:10.5194/acp-9-4575-2009, 2009.

Ripoll, A., Pey, J., Minguillón, M. C., Pérez, N., Pandolfi, M., Querol, X., and Alastuey, A.: Three years of aerosol mass, black carbon and particle number concentrations at Montsec (southern Pyrenees, 1570 m a.s.l.), Atmos. Chem. Phys., 14, 4279–4295, doi:10.5194/acp-14-4279-2014, 2014.

Rodríguez, S., Alastuey, a., Alonso-Pérez, S., Querol, X., Cuevas, E., Abreu-Afonso, J., Viana, M., Pérez, N., Pandolfi, M., and de la Rosa, J.: Transport of desert dust mixed with North African industrial pollutants in the subtropical Saharan Air Layer, Atmos. Chem. Phys., 11, 6663–6685, doi:10.5194/acp-11-6663-2011, 2011.

Rodríguez, S., Querol, X., Alastuey, A., and Mantilla, E.: Origin of high summer PM_{10} and TSP concentrations at rural sites in Eastern Spain, Atmos. Environ., 36, 3101–3112, doi: 10.1016/S1352-2310(02)00256-X, 2002.

Rodríguez, S., Querol, X., Alastuey, A., Viana, M.-M., and Mantilla, E.: Events affecting levels and seasonal evolution of airborne particulate matter concentrations in the Western Mediterranean., Environ. Sci. Technol., 37, 216–222, doi:10.1021/es020106p, 2003.

Seco, R., Peñuelas, J., Filella, I., Llusià, J., Molowny-Horas, R., Schallhart, S., Metzger, A., Müller, M., and Hansel, A.: Contrasting winter and summer VOC mixing ratios at a forest site in the Western Mediterranean Basin: the effect of local biogenic emissions, Atmos. Chem. Phys., 11, 13161–13179, doi:10.5194/acp-11-13161-2011, 2011.

Sicard, M., Rocadenbosch, F., Reba, M. N. M., Comerón, a., Tomás, S., García-Vízcaino, D., Batet, O., Barrios, R., Kumar, D., and Baldasano, J. M.: Seasonal variability of aerosol optical properties observed by means of a Raman lidar at an EARLINET site over Northeastern Spain, Atmos. Chem. Phys., 11, 175–190, doi:10.5194/acp-11-175-2011, 2011.

Takahama, S., Schwartz, R. E., Russell, L. M., Macdonald, A. M., Sharma, S., and Leaitch, W. R.: Organic functional groups in aerosol particles from burning and non-burning forest emissions at a high-elevation mountain site, Atmos. Chem. Phys., 11, 6367–6386, doi:10.5194/acp-11-6367-2011, 2011.

Thurston, G. D. and Spengler, J. D.: A quantitative assessment of source contributions to inhalable particulate matter pollution in metropolitan Boston, Atmos. Environ., 19, 9–25, 1985.

Tositti, L., Riccio, A., Sandrini, S., Brattich, E., Baldacci, D., Parmeggiani, S., Cristofanelli, P., and Bonasoni, P.: Short-term climatology of PM_{10} at a high altitude background station in southern Europe, Atmos. Environ., 65, 142–152, doi:10.1016/j.atmosenv.2012.10.051, 2013.

Wall, S. M., John, W., and Ondo, J. L.: Measurement of aerosol size distributions for nitrate and major ionic species, Atmos. Environ., 22, 1649–1656, doi:10.1016/0004-6981(88)90392-7, 1988.

WHO: Review of Evidence on Health Aspects of Air Pollution – REVIHAAP, First Results, WHO's Regional Office for Europe, Copenhaguen, 28 pp., available at: http://www.euro.who.int/_data/assets/pdf_file/0020/182432/e96762-final.pdf (last access: 16 June 2014), 2013.

Zhuang, H., Chan, C. K., Fang, M., and Wexler, A. S.: Formation of nitrate and non-sea-salt sulfate on coarse particles, Atmos. Environ., 33, 4223–4233, doi:10.1016/S1352-2310(99)00186-7, 1999a.

Zhuang, H., Chan, C. K., Fang, M., and Wexler, A. S.: Size distributions of particulate sulfate , nitrate , and ammonium at a coastal site in Hong Kong, 3, 843–853, doi: 10.1016/S1352-2310(98)00305-7, 1999b.

Supplementary material related to "*Joint analysis of continental and regional background environments in the western Mediterranean: PM_1 and PM_{10} concentrations and composition*"

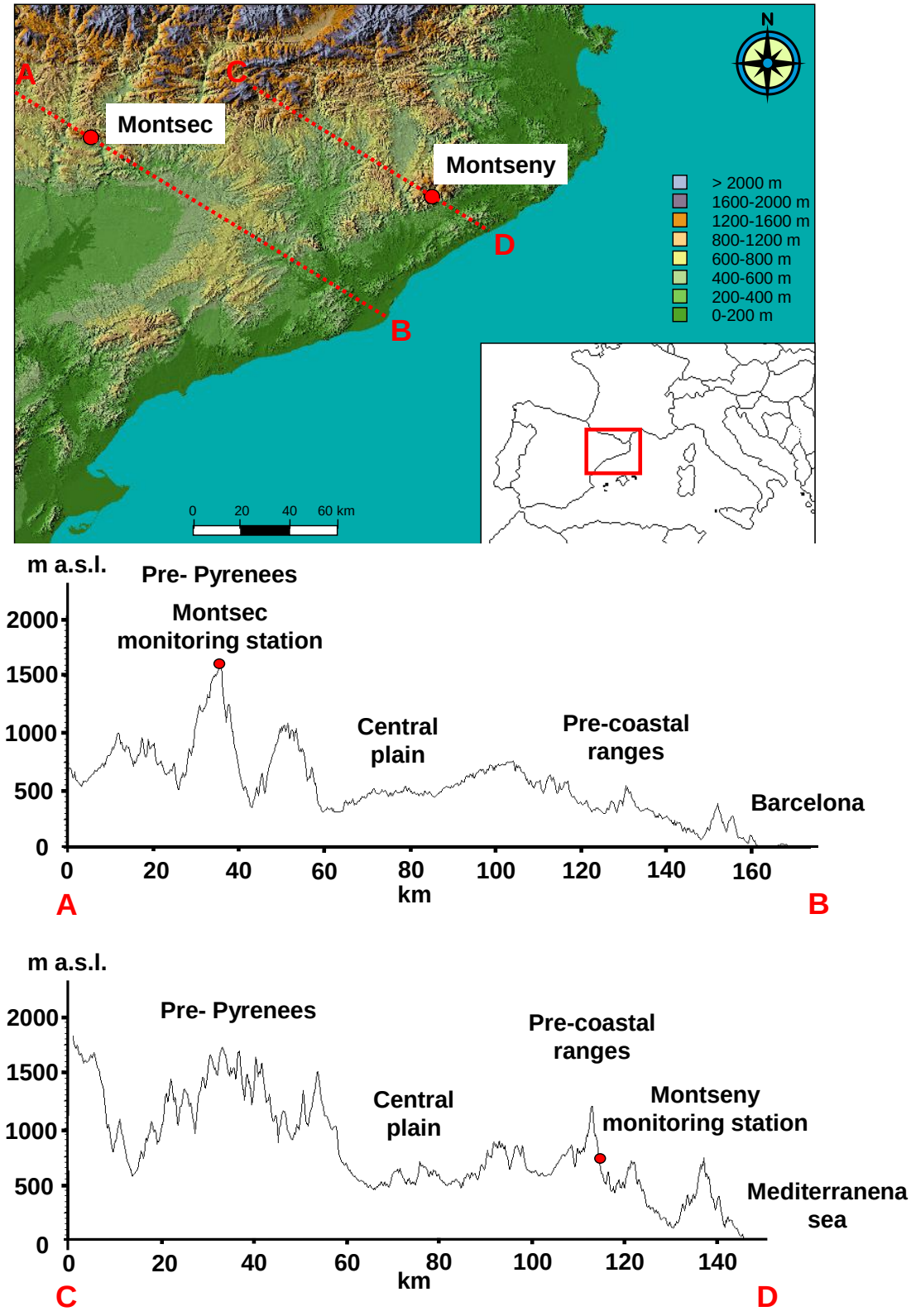

Fig. S1 Top: location of the two monitoring stations (Montsec and Montseny). Bottom: topography of the Montsec and Montseny area.

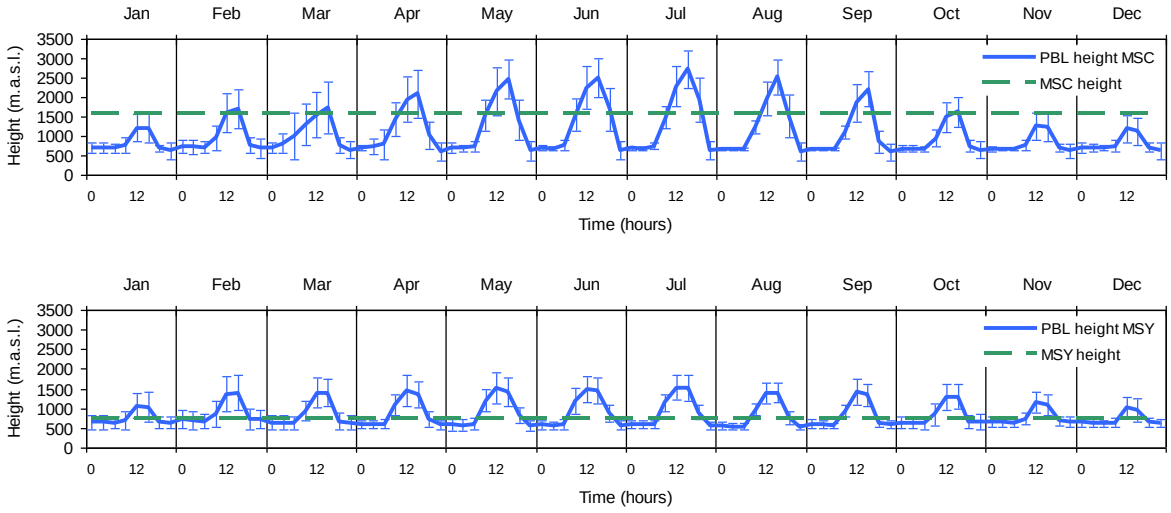

Fig. S2 Diurnal variation of the boundary layer height (computed with HYSPLIT model) averaged for each month at Montsec and Montseny between January 2010 and March 2013.

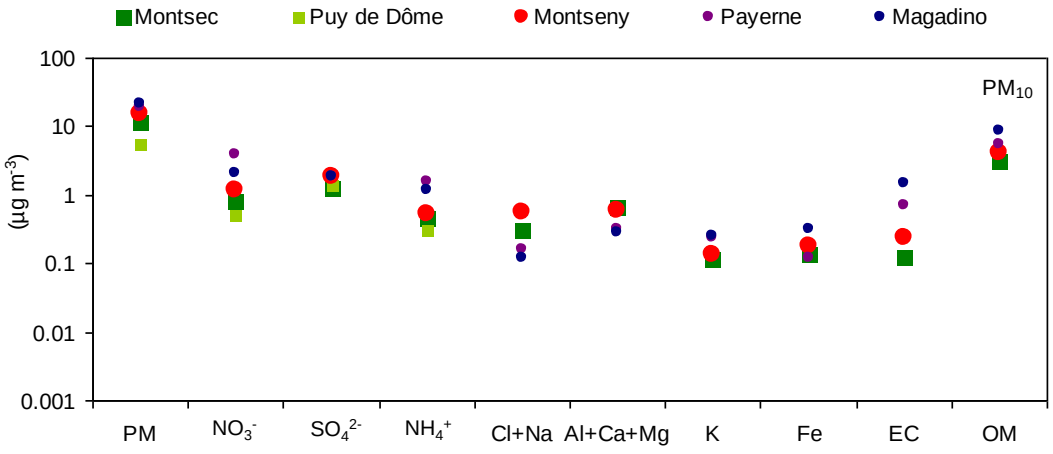

Fig. S3 Average concentrations of PM_{10} major compounds at Montsec (present study), Puy de Dôme (Bourcier et al., 2012)**, Montseny (present study), Payerne and Magadino** (Gianini et al., 2012)**.**

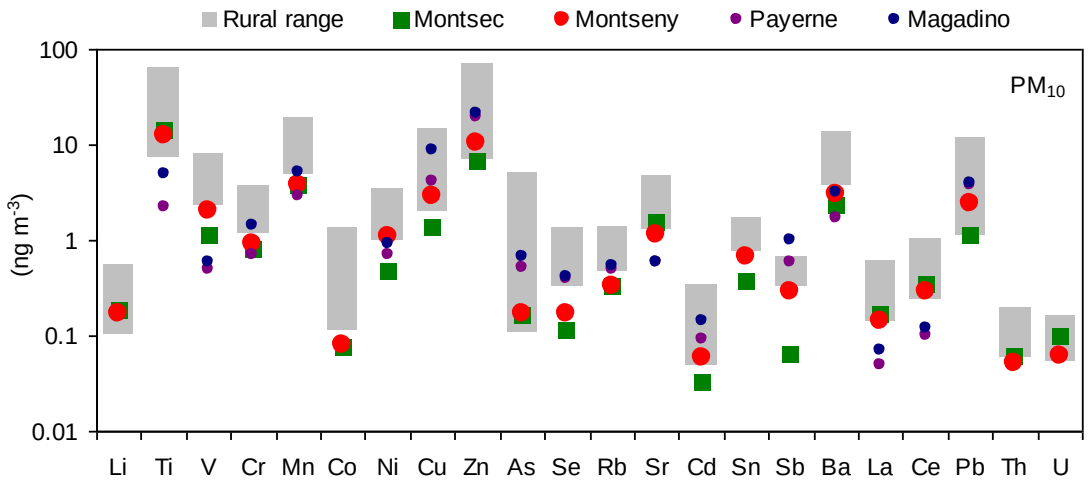

Fig. S4 Average concentrations of PM_{10} trace elements at Montsec and Montseny (present study), and at Payerne and Magadino (Gianini et al., 2012)**, and range of Spanish rural concentrations** (updated from Querol et al., 2007)**.**

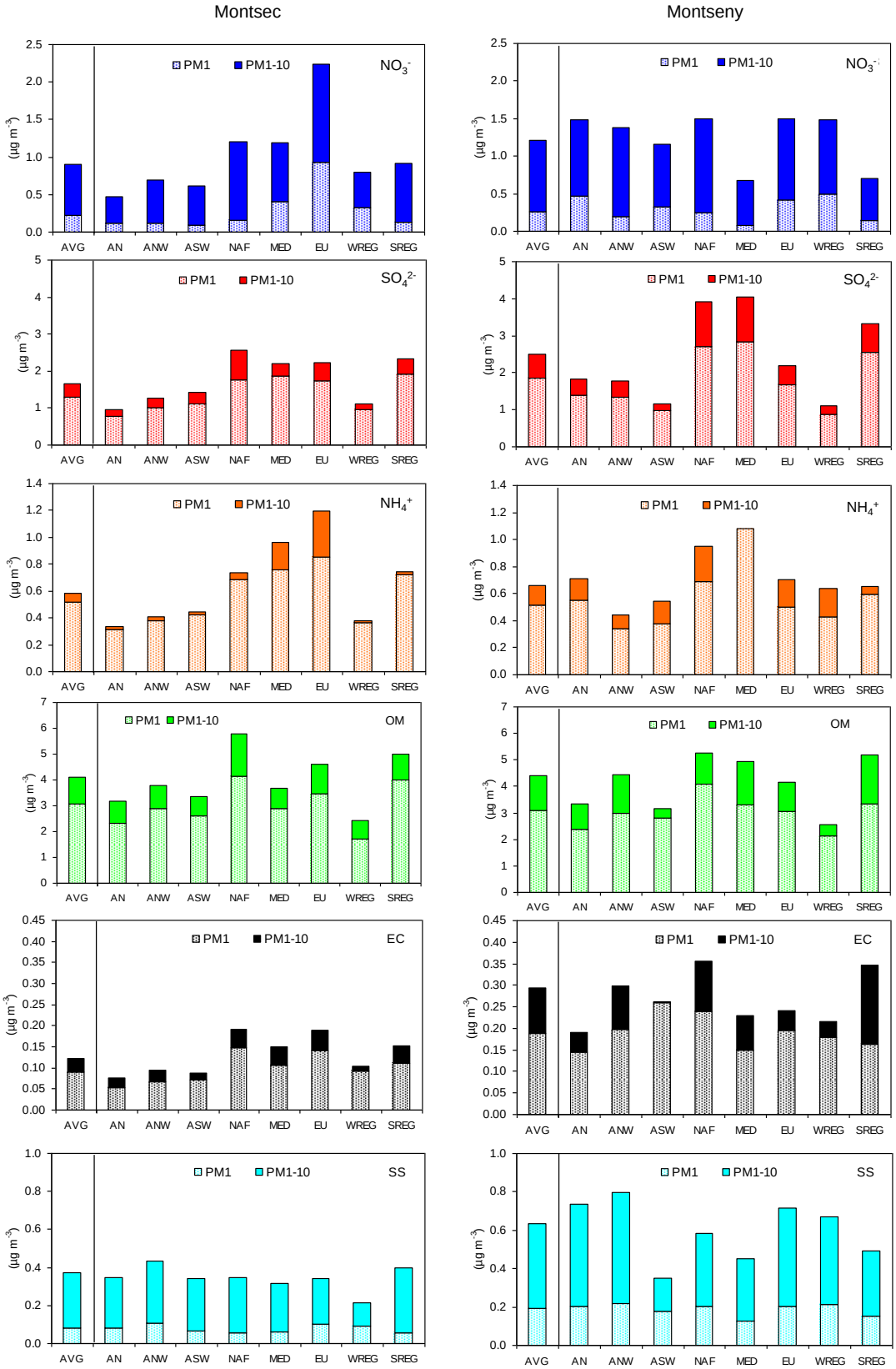

Fig. S5 Average (AVG) concentrations of PM_1 and PM_{1-10} nitrate (NO_3^-), sulfate (SO_4^{2-}), ammonium (NH_4^+), elemental carbon (EC), organic matter (OM) and sea salt (SS) at Montsec and Montseny for different atmospheric episodes based on daily measurements between January 2010 and March 2013.

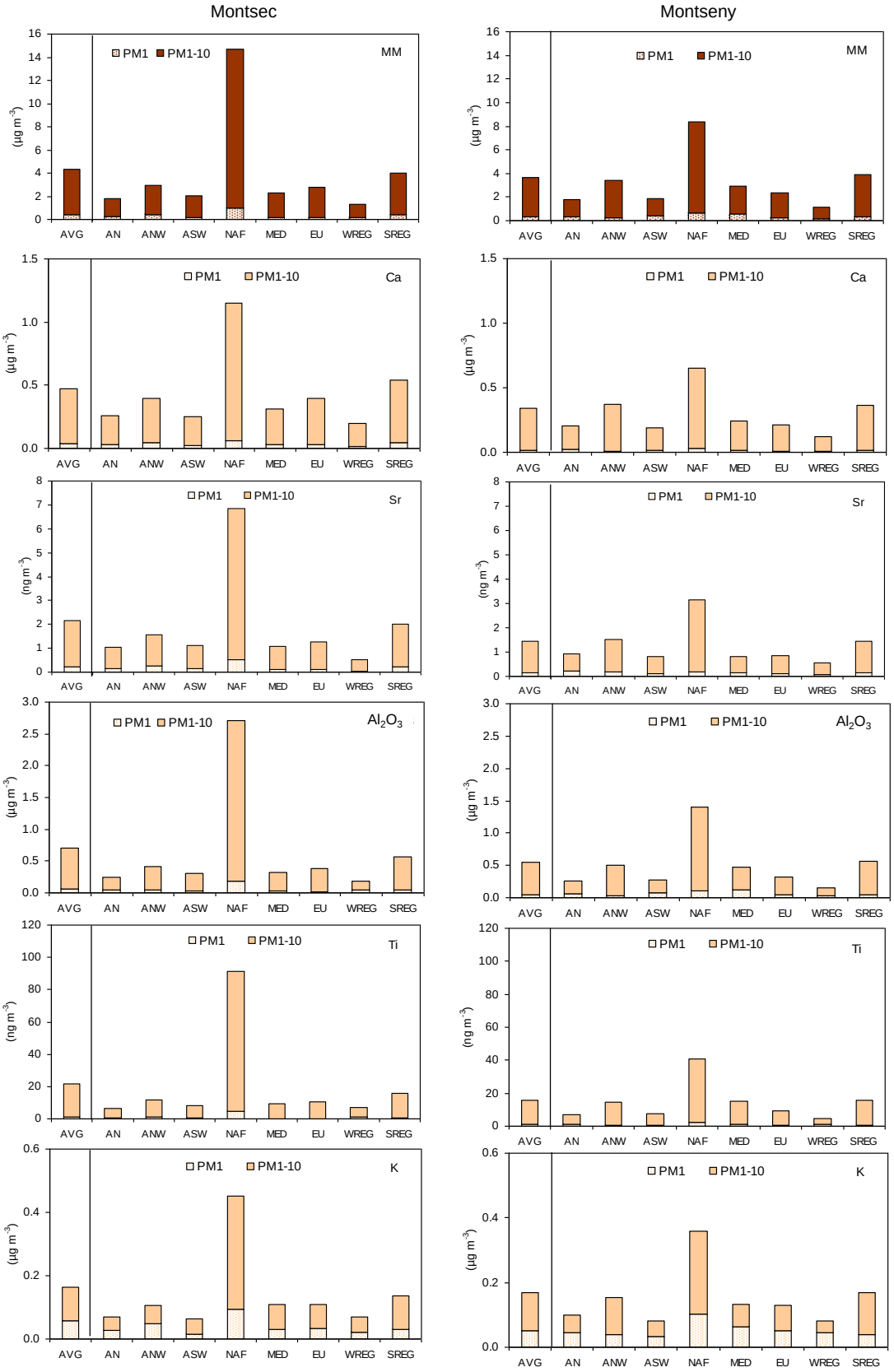

Fig. S6 Average (AVG) concentrations of PM_1 and PM_{1-10} mineral matter (MM), carbonate (CO_3^{2-}), strontium (Sr), aluminium oxide (Al2O3), titanium (Ti) and potassium (K) at Montsec and Montseny for different atmospheric episodes based on daily measurements between January 2010 and March 2013.

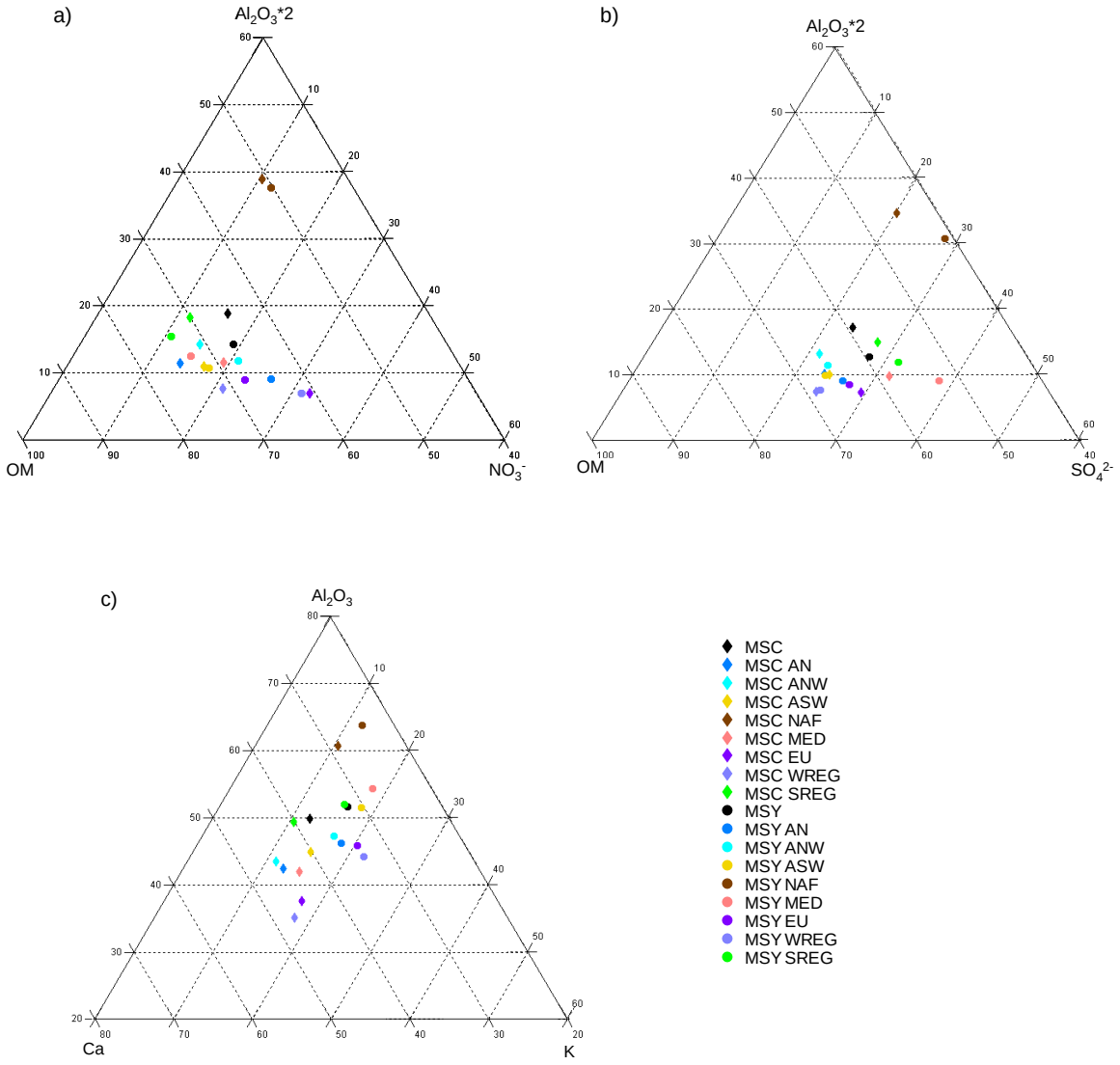

Fig. S7 Ternary plot of (a) organic matter (OM), aluminium oxide (Al_2O_3*2) and nitrate (NO_3^-), (b) organic matter (OM), aluminium oxide (Al_2O_3*2) and sulfate (SO_4^{2-}), and (c) calcium (Ca), aluminium oxide (Al_2O_3) and potassium (K) average concentrations of PM_{10} and average concentrations for different atmospheric episodes at Montsec (MSC) and Montseny (MSY) based on daily measurements between January 2010 and March 2013.

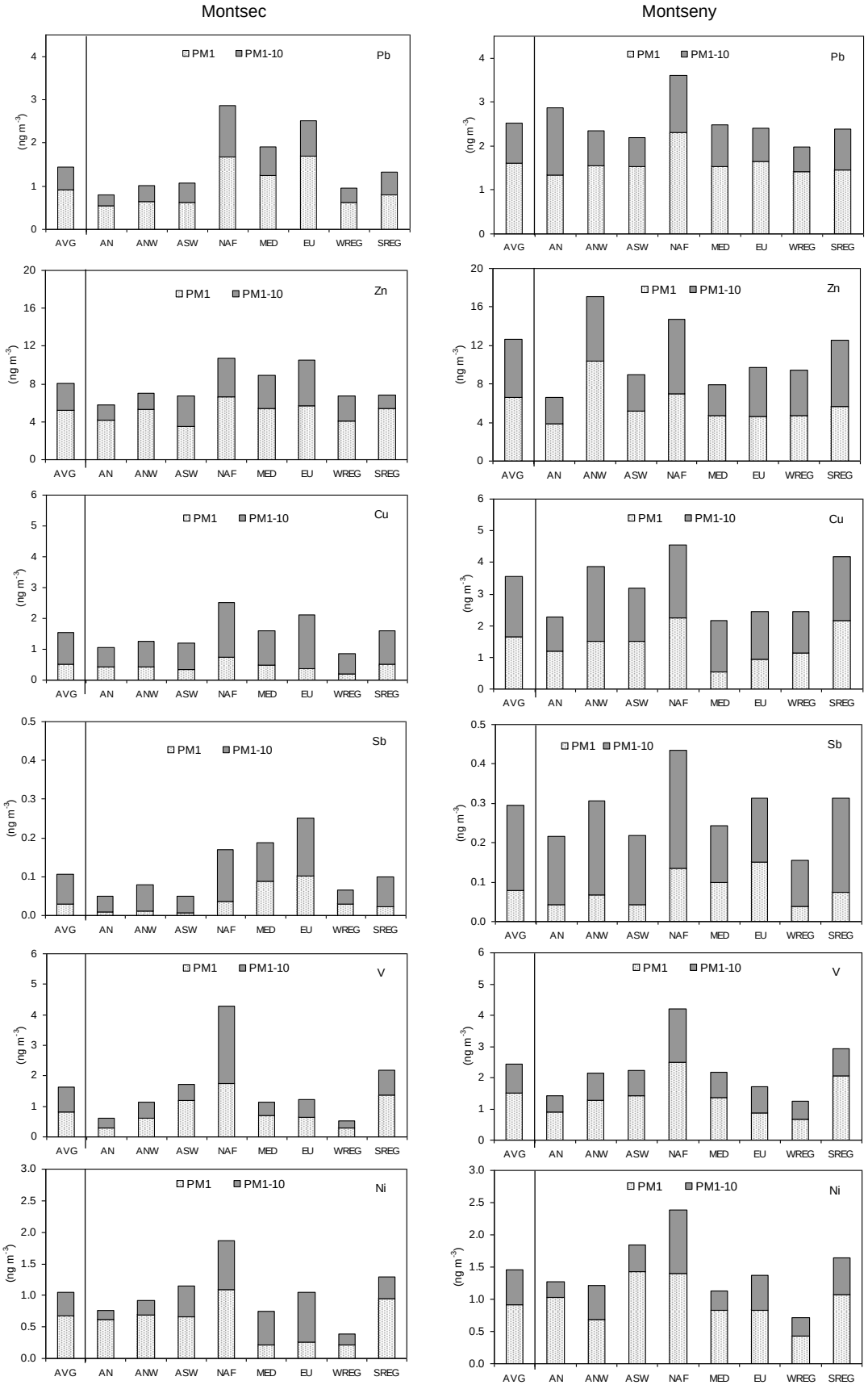

Fig. S8 Average (AVG) concentrations of PM_1 and PM_{1-10} vanadium (V), arsenic (As), cadmium (Cd), copper (Cu), lead (Pb) and antimony (Sb) at Montsec and Montseny for different atmospheric episodes based on daily measurements between January 2010 and March 2013.

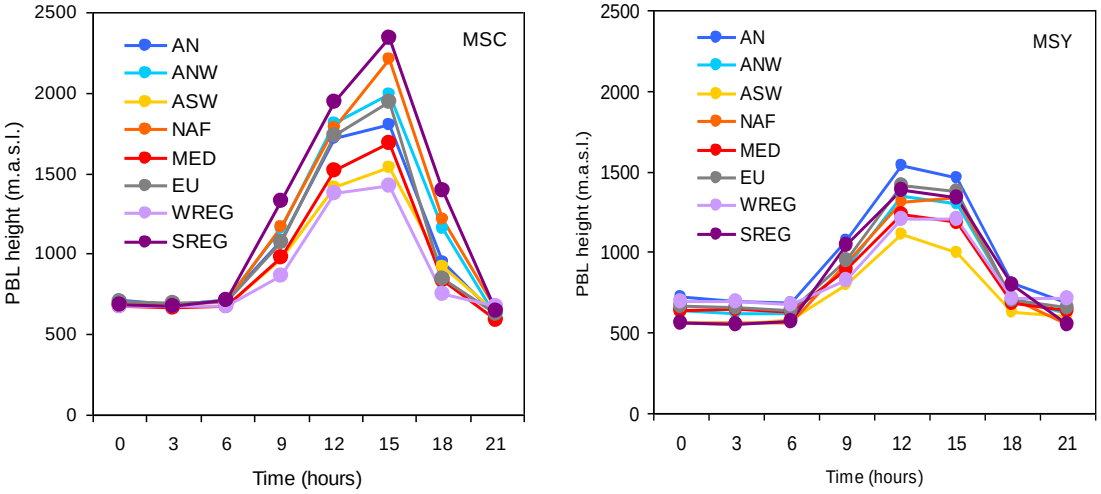

Fig. S9 Diurnal variation of the boundary layer height (computed with HYSPLIT model) averaged for different atmospheric episodes at Montsec (MSC) and Montseny (MSY) between January 2010 and March 2013.

a) African dust outbreak (NAF)

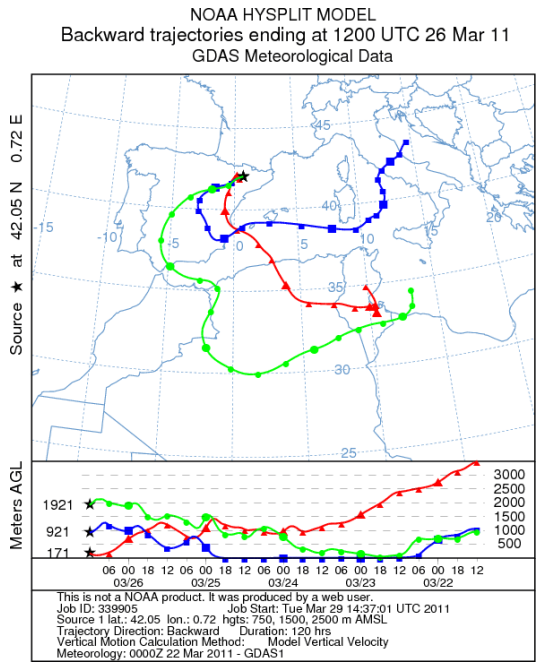

b) European (EU) episode

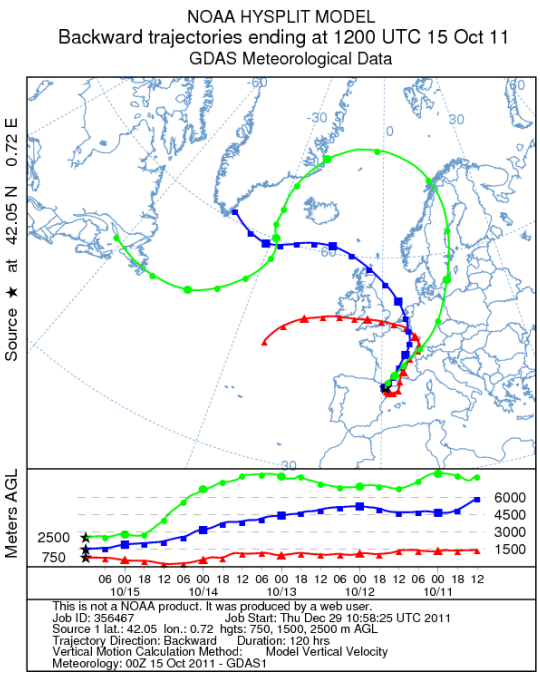

c) Winter regional (WREG) episode

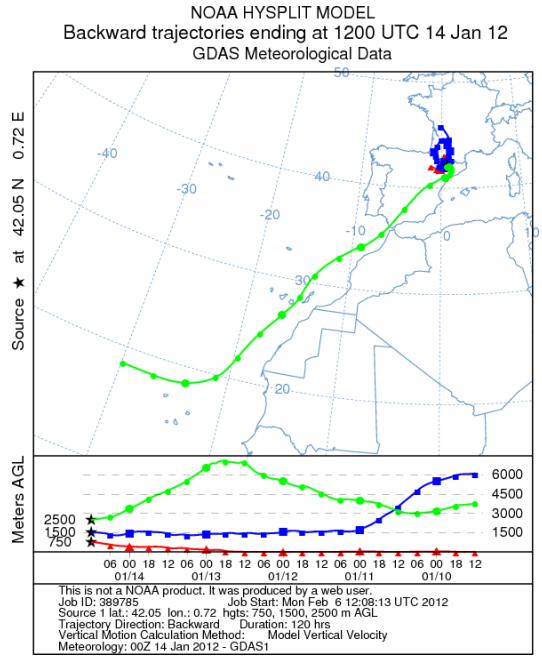

d) Wildfire event

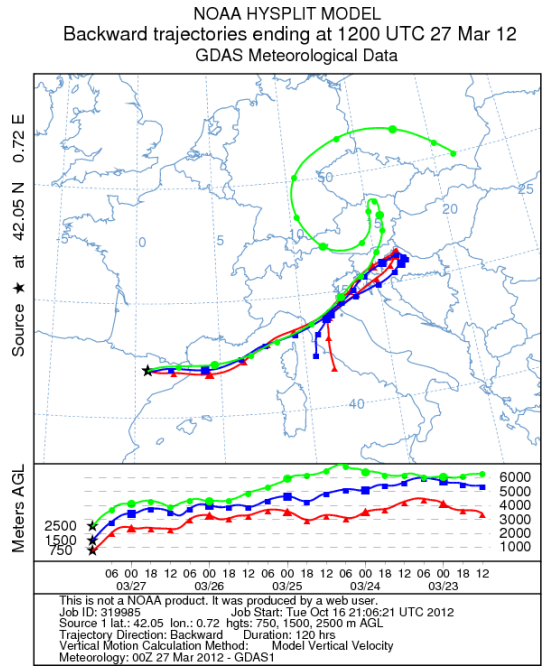

Fig. S10 Backward trajectories corresponding to 4 examples of different atmospheric episodes affecting the study area, (a) African dust outbreak, (b) European episode, (c) winter regional episode, and (d) wildfire event.

a) African dust outbreak (NAF)

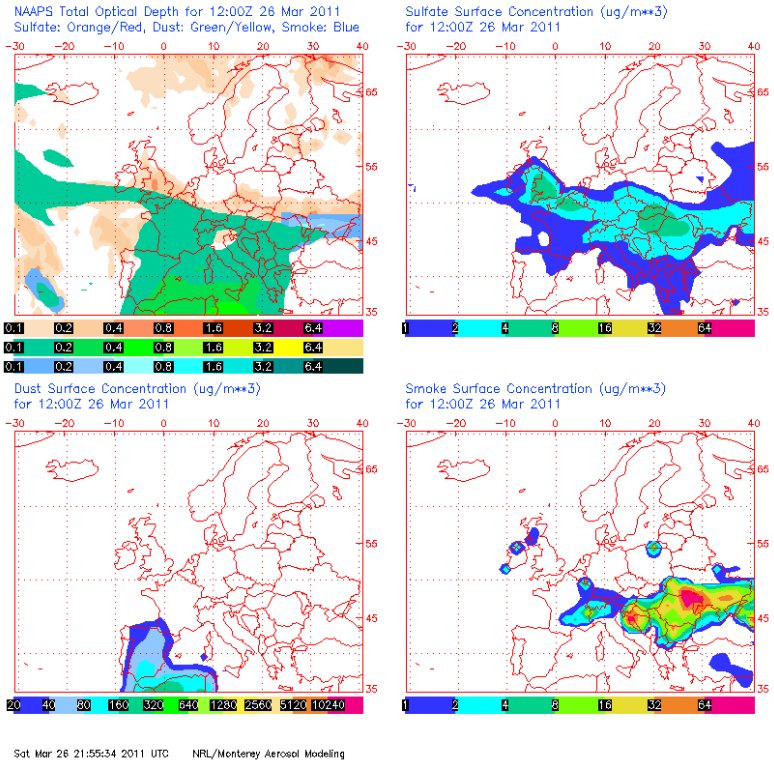

b) European (EU) episode

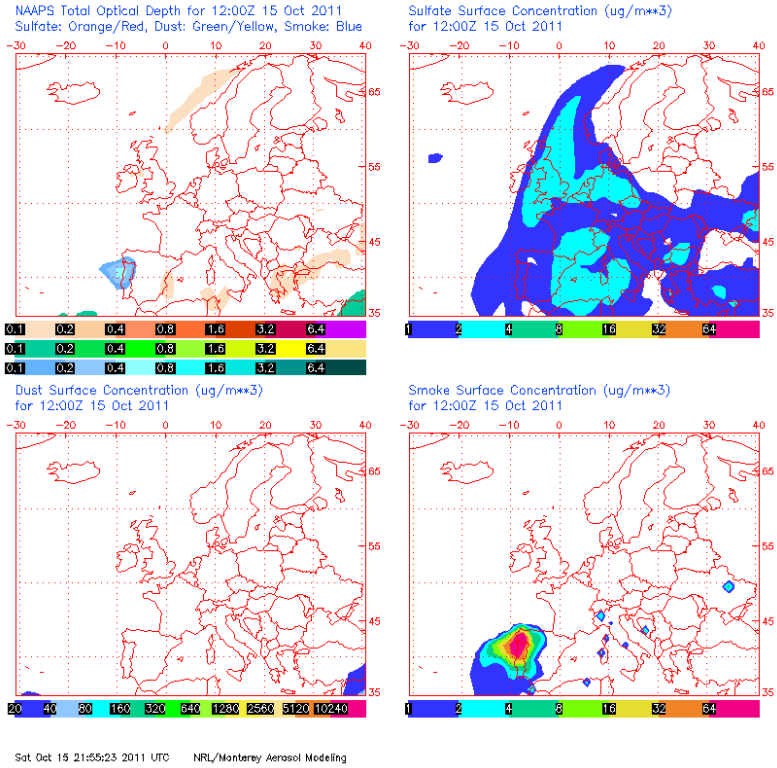

c) Winter regional (WREG) episode

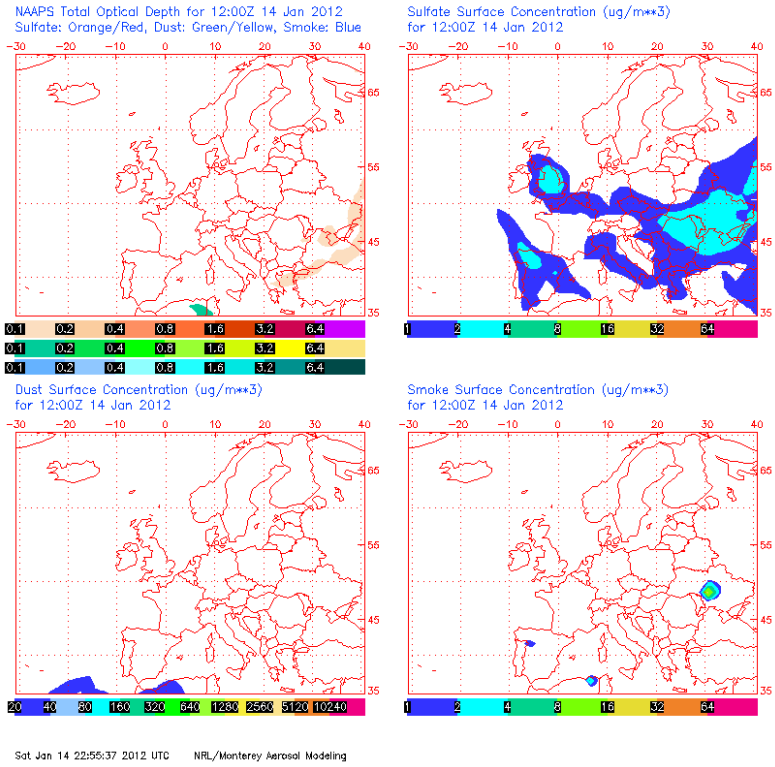

d) Wildfire event

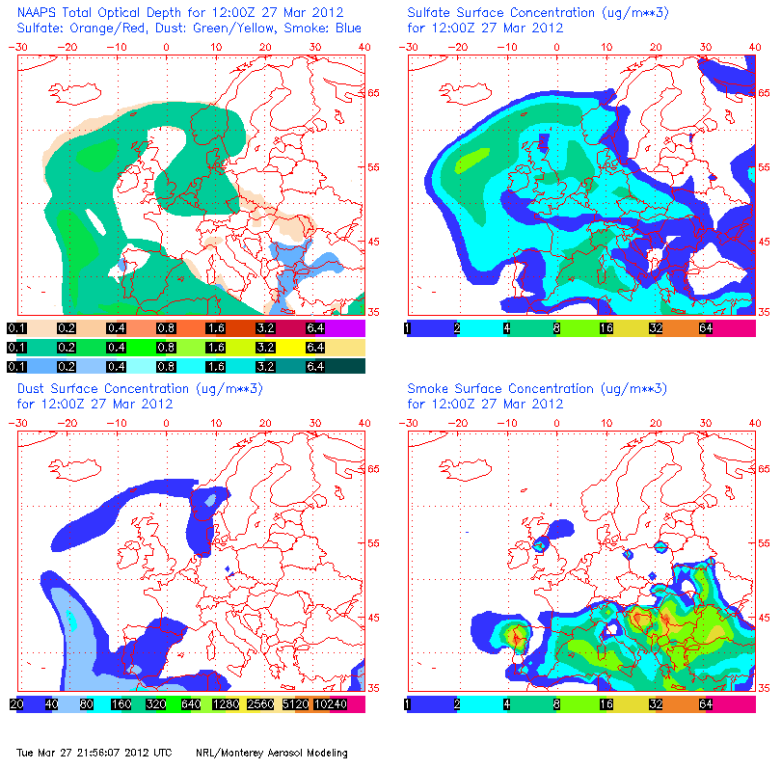

Fig. S11 Total optical depth, sulfate surface concentration, dust surface concentration, and smoke surface concentration from the NAAPS model corresponding to 4 examples of different atmospheric episodes affecting the study area, (a) African dust outbreak, (b) European episode, (c) winter regional episode, and (d) wildfire event.

Table S3. Average (and standard deviation for Montsec and Montseny) of PM_{10} and PM_1 chemical components at different continental and regional background stations in Europe.

	Montsec (1570 m a.s.l.)				Puy de Dôme (1465 m a.s.l.)[1]		Montseny (720 m a.sl.)				Payerne (489 m a.s.l.)[2]	Magadino (200 m a.s.l.)[2]
	January 2010-March 2013		March 2011-March 2013		April 2006 - April 2007		January 2010- March 2013				August 2008 - July 2009	August 2008 - July 2009
	PM_{10}	N=273	PM_1	N=137	PM_{10}	PM_1	PM_{10}	N=249	PM_1	N=240	PM_{10}	PM_{10}
	AVG	SD	AVG	SD	AVG	AVG	AVG	SD	AVG	SD	AVG	AVG
PM mass (µg m^{-3})	**11.5**	**9.3**	**7.1**	**3.9**	**5.6**	**3.9**	**15.5**	**7.9**	**8.2**	**4.1**	**19.1**	**20.9**
Undet (µg m^{-3})	**2.4**	**1.6**	**2.1**	**1.2**	**3.4**	**2.2**	**4.3**	**2.7**	**3.6**	**2.7**	**3.2**	**2.7**
EC (µg m^{-3})	0.12	0.09	0.09	0.07	-	-	0.23	0.13	0.17	0.10	0.7	1.5
OM (µg m^{-3})	3.2	1.8	2.8	1.5	-	-	4.0	1.8	2.9	1.3	5.6	8.8
NO_3^- (µg m^{-3})	0.8	1.0	0.2	0.4	0.5	0.3	1.2	1.2	0.3	0.5	3.8	2.1
NH_4^+ (µg m^{-3})	0.5	0.5	0.5	0.4	0.3	0.3	0.5	0.5	0.5	0.4	1.6	1.2
SO_4^{2-} (µg m^{-3})	1.3	1.1	1.2	1.0	1.4	1.2	1.9	1.4	1.5	1.1	1.9	1.9
Sea salt (µg m^{-3})	**0.3**	**0.3**	**0.07**	**0.1**	**-**	**-**	**0.5**	**0.5**	**0.14**	**0.2**	-	-
Cl^- (µg m^{-3})	0.1	0.2	0.1	0.1	-	-	0.3	0.3	0.1	0.2	0.03	0.05
ss-Na (µg m^{-3})	0.1	0.2	0.02	0.02	-	-	0.3	0.3	0.03	0.03	0.1	0.1
Mineral (µg m^{-3})	**3.0**	**5.7**	**0.26**	**0.4**	**-**	**-**	**2.8**	**3.2**	**0.25**	**0.5**	**1.8**	**1.9**
CO_3^{2-} (µg m^{-3})	0.5	0.7	0.05	0.04	-	-	0.4	0.4	<0.01	<0.01	-	-
SiO_2 (µg m^{-3})	1.1	2.7	0.1	0.2	-	-	1.1	1.4	0.1	0.3	-	-
Al_2O_3 (µg m^{-3})	0.5	1.1	0.03	0.1	-	-	0.4	0.6	0.04	0.1	-	-
nss-Na (µg m^{-3})	0.03	0.07	<0.01	<0.01	-	-	-	-	-	-	0.1	0.1
Al (µg m^{-3})	0.2	0.6	0.02	0.05			0.2	0.3	0.02	0.06	0.1	0.1
Ca (µg m^{-3})	0.3	0.4	0.03	0.02	-	-	0.3	0.3	0.01	0.03	0.2	0.1
K (µg m^{-3})	0.11	0.2	0.02	0.1	-	-	0.14	0.1	0.05	0.03	0.2	0.3
Mg (µg m^{-3})	0.1	0.1	0.01	0.01	-	-	0.1	0.1	<0.01	0.01	0.04	0.04
Fe (µg m^{-3})	0.1	0.3	0.01	0.02	-	-	0.2	0.2	0.01	0.01	0.1	0.3
P (ng m^{-3})	9	8	3	1.8	-	-	11.0	8.4	3.2	4.4	-	-
Ti (ng m^{-3})	14	35	1.1	2.2	-	-	12.4	16.1	0.8	1.2	2.2	4.9
Mn (ng m^{-3})	4	6	0.9	1.1	-	-	3.8	3.0	0.7	0.9	2.9	5.1
Trace elements (µg m^{-3})	**0.02**	**0.02**	**0.02**	**0.01**	**-**	**-**	**0.03**	**0.02**	**0.02**	**0.02**	**0.60**	**0.80**
Li (ng m^{-3})	0.2	0.4	0.01	0.02	-	-	0.2	0.2	0.01	0.02	-	-
Be (ng m^{-3})	0.01	0.02	<0.01	<0.01	-	-	<0.01	0.01	<0.01	<0.01	-	-
V (ng m^{-3})	1.1	1.4	0.7	0.8	-	-	2.0	1.5	1.2	1.1	0.5	0.6
Cr (ng m^{-3})	0.8	1.4	0.7	1.3	-	-	0.9	0.9	0.5	1.0	0.7	1.4
Co (ng m-3)	0.08	0.1	0.05	0.2	-	-	0.08	0.07	0.03	0.05	-	-
Ni (ng m^{-3})	0.5	1.0	0.4	1.1	-	-	1.1	0.8	0.8	0.8	0.7	0.9
Cu (ng m^{-3})	1.1	1.1	0.4	0.4	-	-	3	2	1.5	3	4	9
Zn (ng m^{-3})	7	4	5	3	-	-	10	7	6	14	19	21
As (ng m^{-3})	0.1	0.2	0.06	0.06	-	-	0.2	0.1	0.1	0.09	0.5	0.7
Se (ng m^{-3})	0.1	0.1	0.06	0.07	-	-	0.2	0.1	0.09	0.07	0.4	0.4
Rb (ng m^{-3})	0.3	0.6	0.05	0.05	-	-	0.3	0.3	0.07	0.04	0.5	0.6
Sr (ng m^{-3})	1.5	3	0.1	0.2	-	-	1.1	1.3	0.1	0.3	0.6	0.6
Zr (ng m^{-3})	3	4	3	4	-	-	3	3	3	3	-	-
Nb (ng m^{-3})	0.2	0.5	0.08	0.08	-	-	0.1	0.2	0.02	0.06	-	-
Cd (ng m^{-3})	0.03	0.03	0.02	0.02	-	-	0.06	0.04	0.05	0.05	0.09	0.1
Sn (ng m^{-3})	0.4	0.5	0.2	0.2	-	-	0.7	0.5	0.4	0.3	-	-
Sb (ng m^{-3})	0.06	0.1	<0.01	0.07	-	-	0.3	0.2	0.1	0.1	0.6	1.0
Cs (ng m^{-3})	0.02	0.04	<0.01	<0.01	-	-	0.01	0.02	<0.01	<0.01	-	-
Ba (ng m^{-3})	2	5	1.3	2	-	-	3	3	0.6	2.0	1.7	3
La (ng m^{-3})	0.2	0.3	0.06	0.05	-	-	0.1	0.2	0.03	0.04	0.05	0.07
Ce (ng m^{-3})	0.3	0.7	0.1	0.1	-	-	0.3	0.3	0.06	0.07	0.1	0.1
Pr (ng m^{-3})	0.04	0.08	0.01	0.02	-	-	0.03	0.04	<0.01	0.01	-	-
Nd (ng m^{-3})	0.2	0.3	0.05	0.06	-	-	0.1	0.1	0.02	0.04	0.04	0.05
Hf (ng m^{-3})	0.2	0.2	0.2	0.2	-	-	0.1	0.2	0.1	0.2	-	-
Tl (ng m^{-3})	<0.01	0.01	<0.01	<0.01	-	-	0.01	0.02	<0.01	0.01	-	-
Pb (ng m^{-3})	1.1	1.0	0.8	0.7	-	-	2	2	1.6	1.0	4	4
Bi (ng m^{-3})	0.02	0.03	0.01	0.02	-	-	0.1	0.2	0.05	0.06	0.07	0.08
Th (ng m^{-3})	0.06	0.1	0.02	0.07	-	-	0.05	0.07	0.02	0.04	-	-
U (ng m^{-3})	0.1	0.1	0.08	0.09	-	-	0.06	0.06	0.05	0.07	-	-

[1](Bourcier et al., 2012); [2](Gianini et al., 2012).

Table S4. Factor loadings resulting from the Principal Component Analysis (PCA), using Varimax rotation, on PM_{10} components from Montsec.

MSC				
Factor	Mineral	Industrial + traffic	Fuel oil combustion	Sea salt
Cl^-	0.14	0.05	-0.10	**0.84**
NO_3^-	0.12	**0.81**	-0.09	0.04
NH_4^+	-0.05	**0.88**	0.13	0.03
SO_4^{2-}	0.13	**0.71**	**0.50**	0.26
Al_2O_3	**0.97**	0.13	0.16	0.04
Ca	**0.75**	**0.33**	**0.31**	0.28
K	**0.87**	**0.34**	0.12	0.03
Na	0.29	0.25	**0.45**	**0.62**
Mg	**0.91**	0.19	0.23	0.21
Fe	**0.97**	0.15	0.16	0.04
Li	**0.96**	0.16	0.16	0.10
Ti	**0.96**	0.11	0.15	0.00
V	**0.68**	**0.42**	**0.45**	0.12
Cr	**0.46**	0.00	**0.56**	-0.08
Mn	**0.88**	0.21	0.25	0.13
Ni	**0.32**	0.23	**0.80**	-0.07
Cu	0.29	**0.57**	**0.44**	0.19
Zn	0.24	**0.67**	-0.02	-0.16
As	**0.62**	**0.50**	0.11	0.05
Se	0.30	**0.54**	**0.54**	0.18
Sr	**0.91**	0.17	0.20	0.19
Cd	**0.31**	**0.57**	0.11	0.06
Sb	0.13	**0.80**	0.22	0.12
Pb	**0.38**	**0.79**	0.27	-0.03
OC	**0.34**	**0.59**	**0.45**	0.23
EC	0.14	**0.82**	0.12	0.17
% Var	54	15	5	4

Factor loadings > 0.7 are marked in red, between 0.7 and 0.5 in dark gray, and between 0.5 and 0.3 in bright gray. % Var: percentage of the variance explained by each factor.

Table S5. Factor loadings resulting from the Principal Component Analysis (PCA), using Varimax rotation, on PM_{10} components from Montseny.

MSY				
Factor	Mineral	Industrial + traffic	Fuel oil combustion	Sea salt
Cl^-	0.05	-0.03	-0.07	**0.82**
NO_3^-	0.06	**0.73**	-0.05	0.24
NH_4^+	-0.05	**0.66**	**0.35**	-0.08
SO_4^{2-}	0.23	0.13	**0.88**	0.03
Al_2O_3	**0.97**	0.09	0.13	0.03
Ca	**0.90**	0.21	0.21	0.13
K	**0.89**	0.20	0.28	0.06
Na	0.24	-0.03	0.26	**0.76**
Mg	**0.91**	0.06	0.21	0.25
Fe	**0.75**	0.01	0.27	0.05
Li	**0.97**	0.13	0.06	0.07
Ti	**0.97**	0.11	0.13	0.02
V	**0.62**	0.20	**0.66**	0.07
Cr	**0.63**	0.28	0.20	-0.12
Mn	**0.93**	0.19	0.19	0.02
Ni	**0.43**	0.21	**0.70**	-0.03
Cu	0.12	**0.73**	-0.01	-0.03
Zn	0.14	**0.78**	0.19	0.08
As	**0.64**	**0.47**	**0.31**	0.03
Se	0.25	0.21	**0.61**	0.17
Sr	**0.96**	0.08	0.05	0.14
Cd	0.13	**0.83**	0.02	-0.07
Sb	0.13	**0.75**	0.19	-0.02
Pb	0.21	**0.57**	0.10	-0.13
OC	0.14	**0.52**	**0.53**	-0.02
EC	0.17	**0.69**	**0.37**	-0.02
% Var	46	16	6	5

Factor loadings > 0.7 are marked in red, between 0.7 and 0.5 in dark gray, and between 0.5 and 0.3 in bright gray. % Var: percentage of the variance explained by each factor.

3.4. Article 3: Long-term real-time chemical characterization of submicron aerosols at Montsec (Southern Pyrenees, 1570 m a.s.l.)

Anna Ripoll[1,2], María Cruz Minguillón[1], Jorge Pey[3], Jose-Luis Jimenez[4], Doug Day[4], Yuliya Sosedova[5], Francesco Canonaco[5], André Prévôt[5], Xavier Querol[1], Andrés Alastuey[1]

[1]Institute of Environmental Assessment and Water Research (IDAEA-CSIC), Jordi Girona 18-26, 08034, Barcelona, Spain.

[2]Department of Astronomy and Meteorology, Faculty of Physics, University of Barcelona, Martí i Franquès 1, 08028, Barcelona, Spain.

[3]Aix-Marseille Université, CNRS, LCE FRE 3416, Marseille, 13331, France

[4]Department of Chemistry and Biochemistry, and Cooperative Institute for Research in the Environmental Sciences (CIRES), University of Colorado at Boulder, 80309, CO, USA.

[5]Paul Scherrer Institute, Laboratory of Atmospheric Chemistry, 5232 Villigen PSI, Switzerland.

Atmos. Chem. Phys., 15, 2935-2951,
doi:10.5194/acp-15-2935-2015, 2015

Published: **16 March 2015**

Impact factor of Journal: **5.298**

Resum. En aquest article es presenta la composició química dels aerosols submicromètrics (aerosols amb diàmetre aerodinàmic inferior a 1 μm) mesurada mitjançant un monitor d'especiació química dels aerosols (angl., aerosol chemical speciation monitor, ACSM). Aquest equip és capaç de mesurar en temps real la concentració màssica dels components no refractaris de les partícules submicromètriques, diferenciant la matèria orgànica, el nitrat, el sulfat, l'amoni i el clorur. A més a més, aquest estudi també inclou altres mesures de la composició química dels aerosols submicromètrics en temps real i no real. Aquestes mesures es van dur a terme, per primera vegada a Europa, a una estació remota (Montsec, MSC, 1570 m s.n.m.) durant 10 mesos (juliol 2011-abril 2012).

La variació estacional dels components no refractaris de les partícules submicromètriques va mostrar un patró molt similar al obtingut pels mateixos components mitjançant mostres de PM_1 recollides amb filtres, és a dir, les concentracions més altes es van observar durant l'estiu i les més baixes durant l'hivern, excepte en el cas del nitrat.

Gràcies a la utilització d'un ACSM es van poder estudiar les variacions intradiàries de les concentracions dels components no refractaris. Això va donar com a resultat uns cicles diaris poc definits a l'estiu, excepte pels aerosols orgànics, i molt més clars a l'hivern. La qual cosa va demostrar que la variació d'aquests compostos depèn de factors diferents. D'una banda, els patrons diaris dels compostos inorgànics venen determinats pels vents de muntanya, l'evolució de la capa de barreja, i l'origen de la massa d'aire; mentre que, per l'altra banda, els cicles diaris dels aerosols orgànics depenen més de les condicions meteorològiques, com ara la temperatura i/o la radiació solar.

A més a més, la matriu d'orgànics obtinguda mitjançant les dades del ACSM va permetre investigar els diferents tipus d'aerosol orgànic present al MSC. D'aquesta manera es van poder identificar tres tipus de compostos orgànics diferents a l'estiu, anomenats aerosol orgànic similar als hidrocarburs (angl., hydrocarbon-like organic aerosol, HOA), aerosol orgànic oxigenat semivolàtil (angl., semivolatile oxygenated organic aerosol, SV-OOA), i aerosol orgànic oxigenat de baixa volatilitat (angl., low-volatility oxygenated organic aerosol, LV-OOA), i tres tipus a l'hivern, anomenats HOA, aerosol orgànic de crema de biomassa (angl., biomass burning organic aerosol, BBOA), i un únic aerosol orgànic oxigenat (angl., oxygenated organic aerosol, OOA).

Atmos. Chem. Phys., 15, 2935–2951, 2015
www.atmos-chem-phys.net/15/2935/2015/
doi:10.5194/acp-15-2935-2015
© Author(s) 2015. CC Attribution 3.0 License.

Atmospheric Chemistry and Physics
Open Access

Long-term real-time chemical characterization of submicron aerosols at Montsec (southern Pyrenees, 1570 m a.s.l.)

A. Ripoll[1,2], M. C. Minguillón[1], J. Pey[3], J. L. Jimenez[4], D. A. Day[4], Y. Sosedova[5], F. Canonaco[5], A. S. H. Prévôt[5], X. Querol[1], and A. Alastuey[1]

[1]Institute of Environmental Assessment and Water Research (IDAEA-CSIC), Jordi Girona 18–26, 08034, Barcelona, Spain
[2]Department of Astronomy and Meteorology, Faculty of Physics, University of Barcelona, Martí i Franquès 1, 08028, Barcelona, Spain
[3]Aix-Marseille Université, CNRS, LCE FRE 3416, Marseille, 13331, France
[4]Department of Chemistry and Biochemistry, and Cooperative Institute for Research in the Environmental Sciences (CIRES), University of Colorado at Boulder, CO 80309, USA
[5]Paul Scherrer Institute, Laboratory of Atmospheric Chemistry, 5232 Villigen PSI, Switzerland

Correspondence to: A. Ripoll (anna.ripoll@idaea.csic.es)

Received: 16 October 2014 – Published in Atmos. Chem. Phys. Discuss.: 19 November 2014
Revised: 24 February 2015 – Accepted: 25 February 2015 – Published: 16 March 2015

Abstract. Real-time measurements of inorganic (sulfate, nitrate, ammonium, chloride and black carbon (BC)) and organic submicron aerosols (particles with an aerodynamic diameter of less than 1 µm) from a continental background site (Montsec, MSC, 1570 m a.s.l.) in the western Mediterranean Basin (WMB) were conducted for 10 months (July 2011–April 2012). An aerosol chemical speciation monitor (ACSM) was co-located with other online and offline PM_1 measurements. Analyses of the hourly, diurnal, and seasonal variations are presented here, for the first time, for this region.

Seasonal trends in PM_1 components are attributed to variations in evolution of the planetary boundary layer (PBL) height, air mass origin, and meteorological conditions. In summer, the higher temperature and solar radiation increases convection, enhancing the growth of the PBL and the transport of anthropogenic pollutants towards high altitude sites. Furthermore, the regional recirculation of air masses over the WMB creates a continuous increase in the background concentrations of PM_1 components and causes the formation of reservoir layers at relatively high altitudes. The combination of all these atmospheric processes results in a high variability of PM_1 components, with poorly defined daily patterns, except for the organic aerosols (OA). OA was mostly composed (up to 90 %) of oxygenated organic aerosol (OOA), split in two types: semivolatile (SV-OOA) and low-volatility (LV-OOA), the rest being hydrocarbon-like OA (HOA). The marked diurnal cycles of OA components regardless of the air mass origin indicates that they are not only associated with anthropogenic and long-range-transported secondary OA (SOA) but also with recently produced biogenic SOA.

Very different conditions drive the aerosol phenomenology in winter at MSC. The thermal inversions and the lower vertical development of the PBL leave MSC in the free troposphere most of the day, being affected by PBL air masses only after midday, when the mountain breezes transport emissions from the adjacent valleys and plains to the top of the mountain. This results in clear diurnal patterns of both organic and inorganic concentrations. OA was also mainly composed (71 %) of OOA, with contributions from HOA (5 %) and biomass burning OA (BBOA; 24 %). Moreover, in winter sporadic long-range transport from mainland Europe is observed.

The results obtained in the present study highlight the importance of SOA formation processes at a remote site such as MSC, especially in summer. Additional research is needed to characterize the sources and processes of SOA formation at remote sites.

Published by Copernicus Publications on behalf of the European Geosciences Union.

1 Introduction

Earth's climate system is modulated by atmospheric aerosols. Submicron particles (< 1 μm in aerodynamic diameter) play a dominant role in both cloud formation and scattering or absorbing solar radiation (IPCC, 2013). The complexity of aerosol sources and processes results in an uncertainty in the radiative forcing of climate. Aerosol optical properties are connected to direct and indirect climate forcing effects, and they are dependent on particle composition. Moreover, aerosol composition may provide valuable information on aerosol sources and processes. Consequently, long-term measurements of PM_1 chemical composition are needed to better understand aerosol sources, to quantify their lifetime in the atmosphere and to constrain the uncertainties of their climatic influence.

Long-term PM_1 chemical composition measurements are relatively scarce both offline and online. In the last decade, online PM_1 chemical composition measurements have been performed using aerosol mass spectrometers (AMS) at a number of locations. Measurements of online chemical composition are useful to study hourly variations and daily patterns. Most of these studies, however, correspond to short-term measurement campaigns (typically a month) (e.g., Crippa et al., 2014; Jimenez et al., 2009; Lanz et al., 2010; Ng et al., 2010; Zhang et al., 2007) given the intensive instrument maintenance required and the need of highly qualified personnel for a good quality data set.

In contrast to the use of the AMS in relatively short campaigns, the more recently developed Aerodyne aerosol chemical speciation monitor (ACSM) is becoming a widely used online instrument for long-term measurements of PM_1 chemical composition (Budisulistiorini et al., 2013; Canonaco et al., 2013; Carbone et al., 2013; Petit et al., 2014; Tiitta et al., 2014). The ACSM is built upon the same technology as the AMS, in which an aerodynamic particle focusing lens is combined with high vacuum thermal particle vaporization, electron impact ionization, and mass spectrometry. Modifications in the ACSM design (e.g., lack of particle sizing chamber and components, and use of a simple and compact RGA mass spectrometer detector), however, allow it to be smaller, less costly, and simpler to operate than the AMS (Ng et al., 2011c). The ACTRIS (Aerosols, Clouds, and Trace gases Research InfraStructure) European network is evaluating the use of the ACSM as a reliable instrument, which will provide the opportunity to study long-term data sets of PM_1 chemical composition across the continent.

Recent publications have investigated most of the existing worldwide AMS databases (e.g., Crippa et al., 2014; Jimenez et al., 2009; Lanz et al., 2010; Ng et al., 2010; Zhang et al., 2007) and reflected a prevalence of organic aerosols (20–90 %) in the submicron fraction, largely independent of the region and type of environment. However, our knowledge on organic aerosol (OA) formation, sources, and atmospheric processing is still very incomplete, especially for secondary organic aerosol (SOA) formed from chemical reactions of gas-phase species (e.g., Donahue et al., 2014; Hallquist et al., 2009; Kroll and Seinfeld, 2008; Robinson et al., 2007; Volkamer et al., 2006). Recent progress has been made in identifying primary organic aerosol (POA) sources (e.g., Elbert et al., 2007; Zhang et al., 2005), but significant gaps still remain in our understanding on the atmospheric evolution of POA after emission (de Gouw and Jimenez, 2009). For these reasons, OA measurements and analysis are required to better understand its chemical evolution in the atmosphere.

The lack of long-term online PM_1 chemical composition measurements is especially evident in the western Mediterranean Basin (WMB), which is characterized by particular atmospheric dynamics strongly influenced by its topography (Jorba et al., 2013; Millan et al., 1997). Over this region, arrival of natural and anthropogenic aerosols as a result of long-range transport from Africa and Europe is frequent (e.g., Pey et al., 2013; Querol et al., 2009; Ripoll et al., 2014; Rodríguez et al., 2001) and accumulation and recirculation processes are frequently observed (Rodriguez et al., 2002). The sources and meteorological controls of PM in the regional background of the WMB have been recently investigated during the DAURE (Determination of the sources of atmospheric Aerosols in Urban and Rural Environments in the western Mediterranean) study (Pandolfi et al., 2014a) using an AMS and ^{14}C analyses (Crippa et al., 2014; Minguillón et al., 2011). Furthermore, Ripoll et al. (2015) studied the PM_1 and PM_{10} chemical composition with daily time resolution in the continental and regional background environments in the WMB. In that study, a higher mineral contribution was identified in the continental background due to the preferential transport of African dust at high altitude layers and to the increased regional dust resuspension enhanced by the drier surface and higher convection. Nevertheless, aerosol chemical characterization with higher time resolution is needed to study the origin of specific PM components and the local and/or regional processes, in particular to exploit the information contained in diurnal cycles that is typically not accessible with offline measurements.

In this study we deployed an ACSM at a high altitude site (Montsec, 1570 m a.s.l.) in the NE of the Iberian Peninsula (42°03′ N, 0°44′ E), representative of the continental background conditions of the WMB (Ripoll et al., 2014). This environment is under free tropospheric (FT) influence most of the time, although it is exposed to regional pollutants during the summer time and/or under the influence of mountain breezes, and it is affected by transboundary incursions of natural and anthropogenic aerosols from Europe and North Africa (Ripoll et al., 2014, 2015). Co-located online and offline PM_1 measurements were also carried out to complement the ACSM data set. Hence, the work presented here interprets the real-time variation of inorganic and organic submicron components during 10 months (July 2011–April 2012), and the types of OA are also studied. Special emphasis is placed on the analysis of the diurnal pattern and seasonal

variations of chemical components and the main factors influencing these variations.

2 Methodology

2.1 Sampling site

The Montsec site (MSC) is located on the highest part of the Montsec d'Ares mountain, at an altitude of 1570 m a.s.l., in a plain near the edge of a 1000 m cliff to the south, with no wind obstructions present around. It is located in the NE of the Iberian Peninsula (42°03′ N, 0°43′ E), 50 km S of the Pyrenees and 140 km NW of Barcelona (Fig. S1 in the Supplement.). A detailed description of this site can be found in Ripoll et al. (2014). This station is a member of the GAW (global atmospheric watch) network as a regional station named MSA.

The daily classification of atmospheric episodes affecting MSC was made following the procedure described by Ripoll et al. (2014) using the HYSPLIT (Hybrid Single Particle Lagrangian Integrated Trajectory Model) model from the NOAA Air Resources Laboratory (ARL). Air masses reaching MSC are mainly from the Atlantic (62 % of the days) throughout the year. From March to October, North African (NAF) episodes are more frequent (17 % of the days) and are very often alternated with the summer regional (SREG) scenarios (12 % of the days). The winter regional (WREG) scenarios are detected from October to March (11 % of the days), as well as the European (EU) episodes (11 % of the days). Conversely, the Mediterranean (MED) episodes are detected sporadically (4 % of the days).

The boundary layer height was calculated using the Global Data Assimilation System (GDAS1) model from the NOAA Air Resources Laboratory (http://www.ready.noaa.gov/READYamet.php) (Fig. 1).

2.2 ACSM sampling and data analysis

The ACSM (Aerodyne Research Inc.) was measuring continuously from July 2011 to April 2012. The ACSM provides real-time mass concentration of submicron particulate organics, nitrate, sulfate, ammonium and chloride via thermal vaporization and electron impact ionization, with detection by a quadrupole mass spectrometer (Ng et al., 2011c). The mass concentration of a given species is determined from the sum of the ion signals at each of its mass spectral fragments and its ionization efficiency (IE) (Canagaratna et al., 2007). Since calibration of IEs for all species is not feasible, the relative ionization efficiency (RIE) (compared to that of nitrate) is used (Jimenez et al., 2003). The ammonium nitrate calibration described by Ng et al. (2011b) was performed using an atomizer (TSI, Constant Output Atomizer model 3076) for primary aerosol generation, followed by a silica gel diffusion dryer, a differential mobility analyzer (DMA) model TSI 3081, and a condensation particle counter (CPC, TSI 3772). Monodisperse 300 nm ammonium nitrate aerosol particles were used, covering a range of nitrate concentrations from 2 to 15 $\mu g\,m^{-3}$. Several calibrations were conducted throughout the sampling period, and average values of 2.2×10^{-11} for nitrate IE and 5.4 for RIE for ammonium were used for the whole data set. The RIE values used in this study for the rest of the species were those usually applied in AMS ambient concentrations: 1.4 for OA and 1.1, 1.2, and 1.3 for nitrate, sulfate, and chloride, respectively (Canagaratna et al., 2007). RIE for sulfate was experimentally determined 1 year later and was found to be 1.26, although the default value was used for the current data set. A time resolution of 62 min was used as a result of 12 scans (one open and one filtered) per data point with a scan speed of 1 $s\,amu^{-1}$.

The ACSM data were analyzed with the standard ACSM data analysis software version 1.5.3.2 (Aerodyne Research Inc.) written in Igor Pro 6 (WaveMetrics, Inc., Lake Oswego, OR, USA). As the ACSM was measuring continuously for a long time, the standard correction for instrument sensitivity drifts was applied to the data set based on the inlet pressure and N_2 signal. Finally, mass concentrations were corrected using a collection efficiency (CE) to account for the particle bounce of aerosols on the vaporizer. The composition-dependent CE was calculated as described by Middlebrook et al. (2012) and was close to 0.45 for most of the time. Since for most ambient studies a 0.5 CE value is found to be representative with data uncertainties generally within ± 20 % (Canagaratna et al., 2007) and since our ACSM concentrations using CE = 0.5 were in good agreement with concentrations from other co-located instruments, a CE of 0.5 was used.

The organic components were further investigated by applying the Multilinear Engine (ME-2) (Paatero, 1999) to the organic mass spectra. With the ME-2, the user can introduce a priori information about sources with the so-called a value approach. Hence, the user inputs one or more factor profiles and a constraint defined by the a value, which determines the extent to which the output profile can differ from the profile fed to the model. The source apportionment of OA was performed applying ME-2 using the custom software tool of Source Finder (SoFi) version 4.8 developed by Canonaco et al. (2013). The ME-2 analysis was carried out separately for the summer period (14 July 2011–24 September 2011) and the winter period (10 January 2012–7 March 2012). Only $m/z \leq 100$ were used for source apportionment of OA because (a) the signals of $m/z > 100$ account for a minor fraction of the total organic mass (on average, 2 %), (b) the $m/z > 100$ have larger uncertainties, and (c) the large interference of naphthalene signals (used for m/z calibration of the ACSM) at these m/z (e.g., m/z 127, 128, and 129) (Sun et al., 2012).

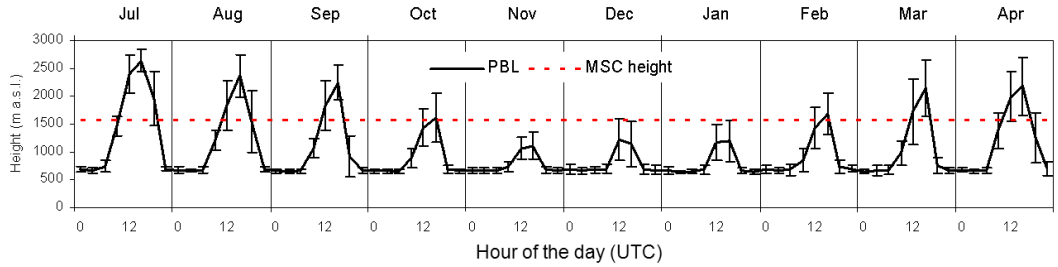

Figure 1. Diurnal variation of the boundary layer height (computed with HYSPLIT model) averaged for each month during the study period at Montsec. Variation bars indicate ± standard deviation.

2.3 Co-located measurements used in this study

MSC has been permanently equipped with aerosol monitoring instrumentation since January 2010 and some of these measurements were used in this study. The 24 h PM_1 samples were collected every 4 days on 150 mm quartz microfiber filters (Pallflex QAT) using high volume samplers (30 $m^3 h^{-1}$, MCV CAV-A/MSb) equipped with MCV PM_1 cutoff inlets. Daily PM_1 mass concentrations were determined by offline gravimetric procedures according to the EN 12341 standard (CEN, 1999), i.e., at 20 °C temperature and 50 % relative humidity. Furthermore, PM_1 chemical composition was obtained as described by Ripoll et al. (2015) using inductively coupled plasma atomic emission spectroscopy (ICP-AES) and mass spectrometry (ICP-MS) for major and trace elements, respectively, ion high performance liquid chromatography (HPLC) and selective electrode for ions concentrations, and the thermal–optical method (using the EUSSAR 2 protocol) for elemental carbon (EC) and organic carbon (OC) concentrations. Real-time PM_1 mass concentrations were continuously measured by an optical particle counter (OPC, model GRIMM 1.107 calibrated with a different latex PSL refraction index 1.59). PM_1 30 min data were averaged daily and subsequently corrected by comparison with 24 h standard gravimetric mass measurements. The absorption coefficient was measured continuously at 637 nm using a multi-angle absorption photometer (MAAP, model 5012, Thermo). Equivalent black carbon (BC) mass concentrations (Petzold et al., 2013) were calculated by the MAAP instrument software by dividing the measured absorption coefficient σ_{ap} (λ) by 6.6 $m^2 g^{-1}$, which is the instrument default mass absorption cross section (MAC) at 637 nm (Müller et al., 2011; Petzold and Schönlinner, 2004). Particle scattering (σ_{sp}; 0–360°) and hemispheric backscattering (σ_{bsp}; 90–270°) coefficients at three wavelengths (450, 525, 635 nm) were measured with a LED-based integrating nephelometer (model Aurora 3000, ECOTECH Pty, Ltd, Knoxfield, Australia).

Finally, all meteorological data were measured by the Catalonian Meteorological Service from the Montsec d'Ares station. Gaseous pollutants (O_3, NO, NO_2, CO and SO_2) were measured using real-time monitors belonging to the Network of Control and Surveillance of Air Quality of the Autonomous Government of Catalonia. NO and NO_2 concentrations were measured using a Thermo Scientific instrument model 42i-TL, CO using a Teledyne 300 EU Gas filter correlation analyzer, O_3 using a MCV 48AV UV photometry analyzer, and SO_2 using a Teledyne 100 EU UV fluorescence analyzer.

In addition to these routine measurements, two intensive campaigns were performed in July–August 2011 and January–February 2012. During these intensive campaigns PM_1 filters were collected daily and a scanning mobility particle sizer (SMPS) was installed to measure particle number size distribution of mobility diameters of 11–350 nm in the summer campaign and of 8–450 nm in the winter campaign. The SMPS system comprises a classifier unit (model TSI 3080) and a differential mobility analyzer (DMA, model TSI 3081) connected to a condensation particle counter (CPC, model TSI 3772). The SMPS data for the winter campaign were also used to estimate the mass concentration to compare with the ACSM data. To this end, the volume size distributions were calculated from the measured particle number distributions assuming sphericity. The total volume concentrations were computed by integrating over the measured particle range and converted to mass concentration using the estimated composition-dependent density, calculated using the chemical composition given by the ACSM and the equation of Salcedo et al. (2006). Average concentrations shown in the whole paper are arithmetic averages unless otherwise specified.

3 Results and discussion

3.1 Submicron aerosol mass concentrations

In order to establish the consistency of the different measurements during this study, the sum of the ACSM species (i.e., sulfate + nitrate + ammonium + OA + chloride) and the BC mass concentrations was compared with the co-located PM_1 and light scattering measurements (Fig. 2). The scatter plots of ACSM plus BC concentrations vs. PM_1 con-

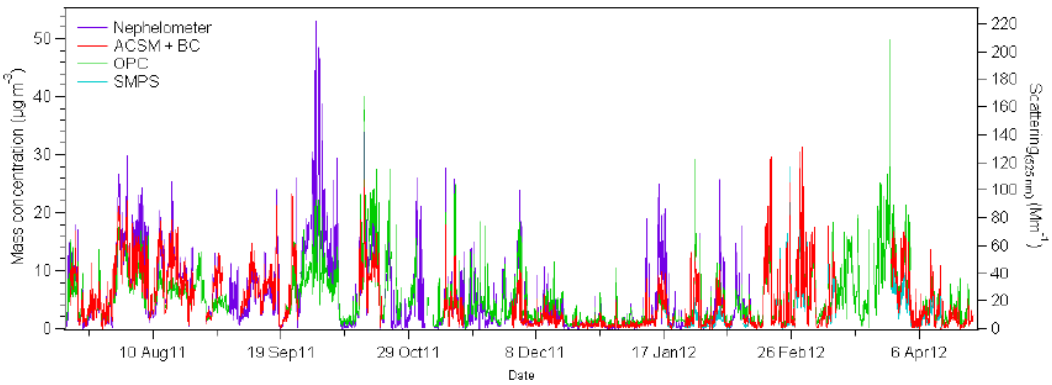

Figure 2. Time series of PM_1 total mass from co-located measurements and light scattering at 525 nm.

centrations from the OPC and SMPS showed strong correlations ($R^2 = 0.72$ and $R^2 = 0.87$, respectively) and slopes close to unity (slope = 0.94 and intercept = 0.09 for the ACSM + BC vs. OPC, and slope = 1.21 and intercept = 0.86 for the ACSM + BC vs. SMPS) (Fig. 3). The differences in the particle size range measured by the different instruments need to be considered when assessing these comparisons. Moreover, ACSM plus BC concentrations were also highly correlated with light scattering at 525 nm determined by the nephelometer ($R^2 = 0.85$, Fig. 3). The high degree of agreement is also apparent in the time series plots of PM_1 shown in Fig. 2.

The average concentration (25th, 50th, 75th percentiles) of the ACSM + BC mass during this study (July 2011–April 2012) was 4.9 μg m^{-3} (0.9, 2.8, 7.9 μg m^{-3}) (Table 1), which is similar to the 2010–2012 average reported by Ripoll et al. (2014) from OPC measurements (5.0 μg m^{-3}). For the sake of brevity only summer (14 July 2011–24 September 2011) and winter (10 January 2012–7 March 2012) hourly variations will be discussed in the following sections, given that hourly variation in spring was similar to that in summer and that in fall was similar to that in winter. The seasonal average PM_1 concentrations were higher in summer (7.5 μg m^{-3} (3.4, 7.1, 10.5 μg m^{-3}), Table 1) than in winter (4.1 μg m^{-3} (0.8, 1.7, 5.6 μg m^{-3}), Table 1). A similar seasonal pattern has been described at other high altitude sites in Europe (e.g., Carbone et al., 2014; Cozic et al., 2008; Freney et al., 2011; Tositti et al., 2013), which are associated with differences in the air mass origin from summer to winter, and also to variations in the planetary boundary layer (PBL) height. The seasonal variation at MSC has been described in detail in recent works (Pandolfi et al., 2014b; Ripoll et al., 2014, 2015), and it has been principally attributed to the seasonal variation of the PBL (Fig. 1). In summer, the stable anticyclonic conditions over this continental area enhance convection, increasing the development of the PBL and favoring the transport of anthropogenic pollutants towards high altitude sites such as MSC. The situation in winter is notably different, as the lower vertical development of the PBL over this area leaves high altitude sites in the FT, isolating MSC from polluted air masses. The seasonal variation of PM concentrations at MSC has been also connected to mesoscale and synoptic processes. At MSC, southern flows and regional recirculation episodes are more frequent in summer, whereas clean Atlantic advections and northeastern winds from mainland Europe are more common in winter (Fig. S2, Table S1) (Pandolfi et al., 2014b; Ripoll et al., 2014, 2015). Moreover, the summer maximum has been ascribed to the more vigorous photochemistry in the atmosphere that enhances the formation of secondary inorganic and organic aerosols (Querol et al., 1999).

3.2 Submicron aerosol chemical composition

Concentrations of ACSM species were averaged daily and compared with offline measurements from 24 h PM_1 samples, and all species showed strong correlations (R^2 between 0.77 and 0.96; Fig. S3). Different slopes (ACSM vs. offline measurements) were found for each of the species: 1.12 for sulfate, 1.31 for ammonium and 1.35 for nitrate. The relatively higher slope for nitrate, with respect to sulfate, could be attributed to a sampling negative artifact due to the volatilization of nitrate on the offline samples (Schaap et al., 2004). Ammonium is present as a counterion for sulfate and nitrate and, thus, its slope is in between those of the two species.

The OM-to-OC ratio cannot be determined for ACSMs based on f_{44} following Aiken et al. (2008) as concluded from an intercomparison of 13 ACSMs (Fröhlich et al., 2015). Therefore, the OM-to-OC in the present study was estimated from the slope of OA, measured by ACSM, vs. OC, obtained from offline measurements. This slope was found to be 3.39; however, values of 2.2 are more common for aged aerosol (e.g., Aiken et al., 2008; Minguillón et al., 2011; Takahama et al., 2011). This disagreement of a factor of 1.54 may be attributed to different reasons. A negative volatilization ar-

Table 1. Diurnal variation of the boundary layer height (computed with HYSPLIT model) averaged for each month during the study period at Montsec. Variation bars indicate ± standard deviation.

	Whole period ($\mu g\,m^{-3}$)	Summer ($\mu g\,m^{-3}$)	Winter ($\mu g\,m^{-3}$)
Period	14 July 2011–23 April 2012	14 July 2011–24 September 2011	10 January 2012–7 March 2012
Organics	2.4 (0.5, 1.4, 3.8)	4.0 (2.1, 4.0, 5.6)	1.9 (0.4, 1.0, 2.6)
Sulfate	1.0 (0.2, 0.5, 1.4)	1.9 (0.7, 1.6, 2.7)	0.5 (0.1, 0.3, 0.7)
Nitrate	0.7 (0.05, 0.2, 0.7)	0.5 (0.1, 0.3, 0.6)	1.0 (0.05, 0.2, 1.0)
Ammonium	0.6 (0.09, 0.3, 0.9)	0.9 (0.3, 0.8, 1.2)	0.5 (0.06, 0.2, 0.7)
Chloride	0.05 (0.01, 0.02, 0.05)	0.04 (0.01, 0.02, 0.05)	0.1 (0.004, 0.02, 0.1)
BC	0.2 (0.04, 0.1, 0.3)	0.2 (0.1, 0.2, 0.3)	0.2 (0.03, 0.1, 0.2)
Total	4.9 (0.9, 2.8, 7.9)	7.5 (3.4, 7.1, 10.5)	4.1 (0.8, 1.7, 5.6)

tifact may occur in the filters, hence resulting in an underestimation of OC. Alternatively it is possible that the RIE for OA in the ACSM is larger than the value of 1.4 determined for the AMS, a topic currently being investigated by the ACSM manufacturer, which would result in an overestimation of OA. Similar series of intercomparisons with a similar discrepancy for OA have been found for a 1-year data set (June 2012–July 2013) with the same instrument at the Montseny site (Minguillón et al., 2015) and for a recently reported study in Atlanta, USA, by Budisulistiorini et al. (2014). Assuming that the disagreement was due to the overestimation by the ACSM, the OA concentrations were corrected dividing by the disagreement factor (1.54) to compare the results with co-located measurements (Fig. 3). The resulting slopes were very similar and, hence, OA concentrations reported in the present paper were not corrected since further research is needed to better estimate the RIE for OA in the ACSM.

The average of PM_1 chemical composition at MSC during this study (July 2011–April 2012) is given in Fig. 4. On average, OA was the largest PM_1 constituent (50 %), followed by sulfate (20 %), nitrate (14 %), ammonium (12 %), BC (4 %) and chloride (1 %). As was the case of PM_1 concentrations, all chemical components increased in summer and decreased in winter, with the exception of nitrate (Fig. 4, Table 1). The higher nitrate concentrations in winter than in summer were also observed in other studies in the Mediterranean region (e.g., Pey et al., 2009; Querol et al., 2009; Ripoll et al., 2015) and this variation was attributed to the high volatility of ammonium nitrate at low humidity and high temperature (Zhuang et al., 1999). At MSC, the summer maximum of the rest of PM components has been mainly ascribed to the higher temperature and solar radiation in summer (Table S1), which enhances atmospheric photochemistry, promoting the formation of secondary inorganic and organic aerosols. All these seasonal characteristics are described in detail in Ripoll et al. (2015).

3.2.1 Summer trends

Time series of PM_1 components during summertime (14 July–24 September 2011) are shown in Fig. 5. Wind direction and wind speed, temperature, precipitation and concentrations of nitrogen oxides, sulfur dioxide, and ozone are also depicted. The daily classification of atmospheric episodes affecting MSC is also illustrated in different background colors. On average, during summer the lowest concentrations of all PM_1 components and gases were recorded under the Atlantic advection conditions since these air masses are associated with precipitation, decreased temperature and solar radiation, and strong winds, leading to cleaner atmospheric conditions. Conversely, summer regional episodes lasted for 6–11 consecutive days and led to sustained increases of the background concentrations of sulfate, OA and BC at MSC. Despite the limited ACSM data availability during North African episodes, relatively high concentrations of PM_1 components were observed under this type of episodes, especially BC (Fig. 5).

The diurnal cycles of PM_1 components, gaseous pollutants and meteorological variables are shown in Fig. 6. The summer concentrations of PM_1 components and gases showed no clear diurnal patterns, except for ozone and OA. This lack of defined daily patterns is similar to the findings obtained at the high altitude Puy-de-Dôme station in central France (Freney et al., 2011, the only similar study found at a remote site). For a high altitude site as MSC, the lack of diurnal cycles can be explained by a combination of factors. In summer, the recirculation of air masses over the WMB induced by an abrupt orography (Fig. S1) causes the formation of reservoir layers at any time at relatively high altitudes (Millan et al., 1997; Rodríguez et al., 2003). Moreover, long-range transport from North Africa, which can be more intense at high altitude layers (Ripoll et al., 2015), could also blur the daily patterns since the occurrence of this transport does not depend on the time of the day. These factors result in a lack of well-defined daily patterns but in a high variability of diurnal cycles even within the same type of episode, which is

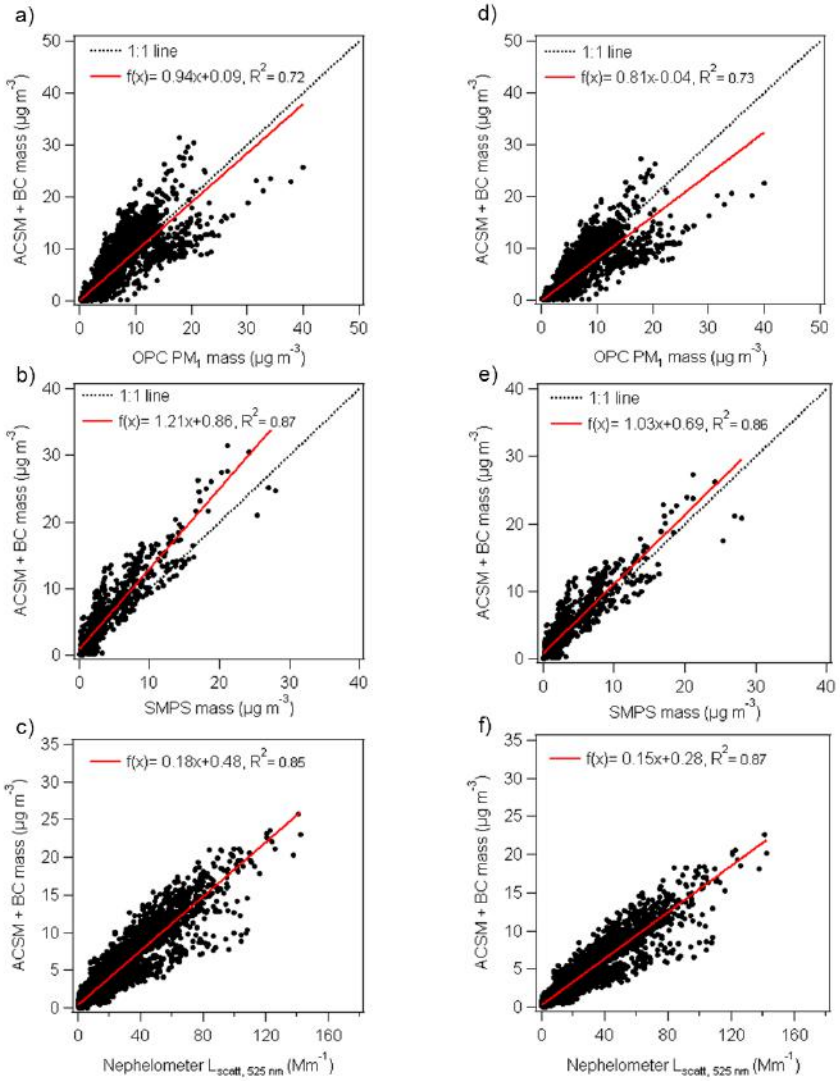

Figure 3. Scatter plots of ACSM plus BC mass vs. PM_1 from **(a)** OPC and **(b)** SMPS (winter campaign), and vs. light scattering at 525 nm from **(c)** nephelometer. Scatter plots of ACSM plus BC mass after dividing OA by 1.54 vs. PM_1 from **(d)** OPC and **(e)** SMPS (winter campaign), and vs. light scattering at 525 nm from **(f)** nephelometer. Data points correspond to hourly values. Equations and red lines correspond to linear regression fits.

reflected in the similar average daily evolutions and the high standard deviations calculated for the average daily patterns when separated by air mass origin (Fig. S4).

The ozone and OA concentrations had a marked diurnal cycle regardless of the air mass origin (Fig. 6, Fig. S4) in summer. These different daily patterns with respect to the rest of the gases and chemical components points to the fact that ozone and OA variations are strongly influenced by local/regional processes and not just dominated by long-range transport. Minimum ozone concentrations were recorded between 08:00 and 09:00 UTC (coordinated universal time, which is local time minus 1 h and local summer time minus 2 h), whereas maximum concentrations were measured between 16:00 and 17:00 UTC. In contrast, the highest OA concentrations were observed around 12:00 UTC and the lowest during the night and in the early morning. The ozone variations may influence those of OA, although the complete understanding of the ozone diurnal evolution is outside the scope of this study. The average increase in OA during the day is likely due to the photooxidation of volatile organic compounds (VOCs). Given that MSC is a remote site, in summer VOCs are most likely dominated by local bio-

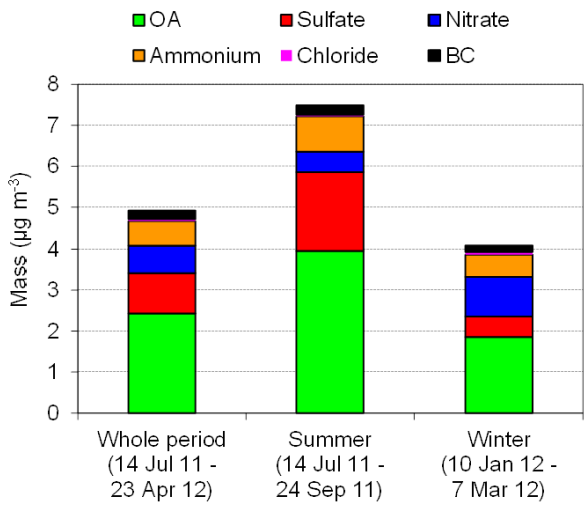

Figure 4. Average concentrations of PM_1 chemical species measured at Montsec during the whole study, in summer and in winter.

genic emissions (BVOCs), as it was found in the Mediterranean forested area of Montseny (Seco et al., 2011). Hence, the midday increase is likely due to recently produced biogenic SOA and, to a lesser degree, photooxidation of anthropogenic VOCs.

Despite the marked diurnal cycle of OA regardless of air mass origin, the average increase during the day with respect to average concentrations during the night was higher under summer regional (2.6 $\mu g\,m^{-3}$) and North African (3.0 $\mu g\,m^{-3}$) episodes than during Atlantic advections (1.3 $\mu g\,m^{-3}$) (Fig. S4). This difference could be caused by the higher SOA formation. This is due to the increase in BVOC emissions and atmospheric photooxidation caused by the higher temperature and solar radiation (Paasonen et al., 2013; Seco et al., 2011) under summer regional and North African episodes. Furthermore, under these episodes higher concentrations of ozone were measured, which also favor the formation of SOA (via direct oxidation and also by leading to higher OH concentrations). The SOA formation registered at MSC is relatively high when compared to other high altitude sites such as Puy-de-Dôme (Freney et al., 2011). This is in agreement with the modeled SOA emissions over Europe, which identified higher SOA concentrations in Mediterranean environments (Bessagnet et al., 2008). This higher SOA formation is probably due to the higher emissions of BVOCs in the Mediterranean forested areas (up to 3 times higher than Boreal forested areas) (Bessagnet et al., 2008; Lang-Yona et al., 2010; Steinbrecher et al., 2009) and the comparable concentrations of tropospheric ozone with other high altitude European sites (Chevalier et al., 2007). On the other hand, the extra formation of SOA under summer regional and North African episodes might also have a contribution from the photooxidation of anthropogenic VOCs since Atlantic advections are associated with cleaner atmospheric conditions.

3.2.2 Winter trends

As in summer, the lowest concentrations of all PM_1 components and gases in winter (10 January 2012–7 March 2012) were recorded under the Atlantic advections, whereas the highest were measured when MSC was affected by air masses from mainland Europe and sporadically under regional conditions (Fig. 7). Mediterranean air masses were detected very infrequently and therefore conclusions on their characteristics will not be drawn in the present paper. The relative contribution of different components was similar, with OA representing a somewhat smaller fraction than in summer.

In contrast to what was found in summer, in winter concentrations of most PM_1 components and gaseous pollutants showed much clearer diurnal patterns, with a minimum around 07:00 UTC and a maximum between 14:00 and 15:00 UTC (Fig. 6). Similar patterns have been observed at the Puy-de-Dôme station during a winter campaign (Freney et al., 2011). These daily cycles are probably caused by the fact that MSC is located most of the day within the FT in winter, whereas PBL air masses are only injected upwards after midday (Fig. 1) Moreover, thermal inversions are very frequent from 20:00 to 07:00 UTC. These situations prevent the transport of pollutants from the lower populated areas towards higher altitudes, especially at night. During the morning, the thermal inversions dissipate due to the radiative warming of the ground and mountain upslope winds develop (e.g., Henne et al., 2004). These mountain winds transport anthropogenic emissions from the adjacent valleys and plains to the top of the mountain, with a maximum upslope transport in the afternoon. Moreover, the biogenic emissions influence cannot be ruled out as average winter temperatures are high enough for them to occur (Seco et al., 2011; Steinbrecher et al., 2009). Thus, mountain breezes play an important role in determining the diurnal variation of PM_1 components in winter (Fig. 6), especially under regional conditions. A clear example of the PM_1 components' diurnal pattern under winter regional episodes was observed from 22 to 25 February 2012 with PM_1 concentrations (and NO_x) increasing several fold during the afternoon (Fig. 7).

The study of the daily cycles as a function of air mass origin (Fig. S5) showed clear diurnal patterns under winter regional episodes, as mentioned above, and less marked daily patterns when MSC is affected by Atlantic advections and long-range transport from mainland Europe. Under Atlantic episodes, the concentrations of PM_1 components were very low and the standard deviations with respect to the average pattern were quite high, resulting in unclear diurnal patterns compared to those under winter regional conditions. During European episodes, which can be more intense at high altitude layers (Ripoll et al., 2015; Sicard et al., 2011), back-

Figure 5. Time series of wind direction, precipitation, temperature, wind speed, concentrations of nitrogen oxides (NO_X), sulfur dioxide (SO_2), ozone (O_3), and PM_1 chemical species (OA, sulfate, nitrate, ammonium, chloride and black carbon (BC)) in summer (14 July 2011–24 September 2011). Background colors correspond to daily classification of atmospheric episodes (summer regional (SREG), North African (NAF), and Atlantic (AT)) and the pie chart corresponds to the average chemical composition for the summer period.

ground concentrations of PM_1 components were higher and the midday increment was lower compared to those under winter regional conditions, resulting in less marked daily patterns. These less-marked diurnal cycles are probably due to the fact that the increase of PM_1 components occurs during these episodes regardless of the time of the day. A good example of this less-marked diurnal variation during European episodes was observed from 17 to 19 February 2012 (Fig. 7).

3.3 Characterization of OA components

In order to better characterize the profiles of OA components, the ME-2 analysis was performed separately for the summer period (14 July–24 September 2011) and the winter period (10 January 2012–7 March 2012), since OA components are expected to vary throughout the year. The solution of the ME-2 analysis selected for each season was based on several tests, with a different number of factors and different a values, taking into account the correlations with external tracers (including nitrate, sulfate, BC and ozone), the daily patterns of each factor, and the residuals. As a result, a solution of three factors was selected for each season. In summer, a hydrocarbon-like OA (HOA), a semivolatile oxygenated OA (SV-OOA) and a low-volatility oxygenated OA (LV-OOA) (Fig. S6) were resolved. The HOA factor was constrained using an average HOA factor from different data sets (Ng et al., 2011b), with an a value of 0.1. The SV-OOA was characterized by a high 43 : 44 ratio, and the LV-OOA was defined by having a dominant peak at m/z 44. In winter the 3 factors identified were HOA, biomass burning OA (BBOA) and OOA (Fig. S6). The HOA and the BBOA factors were constrained based on the profiles from different data sets (Ng et al., 2011b), with an a value of 0.1 in both factors, and including BC as an additional variable to the ME-2 analysis. The OOA was characterized by a 43 : 44 ratio between those found for the LV-OOA and the SV-OOA in summer, and by having a dominant peak at m/z 44. This high signal

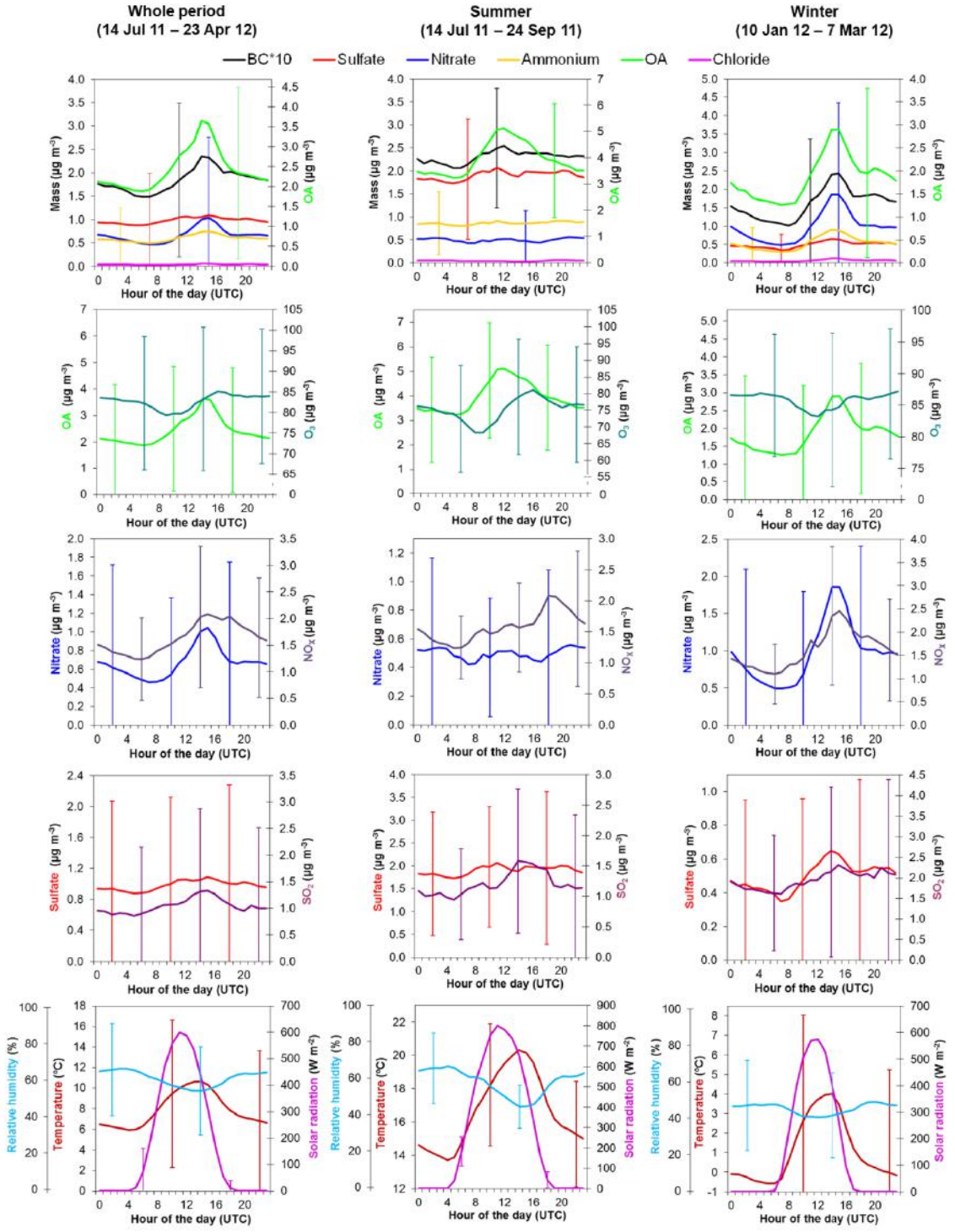

Figure 6. Diurnal cycles of PM_1 chemical species (BC, sulfate, nitrate, ammonium, chloride and OA), gaseous pollutants (O_3, NO_X, and SO_2), and meteorological parameters (relative humidity, temperature and solar radiation) averaged for the whole period, summer and winter. Variation bars indicate ± standard deviation.

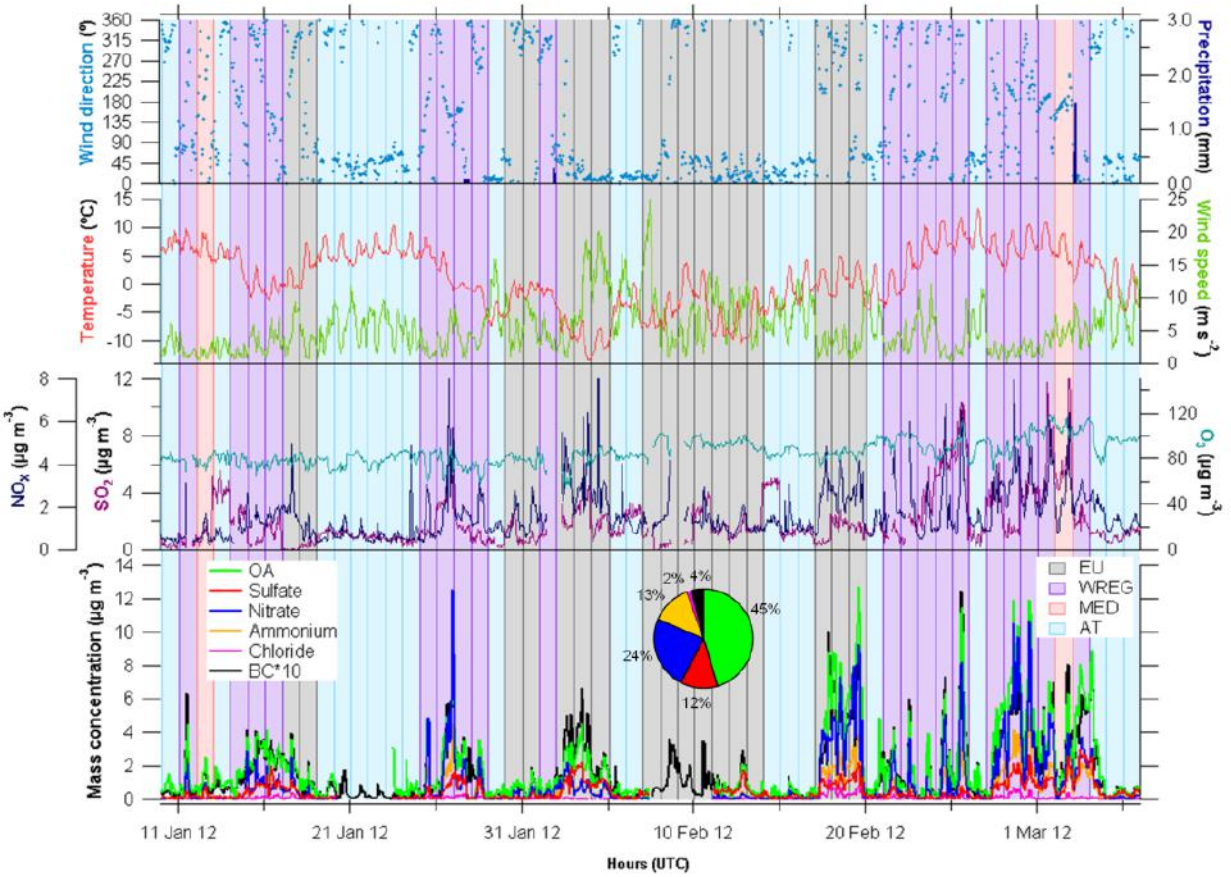

Figure 7. Time series of wind direction (WD) and speed (WS), temperature (T), precipitation (PP), concentrations of NO_x, SO_2, O_3, and PM_1 chemical species (organics, sulfate, nitrate, ammonium, chloride and black carbon (BC)) in winter (10 January 2012–7 March 2012). Background colors correspond to daily classification of atmospheric episodes (European (EU), winter regional (WREG), Mediterranean (MED) and Atlantic (AT)) and the pie chart corresponds to the average chemical composition for the winter period.

of m/z 44 in the winter OOA indicates a high degree of oxidation and, therefore, a dominant aged character during winter. A solution with four factors in winter was investigated in order to split the OOA into SV-OOA and LV-OOA, but the resulting profiles did not represent two different OOA types, and the time series showed that one of the factors was mainly representing noise. The HOA profiles obtained for the summer and winter periods were similar and showed similar deviations from the Ng et al. (2011b) spectrum (Fig. S7), since they were constrained with the same anchor HOA profile.

On average, LV-OOA dominated the OA fraction in summer, contributing 64 %, followed by SV-OOA (26 %) and the HOA (10 %) (Fig. 8), whereas in winter OOA accounted for 71 %, BBOA contributed 24 %, and HOA contribution decreased to 5 % (Fig. 9). The high contribution of OOA components confirms the initial hypothesis of MSC organic components being mostly secondary in their origin, and it is in agreement with what was found in other remote sites (Freney et al., 2011; Raatikainen et al., 2010). Furthermore, the origin of OA has been recently investigated in the Mediterranean forested area of Montseny and it has been found that SOA accounted for 91 % (Minguillón et al., 2011). The low contribution of primary organic components at MSC is in agreement with the location, since the primary organic emissions are mixed and oxidized during their transport from industrial and urban areas to the remote site of MSC.

The diurnal cycles of OA components were studied as a function of air mass origin (Fig. 8, 9). A clear daily pattern of OA components was found regardless of the air mass origin, except for Atlantic advections in winter. In summer, the maximum concentrations of LV-OOA and HOA were measured between 12:00 and 13:00 UTC, whereas those of SV-OOA were observed between 11:00 and 12:00 UTC. The LV-OOA has been generally associated with highly oxidized, aged, and long-range-transported aerosol particles (Lanz et al., 2010). Conversely, the SV-OOA has been described as the less oxy-

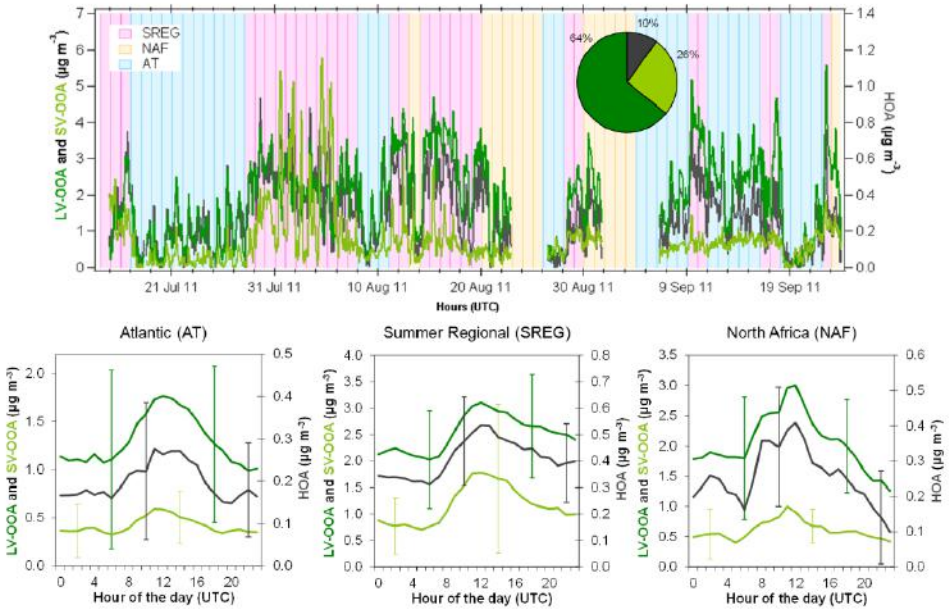

Figure 8. Top: time series of organic species (hydrocarbon-like organic aerosol (HOA), semivolatile oxygenated organic aerosol (SV-OOA) and low-volatility oxygenated organic aerosol (LV-OOA)) concentrations in summer (14 July 2011–24 September 2011). Background colors correspond to daily classification of atmospheric episodes and the pie chart correspond to the average organic species composition for the summer period. Bottom: diurnal cycles of organic species concentrations averaged as a function of atmospheric episode for the summer period. Variation bars indicate ± standard deviation.

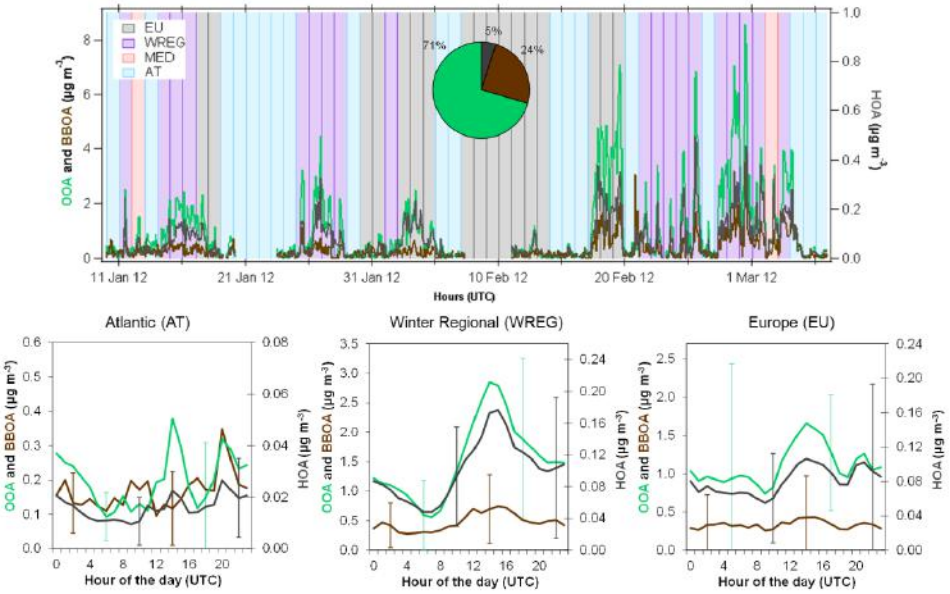

Figure 9. Top: time series of organic species (hydrocarbon-like organic aerosol (HOA), biomass burning organic aerosol (BBOA) and oxygenated organic aerosol (OOA)) concentrations in winter (10 January 2012–7 March 2012). Background colors correspond to daily classification of atmospheric episodes and the pie chart correspond to the average organic species composition for the winter period. Bottom: diurnal cycles of organic species concentrations averaged as a function of atmospheric episode for the winter period. Variation bars indicate ± standard deviation.

genated and semivolatile fraction of OOA (Ng et al., 2011a) and therefore it has been mostly attributed to SOA formation from more local emissions (Jimenez et al., 2009). For this reason, the LV-OOA and HOA hourly variations are more influenced by long-range transport than those of SV-OOA, which are strongly influenced by local/regional processes. In winter, the maximum concentrations of the OA components were observed simultaneously around 14:00 UTC. The different daily patterns between seasons can be attributed to the higher production of SOA in summer as opposed to winter, when the maximum daily concentrations are reached and later driven by the mountain breezes.

4 Conclusions

This work interprets the real-time variation of inorganic and organic submicron components during 10 months (July 2011–April 2012) at a high altitude site in southern Europe (Montsec, 1570 m a.s.l.). The aerosol chemical composition was obtained with an ACSM, and co-located online and offline PM_1 measurements were also carried out. The average concentration of the ACSM plus BC mass during this study was 4.9 $\mu g\,m^{-3}$ and, on average, OA was the foremost PM_1 constituent (50 %), followed by sulfate (20 %), nitrate (14 %), ammonium (12 %), BC (4 %) and chloride (1 %). Discrepancies of OA determined by ACSM with co-located measurements pointed to an overestimation by the ACSM probably caused by the use of the default RIE for OA, which could be lower than the actual one. Further research is needed to better address this issue.

The seasonal variation of PM_1 mass and chemical component concentrations showed similar patterns, with an increase in summer and a decrease in winter, except for nitrate which has high volatility in summer. The seasonal variation was attributed to the evolution of the PBL height throughout the year and to synoptic circulation and meteorological factors. At MSC the higher temperature and solar radiation in summer enhances the convection processes, incrementing the development of the PBL, and augments atmospheric photochemistry, promoting the formation of secondary inorganic and organic aerosols.

The diurnal variation of PM_1 components had no clear diurnal patterns in summer, except for organics. This lack of defined daily patterns was ascribed to the recirculation of air masses that causes the formation of reservoir layers at relatively high altitudes and to the long-range transport from North Africa. These factors result in a high variability of diurnal cycles even within the same type of episode. Nevertheless, organic concentrations had a marked diurnal cycle regardless of the air mass origin, with maximum concentrations around 12:00 UTC. The OA was dominated by LV-OOA (64 %), followed by SV-OOA (26 %), and HOA (10 %). Hence, the midday increase with respect to average concentrations during the night was attributed to the formation of SOA.

In winter, under regional conditions, concentrations of all PM_1 components showed much clearer diurnal patterns than in summer, with a maximum between 14:00 and 15:00 UTC. These daily cycles were connected to the fact that MSC is located most of the day within the FT, whereas PBL air masses are only injected upwards after midday. However, when MSC was affected by long-range transport from mainland Europe, less marked daily patterns of PM_1 components were observed.

The OA in winter was also mainly secondary (71 %), with contributions from BBOA (24 %), and HOA (5 %). The hourly variation of these factors showed a clear diurnal pattern regardless of the air mass origin, except for Atlantic advections.

To the authors' knowledge, this is one of the first times that real-time submicron aerosol chemical composition is characterized and its variation interpreted during a period of almost a year in a continental background environment. The results obtained in the present study highlight the importance of the SOA formation processes at a remote site such as MSC, which could be the objective of further investigations.

The Supplement related to this article is available online at doi:10.5194/acp-15-2935-2015-supplement.

Acknowledgements. This study was supported by the Ministry of Economy and Competitiveness and FEDER funds under the PRISMA (CGL2012-39623-C02-1) and CARIATI (CGL2008-06294/CLI) projects, and by the Generalitat de Catalunya (AGAUR 2009 SGR8 and the DGQA). The research received funding from the European Union Seventh Framework Programme (FP7/2007-2013) ACTRIS under grant agreement no. 262254. We would like to extend their gratitude to the personnel from the COU and the OAdM. We would also like to express our gratitude to the NOAA Air Resources Laboratory (ARL) for the provision of the HYSPLIT transport and dispersion model, and boundary layer height calculation, used in this publication. D. A. Day and J. L. Jimenez thank the DOE (BER/ASR) DE-SC0011105 and NOAA NA13OAR4310063.

Edited by: R. McLaren

References

Aiken, A. C., Decarlo, P. F., Kroll, J. H., Worsnop, D. R., Huffman, J. A., Docherty, K. S., Ulbrich, I. M., Mohr, C., Kimmel, J. R., Sueper, D., Sun, Y., Zhang, Q., Trimborn, A., Northway, M., Ziemann, P. J., Canagaratna, M. R., Onasch, T. B., Alfarra, M. R., Prevot, A. S. H., Dommen, J., Duplissy, J., Metzger, A., Baltensperger, U., and Jimenez, J. L.: O/C and OM/OC ratios

of primary, secondary, and ambient organic aerosols with high-resolution time-of-flight aerosol mass spectrometry, Environ. Sci. Technol., 42, 4478–4485, doi:10.1021/es703009q, 2008.

Bessagnet, B., Menut, L., Curci, G., Hodzic, A., Guillaume, B., Liousse, C., Moukhtar, S., Pun, B., Seigneur, C., and Schulz, M.: Regional modeling of carbonaceous aerosols over Europe-focus on secondary organic aerosols, J. Atmos. Chem., 61, 175–202, doi:10.1007/s10874-009-9129-2, 2008.

Budisulistiorini, S. H., Canagaratna, M. R., Croteau, P. L., Baumann, K., Edgerton, E. S., Kollman, M. S., Ng, N. L., Verma, V., Shaw, S. L., Knipping, E. M., Worsnop, D. R., Jayne, J. T., Weber, R.J., and Surratt, J. D.: Intercomparison of an Aerosol Chemical Speciation Monitor (ACSM) with ambient fine aerosol measurements in downtown Atlanta, Georgia, Atmos. Meas. Tech., 7, 1929–1941, doi:10.5194/amt-7-1929-2014, 2014.

Budisulistiorini, S. H., Canagaratna, M. R., Croteau, P. L., Marth, W. J., Baumann, K., Edgerton, E. S., Shaw, S. L., Knipping, E. M., Worsnop, D. R., Jayne, J. T., Gold, A. and Surratt, J. D.: Real-time continuous characterization of secondary organic aerosol derived from isoprene epoxydiols in downtown Atlanta, Georgia, using the Aerodyne Aerosol Chemical Speciation Monitor., Environ. Sci. Technol., 47, 5686–5694, doi:10.1021/es400023n, 2013.

Canagaratna, M. R., Onasch, T. B., Wood, E. C., Herndon, S. C., Jayne, J. T., Cross, E. S., Miake-Lye, R. C., Kolb, C. E., and Worsnop, D. R.: Chemical and microphysical characterization of ambient aerosols with the aerodyne aerosol mass spectometer, Wiley Intersci., 26, 185–222, doi:10.1002/mas.20115, 2007.

Canonaco, F., Crippa, M., Slowik, J. G., Baltensperger, U., and Prévôt, A. S. H.: SoFi, an IGOR-based interface for the efficient use of the generalized multilinear engine (ME-2) for the source apportionment: ME-2 application to aerosol mass spectrometer data, Atmos. Meas. Tech., 6, 3649–3661, doi:10.5194/amt-6-3649-2013, 2013.

Carbone, S., Saarikoski, S., Frey, A., Reyes, F., Reyes, P., Castillo, M., Gramsch, E., Jayne, J., Worsnop, D. R., and Hillamo, R.: Chemical Characterization of Submicron Aerosol Particles in Santiago de Chile, Aerosol Air Qual. Res., 13, 462–473, doi:10.4209/aaqr.2012.10.0261, 2013.

Carbone, C., Decesari, S., Paglione, M., Giulianelli, L., Rinaldi, M., Marinoni, A., Cristofanelli, P., Didiodato, A., Bonasoni, P., Fuzzi, S., and Facchini, M. C.: 3-year chemical composition of free tropospheric PM1 at the Mt. Cimone GAW global station – South Europe – 2165 m a.s.l., Atmos. Environ., 87, 218–227, doi:10.1016/j.atmosenv.2014.01.048, 2014.

CEN: Air quality – Determination of the PM_{10} fraction of suspended particulate matter. Reference method and field test procedure to demonstrate reference equivalence of measurement methods, EN12341:1999, 1999.

Chevalier, A., Gheusi, F., Delmas, R., Ordóñez, C., Sarrat, C., Zbinden, R., Thouret, V., Athier, G., and Cousin, J.-M.: Influence of altitude on ozone levels and variability in the lower troposphere: a ground-based study for western Europe over the period 2001–2004, Atmos. Chem. Phys., 7, 4311–4326, doi:10.5194/acp-7-4311-2007, 2007.

Cozic, J., Verheggen, B., Weingartner, E., Crosier, J., Bower, K. N., Flynn, M., Coe, H., Henning, S., Steinbacher, M., Henne, S., Collaud Coen, M., Petzold, A., and Baltensperger, U.: Chemical composition of free tropospheric aerosol for PM1 and coarse mode at the high alpine site Jungfraujoch, Atmos. Chem. Phys., 8, 407–423, doi:10.5194/acp-8-407-2008, 2008.

Crippa, M., Canonaco, F., Lanz, V. A., Äijälä, M., Allan, J. D., Carbone, S., Capes, G., Ceburnis, D., Dall'Osto, M., Day, D. A., DeCarlo, P. F., Ehn, M., Eriksson, A., Freney, E., Hildebrandt Ruiz, L., Hillamo, R., Jimenez, J. L., Junninen, H., Kiendler-Scharr, A., Kortelainen, A.-M., Kulmala, M., Laaksonen, A., Mensah, A. A., Mohr, C., Nemitz, E., O'Dowd, C., Ovadnevaite, J., Pandis, S. N., Petäjä, T., Poulain, L., Saarikoski, S., Sellegri, K., Swietlicki, E., Tiitta, P., Worsnop, D. R., Baltensperger, U., and Prévôt, A. S. H.: Organic aerosol components derived from 25 AMS data sets across Europe using a consistent ME-2 based source apportionment approach, Atmos. Chem. Phys., 14, 6159–6176, doi:10.5194/acp-14-6159-2014, 2014.

De Gouw, J. and Jimenez, J. L.: Organic aerosols in the Earth's atmosphere., Environ. Sci. Technol., 43, 7614–7618, doi:10.1021/es9006004, 2009.

Donahue, N. M., Robinson, A. L., Trump, E. R., Riipinen, I., and Kroll, J. H.: Volatility and Aging of Atmospheric Organic Aerosol, Top. Curr. Chem., 339, 97–144, doi:10.1007/128_2012_355, 2014.

Elbert, W., Taylor, P. E., Andreae, M. O., and Pöschl, U.: Contribution of fungi to primary biogenic aerosols in the atmosphere: wet and dry discharged spores, carbohydrates, and inorganic ions, Atmos. Chem. Phys., 7, 4569–4588, doi:10.5194/acp-7-4569-2007, 2007.

Freney, E. J., Sellegri, K., Canonaco, F., Boulon, J., Hervo, M., Weigel, R., Pichon, J. M., Colomb, A., Prévôt, A. S. H., and Laj, P.: Seasonal variations in aerosol particle composition at the puy-de-Dôme research station in France, Atmos. Chem. Phys., 11, 13047–13059, doi:10.5194/acp-11-13047-2011, 2011.

Fröhlich, R., Crenn, V., Setyan, A., Belis, C. A., Canonaco, F., Favez, O., Riffault, V., Slowik, J. G., Aas, W., Aijälä, M., Alastuey, A., Artiñano, B., Bonnaire, N., Bozzetti, C., Bressi, M., Carbone, C., Coz, E., Croteau, P. L., Cubison, M. J., Esser-Gietl, J. K., Green, D. C., Gros, V., Heikkinen, L., Herrmann, H., Jayne, J. T., Lunder, C. R., Minguillón, M. C., Močnik, G., O'Dowd, C. D., Ovadnevaite, J., Petralia, E., Poulain, L., Priestman, M., Ripoll, A., Sarda-Estève, R., Wiedensohler, A., Baltensperger, U., Sciare, J., and Prévôt, A. S. H.: ACTRIS ACSM intercomparison – Part 2: Intercomparison of ME-2 organic source apportionment results from 15 individual, co-located aerosol mass spectrometers, Atmos. Meas. Tech. Discuss., 8, 1559–1613, doi:10.5194/amtd-8-1559-2015, 2015.

Hallquist, M., Wenger, J. C., Baltensperger, U., Rudich, Y., Simpson, D., Claeys, M., Dommen, J., Donahue, N. M., George, C., Goldstein, A. H., Hamilton, J. F., Herrmann, H., Hoffmann, T., Iinuma, Y., Jang, M., Jenkin, M. E., Jimenez, J. L., Kiendler-Scharr, A., Maenhaut, W., McFiggans, G., Mentel, Th. F., Monod, A., Prévôt, A. S. H., Seinfeld, J. H., Surratt, J. D., Szmigielski, R., and Wildt, J.: The formation, properties and impact of secondary organic aerosol: current and emerging issues, Atmos. Chem. Phys., 9, 5155–5236, doi:10.5194/acp-9-5155-2009, 2009.

Henne, S., Furger, M., Nyeki, S., Steinbacher, M., Neininger, B., de Wekker, S. F. J., Dommen, J., Spichtinger, N., Stohl, A., and Prévôt, A. S. H.: Quantification of topographic venting of boundary layer air to the free troposphere, Atmos. Chem. Phys., 4, 497–509, doi:10.5194/acp-4-497-2004, 2004.

IPCC 2013 in: Climate Change 2013: The Physical Science Basis (Contribution of Working Group I to the Fifth Assessment Report of the Intergovernmental Panel on Climate Change), edited by: Stocker, T. F., Qin, D., Plattner, G. K., Tignor, M. M. B., Allen, S. K., Boschung, J., Nauels, A., Xia, Y., Bex, V., and Midgley, P. M., Cambridge Univ. Press, UK and New York, USA, 2013.

Jimenez, J. L., Jayne, J. T., Shi, Q., Kolb, C. E., Worsnop, D. R., Yourshaw, I., Seinfeld, J. H., Flagan, R. C., Zhang, X., Smith, K. A., Morris, J. W., and Davidovits, P.: Ambient aerosol sampling using the Aerodyne Aerosol Mass Spectrometer, J. Geophys. Res., 108, 8425, doi:10.1029/2001JD001213, 2003.

Jimenez, J. L., Canagaratna, M. R., Donahue, N. M., Prevot, A. S. H., Zhang, Q., Kroll, J. H., DeCarlo, P. F., Allan, J. D., Coe, H., Ng, N. L., Aiken, A. C., Docherty, K. S., Ulbrich, I. M., Grieshop, A. P., Robinson, A. L., Duplissy, J., Smith, J. D., Wilson, K. R., Lanz, V. A., Hueglin, C., Sun, Y. L., Tian, J., Laaksonen, A., Raatikainen, T., Rautiainen, J., Vaattovaara, P., Ehn, M., Kulmala, M., Tomlinson, J. M., Collins, D. R., Cubison, M. J., Dunlea, E. J., Huffman, J. A., Onasch, T. B., Alfarra, M. R., Williams, P. I., Bower, K., Kondo, Y., Schneider, J., Drewnick, F., Borrmann, S., Weimer, S., Demerjian, K., Salcedo, D., Cottrell, L., Griffin, R., Takami, A., Miyoshi, T., Hatakeyama, S., Shimono, A., Sun, J. Y., Zhang, Y. M., Dzepina, K., Kimmel, J. R., Sueper, D., Jayne, J. T., Herndon, S. C., Trimborn, A. M., Williams, L. R., Wood, E. C., Middlebrook, A. M., Kolb, C. E., Baltensperger, U., and Worsnop, D. R.: Evolution of organic aerosols in the atmosphere., Science, 326, 1525–1529, doi:10.1126/science.1180353, 2009.

Jorba, O., Pandolfi, M., Spada, M., Baldasano, J. M., Pey, J., Alastuey, A., Arnold, D., Sicard, M., Artiñano, B., Revuelta, M. A., and Querol, X.: Overview of the meteorology and transport patterns during the DAURE field campaign and their impact to PM observations, Atmos. Environ., 77, 607–620, doi:10.1016/j.atmosenv.2013.05.040, 2013.

Kroll, J. H. and Seinfeld, J. H.: Chemistry of secondary organic aerosol: Formation and evolution of low-volatility organics in the atmosphere, Atmos. Environ., 42, 3593–3624, doi:10.1016/j.atmosenv.2008.01.003, 2008.

Lang-Yona, N., Rudich, Y., Mentel, Th. F., Bohne, A., Buchholz, A., Kiendler-Scharr, A., Kleist, E., Spindler, C., Tillmann, R., and Wildt, J.: The chemical and microphysical properties of secondary organic aerosols from Holm Oak emissions, Atmos. Chem. Phys., 10, 7253–7265, doi:10.5194/acp-10-7253-2010, 2010.

Lanz, V. A., Prévôt, A. S. H., Alfarra, M. R., Weimer, S., Mohr, C., DeCarlo, P. F., Gianini, M. F. D., Hueglin, C., Schneider, J., Favez, O., D'Anna, B., George, C., and Baltensperger, U.: Characterization of aerosol chemical composition with aerosol mass spectrometry in Central Europe: an overview, Atmos. Chem. Phys., 10, 10453–10471, doi:10.5194/acp-10-10453-2010, 2010.

Middlebrook, A. M., Bahreini, R., Jimenez, J. L., and Canagaratna, M. R.: Evaluation of Composition-Dependent Collection Efficiencies for the Aerodyne Aerosol Mass Spectrometer using Field Data, Aerosol Sci. Technol., 46, 258–271, doi:10.1080/02786826.2011.620041, 2012.

Millan, M. M., Salvador, R., Mantilla, E., and Kallos, G.: Photooxidant dynamics in the Mediterranean basin in summer: Results from European research projects, J. Geophys. Res., 102, 8811–8823, 1997.

Minguillón, M. C., Perron, N., Querol, X., Szidat, S., Fahrni, S. M., Alastuey, A., Jimenez, J. L., Mohr, C., Ortega, A. M., Day, D. A., Lanz, V. A., Wacker, L., Reche, C., Cusack, M., Amato, F., Kiss, G., Hoffer, A., Decesari, S., Moretti, F., Hillamo, R., Teinilä, K., Seco, R., Peñuelas, J., Metzger, A., Schallhart, S., Müller, M., Hansel, A., Burkhart, J. F., Baltensperger, U., and Prévôt, A. S. H.: Fossil versus contemporary sources of fine elemental and organic carbonaceous particulate matter during the DAURE campaign in Northeast Spain, Atmos. Chem. Phys., 11, 12067–12084, doi:10.5194/acp-11-12067-2011, 2011.

Minguillón, M. C., Ripoll, A., Pérez, N., Prévôt, A. S. H., Canonaco, F., Querol, X., and Alastuey, A.: Chemical characterization of submicron regional background aerosols in the Western Mediterranean using an Aerosol Chemical Speciation Monitor, Atmos. Chem. Phys. Discuss., 15, 965–1000, doi:10.5194/acpd-15-965-2015, 2015.

Müller, T., Henzing, J. S., de Leeuw, G., Wiedensohler, A., Alastuey, A., Angelov, H., Bizjak, M., Collaud Coen, M., Engström, J. E., Gruening, C., Hillamo, R., Hoffer, A., Imre, K., Ivanow, P., Jennings, G., Sun, J. Y., Kalivitis, N., Karlsson, H., Komppula, M., Laj, P., Li, S.-M., Lunder, C., Marinoni, A., Martins dos Santos, S., Moerman, M., Nowak, A., Ogren, J. A., Petzold, A., Pichon, J. M., Rodriquez, S., Sharma, S., Sheridan, P. J., Teinilä, K., Tuch, T., Viana, M., Virkkula, A., Weingartner, E., Wilhelm, R., and Wang, Y. Q.: Characterization and intercomparison of aerosol absorption photometers: result of two intercomparison workshops, Atmos. Meas. Tech., 4, 245–268, doi:10.5194/amt-4-245-2011, 2011.

Ng, N. L., Canagaratna, M. R., Zhang, Q., Jimenez, J. L., Tian, J., Ulbrich, I. M., Kroll, J. H., Docherty, K. S., Chhabra, P. S., Bahreini, R., Murphy, S. M., Seinfeld, J. H., Hildebrandt, L., Donahue, N. M., DeCarlo, P. F., Lanz, V. A., Prévôt, A. S. H., Dinar, E., Rudich, Y., and Worsnop, D. R.: Organic aerosol components observed in Northern Hemispheric datasets from Aerosol Mass Spectrometry, Atmos. Chem. Phys., 10, 4625–4641, doi:10.5194/acp-10-4625-2010, 2010.

Ng, N. L., Canagaratna, M. R., Jimenez, J. L., Chhabra, P. S., Seinfeld, J. H., and Worsnop, D. R.: Changes in organic aerosol composition with aging inferred from aerosol mass spectra, Atmos. Chem. Phys., 11, 6465–6474, doi:10.5194/acp-11-6465-2011, 2011a.

Ng, N. L., Canagaratna, M. R., Jimenez, J. L., Zhang, Q., Ulbrich, I. M., and Worsnop, D. R.: Real-Time Methods for Estimating Organic Component Mass Concentrations from Aerosol Mass Spectrometer Data, Environ. Sci. Technol., 45, 910–916, doi:10.1021/es102951k, 2011b.

Ng, N. L., Herndon, S. C., Trimborn, A., Canagaratna, M. R., Croteau, P. L., Onasch, T. B., Sueper, D., Worsnop, D. R., Zhang, Q., Sun, Y. L., and Jayne, J. T.: An Aerosol Chemical Speciation Monitor (ACSM) for routine monitoring of the composition and mass concentrations of ambient aerosol, Aerosol Sci. Technol., 45, 780–794, doi:10.1080/02786826.2011.560211, 2011c.

Paasonen, P., Asmi, A., Petäjä, T., Kajos, M. K., Äijälä, M., Junninen, H., Holst, T., Abbatt, J. P. D., Arneth, A., Birmili, W., van der Gon, H. D., Hamed, A., Hoffer, A., Laakso, L., Laaksonen, A., Richard Leaitch, W., Plass-Dülmer, C., Pryor, S. C., Räisänen, P., Swietlicki, E., Wiedensohler, A., Worsnop, D. R., Kerminen, V.-M., and Kulmala, M.: Warming-induced increase in

aerosol number concentration likely to moderate climate change, Nat. Geosci., 6, 438–442, doi:10.1038/ngeo1800, 2013.

Paatero, P.: The multilinear engine – a table-driven, least squares program for solving multilinear problems, including the n-way parallel factor analysis model, J. Comput. Graph. Stat., 8, 854–888, doi:10.2307/1390831, 1999.

Pandolfi, M., Querol, X., Alastuey, A., Jimenez, J. L., Jorba, O., Day, D., Ortega, A., Cubison, M. J., Comerón, A., Sicard, M., Mohr, C., Prévôt, A. S. H., Minguillón, M. C., Pey, J., Baldasano, J. M., Burkhart, J. F., Seco, R., Peñuelas, J., van Drooge, B. L., Artiñano, B., Di Marco, C., Nemitz, E., Schallhart, S., Metzger, A., Hansel, A., Lorente, J., Ng, S., Jayne, J., and Szidat, S.: Effects of sources and meteorology on particulate matter in the Western Mediterranean Basin: An overview of the DAURE campaign, J. Geophys. Res. Atmos., 119, 4978–5010, doi:10.1002/2013JD021079, 2014a.

Pandolfi, M., Ripoll, A., Querol, X., and Alastuey, A.: Climatology of aerosol optical properties and black carbon mass absorption cross section at a remote high-altitude site in the western Mediterranean Basin, Atmos. Chem. Phys., 14, 6443–6460, doi:10.5194/acp-14-6443-2014, 2014b.

Petit, J.-E., Favez, O., Sciare, J., Crenn, V., Sarda-Estève, R., Bonnaire, N., Moc˘(nik, G., Dupont, J.-C., Haeffelin, M., and Leoz-Garziandia, E.: Two years of near real-time chemical composition of submicron aerosols in the region of Paris using an Aerosol Chemical Speciation Monitor (ACSm) and a multi-wavelength Aethalometer, Atmos. Chem. Phys. Discuss., 14, 24221–24271, doi:10.5194/acpd-14-24221-2014, 2014.

Petzold, A. and Schönlinner, M.: Multi-angle absorption photometry – a new method for the measurement of aerosol light absorption and atmospheric black carbon, J. Aerosol Sci., 35, 421–441, doi:10.1016/j.jaerosci.2003.09.005, 2004.

Petzold, A., Ogren, J. A., Fiebig, M., Laj, P., Li, S.-M., Baltensperger, U., Holzer-Popp, T., Kinne, S., Pappalardo, G., Sugimoto, N., Wehrli, C., Wiedensohler, A., and Zhang, X.-Y.: Recommendations for reporting"black carbon" measurements, Atmos. Chem. Phys., 13, 8365–8379, doi:10.5194/acp-13-8365-2013, 2013.

Pey, J., Pérez, N., Castillo, S., Viana, M., Moreno, T., Pandolfi, M., López-Sebastián, J. M., Alastuey, A., and Querol, X.: Geochemistry of regional background aerosols in the Western Mediterranean, Atmos. Res., 94, 422–435, doi:10.1016/j.atmosres.2009.07.001, 2009.

Pey, J., Querol, X., Alastuey, A., Forastiere, F., and Stafoggia, M.: African dust outbreaks over the Mediterranean Basin during 2001–2011: PM_{10} concentrations, phenomenology and trends, and its relation with synoptic and mesoscale meteorology, Atmos. Chem. Phys., 13, 1395–1410, doi:10.5194/acp-13-1395-2013, 2013.

Querol, X., Alastuey, A., Lopez-soler, A., Plana, F., and Puicercus, J. A.: Daily evolution of sulphate aerosols in a rural area, northeastern Spain – elucidation of an atmospheric reservoir effect, Environ. Pollut., 105, 397–407, doi:10.1016/S0269-7491(99)00037-8, 1999.

Querol, X., Alastuey, A., Pey, J., Cusack, M., Pérez, N., Mihalopoulos, N., Theodosi, C., Gerasopoulos, E., Kubilay, N., and Koçak, M.: Variability in regional background aerosols within the Mediterranean, Atmos. Chem. Phys., 9, 4575–4591, doi:10.5194/acp-9-4575-2009, 2009.

Raatikainen, T., Vaattovaara, P., Tiitta, P., Miettinen, P., Rautiainen, J., Ehn, M., Kulmala, M., Laaksonen, A., and Worsnop, D. R.: Physicochemical properties and origin of organic groups detected in boreal forest using an aerosol mass spectrometer, Atmos. Chem. Phys., 10, 2063–2077, doi:10.5194/acp-10-2063-2010, 2010.

Ripoll, A., Pey, J., Minguillón, M. C., Pérez, N., Pandolfi, M., Querol, X., and Alastuey, A.: Three years of aerosol mass, black carbon and particle number concentrations at Montsec (southern Pyrenees, 1570 m a.s.l.), Atmos. Chem. Phys., 14, 4279–4295, doi:10.5194/acp-14-4279-2014, 2014.

Ripoll, A., Minguillón, M. C., Pey, J., Pérez, N., Querol, X., and Alastuey, A.: Joint analysis of continental and regional background environments in the western Mediterranean: PM_1 and PM_{10} concentrations and composition, Atmos. Chem. Phys., 15, 1129–1145, doi:10.5194/acp-15-1129-2015, 2015.

Robinson, A. L., Donahue, N. M., Shrivastava, M. K., Weitkamp, E. A., Sage, A. M., Grieshop, A. P., Lane, T. E., Pierce, J. R., and Pandis, S. N.: Rethinking organic aerosols: semivolatile emissions and photochemical aging., Science, 315, 1259–1262, doi:10.1126/science.1133061, 2007.

Rodríguez, S., Querol, X., Alastuey, A., Kallos, G., and Kakaliagou, O.: Saharan dust contributions to PM_{10} and TSP levels in Southern and Eastern Spain, Atmos. Environ., 35, 2433–2447, doi:10.1016/S1352-2310(00)00496-9, 2001.

Rodriguez, S., Querol, X., Alastuey, A., and Mantilla, E.: Origin of high summer PM10 and TSP concentrations at rural sites in Eastern Spain, Atmos. Environ., 36, 3101–3112, doi:10.1016/S1352-2310(02)00256-X, 2002.

Rodríguez, S., Querol, X., Alastuey, A., Viana, M.-M., and Mantilla, E.: Events affecting levels and seasonal evolution of airborne particulate matter concentrations in the Western Mediterranean., Environ. Sci. Technol., 37, 216–222, doi:10.1021/es020106p, 2003.

Salcedo, D., Onasch, T. B., Dzepina, K., Canagaratna, M. R., Zhang, Q., Huffman, J. A., DeCarlo, P. F., Jayne, J. T., Mortimer, P., Worsnop, D. R., Kolb, C. E., Johnson, K. S., Zuberi, B., Marr, L. C., Volkamer, R., Molina, L. T., Molina, M. J., Cardenas, B., Bernabé, R. M., Márquez, C., Gaffney, J. S., Marley, N. A., Laskin, A., Shutthanandan, V., Xie, Y., Brune, W., Lesher, R., Shirley, T., and Jimenez, J. L.: Characterization of ambient aerosols in Mexico City during the MCMA-2003 campaign with Aerosol Mass Spectrometry: results from the CENICA Supersite, Atmos. Chem. Phys., 6, 925–946, doi:10.5194/acp-6-925-2006, 2006.

Schaap, M., Spindler, G., Schulz, M., Acker, K., Maenhaut, W., Berner, A., Wieprecht, W., Streit, N., Müller, K., Brüggemann, E., Chi, X., Putaud, J.-P., Hitzenberger, R., Puxbaum, H., Baltensperger, U., and ten Brink, H.: Artefacts in the sampling of nitrate studied in the "INTERCOMP" campaigns of EUROTRAC-AEROSOL, Atmos. Environ., 38, 6487–6496, doi:10.1016/j.atmosenv.2004.08.026, 2004.

Seco, R., Peñuelas, J., Filella, I., Llusià, J., Molowny-Horas, R., Schallhart, S., Metzger, A., Müller, M., and Hansel, A.: Contrasting winter and summer VOC mixing ratios at a forest site in the Western Mediterranean Basin: the effect of local biogenic emissions, Atmos. Chem. Phys., 11, 13161–13179, doi:10.5194/acp-11-13161-2011, 2011.

Sicard, M., Rocadenbosch, F., Reba, M. N. M., Comerón, A., Tomás, S., García-Vízcaino, D., Batet, O., Barrios, R., Kumar, D., and Baldasano, J. M.: Seasonal variability of aerosol optical properties observed by means of a Raman lidar at an EARLINET site over Northeastern Spain, Atmos. Chem. Phys., 11, 175–190, doi:10.5194/acp-11-175-2011, 2011.

Steinbrecher, R., Smiatek, G., Köble, R., Seufert, G., Theloke, J., Hauff, K., Ciccioli, P., Vautard, R., and Curci, G.: Intra- and inter-annual variability of VOC emissions from natural and semi-natural vegetation in Europe and neighbouring countries, Atmos. Environ., 43, 1380–1391, doi:10.1016/j.atmosenv.2008.09.072, 2009.

Sun, Y., Wang, Z., Dong, H., Yang, T., Li, J., Pan, X., Chen, P., and Jayne, J. T.: Characterization of summer organic and inorganic aerosols in Beijing, China with an Aerosol Chemical Speciation Monitor, Atmos. Environ., 51, 250–259, doi:10.1016/j.atmosenv.2012.01.013, 2012.

Takahama, S., Schwartz, R. E., Russell, L. M., Macdonald, A. M., Sharma, S., and Leaitch, W. R.: Organic functional groups in aerosol particles from burning and non-burning forest emissions at a high-elevation mountain site, Atmos. Chem. Phys., 11, 6367–6386, doi:10.5194/acp-11-6367-2011, 2011.

Tiitta, P., Vakkari, V., Croteau, P., Beukes, J. P., van Zyl, P. G., Josipovic, M., Venter, A. D., Jaars, K., Pienaar, J. J., Ng, N. L., Canagaratna, M. R., Jayne, J. T., Kerminen, V.-M., Kokkola, H., Kulmala, M., Laaksonen, A., Worsnop, D. R., and Laakso, L.: Chemical composition, main sources and temporal variability of PM_1 aerosols in southern African grassland, Atmos. Chem. Phys., 14, 1909–1927, doi:10.5194/acp-14-1909-2014, 2014.

Tositti, L., Riccio, A., Sandrini, S., Brattich, E., Baldacci, D., Parmeggiani, S., Cristofanelli, P., and Bonasoni, P.: Short-term climatology of PM10 at a high altitude background station in southern Europe, Atmos. Environ., 65, 142–152, doi:10.1016/j.atmosenv.2012.10.051, 2013.

Volkamer, R., Jimenez, J. L., San Martini, F., Dzepina, K., Zhang, Q., Salcedo, D., Molina, L. T., Worsnop, D. R., and Molina, M. J.: Secondary organic aerosol formation from anthropogenic air pollution: Rapid and higher than expected, Geophys. Res. Lett., 33, L17811, doi:10.1029/2006GL026899, 2006.

Zhang, Q., Worsnop, D. R., Canagaratna, M. R., and Jimenez, J. L.: Hydrocarbon-like and oxygenated organic aerosols in Pittsburgh: insights into sources and processes of organic aerosols, Atmos. Chem. Phys., 5, 3289–3311, doi:10.5194/acp-5-3289-2005, 2005.

Zhang, Q., Jimenez, J. L., Canagaratna, M. R., Allan, J. D., Coe, H., Ulbrich, I., Alfarra, M. R., Takami, A., Middlebrook, a. M., Sun, Y. L., Dzepina, K., Dunlea, E., Docherty, K., DeCarlo, P. F., Salcedo, D., Onasch, T., Jayne, J. T., Miyoshi, T., Shimono, A., Hatakeyama, S., Takegawa, N., Kondo, Y., Schneider, J., Drewnick, F., Borrmann, S., Weimer, S., Demerjian, K., Williams, P., Bower, K., Bahreini, R., Cottrell, L., Griffin, R. J., Rautiainen, J., Sun, J. Y., Zhang, Y. M., and Worsnop, D. R.: Ubiquity and dominance of oxygenated species in organic aerosols in anthropogenically-influenced Northern Hemisphere midlatitudes, Geophys. Res. Lett., 34, L13801, doi:10.1029/2007GL029979, 2007.

Zhuang, H., Chan, C. K., Fang, M., and Wexler, A. S.: Size distributions of particulate sulfate , nitrate, and ammonium at a coastal site in Hong Kong, Atmos. Environ., 33, 843–853, doi:10.1016/S1352-2310(98)00305-7, 1999.

Supplementary material related to "Long-term real-time chemical characterization of submicron aerosols at Montsec (southern Pyrenees, 1570 m a.s.l.)"

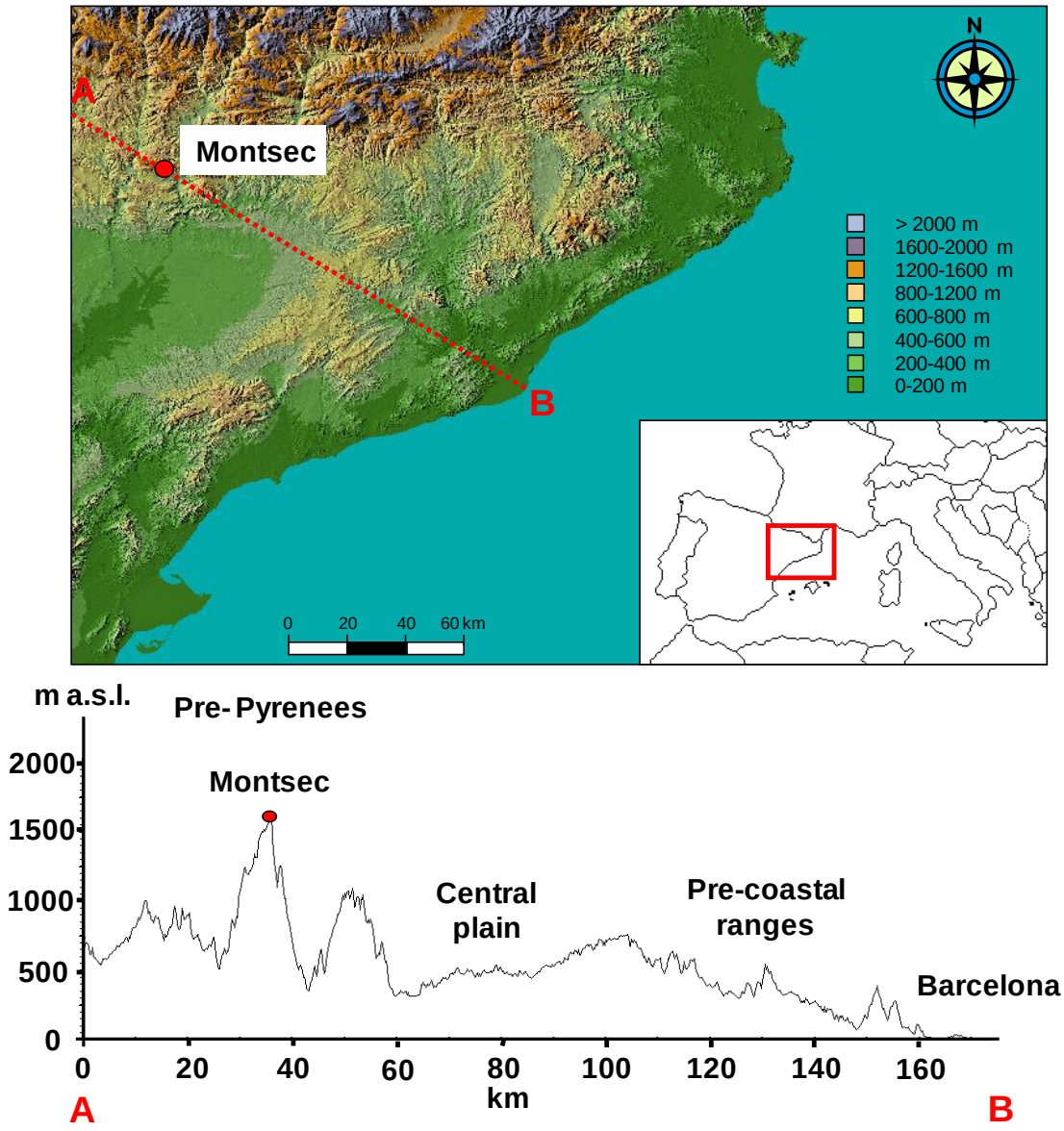

Fig.S1 Top: location of the Montsec sampling site. Bottom: topography of Montsec area following the red line.

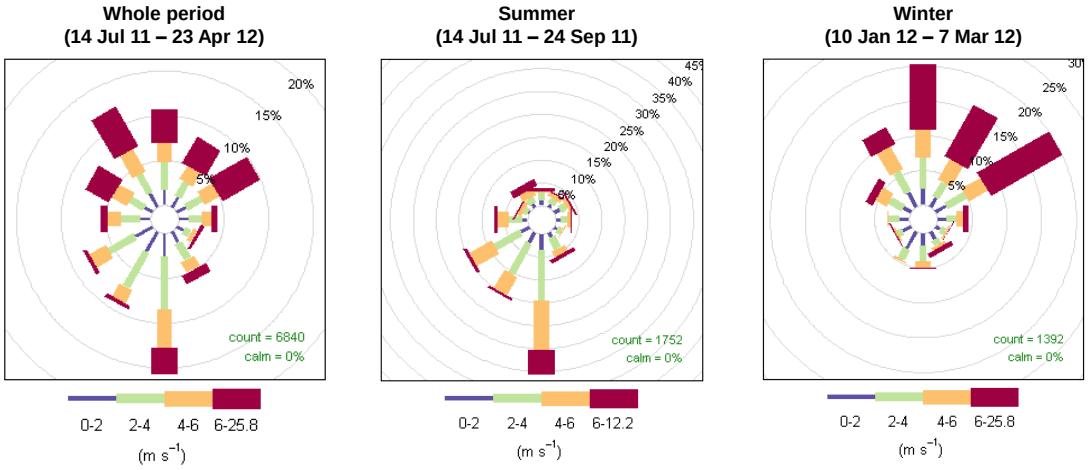

Fig.S2 Wind rose frequency at Montsec during the study.

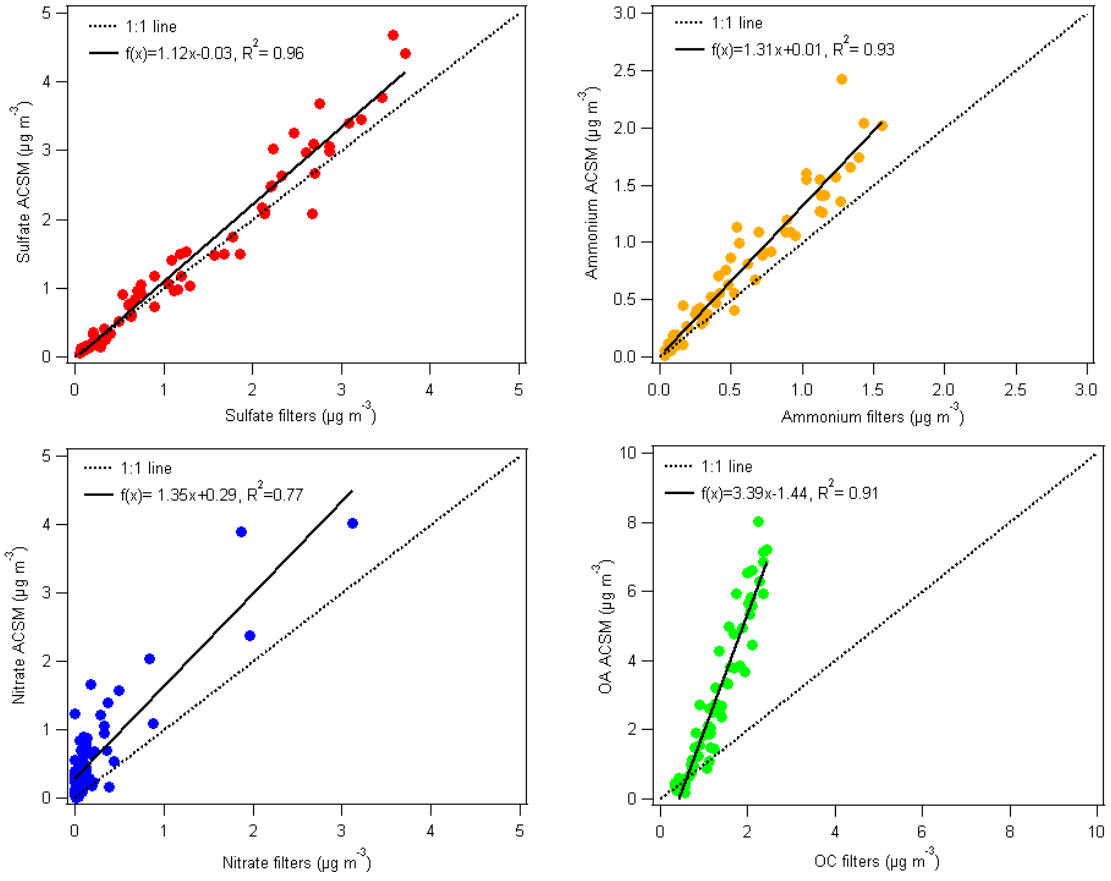

Fig.S3 Scatter plots of chemical species concentrations measured by the ACSM versus those measured off-line in 24-h PM_1 filter samples.

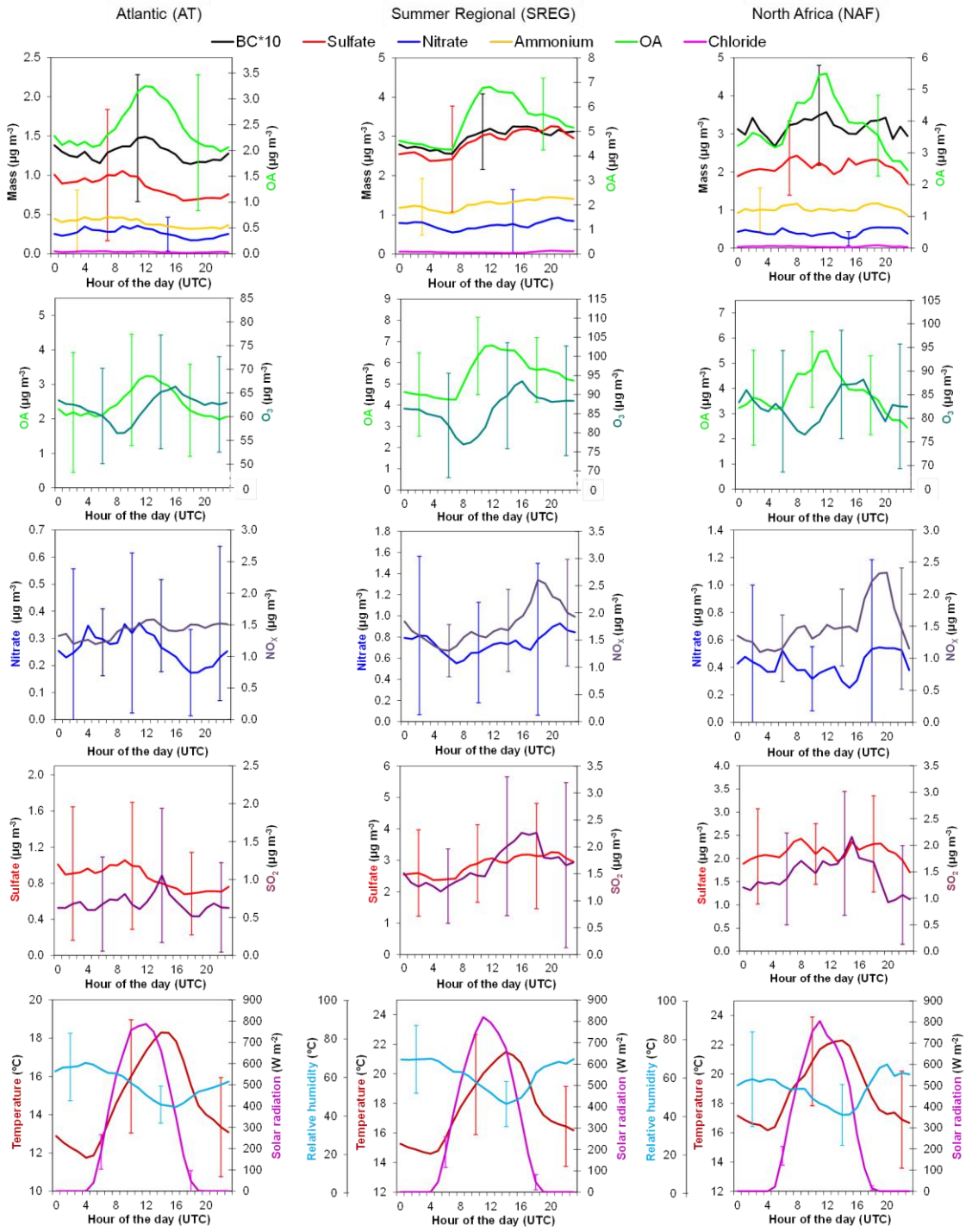

Fig.S4 Diurnal cycles of PM_1 chemical species (black carbon (BC), sulfate, nitrate, ammonium, chloride and OA), gaseous pollutants (ozone (O_3), nitrogen oxides (NO_x), and sulfur dioxide (SO_2)), and meteorological parameters (relative humidity, temperature and solar radiation) averaged as a function of meteorological episode for the summer period (14 Jul 11 – 24 Sep 11). Variation bars indicate ± standard deviation.

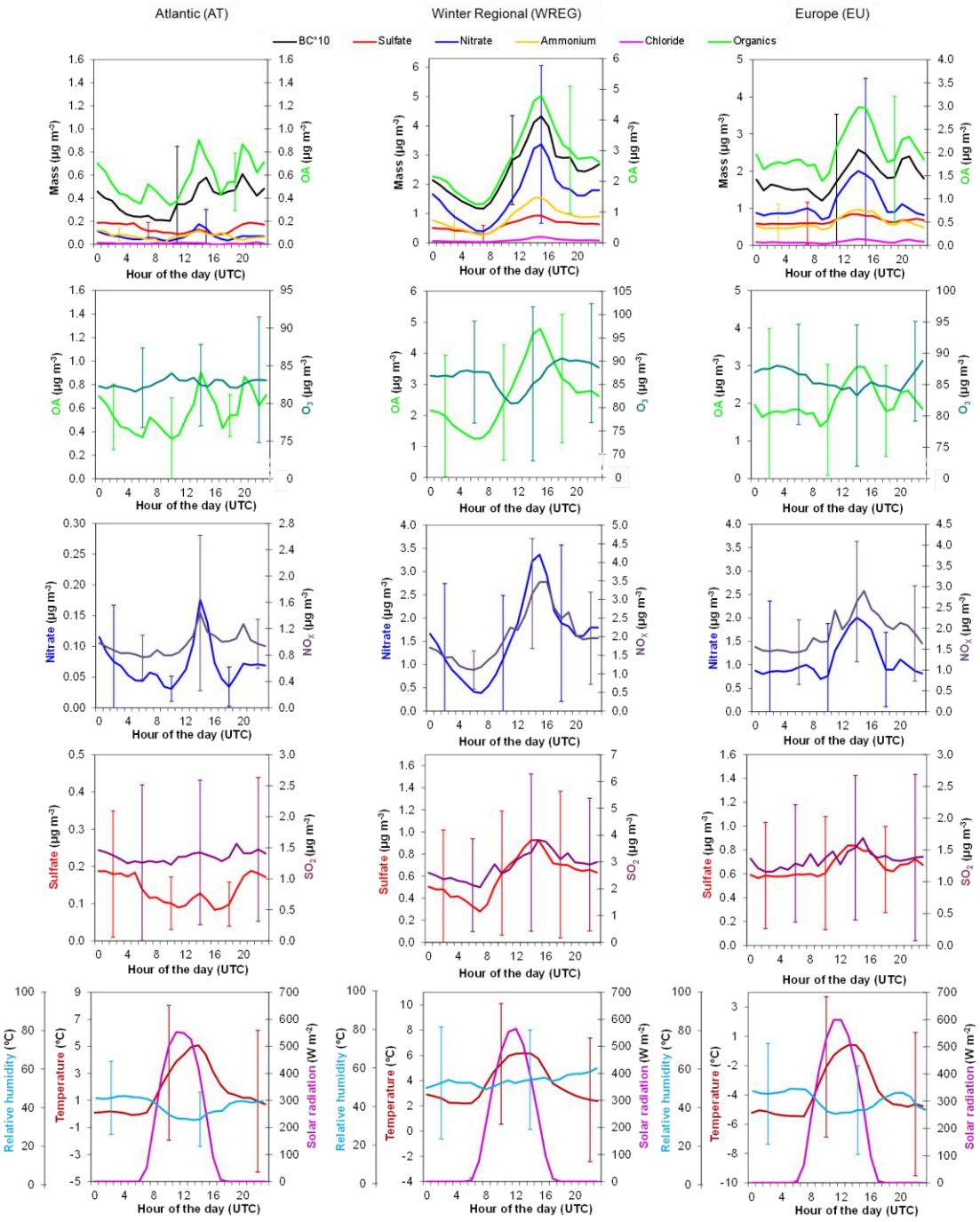

Fig.S5 Diurnal cycles of PM_1 chemical species (black carbon (BC), sulfate, nitrate, ammonium, chloride and OA), gaseous pollutants (ozone (O_3), nitrogen oxides (NO_X), and sulfur dioxide (SO_2)), and meteorological parameters (relative humidity, temperature and solar radiation) averaged as a function of meteorological episode for the winter period (10 Jan 12 – 7 Mar 12). Variation bars indicate ± standard deviation.

a)

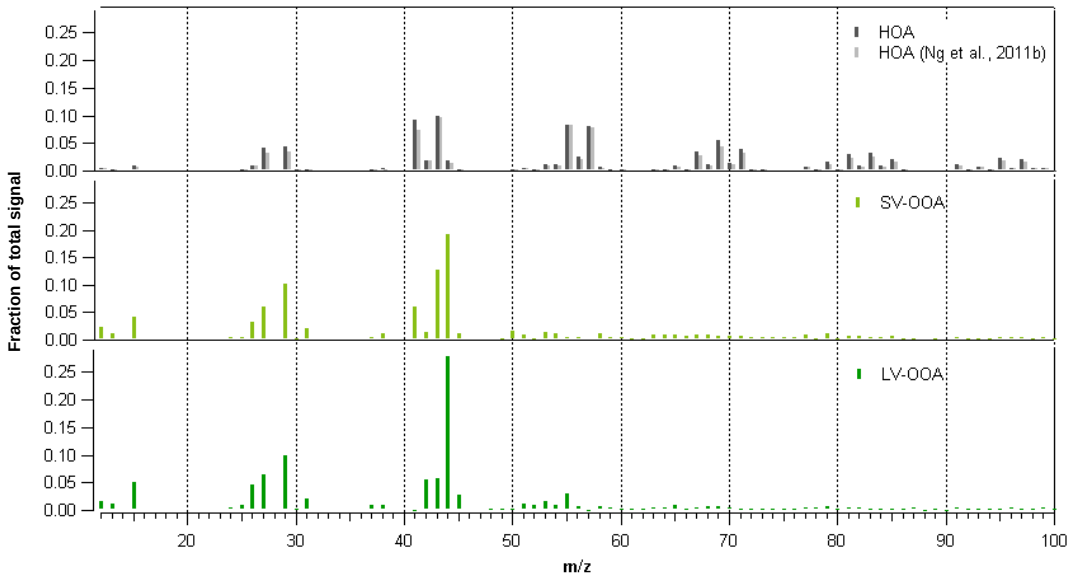

b)

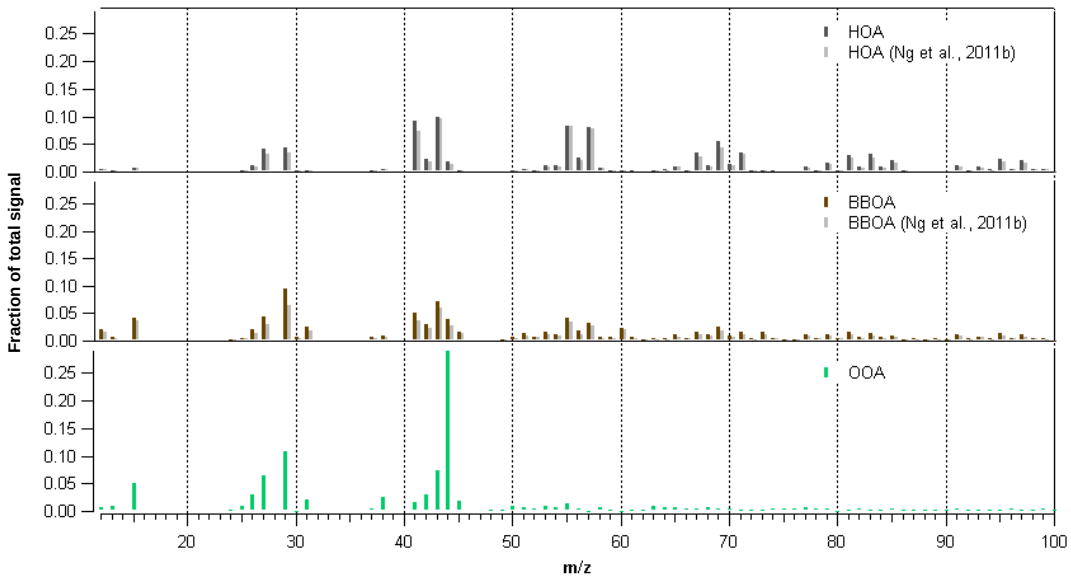

Fig.S6 Organic species profiles extracted from the ME-2 analysis for (a) the summer period (14 Jul 11 – 24 Sep 11) and for the winter period (10 Jan 12 – 7 Mar 12). The hydrocarbon-like organic aerosol (HOA) and the biomass burning organic aerosol (BBOA) were constrained using an average HOA and BBOA factors from different datasets (Ng et al., 2011b) **, with an a-value of 0.1.**

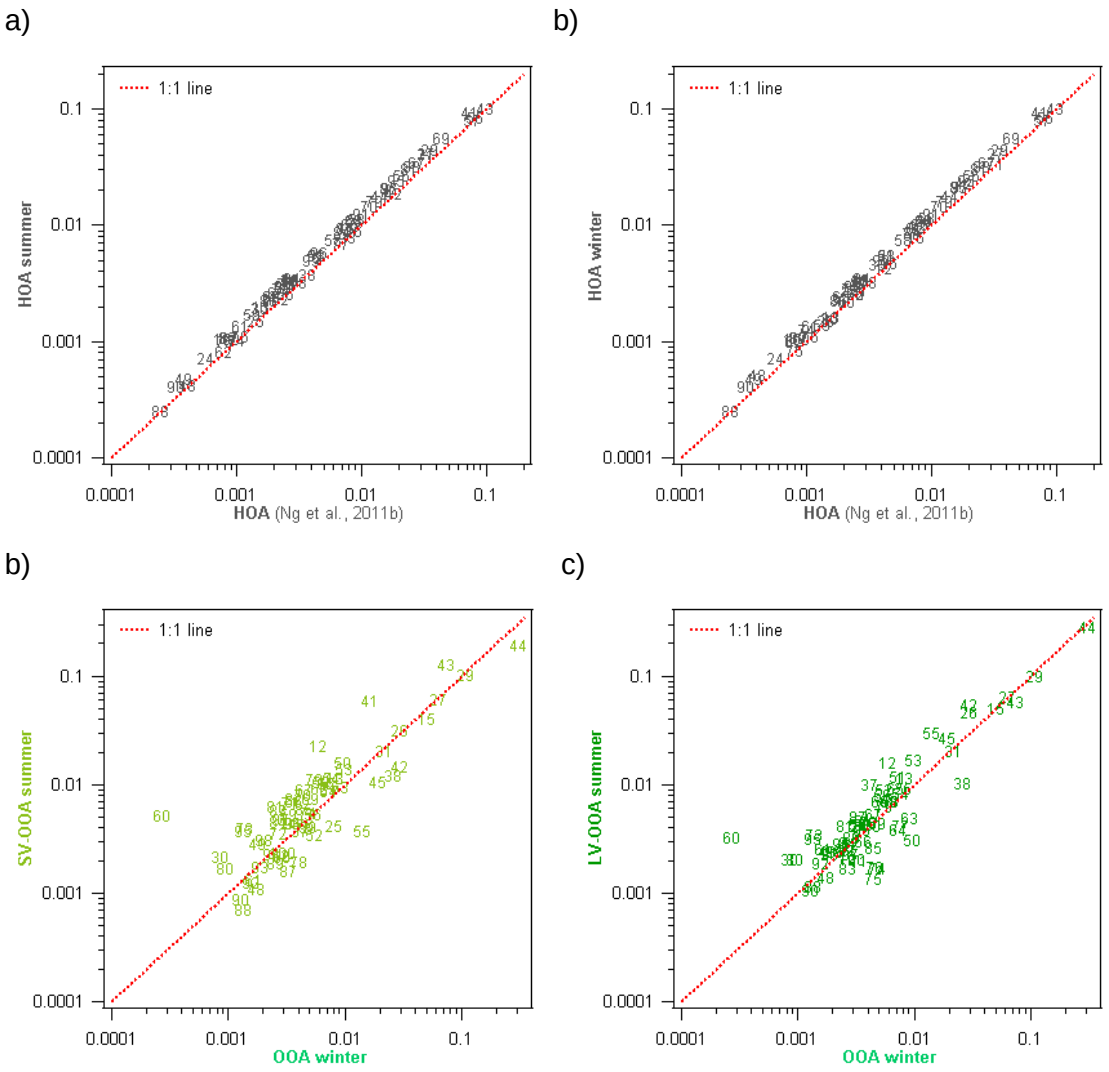

Fig.S7 Scatter plot of organic species profiles, (a) hydrocarbon-like organic aerosol (HOA) for the summer period (14 Jul 11 – 24 Sep 11) versus HOA from Ng et al. (2011b)**, (b) HOA for the winter period (10 Jan 12 – 7 Mar 12) versus HOA from** Ng et al. (2011b)**, (c) semi-volatile oxygenated organic aerosol (SV-OOA) for the summer period versus oxygenated organic aerosol (OOA) for the winter period, and (d) low-volatility oxygenated organic aerosol (LV-OOA) for the summer period versus OOA for the winter period. The numerical markers correspond to *m/z* values.**

Table S6 Average of meteorological parameters recorded at Montsec during the study. Note that the whole period averages include also spring and fall.

	Whole period	Summer	Winter
Period	14 Jul11 - 23 Apr 12	14 Jul 11 - 24 Sep 11	10 Jan 12 - 7 Mar 12
Tavg (ºC)	7.9	16.6	1.1
Tmax (ºC)	28.8	28.8	13.5
Tmin (ºC)	-13.5	5.5	-13.5
RH (%)	59	58	45
TAP* (mm)	422	51	3
WS** (m s^{-1})	0.8	2.0	3.6
WD** (degrees)	347	206	22
P (hPa)	852	853	852
SR (W m^{-2})	180	273	152

*Total Accumulated precipitation

**Vector average

3.5. Article 4: Climatology of aerosol optical properties and black carbon mass absorption cross section at a remote high-altitude site in the western Mediterranean Basin

Marco Pandolfi1, **Anna Ripoll**[1,2], Xavier Querol[1], Andrés Alastuey[1]

[1]Institute of Environmental Assessment and Water Research (IDAEA-CSIC), Jordi Girona 18-26, 08034, Barcelona, Spain.

[2]Department of Astronomy and Meteorology, Faculty of Physics, University of Barcelona, Martí i Franquès 1, 08028, Barcelona, Spain.

Atmos. Chem. Phys., 14, 6443-6460,

doi:10.5194/acp-14-6443-2014, 2014

Published: **27 June 2014**

Impact factor of Journal: **5.298**

Resum. Els coeficients de dispersió (angl., scattering, σ_{sp} i backscattering, σ_{bsp}) i d'absorció (angl., absorption, σ_{ap}) de la llum que generen les partícules atmosfèriques van ser mesurats a l'estació d'alta muntanya del Montsec (MSC; 42º 3' N, 0º 44' E 1570 m s.n.m.), situada a l'oest del mediterrani. Els valors mitjans obtinguts (± desviació estàndard) durant el període d'estudi (juny 2011-juny 2013) i a una longitud d'ona de 635 nm van ser 18.9 ±20.8, 2.6±2.8 i 1.5±1.4 Mm^{-1} per als coeficients de σ_{sp} , σ_{bsp} i σ_{ap}, respectivament. Els valors mitjans del SSA (angl., single-scattering albedo, 635 nm), el SAE (angl., scattering Ångström exponent, 450-635 nm), el *B/S* (backscattering-to-scattering ratio), el *g* (angl., asymmetry parameter, 635 nm), la MAC (angl., Black carbon mass absorption cross section, 637 nm) i el $PM_{2.5}$ MSCS (angl., mass scattering cross section, 635 nm) van ser 0.92±0.03, 1.56±0.88, 0.16±0.09, 0.53±0.16, 10.9±3.5 $m^2\ g^{-1}$ i 2.5±1.3 $m^2\ g^{-1}$, respectivament.

Els valors de les mesures de dispersió obtingudes al MSC es troben a la zona mig-alta del rang publicat per Andrews et al. (2011) corresponent a llocs d'alta muntanya de diferents parts del món. Això és degut al fet que el MSC està influenciat per episodis de recirculació regional i per intrusions saharianes, sobretot a la primavera i a l'estiu, que provoquen la presencia de capes contaminades a les zones altes de la troposfera. A més a més, els vents de muntanya i la influencia de la capa de barreja durant l'estiu, també poden contribuir als valors alts de dispersió al MSC. Aquestes condicions atmosfèriques observades durant l'estiu són probablement les causants de la manca de cicles diaris de les propietats òptiques dels aerosols.

La caracterització de les propietats òptiques dels aerosols en funció de l'origen de les masses d'aire, va revelar que els valors de σ_{sp} , σ_{ap}, MAC i MSCS eren majors durant les intrusions saharianes i els episodis de recirculació regional de l'estiu que durant les adveccions atlàntiques o els episodis anticiclònics de l'hivern. Per altra banda, els valors més baixos de SAE es van observar durant les intrusions saharianes, mentre que els més alts es van registrar durant els episodis de recirculació de l'estiu. Això és un indicatiu de que durant les intrusions saharianes el MSC estava dominat per partícules grans, mentre que durant els episodis de recirculació de l'estiu predominaven les partícules petites.

Atmos. Chem. Phys., 14, 6443–6460, 2014
www.atmos-chem-phys.net/14/6443/2014/
doi:10.5194/acp-14-6443-2014
© Author(s) 2014. CC Attribution 3.0 License.

Atmospheric Chemistry and Physics Open Access

Climatology of aerosol optical properties and black carbon mass absorption cross section at a remote high-altitude site in the western Mediterranean Basin

M. Pandolfi, A. Ripoll, X. Querol, and A. Alastuey

Institute of Environmental Assessment and Water Research (IDAEA-CSIC), Barcelona, Spain

Correspondence to: M. Pandolfi (marco.pandolfi@idaea.csic.es)

Received: 3 December 2013 – Published in Atmos. Chem. Phys. Discuss.: 11 February 2014
Revised: 19 May 2014 – Accepted: 20 May 2014 – Published: 27 June 2014

Abstract. Aerosol light scattering (σ_{sp}), backscattering (σ_{bsp}) and absorption (σ_{ap}) were measured at Montsec (MSC; 42°3′ N, 0°44′ E, 1570 m a.s.l.), a remote high-altitude site in the western Mediterranean Basin. Mean (±SD) σ_{sp}, σ_{bsp} and σ_{ap} were 18.9 ± 20.8, 2.6 ± 2.8 and $1.5 \pm 1.4\,Mm^{-1}$, respectively at 635 nm during the period under study (June 2011–June 2013). Mean values of single-scattering albedo (SSA, 635 nm), the scattering Ångström exponent (SAE, 450–635 nm), backscatter-to-scatter ratio (B/S, 635 nm), asymmetry parameter (g, 635 nm), black carbon mass absorption cross section (MAC, 637 nm) and $PM_{2.5}$ mass scattering cross section (MSCS, 635 nm) were 0.92 ± 0.03, 1.56 ± 0.88, 0.16 ± 0.09, 0.53 ± 0.16, $10.9 \pm 3.5\,m^2\,g^{-1}$ and $2.5 \pm 1.3\,m^2\,g^{-1}$, respectively. The scattering measurements performed at MSC were in the medium/upper range of values reported by Andrews et al. (2011) for other mountaintop sites in Europe due to the frequent regional recirculation scenarios (SREG) and Saharan dust episodes (NAF) occurring mostly in spring/summer and causing the presence of polluted layers at the MSC altitude. However, the development of upslope winds and the possible presence of planetary boundary layer air at MSC altitude in summer may also have contributed to the high scattering observed. Under these summer conditions no clear diurnal cycles were observed for the measured extensive aerosol optical properties (σ_{sp}, σ_{bsp} and σ_{ap}). Conversely, low σ_{sp} and σ_{ap} at MSC were measured during Atlantic advections (AA) and winter regional anticyclonic episodes (WREG) typically observed during the cold season in the western Mediterranean. Therefore, a season-dependent decrease in the magnitude of aerosol extensive properties was observed when MSC was in the free troposphere, with the highest free-troposphere vs. all-data difference observed in winter and the lowest in spring/summer. The location of MSC station allowed for a reliable characterization of aerosols as a function of the main synoptic meteorological patterns. The SAE was the lowest during NAF and showed an inverse correlation with the outbreak intensity, indicating a progressive shift toward larger particles. Moreover, the strength of NAF episodes in the region led to a slope of the scattering vs. absorption relationship among the lowest reported for other mountaintop sites worldwide, indicating that MSC was dominated by dust aerosols at high aerosol loading. As a consequence, SSA showed a nearly monotonic increase with increasing particle concentration and scattering. The SAE was the highest during SREG, indicating the presence of polluted layers dominated by smaller particles. Correspondingly, the asymmetry parameter was lower under SREG compared with NAF. The MAC and MSCS were significantly higher during NAF and SREG compared to AA and WREG, indicating an increase of absorption and scattering efficiencies associated with the summer polluted scenarios. The optical measurements performed at the MSC remote site were compared with those simultaneously performed at a regional background station in the western Mediterranean Basin located at around 700 m a.s.l. upstream of the MSC station.

1 Introduction

Atmospheric aerosols affect the Earth's radiative balance directly, by scattering and absorbing solar and terrestrial radiation, and indirectly, by acting as cloud condensation

Published by Copernicus Publications on behalf of the European Geosciences Union.

nuclei, thus modifying the physical and optical properties of clouds. The measurements of aerosol optical properties such as scattering, backscattering, absorption and extinction are important for aerosol characterization and model validation and, consequently, for a better comprehension of the role of aerosols in the Earth–atmosphere system (IPCC, 2007, 2013). Specific aerosol optical parameters such as single-scattering albedo (SSA), the scattering Ångström exponent (SAE), backscatter-to-scatter ratio (B / S) and asymmetry parameter (g), among others, can be derived from these optical properties. Moreover, the mass scattering cross section (MSCS) and the mass absorption cross section (MAC) of sampled aerosols can be obtained from independent measurements of particulate matter (PM) and elemental carbon (EC) concentrations, respectively, and the measured aerosol scattering and absorption coefficients. The cooling or absorbing potential of atmospheric aerosols mostly depends on these parameters, which are complex functions of aerosols size, shape, chemical composition and refractive index. Most particles scatter the sunlight, causing a net cooling at the top of the atmosphere, whereas black carbon (BC) particles (or EC) absorb radiation over the entire visible spectrum, thus affecting the vertical heating profile and causing a net warming of the Earth–atmosphere system (IPCC, 2007, 2013). BC particles play a role second only to carbon dioxide in climate change and are co-emitted with a variety of other aerosols and precursor gases which can increase the light absorption by BC through an increase in its MAC (e.g. Bond et al., 2013). Given that atmospheric models convert the modelled BC mass concentrations to optical absorption using the MAC, accurate estimates of MAC values and of the possible reasons explaining their variability are important.

Aerosol optical measurements are carried out worldwide by means of both in situ and remote techniques. In order to address the uncertainties related to the geographical variation in aerosols optical properties, networks such as ACTRIS (Aerosols, Clouds, and Trace gases Research InfraStructure Network, www.actris.net) or NOAA's baseline observatory (http://www.esrl.noaa.gov/gmd/) were created. The ACTRIS network aims at integrating three existing European research infrastructures: EUSAAR (European Supersites for Atmospheric Aerosol Research, for in situ aerosol measurements at regional level; www.eusaar.net), EARLINET (European Aerosol Research Lidar Network, for remote aerosol measurements; www.earlinet.org) and CLOUDNET (to provide a systematic evaluation of clouds in forecast models, www.met.rdg.ac.uk/radar/cloudnet/). Thus, the ACTRIS project provides the unique opportunity to integrate in situ and vertical aerosol measurements for the characterization of both the planetary boundary layer (PBL) and the free troposphere (FT). The measurements of aerosols in the FT are especially important given that FT aerosols are more spatially representative of the global atmosphere than the aerosols in the PBL due to their long residence time (of the order of several weeks). Aerosols in the FT can be transported over long distances and have extended climate and air quality impacts (Laj et al., 2009; Andrews et al., 2011). Due to the location of the majority of in situ ACTRIS stations, the in situ measurements are performed mainly within the PBL, whereas the vertical lidar measurements allow for aerosol optical measurements almost in the whole troposphere. However, lidars do not measure key climate variables such as aerosol absorption, SSA, MSCS or MAC. Consequently, the measurements performed at mountaintop observatories provide the opportunity to make long-term, continuous observations of in situ aerosol properties in the free troposphere (FT). Moreover, given their frequent position in the FT, mountaintop stations give the possibility to study aerosols under different atmospheric scenarios without strong interference from closer anthropogenic emissions. However, the number of mountaintop observatories providing long-term in situ aerosol optical measurements worldwide is rather low. Recently, Andrews et al. (2011) presented climatology for free-tropospheric aerosol radiative properties utilizing in situ data from 10 high-altitude stations in the 20–50° N latitude band. Examples of high-altitude aerosol optical measurements were presented by Bodhaine (1983, 1995), McKendry et al. (2011), Marcq et al. (2010), Collaud Coen et al. (2004, 2007, 2011), Cozic et al. (2008), Andrews et al. (2011), Nyeki et al. (1998).

In this work we present the results from two-year measurements (June 2011–June 2013) of aerosol optical properties performed at the high-altitude Montsec station (MSC), which is run following the ACTRIS standards. Data from MSC were compared with data collected at the ACTRIS Montseny station (MSY; 41°19′ N, 02°21′ E, 720 m a.s.l.): a regional background station located around 140 km east of MSC. Seasonal and diurnal variation of extensive (scattering, absorption, extinction) and intensive (SSA, SAE, B / S, and g) aerosol properties as well as MSCS and MAC are presented and discussed. The effects of four main season-dependent synoptic atmospheric scenarios affecting the western Mediterranean Basin (WMB) on the measured optical properties are also discussed. Moreover, the data collected when the MSC station is in the FT are compared with the free-tropospheric aerosol optical properties presented in Andrews et al. (2011) for other mountaintop sites. All acronyms used in this work are reported in Table 1.

2 Measurement site and methodology

2.1 Montsec measurement station

The MSC site (42°3′ N, 0°44′ E, 1570 m a.s.l.) is a high-altitude emplacement located in the NE of the Iberian Peninsula (Fig. 1) and situated in the southern side of the Pre-Pyrenees at the top of Montsec d'Ares. This region is low-density populated and isolated from large pollutant emissions, 140 km from the highly urbanized and industrialized coastline to the southeast, 30 km from the largest city in the

Table 1. Acronyms used in this work.

Acronyms	
Extensive aerosol optical properties	
σ_{sp}:	particle scattering
σ_{bsp}:	particle backscattering
σ_{ap}:	particle absorption
Intensive aerosol optical properties	
SSA:	single-scattering albedo
SAE:	scattering Ångström exponent
B / S:	backscatter-to-scatter ratio
g:	asymmetry parameter
MAC:	mass absorption cross section
MSCS:	mass scattering cross section
Concentration measurements	
BC:	black carbon
EC:	elemental carbon
PM_1:	particles with aerodynamic diameter < 1 µm
PM_{10}:	particles with aerodynamic diameter < 10 µm
Measurement sites	
MSC:	Montsec (NE Spain, mountaintop measurement site)
MSY:	Montseny (NE Spain, regional background measurement site)
Air masses	
AA:	Atlantic Ocean advections
NAF:	North Africa
WREG:	winter-regional scenario
SREG:	summer-regional scenario
Others	
WMB:	western Mediterranean Basin
PBL:	planetary boundary layer
FT:	free troposphere

region (Balaguer, 15 769 inhabitants) to the south, and 50 km from the axial Pyrenees to the north. The ACTRIS regional background station of MSY is located around 140 km from the MSC site. Figure 1 also shows three meteorological stations: Montsec Observatory (800 m), Os de Balaguer (576 m) and Vallfogona de Balaguer (238 m).

Aerosol measurements presented in this work were performed at MSC during the period June 2011–June 2013. Due to the deployment of the nephelometer in measurement campaigns at other locations, scattering and backscattering data were not available from February 2012 to June 2012. Results from the MSC site were compared with those simultaneously obtained at the MSY station (Fig. 1). A description of the MSY site and the optical measurement performed at MSY can be found in Pandolfi et al. (2011).

2.2 Optical measurements

2.2.1 Scattering, hemispheric backscattering and absorption

Particle scattering (σ_{sp}: 10–171°) and hemispheric backscattering (σ_{bsp}: 90–171°) coefficients at three wavelengths (450 nm, 525 nm, 635 nm) were measured with an LED-based integrating nephelometer (model Aurora 3000, ECOTECH Pty Ltd, Knoxfield, Australia). The σ_{sp} and σ_{bsp} data were corrected for truncation errors, allowing scattering

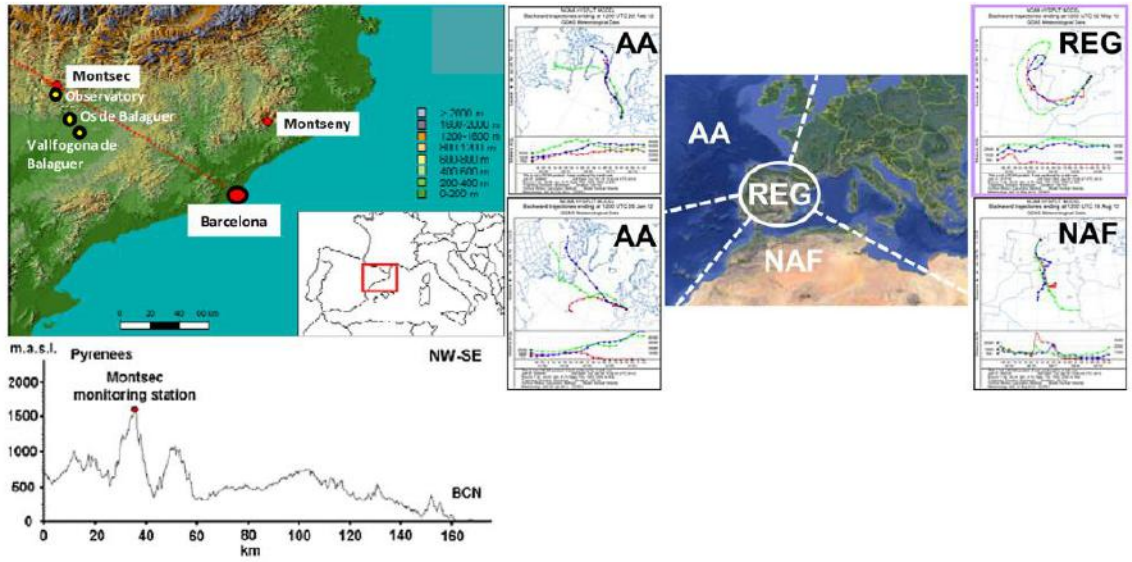

Figure 1. Location of the Montsec (MSC, remote mountaintop site) and Montseny (MSY, regional background) measurement sites. Barcelona is also shown. Yellow dots are meteorological stations (observatory (800 m a.s.l.), Os de Balaguer (576 m) and Vallfogona de Balaguer (238 m)). Air mass back trajectories from the Atlantic Ocean (AA), regional (REG) and North Africa (NAF).

for 0–360° and backscattering for 90–270° to be reported, and for non-ideal (non-Lambertian) illumination function of the light source as described by Müller et al. (2011a). Müller et al. (2011a) provided parameterized correction factors for each wavelength as linear relationship of the Ångström exponents calculated from uncorrected multi-wavelength scattering measurements. A full calibration of the nephelometer was performed four times per year by using CO_2 as span gas, while zero measurements and adjusts were performed once per week by using internally filtered particle free air.

In order to reduce the effects of hygroscopicity enhancing the scattering properties of particles, a relative humidity (RH) threshold of 40 % was set in the sampling cell by using a processor-controlled automatic heater inside the nephelometer. This experimental procedure, which follows the ACTRIS standards, has been applied elsewhere (see, for example, Pereira et al., 2011; Anderson and Ogren, 1998; Pandolfi et al., 2011). The mean RH in the nephelometer sampling cell during the study period was 28.4 ± 9.5 %. Moreover, in-cloud data were removed by selecting only those data with ambient RH < 90 %. The detection limits of Aurora 3000 over 1 min averaging time are 0.11, 0.14 and 0.12 Mm^{-1} for total scattering at 450, 525 and 635 nm, respectively, and 0.12, 0.11 and 0.13 Mm^{-1} for backscattering (Müller et al., 2011a).

Aerosol absorption coefficients (σ_{ap}) at 637 nm (Müller et al., 2011b) were measured with multi-angle absorption photometers (MAAP, model 5012, Thermo). The detection limit of the MAAP instrument is lower than 0.6 Mm^{-1} over 2 min integration. Absorption measurements are converted by the MAAP's software to BC concentration (in $\mu g\,m^{-3}$) assuming a constant MAC of 6.6 $m^2\,g^{-1}$ (Petzold et al., 2004).

The nephelometer and MAAP instruments were connected to two separate sampling lines with cut-off diameters of 2.5 and 10 µm, respectively, and placed at about 1.5 m above the roof of the cabin hosting the instruments. The inlets flow was 1 $m^3\,h^{-1}$ and humidity control was performed by connecting a drier to the sampling inlet. The Reynolds number for the described inlets was around 1300. The scattering, backscattering and absorption measurements reported in this work were adjusted to standard temperature and pressure (STP, $T_{standard} = 273.15$ K and $P_{standard} = 1013.25$).

2.3 PM measurements

Real-time PM_{10}, $PM_{2.5}$ and PM_1 mass concentrations were continuously measured, on an hourly base, by using a GRIMM optical counter (model 1107). Subsequently, the PM_x concentrations were corrected with factors obtained by comparing the real-time and simultaneous in situ gravimetric measurements (Querol et al., 2008). PM_x gravimetric measurements on a 24 h base were performed twice per week with high-volume (Hi-Vol) samplers (DIGITEL and MCV at 30 $m^3\,h^{-1}$) with appropriate PM_x cut-off inlets.

2.4 EC measurements

The sampled 24 h filters from Hi-Vol were analysed by means of a SUNSET OCEC analyser for the determination of elemental carbon (EC) concentrations. The EUSAAR 2 protocol (Cavalli et al., 2010) was used. In this

work the uncertainties for the measured EC concentrations were calculated by adding half of the minimum measured EC concentration to the 7% of the concentrations (Err[EC] = min[EC]/2 + 0.07 · [EC]). With the EUSAAR 2 protocol the EC uncertainties have been estimated to be around 2–7% (JRC report, 2009). The formula applied here gives higher uncertainty to low EC concentrations (e.g. Polissar et al., 1998).

2.5 Data processing

In this work the aerosol scattering, backscattering and absorption coefficients were integrated over 1 h. Six additional parameters (B/S, g, SSA, SAE, MSCS and MAC) were derived from the aerosol optical and mass concentration measurements. The B/S parameter, which is the ratio between hemispherical backscatter and total scatter, is used here to estimate the g of airborne particles used in radiative transfer calculations (Andrews et al., 2006). Values of g can range from -1 for 180° backwards scattering to $+1$ for complete forward scattering (0°), with a value of 0.7 commonly used in radiative transfer models (Ogren et al., 2006). Following Delene and Ogren (2002) and Andrews et al. (2006), g was calculated for the three nephelometer wavelengths as follows:

$$g = -7.14(B/S)^3 + 7.46(B/S)^2 - 3.96(B/S) + 0.9893. \quad (1)$$

The SSA indicates the relative amounts of radiation scattered and absorbed by particles. Thus, SSA is a parameter indicating the potential for aerosols for cooling or warming the atmosphere. It is defined as

$$\mathrm{SSA} = \frac{\sigma_{\mathrm{sp}}}{\sigma_{\mathrm{sp}} + \sigma_{\mathrm{ap}}}. \quad (2)$$

Non-absorbing particles such as sulfate have an SSA of 1 (cooling), while lower SSA values indicate the presence of more absorbing particles. BC particles have an SSA of about 0.2 (warming). In this work SSA was estimated to be 635 nm, as the difference between absorption at 637 nm (MAAP wavelength) and 635 nm was assumed to be negligible.

The SAE (450–635 nm) was calculated from the multi-wavelength nephelometer data as

$$\mathrm{SAE} = -\frac{\log\left(\sigma_{\mathrm{sp}}^{\lambda_1} / \sigma_{\mathrm{sp}}^{\lambda_2}\right)}{\log\left(\lambda_1 / \lambda_2.\right)} \quad (3)$$

The SAE describes the λ dependence of the particle scattering coefficient. An Ångström exponent of 4 represents the scattering from molecules (Rayleigh's regime). A large SAE (higher than 2) implies scattering dominated by submicron particles, while SAE values lower than 1 represent an aerosol distribution dominated by coarser particles (e.g. Schuster et al., 2006).

In order to eliminate issues with measurement noise during clean periods (e.g. when MSC was in the FT), the B/S, g, SSA and SAE parameters were calculated from hourly averaged scattering (635 nm), hemispheric backscattering (635 nm) and absorption above 0.4, 0.4 and 0.6 Mm^{-1}, respectively.

The MAC and MSCS are a measurement of the efficiency of the measured particles to absorb or scatter, respectively, light at a given wavelength and are expressed in $\mathrm{m}^2\,\mathrm{g}^{-1}$. The MAC is the parameter used to convert absorption to concentration of absorbing particles (i.e. BC or EC), and vice versa, and was estimated from error-weighted linear fitting between σ_{ap} from MAAP and EC concentrations from offline filter analysis. MAAP data were averaged over the filter sampling time. The MSCS is the parameter relating the measured scattering to the concentration of PM and was estimated at the three nephelometer wavelengths by averaging the ratios between σ_{sp} and $\mathrm{PM}_{2.5}$ after subtracting the EC mass from PM.

2.6 Main meteorological patterns

In order to determine and classify the atmospheric episodes affecting MSC, HYSPLIT (http://ready.arl.noaa.gov/HYSPLITtraj.php), BSC/DREAM8b (http://www.bsc.es/projects/earthscience/DREAM), SKIRON (http://forecast.uoa.gr/dustindx.php) and NAAPS (http://www.nrlmry.navy.mil/aerosol) models were used. For each day of measurements, 120 h backward trajectories (for 12:00 modelling vertical velocity and for three different heights, 750, 1500 and 2500 m a.g.l) were computed and classified according to their predominant transport direction in the (1) Atlantic Ocean (AA, Atlantic north and Atlantic northwest; 52%), (2) North Africa (NAF, 14%), (3) winter regional (WREG, from November to April; 6%), and (4) summer regional (SREG, from May to October; 9%). The global atmospheric circulation has some seasonal oscillations, and thus MSC is more westerly and northerly influenced in winter, while in summer the prevailing winds come from the south (Ripoll et al., 2014). Consequently, AA episodes are more frequent in winter, whereas continental NAF air masses are more frequent in summer (Pandolfi et al., 2014, 2011; Querol et al., 2009; Pey et al., 2009; Pérez et al., 2008; Rodríguez et al., 2001). The advection of clean Atlantic air masses clears out the previously accumulated pollution in the aged air masses, leading to lower pollutant concentrations. In summer the meteorology of the area is mainly characterized by long dry periods, sporadic but occasionally heavy rains, and a prevalence of NAF outbreaks (Rodriguez et al., 2004). The WREG and SREG scenarios represent mainly air masses from the Iberian Peninsula (IP) (Rodriguez et al., 2004). In winter (WREG) recurrent anticyclonic conditions with weak synoptic winds lead to stagnation of air masses and the accumulation and aging of pollutants over the region. Under these conditions the PBL height mostly determines the dilution of pollutants around the emission sources and the degree of pollution at

more elevated/regional areas in the WMB (e.g. Jorba et al., 2013; Pandolfi et al., 2014). In summer, due to the intense and rapid solar heating of the lower atmospheric layers, convergence of surface winds from the coast to the central IP plateau injects polluted air into the middle troposphere up to 3.5–5 km (Millán et al., 1997; Pérez et al., 2004). This pattern allows for the recirculation and accumulation of aerosol and has the potential to form stratified reservoir layers of aged pollutants which subside over the coastal area and the sea (e.g. Millán et al., 1992, Gangoiti et al., 2001; Pérez et al., 2004).

3 Results and discussion

3.1 General features

Table 2 reports the statistics for the measured parameters, including means, standard deviations, percentiles (1, 10, 25, 50, 75, 99 percentiles), minima and maxima values and skewness. With the exception of SAE, MSCS and MAC, all parameters showed skewness higher than 1, for which almost normal distributions (skewness close to zero) were observed, and SSA and g both showing a negative skewness. Similar SSA skewness was presented by Pandolfi et al. (2011) at the MSY regional background measurement site. Negative skewness for g is a consequence of the high positive skewness observed for B/S.

Hourly σ_{sp} and σ_{bsp} at 635 nm at MSC ranged between 0.1 and 161.1 Mm^{-1} (mean $\pm$SD: $18.9 \pm 20.8\,Mm^{-1}$) and between 0.0 and 17.1 Mm^{-1} ($2.6 \pm 2.8\,Mm^{-1}$), respectively. Mean values of σ_{sp} and σ_{bsp} at 450 nm and 525 nm are reported in Table 2. The σ_{ap} (at 637 nm) ranged between about 0.0 and 12.6 Mm^{-1}, with a mean value of $1.5 \pm 1.4\,Mm^{-1}$. The hourly PM_1 levels at MSC ranged between about 0.1 and 49.9 $\mu g\,m^{-3}$, with a mean value of $5.3 \pm 4.5\,\mu g\,m^{-3}$.

As shown later the lowest scattering, backscattering and absorption at MSC were measured under AA and WREG episodes typically observed during the cold season in the WMB. Conversely, high σ_{sp}, σ_{bsp} and σ_{ap} were measured during NAF and SREG episodes, which predominate in spring/summer.

A comparison between measurements performed at MSC with those reported for other high-altitude sites is reported in the following of this section and in the next sections. It should be taken into account that in some cases the comparison may be affected by the different size cut-off of the particles sampled at the different sites. At the Jungfraujoch high-alpine site (3580 m a.s.l., whole air sampled), Fierz-Schmidhauser et al. (2010) reported mean σ_{sp} at 550 nm of about 12 Mm^{-1}, by excluding NAF episodes, and around 20 Mm^{-1}, considering only the NAF episodes. At Izaña (Canary Islands, $\sim$2400 km a.s.l.; PM_{10} size cut-off) mean σ_{sp} and σ_{ap} at 550 nm of about 10 Mm^{-1} and 0.8 Mm^{-1}, respectively, have been measured (Andrews et al., 2011). Monte Cimone (Italy, $\sim$2200 m a.s.l.; whole air sampled) registered mean σ_{sp} and σ_{ap} of around 11 and 3 Mm^{-1}, respectively, and both parameters increased highly during Saharan dust outbreaks and wildfire emissions over North Africa (Andrews et al., 2011; Cristofanelli et al., 2009). The mean scattering and absorption values measured at MSC were lower than the values reported by Pandolfi et al. (2011) for the MSY regional background station (720 m a.s.l., PM_{10} size cut-off). Mean σ_{sp} (635 nm) and σ_{ap} (637 nm) at MSY were around 26.6 and 2.8 Mm^{-1}, respectively, due to the higher influence of anthropogenic emissions in the lower boundary layer (MSY) compared with higher altitudes (MSC).

The mean B/S (525 nm), SAE (450–635 nm), SSA (635 nm) and g (525) measured at MSC were 0.135 ± 0.066, 1.56 ± 0.88, 0.92 ± 0.03 and 0.59 ± 0.13, respectively. At the alpine Jungfraujoch site, Fierz-Schmidhauser et al. (2010) reported mean B/S, SAE and SSA for dry aerosols (RH < 20 %) within the ranges 0.128–0.122, 1.787–1.671 and 0.91–0.93, respectively. The higher B/S measured at MSC was likely due to the lower size range measured at MSC ($PM_{2.5}$) compared with Jungfraujoch (whole air), whereas the lower SAE at MSC, despite the different size cut-off, may be an indication of the prevalence of slightly coarser aerosols at MSC. This difference was likely due to the fact that more large particles had time to deposit out or be removed via wet scavenging since the altitude of Jungfraujoch is about twice that of the MSC altitude.

At the MSY regional background station the mean B/S (525 nm), SAE (450–635 nm), SSA (635 nm) and g (525 nm) were different by around -16, $+5$, -4 and $+6$ %, respectively, compared to MSC (only contemporary data were used). These differences were small suggesting, on average, similarity in microphysical aerosol properties measured at the MSC and MSY stations. Recently, Ripoll et al. (2014) have shown that the mean chemical composition of particles at MSC and MSY is on average similar, mainly due to the frequency of specific meteorological episodes affecting aerosol properties similarly at both sites. The main difference was observed for B/S, which was higher at MSC, likely because of the lower size cut-off at MSC ($PM_{2.5}$) compared to MSY (PM_{10}). Moreover, the relatively lower SSA and higher SAE at MSY, despite the differences in the size cut-off, suggested the presence of relatively smaller and more absorbing particles at regional level, likely because the proximity of the MSY station to anthropogenic sources.

The mean MAC ($\pm$SD) at MSC was around $11 \pm 4\,m^2\,g^{-1}$ and ranged from 2.4 to $20.8\,m^2\,g^{-1}$. Mean MSCS ($\pm$SD) at 635, 525 and 450 nm were 2.5 ± 1.4, 3.3 ± 1.9 and $4.2 \pm 2.4\,m^2\,g^{-1}$, respectively. As shown later (Sect. 3.5) the MAC and MSCS at MSC showed a clear seasonal dependence. These two parameters can change as a function of aerosol composition and age, and therefore it can differ depending on the area under study and the meteorological scenarios. MACs between 7 and $20\,m^2\,g^{-1}$ have often been reported in the literature (e.g. Quinn and Bates, 2005; Bond and

Table 2. Statistics of the considered aerosol components and parameters for the period June 2011–June 2013 at Montsec site (all data). The wavelength (λ) is given in [nm]; scattering (σ_{sp}), backscattering (σ_{bsp}) and absorption coefficients (σ_{ap}) are given in [Mm^{-1}]; backscattering-to-scattering ratio (B/S), asymmetry parameter (g), single-scattering albedo (SSA) and the Ångström exponent (SAE) are dimensionless; PM_1 concentrations are given in [$\mu g\,m^{-3}$]; and MAC and MSCS is expressed in [$m^2\,g^{-1}$]. Statistics based on hourly mean values (24 h for MAC and MSCS). Optical data were referenced to STP ($T_{standard} = 273.15$ K and $P_{standard} = 1013.25$ hPa).

Hourly base	λ	Counts	Mean	SD	Median (50th perc.)	Min	Max	Skewness	Percentiles				
									1	10	25	75	99
σ_{sp}	635	10 014	18.9	20.8	11.2	0.1	161.1	1.83	0.2	1.1	3.5	28.3	89.8
	525	10 014	25.4	27.5	15.1	0.1	222.2	1.68	0.1	1.6	4.5	38.6	118.5
	450	10 014	32.3	34.7	19.3	0.1	276.2	1.62	0.1	2.0	5.6	49.6	143.6
σ_{bsp}	635	10 014	2.6	2.8	1.7	0.0	17.1	1.25	0.1	0.2	0.4	4.3	11.1
	525	10 014	3.1	3.2	1.9	0.0	36.4	1.31	0.1	0.2	0.5	5.1	12.8
	450	10 014	3.6	3.9	2.2	0.0	96.0	1.21	0.1	0.2	0.5	6.0	14.6
B/S	635	8612	0.16	0.09	0.15	0.02	0.99	4.03	0.04	0.10	0.12	0.18	0.58
	525	8864	0.13	0.07	0.13	0.01	0.98	4.78	0.04	0.09	0.11	0.15	0.44
	450	8761	0.12	0.06	0.11	0.01	1.00	4.95	0.03	0.07	0.10	0.13	0.36
σ_{ap}	637	13 712	1.5	1.4	1.0	0.0	12.6	1.45	0.0	0.1	0.3	2.4	6.2
g	635	8587	0.53	0.16	0.54	−0.99	0.93	−2.51	−0.10	0.39	0.49	0.60	0.85
	525	8858	0.59	0.13	0.59	−0.92	0.94	−3.25	0.09	0.49	0.55	0.64	0.85
	450	8755	0.62	0.11	0.62	−0.79	0.95	−2.15	0.20	0.53	0.58	0.66	0.88
SAE	450–635	9561	1.56	0.88	1.65	−1.96	5.99	0.30	−1.14	0.56	1.22	1.90	4.69
SSA	635	6123	0.92	0.03	0.93	0.45	0.99	−2.59	0.81	0.89	0.91	0.94	0.97
MAC	637	384	10.9	3.5	11.1	2.4	20.8	0.21	3.6	6.2	8.2	13.2	19.8
MSCS	635	228	2.5	1.4	2.4	0.1	7.5	0.66	0.2	0.7	1.3	3.4	6.8
	525	228	3.3	1.9	3.2	0.1	10.3	0.74	0.2	1.1	1.8	4.6	9.3
	450	228	4.2	2.4	4.0	0.2	12.9	0.73	0.3	1.5	2.2	5.9	11.8
PM_1	–	10 949	5.3	4.5	4.0	0.1	49.9	2.06	0.5	1.4	1.9	7.2	21.8

Bergstrom, 2006; Fernandez-Camacho et al., 2010; Arnott et al., 2003, 2005; Reche et al., 2011; Pandolfi et al., 2011; Querol et al., 2013).

3.2 Diurnal cycles and cluster analysis

As shown in Fig. 2 the mean scattering and absorption at MSC exhibited diurnal cycles with lower values at night and higher values in the afternoon. Thus, on average, thermally driven upslope winds and PBL height variations favoured the transport of pollutants toward the MSC site during the warmest hours of the day. Similar diurnal variations at other mountaintop sites have been observed for extensive aerosol optical properties (e.g. Andrews et al., 2011) and physical properties (e.g. Venzac et al., 2009; Marinoni et al., 2008). The absolute values of extensive optical properties and PM mass concentrations and their diurnal cycle amplitudes were higher at the MSY site compared to MSC (Fig. 2), mainly because the proximity of MSY to the highly urbanized/industrialized coastline (Fig. 1) and its lower altitude compared to MSC. As a consequence, the SSA and SAE at the MSY station also showed marked diurnal cycles compared to MSC due to the effectiveness of thermally driven upslope winds in transporting fine highly absorbing particles of anthropogenic origin to MSY (Fig. 2; cf. Pandolfi et al., 2014).

The σ_{sp} and σ_{ap} measured at MSC showed marked differences as a function of the different synoptic scenarios, with the lowest values measured under AA and WREG and the highest measured under NAF and SREG (Fig. 2). The mean scattering at MSC under NAF and SREG scenarios was close to the values measured at the MSY regional background station, whereas lower scattering was measured at MSC under AA and WREG compared to MSY. A similar pattern was observed for fine PM_1 concentrations (Fig. 2). The similarities in σ_{sp} at MSC and MSY under NAF and SREG demonstrate the potential of these two summer atmospheric scenarios in polluting both regional and remote areas in the WMB. The potential of SREG scenarios to produce atmospheric reservoir layers of aged pollutants is also demonstrated by the similarity in the concentrations of fine PM at both sites despite their different altitude and distance from important pollution sources. Conversely, mean σ_{sp} and

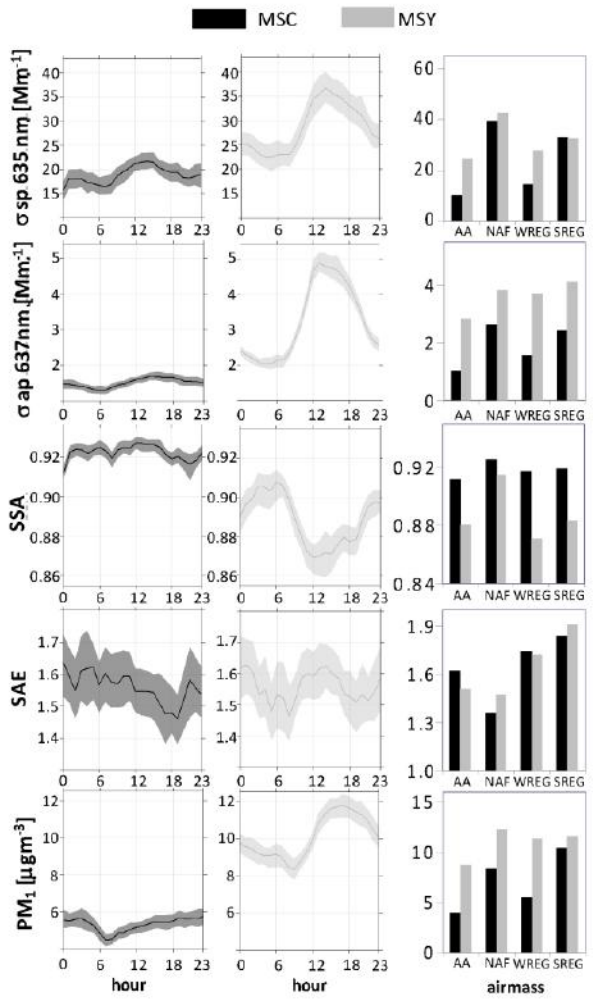

Figure 2. Diurnal cycles and cluster analysis of scattering (σ_{sp} at 635 nm), absorption (σ_{ap} at 637 nm), single-scattering albedo (SSA at 635 nm), scattering Ångström exponent (SAE calculated between 450 and 635 nm) and PM_1 concentrations measured at Montsec site (MSC, black lines) and at Montseny regional background site (MSY, grey lines). Atmospheric scenarios are Atlantic advection (AA), African dust outbreaks (NAF), winter regional anticyclonic episodes (WREG) and summer regional recirculation episodes (SREG).

PM_1 concentrations at MSC under WREG were relatively lower compared to MSY despite the general winter anticyclonic conditions in the WMB, which favour the accumulation of pollutants around the emission sources. However, as already stated, the degree of pollution at rural/remote elevated areas under WREG strongly depends on PBL height. We will show later that MSC was predominantly in the free troposphere in winter when WREG scenarios were observed. Conversely, during WREG the height of the polluted PBL can often reach the altitude of MSY (Pandolfi et al., 2014).

The absorption measured at MSC was lower compared with MSY for all considered scenarios due to the proximity of the MSY station to anthropogenic sources of BC compared to MSC. As a consequence, the SSA was higher at MSC than at MSY irrespective of the atmospheric scenarios. The highest SSA at both sites was measured under NAF scenarios due to the higher relative concentrations of dust particles from Africa enhancing the scattering. Finally, the SAE showed similar characteristics at the two sites with lower values observed under NAF (due to the transport of coarser particles) and higher values under SREG (due to the increased relative concentration in the atmosphere of fine (PM_1) particles of anthropogenic origin).

3.3 FT conditions at MSC station

3.3.1 Identification of FT air

For the identification of FT air we followed the definition given by Andrews et al. (2011, AND2011 from now on) based on the use of data collected between 03:00 and 09:00 LT. As reported in AND2011, this criterion appears to be reasonable for most mountaintop sites and seasons. The limitations of this "time of day" approach are related to the location, height and topography of the site, which determine the strength and frequency of local thermally driven flow and the presence/intensity of polluted residual layers. All these factors make it difficult to rigorously define FT air. In the WMB the frequent SREG and NAF episodes in spring/summer further complicate the identification of the FT air. In order to evaluate when the MSC station was in the FT, we used meteorological data collected at MSC and at three lower altitude meteorological stations (Fig. 1). Thus, contemporary meteorological data collected at MSC station (1570 m a.s.l.), Montsec Observatory (800 m), Os de Balaguer (576 m) and Vallfogona de Balaguer (238 m) were used to study the mean diurnal cycles of potential temperature (Fig. 3a), relative humidity (Fig. 3b) and water vapour mixing ratio (Fig. 3c) as a function of altitude. The potential temperature and water vapour mixing ratio were calculated with the humidity conversion formulas provided by Vaisala (Vaisala Oyj, 2013). Moreover, the diurnal cycles of the gradients of potential temperature (Fig. 3e) and actual temperature (Fig. 3f) were also reported in order to study the strength of the nocturnal and diurnal thermal inversions between the four sites (i.e. between mountain and valley). This analysis may be affected by differences due to different instruments, calibration procedures or local features associated with a specific location (the MSC station and Vallfogona de Balaguer were around 35 km apart). Consequently, we also simulated the mean seasonal PBL diurnal cycles at MSC (Fig. 3d) by means of the HYSPLIT model (http://www.ready.noaa.gov/READYamet.php). Grey and yellow rectangles in Fig. 3 respectively highlight hours when the MSC station was within the PBL and the hours of the time of the day approach (from

03:00 to 09:00 LT) for the identification of FT air proposed by Andrews et al. (2011). In this analysis we assumed that, in a well-mixed mixing layer, the water vapour mixing ratio and potential temperature should be nearly constant with altitude within the PBL. In the free troposphere the water vapour content and potential temperature will decrease and increase, respectively, with altitude. Moreover, if the mixing layer has a uniform distribution of water vapour throughout, then the relative humidity has to increase with altitude. Figure 3 shows that when the relative humidity at MSC was higher compared to the other three stations, the potential temperature and water vapour content were fairly similar. We used these conditions to define the PBL air (grey rectangles). Conversely, at night/in the early morning (yellow rectangles) the relative humidity at MSC was the lowest and the differences in potential temperature and water vapour content among the four stations were the highest. Moreover, the gradients of potential temperature and actual temperature show that strong inversions were on average observed at night between Montsec Observatory and Os de Balaguer with MSC station above the inversion. Conversely, the gradients were lower and rather similar when MSC was within the PBL (grey rectangles). Figure 3 also shows that our estimation of PBL conditions obtained using meteorological data agrees satisfactorily with the simulation performed with HYSPLIT.

Thus, the MSC station was on average above the inversion at night–early morning and within the PBL during the warmest hours of the day in summer, spring and autumn. Thus, the presence of polluted PBL residual layers at MSC altitude at night cannot be excluded. Conversely, in winter the MSC was on average in the FT during the whole day.

Figure 4 shows that the highest diurnal cycle amplitude of scattering at MSC was observed in winter, whereas in spring and summer no clear diurnal cycles were observed. The remarkable diurnal cycle of aerosol scattering in winter was due to the position of MSC station in the free troposphere, whereas thermally driven flows can transport pollutants toward MSC around midday. The observed reduced diurnal cycle for scattering at MSC during spring and summer was mainly due to the frequent occurrence of NAF and SREG episodes and to the possible presence of polluted residual layers at night at the MSC altitude. The NAF and SREG scenarios were also linked with high concentrations of PM and BC during the whole day by Ripoll et al. (2014). Thus, as already observed by Venzac et al. (2009) for the Puy de Dôme station, the seasonal change in FT data at MSC was in part due to the seasonal variability in air mass origin and transport routes.

3.3.2 FT vs. all data: comparison with mountaintop sites presented in AND2011

Figure 5 shows the median values for all periods (June 2011–June 2013) and by season at MSC for the six aerosol optical parameters presented in AND2011. MSC data were scaled to a wavelength of 550 nm (used in AND2011) by using 1.6 as SAE (median values for MSC, this work) and 1.4 as the absorption Ångström exponent (AAE). The AAE was calculated from 1-month absorption measurements performed at MSC with a seven-wavelength Aethalometer (model AE33, Magee Scientific). For MSC the values were calculated for the whole period considered here (ALL, June 2011–June 2013), as well as for autumn (SON), winter (DJF), spring (MAM) and summer (JJA). Red and yellow colours in Fig. 5 represent all data (averaged over 24h) and FT data (averaged between 03:00 and 09:00 LT), respectively. The percentage values in each figure represent the relative difference between the medians calculated for all data and FT data, with positive values indicating lower FT-data medians compared to all data. The non-parametric Mann–Whitney U test was applied to study whether the differences between all-data and FT-data medians were statistically significant. In Fig. 5, bold green numbers indicate statistically significant differences to a significance level of 5 % (p value <0.05), blue bold numbers highlight marginally significant differences ($p < 0.1$), whereas black numbers report differences which were not statistically significant ($p > 0.1$). The six red and yellow rectangles within the blue areas on the right of each figure represent the range of variability of the medians presented by AND2011 calculated for mountaintop sites in the Western Hemisphere (W), Europe (EU) and the Eastern Hemisphere (E).

As reported in Fig. 5 the scattering (median 14.1 Mm^{-1}; Fig. 5a ALL, all data) and the absorption (1.2 Mm^{-1}; Fig. 5b ALL, all data) measured at MSC for the whole data set (ALL) locate the MSC site in the medium/upper range of EU ranges. This is especially marked for scattering data. As reported in Fig. 5 higher scattering and absorption at MSC were measured in summer (JJA, all data; 34.6 Mm^{-1} and 2.4 Mm^{-1}, respectively) compared to winter (DJF, all data; 3.7 Mm^{-1} and 0.3 Mm^{-1}, respectively). As already noted, the NAF and SREG episodes affecting the WMB have the potential to increase the aerosol mass and scattering measured in this area in summer (Fig. 2 and JJA scattering in Fig. 4). At the same time, the lower altitude of MSC station compared with the stations reported in AND2011 (lowest altitude around 2.2 km) may have also contributed to the relatively higher scattering observed at MSC station. Recently, Ripoll et al. (2014) have shown that the MSC site registers higher PM_{10} concentrations than those measured at other high-altitude central European sites and similar or lower BC concentrations. As a consequence, the median value of SSA at MSC (0.93; Fig. 5d ALL, all data) was relatively higher compared with the EU, W and E ranges of variability. Conversely, SAE (1.65; Fig. 5e ALL, all data) and B / S (0.126; Fig. 5f ALL, all data) were in the middle of the corresponding EU ranges. The SSA at MSC did not change considerably as a function of seasons and varied between 0.92 (SON) and 0.94 (DJF). Conversely, SAE was higher in summer (1.74; Fig. 5e JJA, all data) compared to winter (1.39; Fig. 5e DJF,

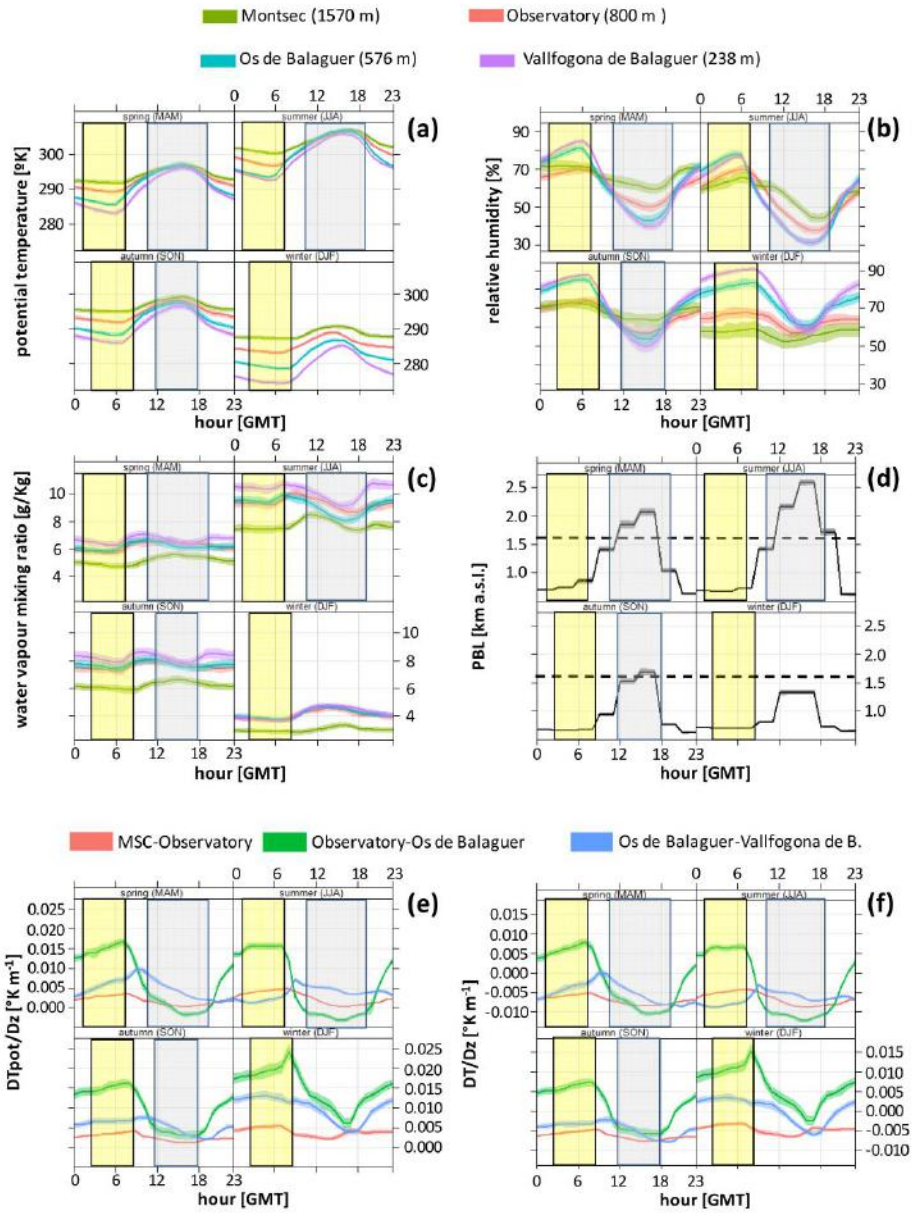

Figure 3. Seasonal diurnal cycles of relative humidity, potential temperature and water vapour mixing ratio measured at Montsec (1570 m a.s.l.), Montsec Observatory (800 m), Os de Balaguer (576 m) and Vallfogona de Balaguer (238 m). Also shown are the diurnal cycles of the planetary boundary layer height (PBL) from HYSPLIT and of the potential temperature and actual temperature gradients. Yellow rectangles highlight the time of the day approach for the identification of FT air proposed in Andrews et al. (2011) and used in this work (from 03:00 to 09:00 LT). Times are reported in GMT. Grey rectangles highlight hours when the MSC station was within the planetary boundary layer. Meteorological data at the four stations were available from 1 January 2011 to 31 December 2012.

all data). The relatively higher SAE observed in summer suggested the prevalence, on average, of finer particles at MSC compared to winter likely due to the frequent SREG scenarios observed during the warm season (cf. Fig. 2). Accordingly, the lowest B / S was measured in winter (0.119; Fig. 5f DJF, all data) and the highest in summer (0.130; Fig. 5f JJA, all data).

All the extensive aerosol properties (scattering, absorption and extinction) showed relatively lower FT-data medians compared with all data (16–19 %; ALL in Fig. 5a, b,

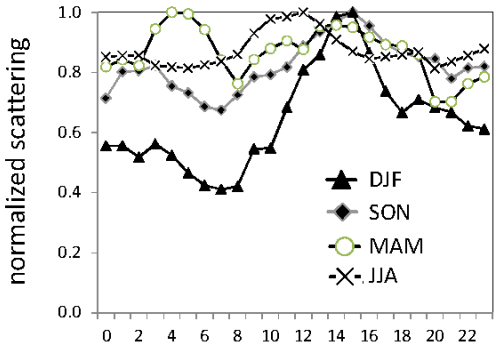

Figure 4. Diurnal cycles of normalized aerosol scattering at 550 nm measured at MSC as a function of the seasons: winter (DJF), autumn (SON), spring (MAM) and summer (JJA).

c). This was a common characteristic for most of the stations presented in AND2011. However, the relative decreases in FT-data extensive properties were clearly seasonal at the MSC site with the highest FT- vs. all-data difference observed in winter (DJF in Fig. 5a, b, c; 21–23 %) and the lowest in spring/summer (MAM and JJA in Fig. 5a, b, c; 0–8 %). The differences between the FT-data and all-data medians were statistically significant for ALL, SON and DJF and marginally significant for JJA. As a consequence of the time of day segregation used for the identification of FT air (03:00–09:00 vs. 24 h) the remote sites showing stronger diurnal cycles tend to have larger decreases in FT aerosol loading compared to all-data (24h) aerosol loading (Andrews et al., 2011). In our case, the high FT- vs. all-data difference observed in winter is consistent with the strong DJF diurnal cycle of normalized scattering presented in Fig. 4.

The lower FT- vs. all-data difference in spring/summer was due to the occurrence of NAF and SREG episodes and to the fact that FT conditions were less frequent in spring/summer due to higher boundary layer. Finally, the differences between the FT-data and all-data medians calculated for the intensive aerosol properties were statistically significant only for SAE in winter (DJF) with slightly higher SAE observed for FT air (1.47; Fig.5e DJF, FT-data).

3.4 Relationships between σ_{sp} and other extensive/intensive aerosol properties

Figure 6 shows the relationships between σ_{sp} and some of the measured extensive (backscattering, absorption, PM_1 concentrations) and intensive (g, SAE, SSA) aerosol properties. Relationships are presented for the whole database (ALL, highlighted by the blue rectangle) and as a function of the main considered meteorological patterns (AA, NAF, SREG, WREG). Similar relationships were investigated, for example, by Delene and Ogren (2002), Pandolfi et al. (2011) and Andrews et al. (2011). However, to our knowledge, this is the first time that these relationships are presented as a function of air mass type. These kind of relationships helps to constrain model parameterizations and to reduce uncertainties in the algorithms used for deriving intensive aerosol properties from remotely sensed data (Delene and Ogren, 2002). In Fig. 6 the frequency distribution of scattering coefficient at 635 nm was calculated for values between 0 and 90 Mm^{-1} with a bin of 5 Mm^{-1} for ALL and NAF scenario. For AA, SREG and WREG scenarios the occurrence for high σ_{sp} was lower, thus limiting the frequency distributions to 75, 75 and 55 Mm^{-1}, respectively.

As shown in Fig. 6 the frequency distribution of aerosol scattering was more right-skewed during AA (sk = 1.93) and WREG (sk = 1.45) compared with NAF (sk = 0.92) and SREG (sk = 0.83) when pollution levels at MSC were higher (Fig. 2).

As reported in Fig. 6 the backscattering and PM_1 concentrations increased with increasing σ_{sp}. If the PM_1 concentrations increase the intensity of light scattered, and also backscattered, increases almost monotonically. Also, the absorption, which is roughly proportional to the concentration of absorbing aerosols in PM samples, increased with increasing scattering and PM_1 concentration. Similar findings were reported by Pandolfi et al. (2011) for the MSY site and by AND2011 (Fig. 6a in AND2011) for the 10 stations considered in their paper. AND2011 observed that the measurement sites which were dominated by dust aerosol at high aerosol loading tend to have a lower slope of the scattering–absorption relationship than the other sites. This is also the case at MSC, which shows a scattering–absorption slope in the lower range of those reported by AND2011 (cf. with Fig. 6a in AND2011). Figure 6 shows that the increase in the extensive aerosol properties with increasing aerosol scattering was fairly similar during the different considered meteorological scenarios, thus leading to very similar SSA as also reported in Fig. 2. Conversely, the most remarkable difference among the scenarios was observed for SAE, which decreased with increasing scattering during NAF reaching values around 0.8 at $\sigma_{sp} = 90\ Mm^{-1}$. Thus, the SAE was clearly a function of NAF intensity. Conversely, during SREG SAE was higher and nearly constant (around 1.8 for $0 < \sigma_{sp} < 90\ Mm^{-1}$), indicating the prevalence of smaller particles with a relatively lower g (0.53 during SREG compared with 0.57 during NAF). No remarkable differences were observed for the intensive aerosol properties between the less polluted WREG and AA scenarios.

On average (ALL in Fig. 6) the parameters g and SAE measured at MSC showed inverse relationships with σ_{sp}: when σ_{sp} increased above around 45–50 Mm^{-1}, SAE decreased, indicating the shift toward larger particles with relatively higher g and SSA. The observed decrease of SAE was due to the prevalence of dust (i.e. large, primarily scattering) particles at high aerosol load at MSC.

To further investigate the effect of NAF episodes on SAE, in Fig. 7 we report the distribution of σ_{sp} as a function of SAE by means of atmospheric scenarios (Fig. 7a) and levels

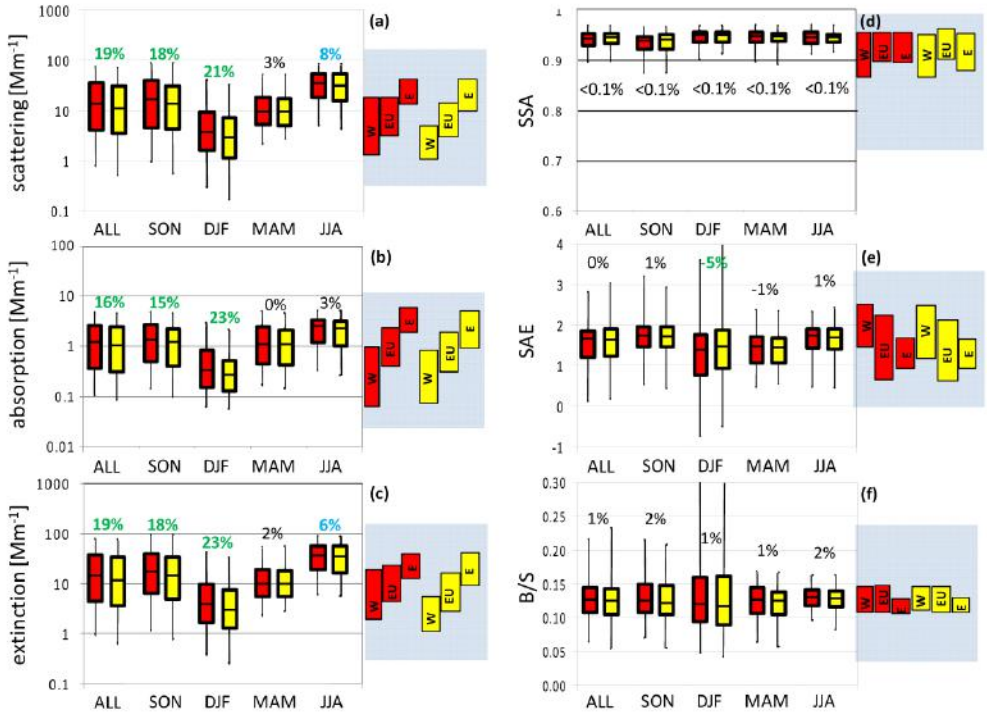

Figure 5. Aerosol optical properties for all data and FT data. Data are reported at 550 nm. Red represents all data, and yellow represents FT data. Horizontal lines within the boxes are the medians (50th percentile), the bottom and top of each box are 25th and 75th percentiles, respectively, and whiskers are 5th and 95th percentiles. The Ångström exponent is calculated for 450/635 nm pair. For MSC, values are calculated for the whole period considered here (ALL), and for autumn (SON), winter (DJF), spring (MAM) and summer (JJA). The percentage values represent the relative difference between the medians calculated for all data and FT data. Green bold numbers indicate statistically significant differences (p value < 0.05); blue bold numbers highlight marginally significant differences ($p < 0.1$); black numbers indicate differences which were not statistically significant ($p > 0.1$). The red and yellow rectangles within the blue areas on the right of each figure represent the range of variability of the medians presented by Andrews et al. (2011) calculated for sites in the Western Hemisphere (W), Europe (EU) and the Eastern Hemisphere (E).

of PM_1 / PM_{10} ratio (Fig. 7b). As shown in Fig. 7a, high scattering and relatively low SAE (< 1) were associated with NAF episodes (yellow). Correspondingly, the PM_1 / PM_{10} ratio was among the lowest (0.2–0.3, Fig. 7b), indicating the prevalence of coarser particles. The AA scenarios (blue in Fig. 7a) were mainly associated with relatively lower scattering ($11.7 \pm 13.9\,Mm^{-1}$ at 635 nm), a broad range of SAE values (from −2 to 4) and PM_1 / PM_{10} ratios around 0.3–0.5. Cermac et al. (2010) suggested that negative SAE could be an indication of reduced anthropogenic emissions with prevalence of coarse-mode particles. For example negative SAE and high aerosol optical depth (AOD) were related to transport of coarse-mode dust in northern India by Singh et al. (2004). However, extremely negative values of SAE are unfeasible for atmospheric aerosols. Similarly, the SAE cannot be higher than about 4, which represents the limit given by the Rayleigh regimen for the molecular scattering. In the present case 123 hourly values of SAE out of 9561 were smaller than −1 (1.2 %) and 150 values were higher than 4 (1.6 %). Consequently, the measured negative SAE at MSC were likely due to both the presence of relatively larger particles during low aerosol concentration (Fig. 7b) and the instrumental noise under low scattering conditions. Similar behaviour of SAE was also observed in a remote subarctic site by Aaltonen et al. (2006) and at the MSY station by Pandolfi et al. (2011). Finally, the SREG episodes mainly (red, Fig. 7a), and to a lesser extent WREG (orange), were associated with relatively larger SAE compared with NAF and high PM_1 / PM_{10} ratios, indicative of the prevalence of mainly fine particles of anthropogenic origin.

For σ_{sp} between around 20 and 40 Mm^{-1} (ALL in Fig. 6) both g and SAE showed relatively constant values around 0.55 (g) and 1.65 (SAE), which were close to the averages reported in Table 2 for these two parameters. When σ_{sp} was below around 15–20 Mm^{-1}, SAE decreased, indicating again the shift toward relatively larger particles associated with relatively clean atmosphere ($PM_1 < 5\,\mu g\,m^{-3}$). This decrease was more pronounced for AA and WREG compared with

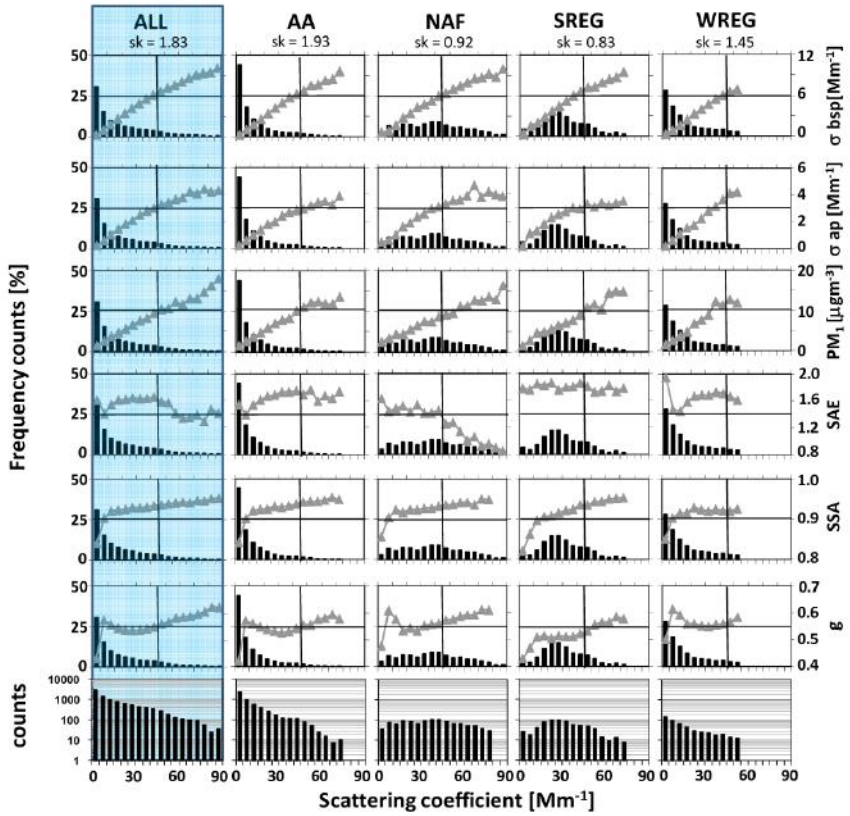

Figure 6. Correlation between the frequency distribution of aerosol scattering coefficients (σ_{sp}) at 635 nm and backscattering coefficient (σ_{bsp} at 635 nm), absorption coefficient (σ_{ap} at 637 nm), PM_1 concentrations (PM_1), asymmetry parameter (g at 635 nm), scattering Ångström exponent (SAE, 450–635 nm) and single-scattering albedo (SSA at 635 nm). Correlations are presented for all data (ALL) and for the different atmospheric scenarios (Atlantic advection, AA; Saharan dust outbreaks, NAF; summer regional recirculation scenario, SREG; and winter anticyclonic scenario, WREG). Frequency count (%) and the absolute number of hourly values (counts) in each been are reported.

NAF and SREG (Fig. 6). However, under very low PM_1 concentrations at MSC ($PM_1 < 1.5\ \mu g\ m^{-3}$) SSA and g reached very low values around 0.84 and 0.43 (ALL in Fig. 6), respectively, whereas the SAE increased. These low PM conditions at MSC were associated with the prevalence of small particles with relatively higher absorption properties irrespective of the scenario considered. Low values of SSA at very low aerosol loading have been observed in AND2011 and associated with an aerosol mixture in which large scattering aerosol particles have been preferentially removed (e.g. by cloud scavenging and/or deposition), leaving behind a relatively smaller and darker aerosol (e.g. AND2011; Berkowitz et al., 2011; Marcq et al., 2010; Targino et al., 2005; Sellegri et al., 2003).

3.5 MAC and MSCS climatology

Mean MAC, determined at Montsec as the error-weighted slope of the absorption–EC scatterplot, was $11.1 \pm 0.3\ m^2\ g^{-1}$ ($R^2 = 0.82$). Given that σ_{ap} and EC concentrations measurements have been available since the end of 2009, the mean MAC presented here was calculated over the period November 2009–June 2013 (384 sample pairs on 24 h basis). Mean MSCS at 635 nm (228 sample pairs) was $2.5 \pm 1.3\ m^2\ g^{-1}$. MSCS at 525 nm and 450 nm are reported in Table 2. On average, lower MAC values were observed during AA ($9.7 \pm 0.7\ m^2\ g^{-1}$, $R^2 = 0.77$) and WREG ($9.4 \pm 1.0\ m^2\ g^{-1}$, $R^2 = 0.88$) scenarios compared to NAF ($11.9 \pm 0.7\ m^2\ g^{-1}$, $R^2 = 0.61$) and SREG ($12.6 \pm 1.0\ m^2\ g^{-1}$, $R^2 = 0.74$) scenarios. Similarly, a low MSCS was on average observed during AA and WREG ($2.0 \pm 1.1\ m^2\ g^{-1}$ and $1.5 \pm 0.6\ m^2\ g^{-1}$, respectively, at 635 nm), whereas MSCS was higher during NAF and SREG ($3.7 \pm 1.4\ m^2\ g^{-1}$ and $3.5 \pm 0.7\ m^2\ g^{-1}$, respectively). The non-parametric Kruskal–Wallis test was used for testing the equality of medians among the four selected categories (scenarios). The difference between the NAF and SREG medians was not statistically significant ($p > 0.5$) for both MAC and MSCS. The same was observed for the AA and WREG medians ($p > 0.3$). Conversely, statistically

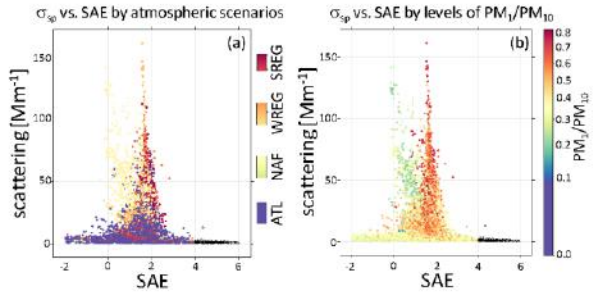

Figure 7. Scattering coefficient (σ_{sp}) distribution at 635 nm as a function of the scattering Ångström exponent (SAE) by atmospheric scenarios **(a)** and by levels of PM_1 / PM_{10} ratio **(b)**. Dark data points indicate SAE > 4.

significant differences ($p < 0.001$) were observed between the medians calculated for WREG and AA and those calculated for NAF and SREG. The higher MAC and MSCS under NAF and SREG compared to AA and WREG were likely due to differences in particles' origin and particle properties during these scenarios. The SREG scenario is a summer scenario (cf. Fig. 8) which favours the recirculation and aging of pollutants in the WMB. Several publications have shown higher sulfate (e.g. Pey et al., 2009; Querol et al., 1999) and organic matter concentrations (e.g. Querol et al., 2013; Pandolfi et al., 2014) in summer compared to winter in the WMB at regional and remote levels. The summer sulfate and organic matter maxima were due to higher temperatures and increased photochemistry in the atmosphere enhancing the SO_2 oxidation and the formation of secondary organic aerosols from biogenic emissions from vegetation (Seco et al., 2011).

Moreover, Ripoll et al. (2014) have shown higher concentrations of BC particles in the warmer months at MSC attributed to the impact of the SREG episodes and to the higher occurrence of wildfires in North Africa and/or in the WMB (Cristofanelli et al., 2009). Once formed, these particles can recirculate and age under the SREG scenario in the WMB. On the other hand, the NAF scenarios, which are more frequent in summer in the WMB (Pey et al., 2013), increase the concentration of mineral dust in the atmosphere. Moreover, Rodríguez et al. (2011) and Ripoll et al. (2014) have shown that pollutants such as sulfate and BC may be transported together with dust across the WMB during NAF episodes.

The mixing of BC particles with other chemical components, such as sulfate and organics, has the potential to increase the absorption properties of BC particles (e.g. Bond et al., 2013) and could explain the higher MAC observed at MSC during NAF and SREG. At the same time, the MSCS was also higher during NAF and SREG, indicating higher scattering efficiency of PM. Similar dependence of the MAC with atmospheric scenarios was reported by Pandolfi et al. (2011) for the MSY station. An exception was observed for the MAC calculated at Montseny during WREG, which was the highest compared to AA, SREG and NAF. The likely reason for the different MAC at MSC and MSY under WREG was the lower altitude of the MSY station, which was often within the polluted PBL under WREG winter scenarios (i.e. Pandolfi et al., 2014), whereas the MSC was above.

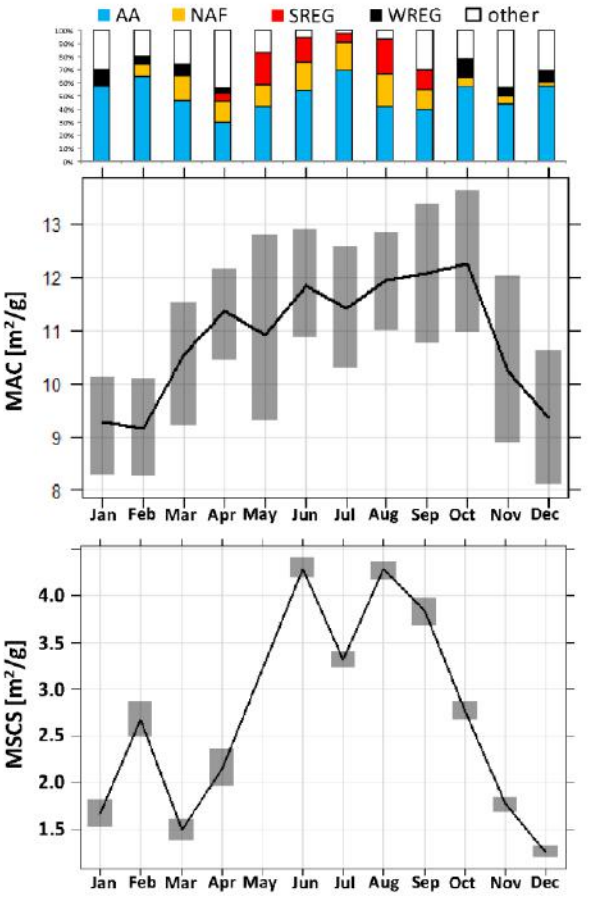

Figure 8. Monthly mean mass absorption cross section (MAC) and mass scattering cross section (MSCS) at MSC station and occurrence (%) of the main atmospheric scenarios (AA: Atlantic advections; NAF: Saharan dust outbreaks; SREG: summer regional recirculation scenarios; and WREG: winter anticyclonic scenarios). Bars represent 95 % confidence intervals.

As a consequence of the observed variations of MAC and MSCS as a function of the four considered season-dependent scenarios, the MAC and MSCS at MSC showed a clear annual cycle, with the lowest values observed in winter and the highest in summer (Fig. 8). Similar seasonal dependence of the MAC with higher values in summer was observed at the Jungfraujoch high-alpine site (Cozic et al., 2008).

4 Conclusions

The measurements of aerosol optical properties presented in this work and performed at the remote Montsec site (MSC; 42°3′ N, 0°44′ E, 1570 m a.s.l.) add useful information on the limited amount of in situ aerosol optical data obtained at high-altitude/mountaintop sites worldwide. The aerosol scattering measurements performed at MSC located this site in the medium/upper range of values reported for other mountaintop sites in Europe (EU). The frequent African dust (NAF) outbreaks and regional recirculation (SREG) scenarios, typical of the WMB in spring/summer, were mainly responsible for these relatively high values. Moreover, the lower altitude of MSC station compared with other mountaintop sites and the strong summer insolation in the Mediterranean regions, favouring the development of thermally driven upslope winds, may have also contributed to the relatively higher scattering observed at MSC. The mean scattering at MSC during the NAF and SREG scenarios was close to the values measured at a regional background station (Montseny, 720 m a.s.l.), thus demonstrating the potential of these two summer atmospheric scenarios in polluting the whole lower troposphere in the western Mediterranean. As a consequence, in spring and summer no clear diurnal cycles were observed for the extensive aerosol optical properties due to the presence of polluted layer at the MSC altitude. Thus, the diurnal variation of scattering at MSC during spring and summer was subject to synoptic circulation, which partially masked the mountain breezes and the dynamics transport at a more local scale. Conversely, during Atlantic advection (AA) and winter regional anticyclonic (WREG) episodes, mainly registered during the cold season, the extensive aerosol properties at MSC were considerably lower compared to Montseny and the highest diurnal cycle amplitudes were observed. The AA scenario in the WMB is typically characterized by high wind speed with air masses coming from the Atlantic Ocean, thus favouring the dispersion of the accumulated pollution with consequent reduction of the concentrations of pollutants, which is more effective at remote levels. The WREG scenario is mainly characterized by weak synoptic winds leading to stagnation of air masses and to the accumulation and aging of pollutants over the region, whereas the PBL height mostly determines the dilution of pollutants around the emission sources and the degree of pollution at more elevated/regional areas in the WMB. Absorption at MSC was not as high as scattering compared with most of measurements in EU, thus leading to relatively higher single-scattering albedo (SSA) compared with EU data. Conversely, the scattering Ångström exponent (SAE) and backscatter-to-scatter ratios (B / S) were in the middle of the corresponding EU ranges.

All the extensive aerosol properties measured at MSC showed relatively lower medians when MSC was in the free troposphere (FT data) compared with the whole database (all data). These decreases were clearly seasonal at the MSC site, with the highest and statistically significant FT- vs. all-data difference observed in winter and the lowest (and not statistically significant) in spring/summer. The frequent NAF and SREG scenarios in summer, and the less frequent FT conditions due to higher boundary layer, explained the lower FT- vs. all-data differences observed in summer compared to winter.

The aerosol optical measurements performed demonstrated that the MSC measurement site provides reliable information for a suitable characterization of the main synoptic meteorological patterns affecting the region. Clear differences were observed between NAF and SREG scenarios in terms of intensive aerosol optical properties. SAE during NAF was the lowest, indicating the presence of larger particles, and was clearly anticorrelated with the intensity of Saharan dust outbreaks, whereas nearly constant and higher SAE was measured under SREG, indicating an aerosol mode dominated by finer particles. Correspondingly, the asymmetry parameter was higher during NAF compared to SREG. The analysis of the relationships between scattering and other extensive/intensive aerosol properties measured at MSC showed a scattering–absorption slope in the lower range of slopes calculated worldwide, indicating that the MSC site is dominated by dust aerosols at high aerosol loading. As a consequence, SSA increased nearly monotonically with increasing scattering.

The MAC estimated at MSC showed a clear annual cycle, with higher values in summer when the occurrence of NAF and SREG scenarios favoured the presence of polluted atmospheric layers containing aged BC particles likely mixed with other chemical components such as organics and sulfate. These summer conditions were also linked with higher scattering efficiency of PM.

Acknowledgements. This work was supported by the MINECO (Spanish Ministry of Economy and Competitiveness), the MAGRAMA (Spanish Ministry of Agriculture, Food and Environment) and FEDER funds: the projects PRISMA (CGL2012-39623-C02/00) and VAMOS (CLG2010-19464). The research received funding from the European Union Seventh Framework Programme (FP7/2007–2013) ACTRIS under grant agreement no. 262254. M. Pandolfi was funded by the JAE-Doc CSIC programme, co-funded by the European Social Fund (ESF). The authors wish to thank D. C. Carslaw and K. Ropkins for providing the Openair software used in this paper (Carslaw and Ropkins, 2012; Carslaw, 2012). The authors wish to thank A. Tobias for the statistical analysis related with Fig. 5. The authors are grateful for the use of the HYSPLIT model, SKIRON, BSC-DREAM and NRL-NAAPS aerosol maps, NCEP/NCAR meteorological database NOAA NAO index data, and image products from MODIS and SeaWiFs NASA satellites used in this publication. The authors would like to extend their gratitude to the personnel from the OAdM. We would also like to express our gratitude to METEOCAT for the meteorological data.

Edited by: S. Gilardoni

References

Aaltonen, V., Lihavainen, H., Kerminen, V.-M., Komppula, M., Hatakka, J., Eneroth, K., Kulmala, M., and Viisanen, Y.: Measurements of optical properties of atmospheric aerosols in Northern Finland, Atmos. Chem. Phys., 6, 1155–1164, doi:10.5194/acp-6-1155-2006, 2006.

Anderson, T. L. and Ogren, J. A.: Determining Aerosol Radiative Properties Using the TSI 3563 Integrating Nephelometer, Aerosol Sci. Tech., 29, 57–69, 1998.

Andrews, E., Sheridan, P. J., Fiebig, M., McComiskey, A., Ogren, J. A., Arnott, P., Covert, D., Elleman, R., Gasparini, R., Collins, D., Jonsson, H., Schmid, B., and Wang, J.: Comparison of methods for deriving aerosol asymmetry parameter, J. Geophys. Res. Atmos., 111, D05S04, doi:10.1029/2004JD005734, 2006.

Andrews, E., Ogren, J. A., Bonasoni, P., Marinoni, A., Cuevas, E., Rodríguez, S., Sun, J. Y., Jaffe, D. A., Fischer, E. V., Baltensperger, U., Weingartner, E., Collaud Coen, M., Sharma, S., Macdonald, A. M., Leaitch, W. R., Lin, N.-H., Laj, P., Arsov, T., Kalapov, I., Jefferson, A., and Sheridan, P.: Climatology of aerosol radiative properties in the free troposphere, Atmos. Res., 102, 365–393, doi:10.1016/j.atmosres.2011.08.017, 2011.

Arnott, W. P., Moosmüller, H., Sheridan, P. J., Ogren, J. A., Raspet, R., Slaton, W. V., Hand, J. L., Kreidenweis, S. M., and Collett Jr., J. L.: Photoacoustic and Filter-Based Ambient Aerosol Light Absorption Measurements: Instrument Comparisons and the Role of Relative Humidity, J. Geophys. Res., 108, 4034, doi:10.1029/2002JD002165, 2003.

Arnott, W. P., Hamasha, K., Moosmüller, H., Sheridan, P. J., and Ogren, J. A.: Towards Aerosol Light Absorption Measurements with a 7-wavelength Aethalometer: Evaluation with a Photoacoustic Instrument and 3 wavelength Nephelometer, Aerosol Sci. Tech., 39, 17–29, 2005.

Berkowitz, C., Berg, L. K., Yu, X.-Y., Alexander, M. L., Laskin, A., Xie, Y., Jobson, B. T., Andrews, E., and Ogren, J.: A statistical overview of aerosol optical, chemical and physical measurements at a coastal northern California site during the summer of 2005, Atmos. Environ., 45, 2559–2568, doi:10.1016/j.atmosres.2011.08.017, 2011.

Bodhaine, B.: Aerosol measurements at four background sites, J. Geophys. Res. 88, 10753–10768, doi:10.1029/JC088iC15p10753, 1983.

Bodhaine, B.: Aerosol absorption measurements at Barrow, Mauna Loa and the South Pole. J. Geophys. Res., 100, 8967–8975, doi:10.1029/95JD00513, 1995.

Bond, T. C. and Bergstrom, R. W.: Light absorption by carbonaceous particles: An investigative review, Aerosol Sci. Tech., 40, 27–67, doi:10.1080/02786820500421521, 2006.

Bond, T. C., Doherty, S. J., Fahey, D. W., Forster, P. M., Berntsen, T., DeAngelo, B. J., Flanner, M. G., Ghan, S., Kärcher, B., Koch, D., Kinne, S., Kondo, Y., Quinn, P. K., Sarofim, M. C., Schultz, M. G., Schulz, M., Venkataraman, C., Zhang, H., Zhang, S., Bellouin, N., Guttikunda, S. K., Hopke, P. K., Jacobson, M. Z., Kaiser, J. W., Klimont, Z., Lohmann, U., Schwarz, J. P., Shindell, D., Storelvmo, T., Warren S. G., and Zender, C. S.: Bounding the role of black carbon in the climate system: A scientific assessment, J. Geophys. Res. 118, 11, 5380–5552, doi:10.1002/jgrd.50171, 2013.

Carslaw, D. C.: The openair manual – open-source tools for analysing air pollution data, Manual for version 0.7-0, King's College, London, 2012.

Carslaw, D. C. and Ropkins, K.: openair – an R package for air quality data analysis, Environ. Modell. Softw., 27–28, 52–61, 2012.

Cavalli, F., Viana, M., Yttri, K. E., Genberg, J., and Putaud, J.-P.: Toward a standardised thermal-optical protocol for measuring atmospheric organic and elemental carbon: the EUSAAR protocol, Atmos. Meas. Tech., 3, 79–89, doi:10.5194/amt-3-79-2010, 2010.

Cermak, J., Wild, M., Knutti, R., Mishchenko, M. I., and Heidinger A. K.: Consistency of global satellite-derived aerosol and cloud data sets with recent brightening observations, Geophys. Res. Lett., 37, L21704, doi:10.1029/2010gl044632, 2010.

Collaud Coen, M., Weingartner, E., Schaub, D., Hueglin, C., Corrigan, C., Henning, S., Schwikowski, M., and Baltensperger, U.: Saharan dust events at the Jungfraujoch: detection by wavelength dependence of the single scattering albedo and first climatology analysis, Atmos. Chem. Phys., 4, 2465–2480, doi:10.5194/acp-4-2465-2004, 2004.

Collaud Coen, M., Weingartner, E., Nyeki, S., Cozic, J., Henning, S., Verheggen, B., Gehrig, R., and Baltensperger, U.: Long-term trend analysis of aerosol variables at the high-alpine site Jungfraujoch, J. Geophys. Res., 112, D13213, doi:10.1029/2006JD007995, 2007.

Collaud Coen, M., Weingartner, E., Furger, M., Nyeki, S., Prévôt, A. S. H., Steinbacher, M., and Baltensperger, U.: Aerosol climatology and planetary boundary influence at the Jungfraujoch analyzed by synoptic weather types, Atmos. Chem. Phys., 11, 5931–5944, doi:10.5194/acp-11-5931-2011, 2011.

Cozic, J., Verheggen, B., Weingartner, E., Crosier, J., Bower, K. N., Flynn, M., Coe, H., Henning, S., Steinbacher, M., Henne, S., Collaud Coen, M., Petzold, A., and Baltensperger, U.: Chemical composition of free tropospheric aerosol for PM1 and coarse mode at the high alpine site Jungfraujoch, Atmos. Chem. Phys., 8, 407–423, doi:10.5194/acp-8-407-2008, 2008.

Cristofanelli, P., Marinoni, A., Arduini, J., Bonafè, U., Calzolari, F., Colombo, T., Decesari, S., Duchi, R., Facchini, M. C., Fierli, F., Finessi, E., Maione, M., Chiari, M., Calzolai, G., Messina, P., Orlandi, E., Roccato, F., and Bonasoni, P.: Significant variations of trace gas composition and aerosol properties at Mt. Cimone during air mass transport from North Africa – contributions from wildfire emissions and mineral dust, Atmos. Chem. Phys., 9, 4603–4619, doi:10.5194/acp-9-4603-2009, 2009.

Delene, D. J. and Ogren, J. A.: Variability of aerosol optical properties at four North American surface monitoring sites, J. Atmos. Sci., 59, 1135–1150, 2002.

Fernández-Camacho, R., Rodríguez, S., de la Rosa, J., Sánchez de la Campa, A. M., Viana, M., Alastuey, A., and Querol, X.: Ultrafine particle formation in the inland sea breeze airflow in Southwest Europe, Atmos. Chem. Phys., 10, 9615–9630, doi:10.5194/acp-10-9615-2010, 2010.

Fierz-Schmidhauser, R., Zieger, P., Gysel, M., Kammermann, L., DeCarlo, P. F., Baltensperger, U., and Weingartner, E.: Measured and predicted aerosol light scattering enhancement factors at the high alpine site Jungfraujoch, Atmos. Chem. Phys., 10, 2319–2333, doi:10.5194/acp-10-2319-2010, 2010.

Gangoiti, G., Millán, M. M., Salvador, R., and Mantilla E.: Long-Range transport and recirculation of pollutants in the western

Mediterranean during the project Regional Cycles of Air Pollution in the west-central Mediterranean Area, Atmos. Environ., 35, 6267–6276, 2001.

IPCC 2007, in: Climate Change 2007: The Physical Science Basis (Contribution of Working Group I to the Fourth Assessment Report of the Intergovernmental Panel on Climate Change) edited by: Solomon, S., Qin, D. Manning, M., Chen, Z., Marquis, M., Averyt, K. B., Tignor, M., and Miller, H. L., Cambridge Univ. Press, New York, USA, 131–217, 2007.

IPCC 2013, in Climate Change 2013: The Physical Science Basis. Working Group I contribution to the IPCC fifth assessment report. Final Draft Underlying Scientific-Technical Assessment, Cambridge University Press, Cambridge, United Kingdom and New York, NY, USA, 2013.

Jorba, O., Pandolfi, M., Spada, M., Baldasano, J. M., Pey, J., Alastuey, A., Arnold, D., Sicard, M., Artinano, B., Revuelta, M. A., and Querol, X.: Meteorological overview and transport patterns of the DAURE field campaign: link to PM observations, Atmos. Environ., 77, 607–620, 2013.

JRC Report: Measurement of Elemental and Organic Carbon in Europe, Scientific and Technical Reports, EUR 23922 EN-2009, Joint Research Center, Ispra, Italy, 2009.

Laj, P., Klausen, J., Bilde, M., Plaß-Duelmer, C., Pappalardo, G., Clerbaux, C., Baltensperger, U., Hjorth, J., Simpson, D., Reimann, S., Coheur, P.-F., Richter, A., De Mazière, M., Rudich, Y., McFiggans, G., Torseth, K., Wiedensohler, A., Morin, S., Schulz, M., Allan, J. D., Attié, J.-L., Barnes, I., Birmili, W., Cammas, J. P., Dommen, J., Dorn, H.-P., Fowler, D., Fuzzi, S., Glasius, M., Granier, C., Hermann, M., Isaksen, I. S. A., Kinne, S., Koren, I., Madonna, F., Maione, M., Massling, A., Moehler, O., Mona, L., Monks, P. S., Müller, D., Müller, T., Orphal, J., Peuch, V.-H., Stratmann, F., Tanré, D., Tyndall, G., Abo Riziq, A., Van Roozendael, M., Villani, P., Wehner, B., Wex, H., and Zardini, A. A.: Measuring atmospheric composition change, Atmos. Environ., 43, 5351–5414, doi:10.1016/j.atmosenv.2009.08.020, 2009.

Marcq, S., Laj, P., Roger, J. C., Villani, P., Sellegri, K., Bonasoni, P., Marinoni, A., Cristofanelli, P., Verza, G. P., and Bergin, M.: Aerosol optical properties and radiative forcing in the high Himalaya based on measurements at the Nepal Climate Observatory-Pyramid site (5079 m a.s.l.), Atmos. Chem. Phys., 10, 5859–5872, doi:10.5194/acp-10-5859-2010, 2010.

Marinoni, A., Cristofanelli, P., Calzolari, F., Roccato, F., Bonafe, U., and Bonasoni, P.: Continuous measurements of aerosol physical parameters at the Mt. Cimone GAW station (2165 m a.s.l., Italy), Sci. Total. Environ., 391, 241–251, 2008.

McKendry, I., Strawbridge, K., Karumudi, M. L., O'Neill, N., Macdonald, A. M., Leaitch, R., Jaffe, D., Cottle, P., Sharma, S., Sheridan, P., and Ogren, J.: Californian forest fire plumes over Southwestern British Columbia: lidar, sunphotometry, and mountaintop chemistry observations, Atmos. Chem. Phys., 11, 465–477, doi:10.5194/acp-11-465-2011, 2011.

Millán, M. M., Artiñano, B., Alonso, L., Castro, M., Fernández-Patier, R., and Goberna, J.: Meso-meteorological Cycles of Air Pollution in the Iberian Peninsula, (MECAPIP), Contract EV4V-0097-E, Air Pollution Research Report 44, (Eur No. 14834) CEC-DG XII/E-1, Rue de la Loi, 200, 1040, Bruselas, 219 pp., 1992.

Millán, M. M., Salvador, R., Mantilla, E., and Kallos, G.: Photooxidant dynamics in the Mediterranean basin in summer: Results from European research projects, J. Geophys. Res., 102, 8811–8823, doi:10.1029/96JD03610, 1997.

Müller, T., Laborde, M., Kassell, G., and Wiedensohler, A.: Design and performance of a three-wavelength LED-based total scatter and backscatter integrating nephelometer, Atmos. Meas. Tech., 4, 1291–1303, doi:10.5194/amt-4-1291-2011, 2011a.

Müller, T., Henzing, J. S., de Leeuw, G., Wiedensohler, A., Alastuey, A., Angelov, H., Bizjak, M., Collaud Coen, M., Engström, J. E., Gruening, C., Hillamo, R., Hoffer, A., Imre, K., Ivanow, P., Jennings, G., Sun, J. Y., Kalivitis, N., Karlsson, H., Komppula, M., Laj, P., Li, S.-M., Lunder, C., Marinoni, A., Martins dos Santos, S., Moerman, M., Nowak, A., Ogren, J. A., Petzold, A., Pichon, J. M., Rodriquez, S., Sharma, S., Sheridan, P. J., Teinilä, K., Tuch, T., Viana, M., Virkkula, A., Weingartner, E., Wilhelm, R., and Wang, Y. Q.: Characterization and intercomparison of aerosol absorption photometers: result of two intercomparison workshops, Atmos. Meas. Tech., 4, 245-268, doi:10.5194/amt-4-245-2011, 2011b.

Nyeki, S., Baltensperger, U., Colbeck, I., Jost, D. T., Weingartner, E., Gaggeler, H. W.: The Jungfraujoch high-alpine research station (3454 m) as a background clean continental site for the measurement of aerosol parameters, J. Geophys. Res., 103, 6097–6107, doi:10.1029/97JD03123, 1998.

Ogren, J. A., Andrews, E., McComiskey, A., Sheridan, P., Jefferson, A., and Fiebig, M.: New insights into aerosol asymmetry parameter, in: Proceedings of the 16th ARM Science Team Meeting, Albuquerque, NM, USA, 2006.

Pandolfi, M., Cusack, M., Alastuey, A., and Querol, X.: Variability of aerosol optical properties in the Western Mediterranean Basin, Atmos. Chem. Phys., 11, 8189–8203, doi:10.5194/acp-11-8189-2011, 2011.

Pandolfi, M., Querol, X., Alastuey, A., Jimenez, J. L., Jorba, O., Day, D., Ortega, A., Cubison, M. J., Comerón, A., Sicard, M., Mohr, C., Prévôt, A. S. H., Minguillón, M. C., Pey, J., Baldasano, J. M., Burkhart, J. F., Seco, R., Peñuelas, J., van Drooge, B. L., Artiñano, B., Di Marco, C., Nemitz, E., Schallhart, S., Metzger, A., Hansel, A., Lorente, J., Ng, S., Jayne, J., and Szidat, S.: Effects of sources and meteorology on particulate matter in the Western Mediterranean Basin: An overview of the DAURE campaign, J. Geophys. Res. Atmos., 119, 4978–5010, doi:10.1002/2013JD021079, 2014.

Pereira, S. N., Wagner, F., and Silva, A. M.: Seven years of measurements of aerosol scattering properties, near the surface, in the southwestern Iberia Peninsula, Atmos. Chem. Phys., 11, 17–29, doi:10.5194/acp-11-17-2011, 2011.

Pérez, C., Sicard, M., Jorba, O., Comerón, A., and Baldasano J. M.: Summertime re-circulations of air pollutants over the northeastern Iberian coast observed from systematic EARLINET lidar measurements in Barcelona, Atmos. Environ., 38, 3983–4000, doi:10.1016/j.atmosenv.2004.04.010, 2004.

Pérez, N., Pey, J., Castillo, S., Viana, M., Alastuey, A., and Querol, X.: Interpretation of the variability of levels of regional background aerosols in the Western Mediterranean, Sci. Total Environ., 407, 527–540, doi:10.1016/j.scitotenv.2008.09.006, 2008.

Petzold, A. and Schönlinner, M.: Multi-angle absorption photometry – a new method for the measurement of aerosol light absorption and atmospheric black carbon, J. Aerosol Sci., 35, 421–441, doi:10.1016/j.jaerosci.2003.09.005, 2004.

Pey, J., Pérez, N., Castillo, S., Viana, M., Moreno, T., Pandolfi, M., López-Sebastián, J. M., Alastuey, A., and Querol, X.: Geochemistry of regional background aerosols in the Western Mediterranean, Atmos. Res., 94, 422–435, doi:10.1016/j.atmosres.2009.07.001, 2009.

Pey, J., Querol, X., Alastuey, A., Forastiere, F., and Stafoggia, M.: African dust outbreaks over the Mediterranean Basin during 2001–2011: PM10 concentrations, phenomenology and trends, and its relation with synoptic and mesoscale meteorology, Atmos. Chem. Phys., 13, 1395–1410, doi:10.5194/acp-13-1395-2013, 2013.

Polissar, A. V., Hopke, P. K., Malm, W. C., and Sisler, J. F.: Atmospheric aerosols over Alaska: 2. Elemental Composition and Sources, J. Geophys. Res., 103, 19045–19057, doi:10.1029/98JD01212, 1998.

Querol, X., Alastuey, A., Lopez-soler, A., Plana, F. and Puicercus, J. A.: Daily evolution of sulphate aerosols in a rural area, northeastern Spain – elucidation of an atmospheric reservoir effect, Environ. Pollut., 105, 397–407, doi:10.1016/S0269-7491(99)00037-8, 1999.

Querol, X., Pey, J., Minguillón, M. C., Pérez, N., Alastuey, A., Viana, M., Moreno, T., Bernabé, R. M., Blanco, S., Cárdenas, B., Vega, E., Sosa, G., Escalona, S., Ruiz, H., and Artíñano, B.: PM speciation and sources in Mexico during the MILAGRO-2006 Campaign, Atmos. Chem. Phys., 8, 111–128, doi:10.5194/acp-8-111-2008, 2008.

Querol, X., Alastuey, A., Pey, J., Cusack, M., Pérez, N., Mihalopoulos, N., Theodosi, C., Gerasopoulos, E., Kubilay, N., and Koçak, M.: Variability in regional background aerosols within the Mediterranean, Atmos. Chem. Phys., 9, 4575–4591, doi:10.5194/acp-9-4575-2009, 2009.

Querol, X., Alastuey, A., Viana, M., Moreno, T., Reche, C., Minguillón, M. C., Ripoll, A., Pandolfi, M., Amato, F., Karanasiou, A., Pérez, N., Pey, J., Cusack, M., Vázquez, R., Plana, F., Dall'Osto, M., de la Rosa, J., Sánchez de la Campa, A., Fernández-Camacho, R., Rodríguez, S., Pio, C., Alados-Arboledas, L., Titos, G., Artíñano, B., Salvador, P., García Dos Santos, S., and Fernández Patier, R.: Variability of carbonaceous aerosols in remote, rural, urban and industrial environments in Spain: implications for air quality policy, Atmos. Chem. Phys., 13, 6185–6206, doi:10.5194/acp-13-6185-2013, 2013.

Quinn, P. K. and Bates, T. S.: Regional aerosol properties: Comparisons of boundary layer measurements from ACE 1, ACE 2, Aerosols99, INDOEX, ACE Asia, TARFOX, and NEAQS, J. Geophys. Res., 110, D14202, doi:10.1029/2004JD004755, 2005.

Reche, C., Querol, X., Alastuey, A., Viana, M., Pey, J., Moreno, T., Rodríguez, S., González, Y., Fernández-Camacho, R., de la Rosa, J., Dall'Osto, M., Prévôt, A. S. H., Hueglin, C., Harrison, R. M., and Quincey, P.: New considerations for PM, Black Carbon and particle number concentration for air quality monitoring across different European cities, Atmos. Chem. Phys., 11, 6207–6227, doi:10.5194/acp-11-6207-2011, 2011.

Ripoll, A., Pey, J., Minguillón, M. C., Pérez, N., Pandolfi, M., Querol, X., and Alastuey, A.: Three years of aerosol mass, black carbon and particle number concentrations at Montsec (southern Pyrenees, 1570 m a.s.l.), Atmos. Chem. Phys., 14, 4279–4295, doi:10.5194/acp-14-4279-2014, 2014.

Rodríguez, S., Querol, X., Alastuey, A., Kallos, G., and Kakaliagou, O.: Saharan dust contributions to PM_{10} and TSP levels in Southern and Eastern Spain, Atmos. Environ., 35, 2433–2447, 2001.

Rodríguez, S., Querol, X., Alastuey, A., Viana, M. M., Alarcón, M., Mantilla, E., and Ruiz, C. R.: Comparative PM_{10}-$PM_{2.5}$ source contribution study at rural, urban and industrial sites during PM episodes in Eastern Spain, Sci. Total Environ., 26, 95–113, doi::10.1016/S0048-9697(03)00411-X, 2004.

Rodríguez, S., Alastuey, A., Alonso-Pérez, S., Querol, X., Cuevas, E., Abreu-Afonso, J., Viana, M., Pérez, N., Pandolfi, M., and de la Rosa, J.: Transport of desert dust mixed with North African industrial pollutants in the subtropical Saharan Air Layer, Atmos. Chem. Phys., 11, 6663–6685, doi:10.5194/acp-11-6663-2011, 2011.

Schuster, G. L., Dubovik, O., and Holben, B. N.: Ångström exponent and bimodal aerosol size distributions, J. Geophys. Res., 111, D07207, doi:101029/2005JD006328, 2006.

Seco, R., Peñuelas, J., Filella, I., Llusià, J., Molowny-Horas, R., Schallhart, S., Metzger, A., Müller, M., and Hansel, A.: Contrasting winter and summer VOC mixing ratios at a forest site in the Western Mediterranean Basin: the effect of local biogenic emissions, Atmos. Chem. Phys., 11, 13161–13179, doi:10.5194/acp-11-13161-2011, 2011.

Sellegri, K., Laj, P., Dupuy, R., Legrand, M., Preunkert, S., and Putaud, J.-P.: Size-dependent scavenging efficiencies of multicomponent atmospheric aerosols in clouds, J. Geophys. Res., 108, 4334, doi:10.1029/2002JD002749, D11, 2003.

Singh, R. P., Dey, S., Tripathi, S. N., Tare, V., and Holben, B. N.: Variability of aerosol parameters over Kanpur city, northern India, J. Geophys. Res., 109, D23206, doi:10.1029/2004JD004966, 2004.

Targino, A. C., Noone, K. J., and Ostrom, E.: Airborne in-situ characterization of dry aerosol optical properties in a multisource influenced marine region, Tellus B, 57, 247–260, doi:10.1111/j.1600-0889.2005.00147.x, 2005.

Vaisala Oyj.: Humidity Conversion Formulas, published by Vaisala, Helsinki, http://www.vaisala.com/Vaisala%20Documents/Application%20notes/Humidity_Conversion_Formulas_B210973EN-F.pdf (last access: 2014), 2013.

Venzac, H., Sellegri, K., Villani, P., Picard, D., and Laj, P.: Seasonal variation of aerosol size distributions in the free troposphere and residual layer at the puy de Dôme station, France, Atmos. Chem. Phys., 9, 1465–1478, doi:10.5194/acp-9-1465-2009, 2009.

4

Summarized results and discussion

This thesis aims to characterize the physical and chemical properties of continental background aerosols in the western Mediterranean. To this end, a station equipped with aerosol monitoring instrumentation was set up at Montsec mountain range (MSC, 1570 m a.s.l.), which allowed for the in-situ measurement of: a) real-time PM_{10}, $PM_{2.5}$, and PM_1 concentrations; b) PM_{10} and PM_1 chemical composition with offline techniques; c) real-time non-refractory submicron aerosol species with an aerosol chemical speciation monitor (ACSM); d) real-time N concentrations; and e) real-time aerosol absorption and scattering coefficients. The results obtained in this continental background environment were compared to those simultaneously measured at the regional background station of MSY, also located in the western Mediterranean, providing an in-depth analysis of the aerosol phenomenology of this particular region, and valuable information for air quality and climate models, and policy makers.

The main results of this study are shown in four specific scientific articles presented in the previous section. The principal findings from the aforementioned articles will be summarized and discussed below in an integrated manner.

4.1. Average concentrations of aerosols and comparison with other high-altitude and regional background European sites

The three-year (2010 - 2012) average concentrations of PM_x measured at MSC (12, 8 and 5 µg m^{-3} of PM_{10}, $PM_{2.5}$ and PM_1, respectively) were relatively low compared with those observed at MSY (18, 13 and 10 µg m^{-3} of PM_{10}, $PM_{2.5}$ and PM_1, respectively). However, they were relatively high with respect to those at other high-altitude European stations such as Jungfraujoch, Rigi, Chaumont, Mt. Cimone, Vorhegg and Schauinsland, where average PM_{10} concentrations ranged from 3 to 9 µg m^{-3}, (Ripoll et al., 2014; ACTRIS database, http://ebas.nilu.no/). The higher concentrations at MSC were attributed to the fact that some of the above stations are located at higher altitudes (Jungfraujoch and Mt. Cimone), so that they are more affected by the free troposphere (FT) conditions, and that they are at higher latitudes, therefore they are much less influenced by African dust outbreaks, which are a major natural source of PM in the Mediterranean basin (Pey et al., 2013b; Querol et al., 2009a; Ripoll et al., 2015b).

The important contribution of African dust to ambient PM in the Mediterranean region was further confirmed with the complete chemical characterization of PM_{1-10} at MSC and MSY, since this PM size fraction was mainly composed of mineral matter at both sites (55% at MSC and 39% at MSY), followed by organic matter (OM: 14 and 15 %), nitrate (9 and 11 %), sulfate (5 and 7 %), sea salt (3 and 5 %), ammonium (1 and 2 %), and elemental carbon (EC: 0.4 and 1 %) (Ripoll et al., 2015b). Comparison of the PM_{10} composition at MSC and MSY with that at Payerne, rural site in the north of the Alps, and Magadino, rural site in south of the Alps, corroborated the higher contribution of mineral matter in the Mediterranean region. PM_{10} mineral major (Al+Ca+Mg) and trace (Ti, Sr, La or Ce) elements at MSC and MSY (0.6 µg m^{-3}) were recorded in concentrations twice as high as those at Payerne (0.3 µg m^{-3}) and Magadino (0.2 µg m^{-3}). The only exception was K, higher at Payerne (0.2 µg m^{-3}) and Magadino (0.3 µg m^{-3}) than at MSC and MSY (0.1 µg m^{-3}), probably due to the higher influence of biomass burning emissions, as suggested by the higher EC and OM concentrations at these stations (Payerne: 0.7 and 5.6 µg m^{-3}, and Magadino: 1.5 and 8.8 µg m^{-3}, of EC and OM, respectively, Gianini et al., 2012) than at MSC and MSY (MSC: 0.12 and 3.2 µg m^{-3}, and MSY: 0.23 and 4.0 µg m^{-3}, of EC and OM, respectively, Ripoll et al., 2015b).

The three-year (2010 - 2012) average concentration of BC measured at MSC (0.19 µg m^{-3}) was clearly lower than the concentration found at MSY (0.41 µg m^{-3}) due to the fact that MSY site is located closer to the anthropogenic sources. Concentrations of BC

were calculated by using the instrument default MAC, however, during the development of this thesis, the specific MAC for MSC was found to be 9.1 m^2 g^{-1} (Ripoll et al., 2014), which explains the difference between BC and EC concentrations. BC concentrations at MSC were also lower than those reported at other high-altitude stations from central Europe such as Schneefernerhaus, Puy de Dôme, Mt. Cimone and Schauinsland (where average BC concentrations ranged from 0.22 to 0.38 µg m^{-3}) (Ripoll et al., 2014). This was ascribed to the higher influence of solid fuel used for power plants and domestic heating in central Europe (Gelencsér et al., 2007). A lower contribution of industrial emissions was also observed at MSC since PM_{10} concentrations of typical industrial trace elements were lower with respect to those measured at lower altitudes such as at MSY, Payerne and Magadino. The only exception was V, higher at MSC (1.1 µg m^{-3}) and MSY (2.0 µg m^{-3}) than at Payerne (0.5 µg m^{-3}) and Magadino (0.6 µg m^{-3}) (Gianini et al., 2012; Ripoll et al., 2015b) probably due to the greater influence of shipping emissions in the Mediterranean region.

Concentrations of PM_{10} secondary inorganic aerosols (nitrate, sulfate and ammonium) at MSC and MSY were also compared with those at Puy de Dôme continental background station (Bourcier et al., 2012), Payerne and Magadino. Nitrate and ammonium concentrations at MSC (0.8 and 0.5 µg m^{-3}, respectively) were slightly higher than those at Puy de Dôme (0.5 and 0.3 µg m^{-3}), whereas the concentrations registered at MSY (1.2 and 0.5 µg m^{-3}) were lower than those measured at Payerne (3.8 and 1.6 µg m^{-3}) and Magadino (2.1 and 1.2 µg m^{-3}). The similar sulfate concentrations at all stations was linked to the long residence time of sulfate aerosols in the atmosphere.

The chemical characterization of PM_1 fraction at MSC and MSY, during the period January 2010 – March 2013, showed very similar relative chemical composition and absolute concentrations, in spite of their altitudinal and longitudinal differences. The foremost PM_1 constituent at both sites was OM (39% at MSC and 34% at MSY) followed by sulfate (17 and 21 %), ammonium (7 and 6 %), mineral matter (5 and 4 %), nitrate (3 %), EC (1.2 and 2%), and sea salt (1 and 2 %) (Ripoll et al., 2015b). These similarities were more pronounced in the warmer months, when recirculation processes at a regional scale are recurrent in the western Mediterranean (Millán et al., 1997), and a strong development of the PBL occurs over continental areas, favoring the transport of surface pollutants towards remote sites such as MSC. These processes cause a homogenization of PM concentrations and composition throughout the region. Despite these aerosol compositional similarities for both PM_1 and PM_{10}, the continental-to-regional background increase, in this particular region of the western Mediterranean,

was estimated to be 1.1 μg m^{-3} for PM_1 and 4.0 μg m^{-3} for PM_{10} on average. The PM_1 increase is attributed to the higher concentrations of sulfate, EC, and OM at the regional background environment, whereas the PM_{10} increase is attributed to higher concentrations of OM, sulfate, nitrate and sea salt. This is due to the fact that regional background site is located closer to the anthropogenic sources and the sea, and that it is within the PBL most of the days owing to its lower altitude (720 m a.s.l.).

Given that the foremost PM_1 constituent at both sites was OM, an in-depth analysis of submicron organic aerosol (OA) was performed at MSC (July 2011 - April 2012; Ripoll et al., 2015a) and MSY (June 2012 - July 2013; Minguillón et al., 2015). The results from this study revealed that the oxygenated organic aerosol (OOA) dominated the OA fraction at both sites (on average at MSC OOA accounted for 81% and at MSY for 73%). This points to the fact that organic components in this region are mostly secondary in their origin, and it is in agreement with what was found at other remote sites (Freney et al., 2011; Raatikainen et al., 2010). In winter biomass burning organic aerosol (BBOA) was identified at both sites and contributed 24% at MSC and 29% at MSY. The low contribution of the hydrocarbon-like organic aerosol (HOA) at both sites (8% at MSC and 13% at MSY on average) is in agreement with their location, since the primary organic emissions are oxidized during their transport from industrial and urban areas to these sites.

Regarding particles number, the average N_3 and N_7 concentrations at MSC (3716 and 2140 # cm^{-3}, respectively) were similar to the average N_{10} concentrations measured at MSY (3475 # cm^{-3}), but higher than N_{10} concentrations reported at Jungfraujoch, Mt. Cimone and Puy de Dôme (634, 1847 and 2070 # cm^{-3}, respectively) (Ripoll et al., 2014). In addition to the differences attributable to the particles between 3 or 7 nm and 10 nm, the higher N concentrations at MSC and MSY were ascribed to the higher frequency of new particle formation (NPF) events as a source of particles. The NPF processes in the western Mediterranean are enhanced by the relevant role of photochemical oxidation (Querol et al., 1999) as a result of higher solar radiation, and by the higher emissions of biogenic particle precursors (up to 3 times higher than Boreal forested areas) (Bessagnet et al., 2008; Lang-Yona et al., 2010; Steinbrecher et al., 2009) as a result of higher temperature (Seco et al., 2011). This is in agreement with the higher N_3 concentrations with respect to those of N_7 at MSC.

Furthermore, aerosol optical measurements were carried out at MSC during a period of two years (June 2011 - June 2013) (Pandolfi et al., 2014b). The results obtained in this study revealed that aerosol light absorption (σ_{ap}) and scattering (σ_{sp}) coefficients at MSC (medians 1.2 and 14.1 Mm^{-1} of σ_{ap} and σ_{sp} respectively) were in the medium/upper range of the high-altitude stations in the northern hemisphere (median

σ_{ap} from 0.08 to 3 Mm^{-1}, and median σ_{sp} from 2 to 40 Mm^{-1}) presented by Andrews et al. (2011). The relatively higher values observed at MSC were attributed to its higher influence of African dust outbreaks.

Thus, aerosol measurements from MSC were found to be comparable in magnitude to those from other remote sites in Europe, after removing African dust outbreaks influence, but also reflected the peculiarities of the western Mediterranean aerosols. This suggests that a *continental background* designation for MSC site is applicable. The differences between MSC and the other high-altitude European sites highlight the lower contribution of combustion processes, the greater impact of shipping emissions, the higher influence of biogenic emissions, and the importance of NPF processes. Moreover, these differences corroborate the important contribution of long-range transport of mineral dust in the western Mediterranean region.

4.2. Seasonal variation of aerosols

The relatively long-term series of aerosol measurements performed at MSC and MSY enabled the investigation of the main factors influencing the seasonal variation of aerosols in the western Mediterranean. All the aerosol parameters showed a clear seasonal variation with the higher values in summer and the lowest in winter, with the exception of nitrate. This seasonal pattern was ascribed to different factors described below.

In the western Mediterranean, southern flows and regional recirculation episodes are more frequent in summer, whereas Atlantic advections and northeastern winds from mainland Europe are more common in winter. Thus, changes in the air mass origin from summer to winter caused a seasonal variation of certain components such as mineral matter.

The higher frequency of African dust outbreaks and the enhanced regional dust resuspension in the warmer months increased mineral matter concentrations affecting both PM_1 and PM_{10} fractions (Pey et al., 2013b; Querol et al., 2009a; Rodríguez et al., 2001). The PM_{1-10} mineral matter concentrations under North African episodes were usually higher at MSC (14 µg m^{-3}) than at MSY (8 µg m^{-3}) owing to the fact that long-range Saharan dust transport occurs preferentially at high altitude layers. The net contribution of African dust to the PM_{10} concentrations was estimated in 16% at MSC and 11% at MSY (Ripoll et al., 2015b). In addition, during these episodes measurements of aerosol optical properties at MSC showed the highest values of σ_{sp} (90 Mm^{-1}), whereas the scattering Ångström exponent (SAE) was the lowest (0.8), indicating the presence of larger particles (Pandolfi et al., 2014b).

During North African episodes concentrations of nitrate and sulfate also increased, demonstrating that dust can be transported together with anthropogenic pollutants such as emissions from oil refineries in North Africa (Perrino et al., 2010; Rodríguez et al., 2011), and that regional anthropogenic pollutants can react with and/or be adsorbed onto dust (Alastuey et al., 2005). This anthropogenic and natural mix was also confirmed by the higher concentrations of BC during African dust outbreaks. Nevertheless, in some cases high absorption values were measured simultaneously with very low EC concentrations (Ripoll et al., 2014). In these cases mineral dust concentrations were very high (pure Saharan dust episode), which means that some mineral matter constituents (such as Fe) may interfere in the absorption measurements and lead to an increase in the absorption values (BC artifact), as observed elsewhere (Vrekoussis et al., 2005). Moreover, during North African episodes a compression of

the PBL is observed at regional scale (Alastuey et al., 2005; Pandolfi et al., 2013), and a dominance of southern winds during the whole day breaks the regular sea breeze circulation (Jorba et al., 2013). These processes enhance the concentration of regional pollutants in the lowest part of the troposphere and inhibit the sea breeze "clean-up" effect. This is reflected in the concentrations of PM_1 sulfate, EC, and industrial and traffic trace elements measured simultaneously at MSC and MSY, since these were in higher concentrations at the regional background environment than at the continental background site (Ripoll et al., 2015b).

Regional recirculation of air masses during summer also accounts for the accumulation of airborne particulates, leading to an increase in concentrations of sulfate, OM, EC, industrial, traffic, and fuel oil combustion tracers at both continental and regional background environments (Ripoll et al., 2015b). Moreover, measurements of aerosol optical properties at MSC during summer regional recirculation scenarios showed higher and nearly constant values of SAE (around 1.8 for $0 < \sigma_{sp} < 90$ Mm^{-1}), indicating the prevalence of smaller particles with a relatively lower g (0.53 during summer regional compared with 0.57 during North African episodes) (Pandolfi et al., 2014b).

In the warmer months the more intense sea breeze circulation favors the transport of shipping emissions from the Mediterranean to the continental areas and thereby increased the concentrations of sulfate, EC, and fuel-oil-combustion-related trace elements at MSC and MSY (Ripoll et al., 2015b). Furthermore, wildfires across the Mediterranean region are more frequent in summer (Cristofanelli et al., 2009), and therefore contributed to an extra increment of the OM and EC concentrations at both continental and regional background sites.

Additionally, the higher temperature and solar radiation in the warmer months augment atmospheric photochemistry and increase biogenic emissions in the western Mediterranean region (Seco et al., 2011), promoting the formation of secondary inorganic and organic aerosols, and thus incrementing markedly the concentration of certain components such as sulfate (Querol et al., 1999) and OM. Conversely, nitrate is not abundant in summer due to the high volatility of ammonium nitrate at relative high temperatures and low humidity (Zhuang et al., 1999b). The increase of NPF processes during the warmer months is also reflected in the concentrations of N, which were higher in summer at MSC (N_3: 5704 # cm^{-3} and N_7: 2739 # cm^{-3}) and MSY (N_{10}: 5014 # cm^{-3}) than in winter (MSC N_3: 2146 # cm^{-3} and N_7: 1500 # cm^{-3}, and MSY N_{10}: 2568 # cm^{-3}) (Ripoll et al., 2014).

As mentioned earlier, the source apportionment of the OA at MSC (Ripoll et al., 2015a) and MSY (Minguillón et al., 2015) further confirmed the importance of SOA

formation processes as an OA source during summer in the western Mediterranean (Figures 4.1 and 4.3). This study allowed for the identification of three types of submicron OA at both sites in summer and three types in winter. The OA in summer was made of HOA, semivolatile oxygenated organic aerosol (SV-OOA) and low-volatility oxygenated organic aerosol (LV-OOA). In winter the three types of OA identified were HOA, BBOA and one single OOA. At MSC the LV-OOA dominated the OA fraction in summer, contributing 64%, followed by the SV-OOA (26%) and the HOA (10%), whereas in winter the OOA accounted for 71%, the BBOA contributed 24%, and the HOA contribution decreased to 5% of the total OA. At MSY the major OA constituent in summer was also the LV-OOA, with 45% on average, followed by the SV-OOA (42%) and the HOA (13%), whereas in winter the OOA accounted for 59%, the BBOA for 29% and the HOA for 12% of the total OA.

In the colder months, the higher occurrence and intensity of Atlantic advections prevents the accumulation of regional pollution and consequently very low values of all aerosol parameters were recorded at MSC and MSY sites. Moreover, the lower vertical development of the PBL and the higher frequency of thermal inversions during winter leaved MSC (1570 m a.s.l.) in the FT on most days, whereas MSY was frequently located within the PBL due to its lower elevation (720 m a.s.l.). Nevertheless, the sporadic transport of polluted air masses from Europe towards the western Mediterranean increased the concentrations of nitrate, OM, EC, and industrial and traffic-related trace elements at continental and regional background sites. The impact of these polluted air masses on the concentrations of PM_x components was usually more evident at MSC than at MSY, since this transport from Europe occurs preferentially at high altitude layers (Sicard et al., 2011). Occasionally, intense peaks of nitrate, OM, and EC were measured at the regional background site during the winter anticyclonic episodes. These stagnant conditions cause the accumulation of pollutants around the emission sources (such as the Barcelona metropolitan area), which can be transported towards relatively nearby areas under favorable conditions (Pey et al., 2010a). The distance from MSC to large anthropogenic sources and its altitude are restricting factors for the occurrence of this process.

The chemical composition and particle size determine the aerosol optical properties, for this reason seasonal variations of these parameters also caused a significant variation of the extensive aerosol optical properties and the MAC and the mass scattering cross section (MSCS), with the highest values in summer (σ_{ap}: 2.4 Mm^{-1}, σ_{sp}: 34.6 Mm^{-1}, MAC: 11.8 $m^2\ g^{-1}$ and MSCS: 4.0 $m^2\ g^{-1}$) and the lowest in winter (σ_{ap}: 0.3 Mm^{-1}, σ_{sp}: 3.7 Mm^{-1}, MAC: 9.3 $m^2\ g^{-1}$ and MSCS: 1.9 $m^2\ g^{-1}$). These properties showed lower medians when MSC was in the FT compared with the whole dataset.

This difference was higher and statistically significant in winter and lower (and not statistically significant) in spring/summer.

4.3. Intra-day variation of aerosols

The relatively long-term series of real-time aerosol measurements conducted at MSC and MSY has allowed for the investigation of the principal factors influencing the intra-day variation of aerosols in the western Mediterranean. At the continental background site, most of the aerosol parameters showed a poorly defined daily pattern in summer and a clearer in winter, except for N and OA concentrations, which showed marked diurnal cycles throughout the year and regardless of the air mass origin. Conversely, at the regional background site marked daily patterns were observed for all aerosol parameters throughout the year. The differences between diurnal cycles of aerosol parameters at continental and regional background sites were attributed to different influence of atmospheric processes. Whereas intra-day variations at MSC were more affected by long-range transport and mesoscale meteorology, daily patterns at MSY depended more on local and regional processes (Ripoll et al., 2014, 2015a).

In the western Mediterranean during the warmer months, the more intense sea breeze circulation and the abrupt orography induces the recirculation of air masses over the region. Such recirculation causes the formation of reservoir layers at relatively high altitude (Millán et al., 1997), which can be persistent at night. Furthermore, Mediterranean region is highly affected by long-range transport from North Africa especially during the warmer months (24% of the days vs. 5% in the colder months). This transport can be more intense at high altitude layers (Ripoll et al., 2015b) and does not depend on the time of the day. All these factors cause an increase of nocturnal aerosol concentrations at relatively high altitude sites such as MSC, and mask the mountain breezes and the local transport. For these reasons a lack of well-defined daily patterns of PM_x, BC, σ_{sp} and submicron major inorganic components (sulfate, nitrate, ammonium and chloride) was observed, and a high variability of diurnal cycles even within the same type of episode was reported at MSC in summer (Pandolfi et al., 2014b; Ripoll et al., 2014, 2015a) (Figure 4.1). Similar intra-day variations of submicron major inorganic components have been observed at the Puy-de-Dôme station in central France (Freney et al., 2011). The fact that MSY is closer to the sea, therefore more affected by sea breeze, and that it is located at lower altitude, are restricting factors for the occurrence of these processes. At MSY all aerosol parameter showed marked daily patterns with a maximum at midday and a minimum at night (Cusack et al., 2013b; Pérez et al., 2008) (Figure 4.1).

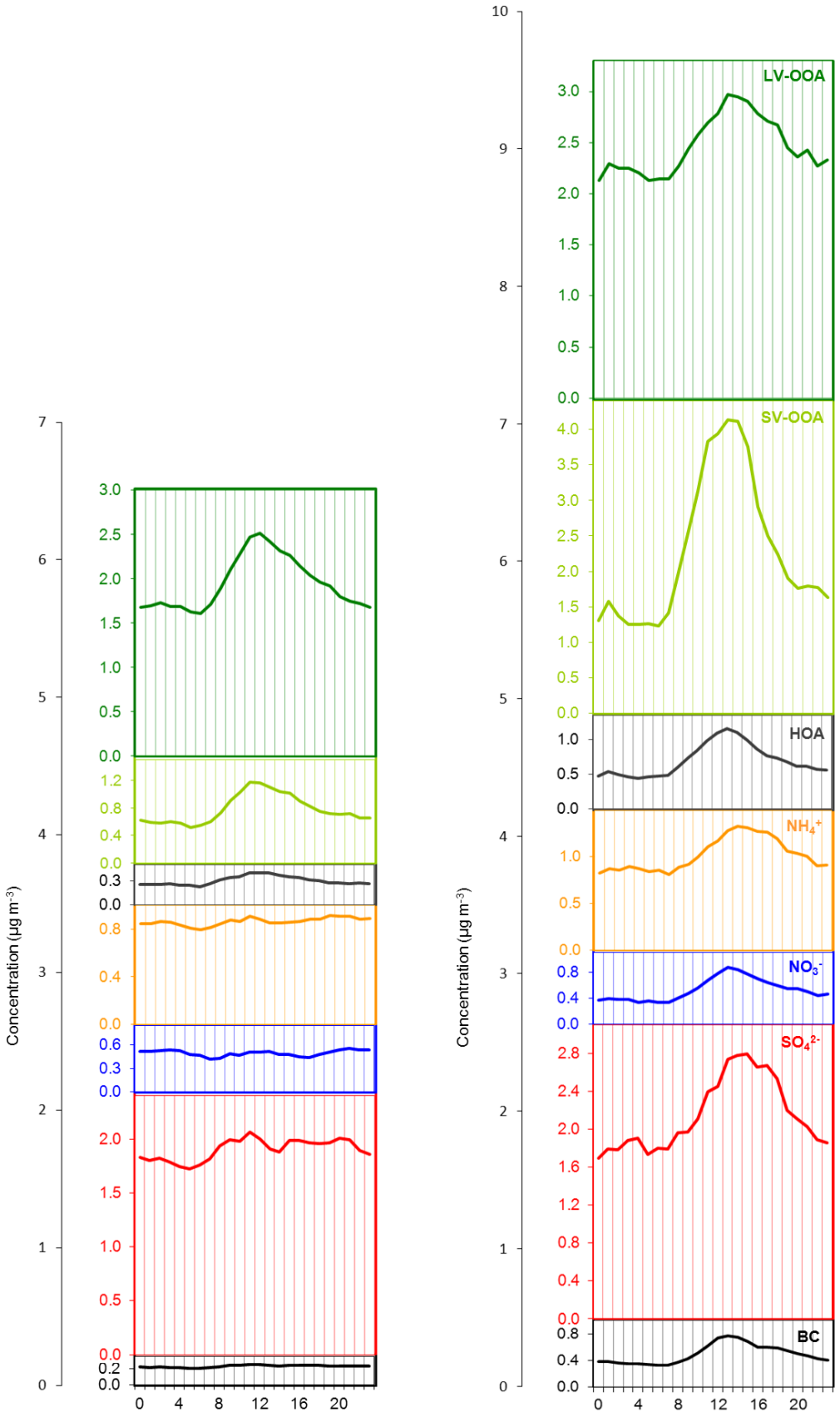

Figure 4.1 First Y axis: average concentrations of submicron aerosols during summer at Montsec (14 Jul - 24 Sep 2011) and Montseny (14 June - 9 Oct 2012). Second Y axis: average daily cycles.

In summer, the higher temperature and solar radiation at midday increases atmospheric photochemistry and biogenic emissions in the western Mediterranean region (Seco et al., 2011), incrementing the frequency of NPF events at midday. This is reflected in the concentrations of N, which showed a clear diurnal cycle, with the highest concentrations between 12:00 and 16:00 UTC and the lowest at night and in the early morning, peaking almost at the same time than temperature and solar radiation. Similar intra-day variation of N has been observed at Puy-de-Dôme site (Venzac et al., 2009). Moreover, the daily amplitude of N concentrations was higher in the warmer months than in the colder months. This difference was more evident for N_3 than for N_7 concentrations. At night (20:00 – 07:00 UTC), average N_3 concentrations were more than 2100 # cm^{-3} in the warmer months and about 1300 # cm^{-3} in the colder months, whereas during the day (08:00 –19:00 UTC) these concentrations rose to 7000 # cm^{-3} in the warmer months and only to 2300 # cm^{-3} in the colder months (Ripoll et al., 2014). The statement of the increase in N concentrations at midday attributed to NPF processes was further demonstrated by the particle number size distribution measurements carried out during two intensive campaigns at MSC in July - August 2011 and January - March 2012. These data showed high frequency of events with the typical banana-like profile characterized by the nucleation episodes followed by growing processes of these newly-formed particles to larger sizes (Figure 4.2). A detailed study of these data is ongoing.

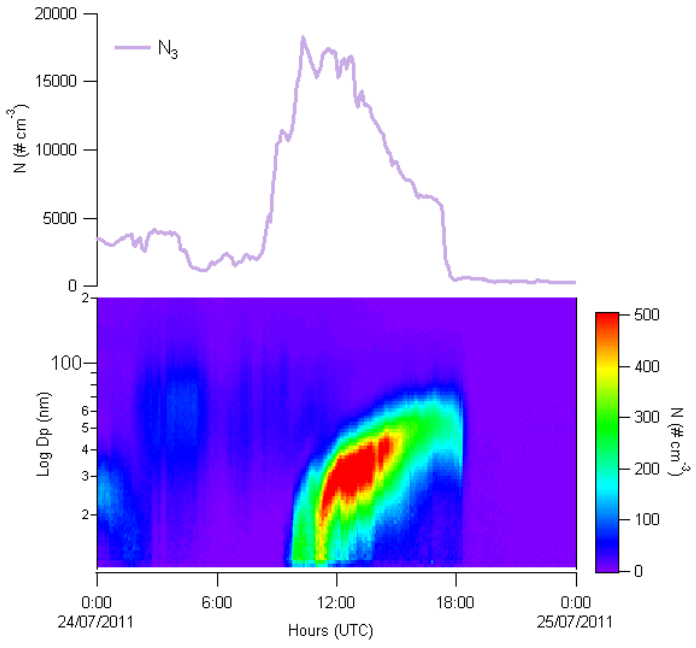

Figure 4.2 An example of a typical formation and subsequent growth event of atmospheric aerosols measured during an intensive campaign (July - August 2011) at MSC. Top: concentrations of N_3. Bottom: concentrations of particle number size distribution.

The diurnal cycles of the different OA types at MSC (Ripoll et al., 2015a) further confirmed the importance of SOA formation processes around midday during summer, since maximum concentrations of SV-OOA were observed between 11:00 and 12:00 UTC, whereas those of LV-OOA and HOA were measured between 12:00 and 13:00 UTC (Figure 4.1). The midday increase of the SV-OOA is attributed to the recently produced biogenic SOA due to photooxidation of local/regional biogenic emissions (BVOCs), given that MSC is a remote site isolated from local anthropogenic emissions, whereas the origin of LV-OOA is more associated with the regional transported SOA. Comparison of these results with those at MSY revealed that the midday increase of the SV-OOA is higher at the regional background site (Figure 4.1). This confirmed that MSY is more influenced by anthropogenic precursors and/or emissions of biogenic precursors, which enhance the formation of SOA around midday.

In the colder months MSC is located most of the day within the FT, whereas PBL air mass is usually only advected to the site during the central hours of the day. Moreover, thermal inversions are very frequent from 20:00 to 07:00 UTC. These situations prevent the transport of pollutants from the most populated areas towards high altitudes, especially at night. In the morning, mountain breezes develop, with an intensity sufficient to transport the pollutants from the adjacent valleys and plains to the top of the mountain arriving later in the afternoon. All these factors accounted for clearer daily patterns of all aerosol parameters, with an increase around 14:00 UTC, in winter at MSC (Pandolfi et al., 2014b; Ripoll et al., 2014, 2015a) (Figure 4.3). Similar intra-day variations have been observed at Jungfraujoch (Baltensperger et al., 1997), Mt. Cimone (Marinoni et al., 2008), Himalayas (Marinoni et al., 2010), and Puy-de-Dôme (Freney et al., 2011).

Thus, in the western Mediterranean continental background environment intra-day variations of PM_x, BC, σ_{sp} and PM_1 major inorganic components (sulfate, nitrate, ammonium and chloride) are not equally influenced by the emission sources and atmospheric processes influencing N and submicron OA variations during the warmer months. Conversely, during the colder months all aerosol parameters were mainly governed by mountain breezes.

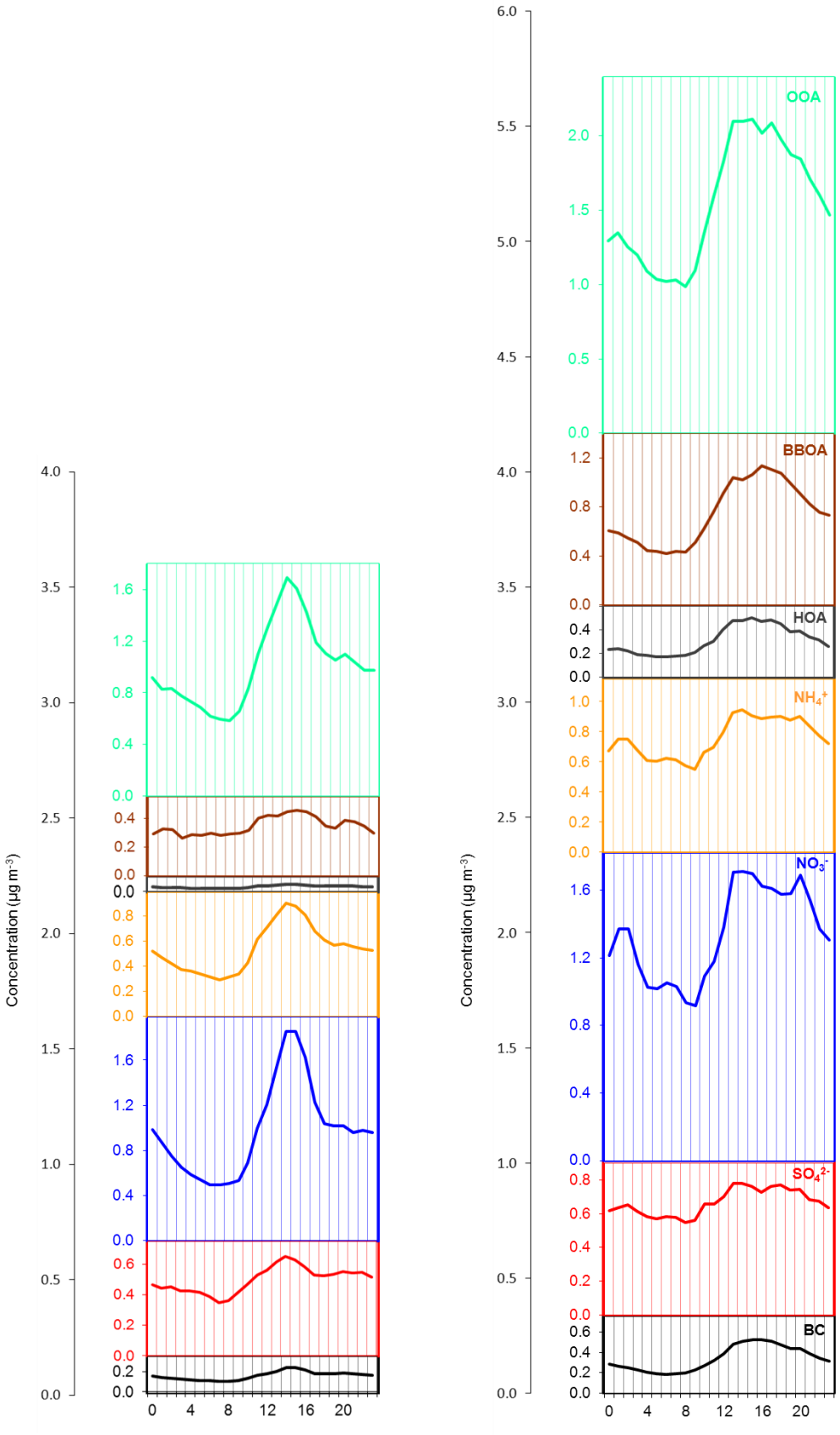

Figure 4.3 First Y axis: average concentrations of submicron aerosols during winter at Montsec (10 Jan - 7 Mar 2012) and Montseny (28 Oct 2012 - 7 Apr 2013). Second Y axis: average daily cycles.

5

Conclusions

The installation of a permanent station equipped with aerosol monitoring instrumentation at Montsec (MSC) observatory has allowed for the investigation of the continental background aerosols in the western Mediterranean. For the first time, the sampling and chemical characterization of PM_1 was performed using offline and online techniques at a remote site in the western Mediterranean. Furthermore, the inclusion of measurements of particle number, aerosol absorption coefficients, as well as aerosol scattering and backscattering coefficients, allowed for a greater understanding of aerosol phenomenology occurring in this region. The main conclusions that can be drawn from the work presented in this thesis are as follows:

- Aerosol measurements (particle mass (PM), particle number (N), scattering and absorption) from MSC were found to be comparable in magnitude to other remote sites in Europe, when removing African dust outbreaks influence. This suggests that a continental background designation for the MSC site is applicable. The closer compositional similarities between regional and continental background aerosols in the western Mediterranean, especially for the fine fraction (PM_1) and during the warmer months, reflects a large homogenization of concentrations and composition throughout the region. Moreover, weekly variation of PM_1 and black carbon (BC) concentrations showed that the reduced human activity at the weekend is reflected in their concentrations with a delay of one day (minimum on Sunday and Monday), which also confirms that MSC is located at a sufficient distance from anthropogenic emissions.

- Continental background aerosols in the western Mediterranean are affected by natural and anthropogenic emissions which results in a PM_1 mainly made up of organic matter (OM), sulfate, ammonium, mineral matter (MM) and nitrate. The foremost PM_{1-10} constituent is MM, followed by OM, nitrate, sulfate and sea salt (SS). Anthropogenic aerosols are principally associated with the fine fraction (PM_1), whereas natural aerosols are more connected to the PM_{1-10} fraction, with some exceptions such as biogenic SOA.

- Three main groups of trace elements in PM_{10} with common origin and variation were identified at MSC continental background site. Ordered by their contribution to the total mass of trace elements these groups were: mineral, industrial and road traffic, and fuel oil combustion related elements. Mineral group was constituted by typical crustal elements (Ti, Mn, Li, and Sr), as well as elements found in clay mineral assemblages (V, Cr, Co, Ni, and As). Industrial and road traffic trace elements (Cu, Zn, As, Cd, Pb, Sb, and Sn) were grouped together due to their mixing during the transportation from industrial and urban areas to MSC, and the fuel oil combustion group was traced by V and Ni.

- The continental to regional background increase in the western Mediterranean is estimated in 1.1 μg m^{-3} for PM_1 and 4.0 μg m^{-3} for PM_{10}. The PM_1 increase is attributed to the higher concentrations of sulfate, elemental carbon (EC), OM, and some anthropogenic trace elements (V, Ni, Cu, Zn, and Pb) at the regional background site, whereas the PM_{10} increase is attributed to higher concentrations of OM, sulfate, nitrate and SS. This is due to the fact that regional background site is located closer to the anthropogenic sources and the sea, and that it is within the planetary boundary layer (PBL) most of the days.

- The MAC is the parameter used to convert absorption to concentration of absorbing particles (i.e. BC). MAAP's software uses a constant MAC of 6.6 m^2 g^{-1}, however it has been found that MAC can change as a function of aerosol composition, and therefore it can differ depending on the region under study and the meteorological scenarios. At MSC, comparison of absorption measurements with those of EC determined by thermal-optical methods revealed an average MAC of 9.1 m^2 g^{-1}.

- For the first time in Europe, real-time measurements of submicron inorganic (sulfate, nitrate, ammonium, and chloride) and organic aerosols (OA) were performed, during almost a year, in a continental background environment, using an aerosol chemical

speciation monitor (ACSM). Long-term series of PM_1 composition (187 samples) was compared with daily averaged ACSM species and all species showed strong correlations (R^2 between 0.77 and 0.96). However, different slopes (ACSM vs. offline measurements) were found for each of the species ranging from 1.12 to 1.35 for sulfate, ammonium and nitrate. The OA concentrations vs. OC concentrations determined offline resulted in a slope of 3.39, pointing to an overestimation by the ACSM probably caused by the use of the default relative ionization efficiency (RIE) for OA, which could be lower than the actual one.

- As previous studies have shown, the Mediterranean region is highly affected by long-range transport of mineral dust. The present study corroborates this important contribution of dust to the ambient concentrations of PM_x in the western Mediterranean, even at high-altitude sites. Concentrations of PM_{10} and MM in the PM_{10} fraction measured at MSC were higher than those reported at other high-altitude sites in Europe. Furthermore, simultaneous measurements at regional and continental background environments demonstrated that long-range transport of African dust occurs preferentially at high altitude layers resulting in higher PM_{1-10} MM concentrations at MSC (14 µg m^{-3}) than at MSY (8 µg m^{-3}). The net contribution of African dust to the PM_{10} concentrations is estimated in 16% at MSC and 11% at MSY. Moreover, under North African episodes the highest scattering values were recorded at MSC, whereas the scattering Ångström exponent (SAE) was the lowest, indicating the presence of larger particles. It has been also found that MM constituents interfere with absorption measurements in some cases, leading to increased BC concentrations when EC concentrations are low. In some other cases, both BC and EC concentrations increase at the same time as MM concentrations, which demonstrated that dust can be transported together with other pollutants.

- During North African episodes a compression of the PBL is observed at regional scale, and a dominance of southern winds during the whole day breaks the regular sea breeze circulation. These processes enhance the concentration of regional pollutants in the lowest part of the troposphere and inhibit the sea breeze “clean-up” effect. This is reflected in the concentrations of PM_1 sulfate, EC, and industrial and traffic trace elements measured simultaneously at MSC and MSY, since they were higher at the regional background environment than at the continental background site.

- The impact of polluted air masses from central and eastern Europe has been identified for the first time on the continental background aerosols in the western

Mediterranean. Concentrations of PM_1, BC, nitrate, OM, EC, and industrial and traffic-related trace elements underwent an increase when these polluted air masses were transported towards the western Mediterranean region. This increase is usually higher at the continental background site than at the regional background station, which demonstrates that the transport from Europe occurs preferentially at high altitude layers.

- Seasonal variation of the majority of the aerosol measurements in the western Mediterranean continental background showed high values in summer and low in winter, with the exception of nitrate. The higher nitrate concentrations in winter than in summer are attributed to the high volatility of ammonium nitrate at low humidity and high temperature. The summer maximum of the rest of aerosol measurements is caused by a variety of factors: 1) the increase in the PBL height, which favors the transport of anthropogenic pollutants towards high-altitude sites; 2) the higher intensity of convection processes that increase the regional dust resuspension; 3) the regional recirculation of air masses over the western Mediterranean inducing the accumulation of pollutants across the region; 4) the higher intensity of solar radiation, which enhances atmospheric photochemistry, promoting the formation of secondary inorganic and organic aerosols; 5) the higher temperature that increases biogenic emissions; 6) the lower precipitation that prevents atmospheric wet-scavenging processes, and 7) the higher frequency of African dust episodes. In winter very different conditions drive the aerosol phenomenology at MSC. The combination of (1) the higher frequency of thermal inversions and (2) the lower vertical development of the PBL, which leave MSC in the free troposphere most of the day, together with (3) the higher occurrence and intensity of Atlantic advections, accounts for the markedly reduced aerosol concentrations in winter.

- At MSC the intra-day variation of PM_x, BC, scattering and PM_1 major inorganic components (sulfate, nitrate, ammonium and chloride) is not equally influenced by the emission sources and atmospheric processes influencing N and submicron OA variation. Thus, in the western Mediterranean continental background environment these aerosol parameters are governed by different factors. Whereas daily patterns of PM_x, BC, scattering, and PM_1 major inorganic components are driven by mountain breezes, PBL evolution, and air mass origin, diurnal cycles of N and submicron OA concentrations are less affected by the air mass origin and depend more on meteorological variables such as temperature and solar radiation. The midday increase of N concentrations was partially attributed to nucleation processes and highlighted the

importance of NPF as a source of particles. The combination of all these atmospheric processes at local, regional and continental scales results in a high variability of these aerosol parameters, with poorly defined daily patterns in summer, except for N and submicron OA concentrations, with a peak at midday.

- The characterization of OA components at MSC using source apportionment analysis (ME-2) of the organic fraction from the ACSM mass spectra was performed separately for the summer and winter period, and a solution of three factors was selected for each season. In summer, a hydrocarbon-like OA (HOA), a semivolatile oxygenated OA (SV-OOA), and a low-volatility oxygenated OA (LV-OOA) were resolved, and in winter the three factors were: HOA, biomass burning OA (BBOA), and one single oxygenated OA (OOA). The OOA in winter showed higher degree of oxidation than any of the OOA in summer, since it had a dominant peak at *m/z* 44 with higher value than that from the SV-OOA and the LV-OOA. The major OA constituent in summer was the LV-OOA, with 64% on average, followed by the SV-OOA (26%) and the HOA (10%), whereas in winter the OOA accounted for 71%, the BBOA contributed 24%, and the HOA contribution decreased to 5%. A clear daily pattern of OA components was found throughout the year regardless of the air mass origin, except for Atlantic advections in winter. Nevertheless, in summer the maximum concentration of SV-OOA were measured between 11:00 and 12:00 UTC, whereas those of LV-OOA and HOA were measured between 12:00 and 13:00 UTC. Conversely, in winter the maximum concentrations of HOA, BBOA, and OOA were observed simultaneously around 14:00 UTC. The different daily patterns between seasons can be attributed to the higher production of SOA in summer as opposed to winter, when the maximum daily concentrations are reached later driven by the mountain breezes. (HOA), (SV-OOA) and (LV-OOA).

Future prospects

The results obtained from the present study have shown the main physical, chemical and optical properties of continental background aerosols in the western Mediterranean, and have led to further open questions and gaps in knowledge that future research will hopefully shed light on. Some of these gaps are briefly described below:

- As shown in this thesis, PBL height appears to be an important factor affecting aerosol variations at MSC site, but calculations of PBL heights at mountain sites using models have significant limitations and results are frequently biased. A ceilometer was installed at the valley of Àger (800 m a.s.l.) in March 2014. This device uses a laser to determine the height of cloud base; however, PBL height can be also deduced. The data from this instrument is being analyzed and will provide essential information to ascertain the causes of aerosol variations suggested in the present study.

- Results of particle number size distribution from two intensive campaigns carried out at MSC in Jul-Aug 2011 and Jan-Mar 2012 are not included in the present work, but a detailed study of these data is ongoing and demonstrated the importance of NPF processes as a particle source. Therefore, it would have a strong scientific interest if continuous measurements of particle number size distribution were implemented at the

MSC station. These measurements allow for the identification of sub-micron particle processes and sources.

- As indicated by the present work, the intra-day variations of organic aerosol and N concentrations have similar patterns with a maximum at midday, which could reflect its similar origin. An in-depth study of organic compound transformations would be crucial to understand the role of these compounds on the NPF processes in continental background environments. To this end, measurements of the VOCs were performed at MSC in July 2011 using a proton transfer reaction-mass spectrometer (PTR-MS), but unfortunately only 15 days are available. The processing and interpretation of these data is under preparation. However, it would be very advisable if measurements of VOCs were performed for longer period, and together with measurements of particle number size distribution and chemical composition of particles with an aerodynamic diameter (Dp) lower than 100 nm, and interpreted with O_3 and NO_x concentrations.

- The intra-day variation of PM_x, BC, scattering and PM_1 major inorganic components (sulfate, nitrate, ammonium and chloride) did not show a clear pattern during the warm periods. It was attributed to a combination of atmospheric processes, which do not depend on the time of the day. More information about this will verify the reasons suggested in the present work. To this end, vertical profiles of aerosol concentrations are necessary, although aircraft campaings and sampling PM_x and analyzing its chemical composition separately for day time and night time could also help.

- The long-term series of PM_x and PM chemical composition at this site would provide valuable information for the analysis of trends and the causes of changes. The long-term series of PM chemical composition are scarce in this region, especially for PM_1 which is more influenced by anthropogenic emissions. Thus, it is essential to continue the PM sampling and chemical analyses.

- The continuation of measuring PM chemical composition together with aerosol optical properties would present the unique opportunity to investigate the optical properties of specific chemical components. These studies are important for determining the radiative forcing potential of

specific components of PM, such as BC, sulfate, nitrate and/or organic matter, and would thus provide valuable information for long-term climate studies in the region.

Scientific contributions

Articles in peer-reviewed journals

Publications included in this thesis

The scientific articles included in this thesis are:

Ripoll, A., Minguillón, M. C., Pey, J., Jimenez, J. L., Day, D. A., Sosedova, Y., Canonaco, F., Prévôt, A. S. H., Querol, X., and Alastuey, A.: Long-term real-time chemical characterization of submicron aerosols at Montsec (southern Pyrenees, 1570 m a.s.l.), Atmos. Chem. Phys., 15, 2935-2951, doi:10.5194/acp-15-2935-2015, 2015a.

Ripoll, A., Minguillón, M. C., Pey, J., Pérez, N., Querol, X., and Alastuey, A.: Joint analysis of continental and regional background environments in the western Mediterranean: PM1 and PM10 concentrations and composition, Atmos. Chem. Phys., 15, 1129-1145, doi:10.5194/acp-15-1129-2015, 2015b.

Ripoll, A., Pey, J., Minguillón, M. C., Pérez, N., Pandolfi, M., Querol, X., and Alastuey, A.: Three years of aerosol mass, black carbon and particle number concentrations at Montsec (southern Pyrenees, 1570 m a.s.l.), Atmos. Chem. Phys., 14, 4279-4295, doi:10.5194/acp-14-4279-2014, 2014.

Pandolfi, M., **Ripoll, A.**, Querol, X., and Alastuey, A.: Climatology of aerosol optical properties and black carbon mass absorption cross section at a remote high-altitude site in the western Mediterranean Basin, Atmos. Chem. Phys., 14, 6443-6460, doi:10.5194/acp-14-6443-2014, 2014.

Publications derived from this thesis

The results obtained during this thesis have been published in the following articles:

Minguillón M.C., **Ripoll A.**, Pérez N., Prévôt A.S.H., Canonaco F., Querol X., Alastuey A.: Chemical characterization of submicron regional background aerosols in the Western Mediterranean using an Aerosol Chemical Speciation Monitor. Atmos. Chem. Phys. Discuss., 15, 965-1000, doi:10.5194/acpd-15-965-2015, 2015.

Querol, X., Alastuey, A., Viana, M., Moreno, T., Reche, C., Minguillón, M. C., **Ripoll, A.**, Pandolfi, M., Amato, F., Karanasiou, A., Pérez, N., Pey, J., Cusack, M., Vázquez, R., Plana, F., Dall'Osto, M., de la Rosa, J., Sánchez de la Campa, A., Fernández-Camacho, R., Rodríguez, S., Pio, C., Alados-Arboledas, L., Titos, G., Artíñano, B., Salvador, P., García Dos Santos, S., and Fernández Patier, R.: Variability of carbonaceous aerosols in remote, rural, urban and industrial environments in Spain: implications for air quality policy, Atmos. Chem. Phys., 13, 6185-6206, doi:10.5194/acp-13-6185-2013, 2013.

Other related publications

The publications derived from the participation in other studies are:

Crenn, V., Sciare, J., Croteau, P. L., Verlhac, S., Fröhlich, R., Belis, C. A., Aas, W., Äijälä, M., Alastuey, A., Artiñano, B., Baisnée, D., Bonnaire, N., Bressi, M., Canagaratna, M., Canonaco, F., Carbone, C., Cavalli, F., Coz, E., Cubison, M. J., Gietl, J. K., Green, D. C., Gros, V., Heikkinen, L., Lunder, C., Minguillón, M. C., Močnik, G., O'Dowd, C. D., Ovadnevaite, J., Petit, J.-E., Petralia, E., Poulain, L., Priestman, M., Riffault, V., **Ripoll, A.**, Sarda-Estève, R., Slowik, J., Setyan, A., Baltensperger, U., Prévôt, A. S. H., Jayne, J. T. and Favez, O.: ACTRIS ACSM intercomparison: Part 1 – Intercomparison of concentration and fragment results from 13 individual co-located aerosol chemical speciation monitors (ACSM), Atmos. Meas. Tech. Discuss., submitted, 2015.

Fröhlich, R., Crenn, V., Setyan, A., Belis, C. A., Canonaco, F., Favez, O., Riffault, V., Slowik, J. G., Aas, W., Aijälä, M., Alastuey, A., Artiñano, B., Bonnaire, N., Bozzetti, C., Bressi, M., Carbone, C., Coz, E., Croteau, P. L., Cubison, M. J., Esser-Gietl, J. K., Green, D. C., Gros, V., Heikkinen, L., Herrmann, H., Jayne, J. T., Lunder, C. R., Minguillón, M. C., Močnik, G., O'Dowd, C. D., Ovadnevaite, J., Petralia, E., Poulain, L., Priestman, M., **Ripoll, A.**, Sarda-Estève, R., Wiedensohler, A., Baltensperger, U., Sciare, J., and Prévôt, A. S. H.: ACTRIS ACSM intercomparison – Part 2: Intercomparison of ME-2 organic source apportionment results from 15 individual, co-located aerosol mass spectrometers, Atmos. Meas. Tech. Discuss., 8, 1559-1613, doi:10.5194/amtd-8-1559-2015, 2015.

Dall'Osto, M., Querol, X., Alastuey, A., Minguillon, M. C., Alier, M., Amato, F., Brines, M., Cusack, M., Grimalt, J. O., Karanasiou, A., Moreno, T., Pandolfi, M., Pey, J., Reche, C., **Ripoll, A.**, Tauler, R., Van Drooge, B. L., Viana, M., Harrison, R. M., Gietl, J., Beddows, D., Bloss, W., O'Dowd, C., Ceburnis, D., Martucci, G., Ng, N. L., Worsnop, D., Wenger, J., Mc Gillicuddy, E., Sodeau, J., Healy, R., Lucarelli, F., Nava, S., Jimenez, J. L., Gomez Moreno, F., Artinano, B., Prévôt, A. S. H., Pfaffenberger, L., Frey, S., Wilsenack, F., Casabona, D., Jiménez-Guerrero, P., Gross, D., and Cots, N.: Presenting SAPUSS: Solving Aerosol Problem by Using Synergistic Strategies in Barcelona, Spain, Atmos. Chem. Phys., 13, 8991-9019, doi:10.5194/acp-13-8991-2013, 2013.

Pey, J., Van Drooge, B. L., **Ripoll, A.**, Moreno, T., Grimalt, J. O., Querol, X., Alastuey, A.: An evaluation of mass, number concentration, chemical composition and types of particles in a cafeteria before and after the passage of an antismoking law. Particuology, 11(5), 527-532. doi:10.1016/j.partic.2013.02.007, 2013.

De Nazelle A., Fruin S., Westerdahl D., Martinez D., **Ripoll A.**, Kubesch N., Nieuwenhuijsen M.: A travel mode comparison of commuters' exposures to air pollutants in Barcelona, Atmos. Environ., 59, 151-159, doi:10.1016/j.atmosenv.2012.05.013, 2012.

Reche, C., Viana, M., Pandolfi, M., Alastuey, A., Moreno, T., Amato, F., **Ripoll, A.**, Querol, X.: Urban NH3 levels and sources in a Mediterranean environment, Atmos. Environ., 57, 153-164, doi:10.1016/j.atmosenv.2012.04.021, 2012.

Contributions to conferences and workshops

Some of the results obtained from this work have been also presented in different international and national conferences:

Ripoll, A., Minguillón, M. C., Pey, J., Pérez, N., Querol, X., Alastuey, A: Joint analysis of continental and regional background environments in the Western Mediterranean: PM1 and PM10 concentrations and composition. Poster, 4th ACTRIS General Assembly, Clermont-Ferrand, France, 10-13 June 2014.

Ripoll A., Minguillón M.C., Pey J., Querol X., Alastuey A.: Chemical composition of PM_{10} and PM_1 at a remote mountain site in NE of Spain. Poster, European Aerosol Conference, EAC 2013, Prague, Czech Republic, 1- 6 September 2013.

Ripoll A., Minguillón M.C., Pey J., Querol X., Alastuey A.: Chemical composition of PM_{10} and PM_1 at a remote mountain site in NE of Spain. Poster, 1st Iberian Meeting on Aerosol Science and Technology, RICTA 2013, Évora, Portugal, 1- 3 July 2013.

Ripoll A., Minguillón M.C., Pey J., Pandolfi M., Alastuey A., Querol X., Jimenez J.L., Day D.: Characterization of tropospheric aerosols in a remote mountain site in NE of Spain with an Aerosol Chemical Speciation Monitor. Poster, American Association for Aerosol Research (AAAR) Annual Conference 2012, Minneapolis, Minnesota, USA, 8- 12 October 2012.

Ripoll A., Pey J., Minguillón M.C., Alastuey A., Querol X.: Two years of measurements of atmospheric aerosols at a remote mountain site in NE Spain. Poster, American Association for Aerosol Research (AAAR) Annual Conference 2012, Minneapolis, Minnesota, USA, 8- 12 October 2012.

Ripoll A., Minguillón M.C., Pey J., Querol X., Alastuey A.: Two years of measurements of atmospheric aerosols at a remote mountain site in NE Spain. Poster, European Aerosol Conference, EAC 2012, Granada, Spain, 3-7 September 2012.

Ripoll A., Pey J., Alastuey A., Minguillón M.C., Querol X.: Two years of measurements of atmospheric aerosols at a remote mountain site in NE Spain. Oral, 2nd

Workshops on Advanced Scientific Results from IDAEA, Observatorio del Ebro (CSIC), Roquetes, Spain, 14-15 May 2012.

Ripoll A., Pey J., Alastuey A., Pandolfi M., Pérez N., Querol X.: Atmospheric PM episodes affecting a remote site (Montsec) in the Western Mediterranean Basin. Poster, V Reunión Española de Ciencia y Tecnología de Aerosoles (RECTA 2011), Centro de Investigaciones Energéticas, Medioambientales y Tecnológicas (CIEMAT), Madrid, Spain, 28-29 June 2011.

Ripoll A., Pey J., Alastuey A., Pandolfi M., Pérez N., Cusack M., Querol X.: Atmospheric PM episodes affecting a continental background site in the Western Mediterranean Basin. Poster, IV Reunión Española de Ciencia y Tecnología de Aerosoles (RECTA 2010), Universidad de granada, Granada, Spain, 29-30 June 2010.

Ripoll A., Pey J., Alastuey A., Pandolfi M., Pérez N., Cusack M., Querol X.: Atmospheric PM episodes affecting a continental background site in the Western Mediterranean Basin. Oral, 1st Workshops on Advanced Scientific results from IDAEA, Centro de Estudios Avanzados de Blanes (CSIC), Blanes, Spain, 9-11 June 2010.

References

Aerodyne Research: ACSM data acquisition software manual. Version 1.4.07, April 2011.

Alastuey, A., Querol, X., Castillo, S., Escudero, M., Avila, A., Cuevas, E., Torres, C., Romero, P., Exposito, F. and Garcia, O.: Characterisation of TSP and PM2.5 at Izaña and Sta. Cruz de Tenerife (Canary Islands, Spain) during a Saharan Dust Episode (July 2002), Atmos. Environ., 39(26), 4715–4728, doi:10.1016/j.atmosenv.2005.04.018, 2005.

Alfaro, S. C., Lafon, S., Rajot, J. L., Formenti, P., Gaudichet, A. and Maillé, M.: Iron oxides and light absorption by pure desert dust: An experimental study, J. Geophys. Res., 109(D8), D08208, doi:10.1029/2003JD004374, 2004.

Alfarra, M. R., Prevot, A. S. H., Szidat, S., Sandradewi, J., Weimer, S., Schreiber, D., Mohr, M. and Baltensperger, U.: Identification of the mass spectral signature of organic aerosols from wood burning emissions, Environ. Sci. Technol., 41, 5770–5777, 2007.

Amato, F., Pandolfi, M., Escrig, A., Querol, X., Alastuey, A., Pey, J., Perez, N. and Hopke, P. K.: Quantifying road dust resuspension in urban environment by Multilinear Engine: A comparison with PMF2, Atmos. Environ., 43(17), 2770–2780, doi:10.1016/j.atmosenv.2009.02.039, 2009.

Andreae, M. O. and Gelencsér, A.: Black carbon or brown carbon ? The nature of light-absorbing carbonaceous aerosols, Atmos. Chem. Phys., 6, 3131–3148, doi:10.5194/acp-6-3131-2006, 2006.

Andrews, E., Ogren, J. A., Bonasoni, P., Marinoni, A., Cuevas, E., Rodríguez, S., Sun, J. Y., Jaffe, D. A., Fischer, E. V., Baltensperger, U., Weingartner, E., Coen, M. C., Sharma, S., Macdonald, A. M., Leaitch, W. R., Lin, N.-H., Laj, P., Arsov, T.,

Kalapov, I., Jefferson, A. and Sheridan, P.: Climatology of aerosol radiative properties in the free troposphere, Atmos. Res., 102(4), 365–393, doi:10.1016/j.atmosres.2011.08.017, 2011.

Anenberg, S. C., Horowitz, L. W., Tong, D. Q. and West, J. J.: An estimate of the global burden of anthropogenic ozone and fine particulate matter on premature human mortality using atmospheric modeling., Environ. Health Perspect., 118(9), 1189–1195, doi:10.1289/ehp.0901220, 2010.

Asmi, A., Collaud Coen, M., Ogren, J. A., Andrews, E., Sheridan, P., Jefferson, A., Weingartner, E., Baltensperger, U., Bukowiecki, N., Lihavainen, H., Kivekäs, N., Asmi, E., Aalto, P. P., Kulmala, M., Wiedensohler, A., Birmili, W., Hamed, A., O'Dowd, C., G Jennings, S., Weller, R., Flentje, H., Fjaeraa, A. M., Fiebig, M., Myhre, C. L., Hallar, A. G., Swietlicki, E., Kristensson, A. and Laj, P.: Aerosol decadal trends – Part 2: In-situ aerosol particle number concentrations at GAW and ACTRIS stations, Atmos. Chem. Phys., 13(2), 895–916, doi:10.5194/acp-13-895-2013, 2013.

Asmi, A., Wiedensohler, A., Laj, P., Fjaeraa, A.-M., Sellegri, K., Birmili, W., Weingartner, E., Baltensperger, U., Zdimal, V., Zikova, N., Putaud, J.-P., Marinoni, A., Tunved, P., Hansson, H.-C., Fiebig, M., Kivekäs, N., Lihavainen, H., Asmi, E., Ulevicius, V., Aalto, P. P., Swietlicki, E., Kristensson, A., Mihalopoulos, N., Kalivitis, N., Kalapov, I., Kiss, G., de Leeuw, G., Henzing, B., Harrison, R. M., Beddows, D., O'Dowd, C., Jennings, S. G., Flentje, H., Weinhold, K., Meinhardt, F., Ries, L. and Kulmala, M.: Number size distributions and seasonality of submicron particles in Europe 2008–2009, Atmos. Chem. Phys., 11(11), 5505–5538, doi:10.5194/acp-11-5505-2011, 2011.

Baltensperger, U., Gfiggeler, H. W., Jost, D. T., Lugauer, M., Schwikowski, M. and Weingartner, E.: Aerosol climatology at the high-alpine site Jungfraujoch, Switzerland, J. Geophys. Res., 102, 19,707–19,715, doi:10.1029/97JD00928, 1997.

Barmpadimos, I., Keller, J., Oderbolz, D., Hueglin, C. and Prévôt, A. S. H.: One decade of parallel fine (PM2.5) and coarse (PM10–PM2.5) particulate matter measurements in Europe: trends and variability, Atmos. Chem. Phys., 12(7), 3189–3203, doi:10.5194/acp-12-3189-2012, 2012.

Basart, S., Pérez, C., Nickovic, S., Cuevas, E. and Baldasano, J. M.: Development and evaluation of the BSC-DREAM8b dust regional model over Northern Africa, the Mediterranean and the Middle East, Tellus B, 64, doi:10.3402/tellusb.v64i0.18539, 2012.

Belis, C. A., Karagulian, F., Larsen, B. R. and Hopke, P. K.: Critical review and meta-analysis of ambient particulate matter source apportionment using receptor models in Europe, Atmos. Environ., 69, 94–108, doi:10.1016/j.atmosenv.2012.11.009, 2013.

Bessagnet, B., Menut, L., Curci, G., Hodzic, A., Guillaume, B., Liousse, C., Moukhtar, S., Pun, B., Seigneur, C. and Schulz, M.: Regional modeling of carbonaceous aerosols over Europe-focus on secondary organic aerosols, J. Atmos. Chem., 61(3), 175–202, doi:10.1007/s10874-009-9129-2, 2008.

Birmili, W., Berresheim, H., Plass-Dülmer, C., Elste, T., Gilge, S., Wiedensohler, A. and Uhrner, U.: The Hohenpeissenberg aerosol formation experiment (HAFEX): a long-term study including size-resolved aerosol, H2SO4, OH, and monoterpenes measurements, Atmos. Chem. Phys. Discuss., 3, 361–376, doi:10.5194/acpd-2-1655-2002, 2003.

Birmili, W., Wiedensohler, A., Heintzenberg, J. and Lehmann, K.: Atmospheric particle number size distribution in central Europe: Statistical relations to air masses and meteorology, J. Geophys. Res. Atmos., 106(D23), 32005–32018, 2001.

Bond, T. C., Doherty, S. J., Fahey, D. W., Forster, P. M., Berntsen, T., DeAngelo, B. J., Flanner, M. G., Ghan, S., Kärcher, B., Koch, D., Kinne, S., Kondo, Y., Quinn, P. K., Sarofim, M. C., Schultz, M. G., Schulz, M., Venkataraman, C. , Zhang, H., Zhang, S., Bellouin, N., Guttikunda, S. K., Hopke, P. K., Jacobson, M. Z., Kaiser, J. W., Klimont, Z., Lohmann, U., Schwarz, J. P., Shindell, D., Storelvmo, T., Warren, S. G. and Zender, C. S.: Bounding the role of black carbon in the climate system: A scientific assessment, J. Geophys. Res. Atmos., 118(11), 5380–5552, doi:10.1002/jgrd.50171, 2013.

Boucher, O., Randall, D., Artaxo, P., Bretherton, C., Feingold, G., Forster, P., Kerminen, V.-M., Kondo, Y., Liao, H., Lohmann, U., Rasch, P., Satheesh, S.K., Sherwood, S., Stevens, B. and Zhang, X.Y.: Clouds and Aerosols. In: Climate Change 2013: The Physical Science Basis. Contribution of Working Group I to the Fifth Assessment Report of the Intergovernmental Panel on Climate Change [Stocker, T.F., D. Qin, G.-K. Plattner, M. Tignor, S.K. Allen, J. Boschung, A. Nauels, Y. Xia, V. Bex and P.M. Midgley (eds.)]. Cambridge University Press, Cambridge, United Kingdom and New York, NY, USA, 2013.

Bourcier, L., Sellegri, K., Chausse, P., Pichon, J. M. and Laj, P.: Seasonal variation of water-soluble inorganic components in aerosol size-segregated at the puy de Dôme station (1,465 m a.s.l.), France, J. Atmos. Chem., 69(1), 47–66, doi:10.1007/s10874-012-9229-2, 2012.

Brown, S. G., Lee, T., Norris, G. A., Roberts, P. T., Paatero, P. and Worsnop, D. R.: Receptor modeling of near-roadway aerosol mass spectrometer data in Las Vegas, Nevada, with EPA PMF, Atmos. Chem. Phys., 12(1), 309–325, doi:10.5194/acp-12-309-2012, 2012.

Burkhardt, J. and Pariyar, S.: Particulate pollutants are capable to “degrade” epicuticular waxes and to decrease the drought tolerance of Scots pine (Pinus sylvestris L.)., Environ. Pollut., 184, 659–67, doi:10.1016/j.envpol.2013.04.041, 2014.

Canagaratna, M. R., Onasch, T. B., Wood, E. C., Herndon, S. C., Jayne, J. T., Cross, E. S., Miake-Lye, R. C., Kolb, C. E. and Worsnop, D. R.: Chemical and microphysical characterization of ambient aerosols with the aerodyne aerosol mass spectometer, Mass Spectrom. Rev., 26(2), 185–222, doi:10.1002/mas.20115, 2007.

Canonaco, F., Crippa, M., Slowik, J. G., Baltensperger, U. and Prévôt, A. S. H.: SoFi, an IGOR-based interface for the efficient use of the generalized multilinear engine (ME-2) for the source apportionment: ME-2 application to aerosol mass spectrometer data, Atmos. Meas. Tech., 6(12), 3649–3661, doi:10.5194/amt-6-3649-2013, 2013.

Casati, R., Scheer, V., Vogt, R. and Benter, T.: Measurement of nucleation and soot mode particle emission from a diesel passenger car in real world and laboratory in situ dilution, Atmos. Environ., 41(10), 2125–2135, doi:10.1016/j.atmosenv.2006.10.078, 2007.

Cassee, F. R., Héroux, M.-E., Gerlofs-Nijland, M. E. and Kelly, F. J.: Particulate matter beyond mass: recent health evidence on the role of fractions, chemical constituents and sources of emission., Inhal. Toxicol., 25(14), 802–12, doi:10.3109/08958378.2013.850127, 2013.

Castillo, S.: Impacto de las masas de aire africano sobre los niveles y composición del material particulado atmosférico en Canarias y el NE de la Península Ibérica, PhD Thesis, Universitat Politècnica de Catalunya (UPC), 2006.

Cavalli, F., Viana, M., Yttri, K. E., Genberg, J. and Putaud, J. P.: Toward a standardised thermal-optical protocol for measuring atmospheric organic and elemental carbon: the EUSAAR protocol, Atmos. Meas. Tech., 3(1), 79–89, doi:10.5194/amt-3-79-2010, 2010.

CEN: Air quality – Determination of the PM10 fraction of suspended particulate matter. Reference method and field test procedure to demonstrate reference equivalence of measurement methods, EN12341:1999, 1999.

Collaud Coen, M., Andrews, E., Asmi, A., Baltensperger, U., Bukowiecki, N., Day, D., Fiebig, M., Fjaeraa, A. M., Flentje, H., Hyvärinen, A., Jefferson, A., Jennings, S. G., Kouvarakis, G., Lihavainen, H., Lund Myhre, C., Malm, W. C., Mihapopoulos, N., Molenar, J. V., O'Dowd, C., Ogren, J. A., Schichtel, B. A., Sheridan, P., Virkkula, A., Weingartner, E., Weller, R. and Laj, P.: Aerosol decadal trends – Part 1: In-situ optical measurements at GAW and IMPROVE stations, Atmos. Chem. Phys., 13(2), 869–894, doi:10.5194/acp-13-869-2013, 2013.

Colomé, J., Ribas, I., Francisco, X., Casteels, K., Fernández, D., Isern, J., Palau, X. and Torra, J.: The OAdM Robotic Observatory, Adv. Astron., 2010, 1–8, doi:10.1155/2010/183016, 2010.

Crenn, V., Sciare, J., Croteau, P. L., Favez, O., Verlhac, S., Belis, C. A., Fröhlich, R., Aas, W., Äijälä, M., Alastuey, A., Artiñano, B., Baisnée, D., Baltensperger, U., Bonnaire, N., Bressi, M., Canagaratna, M., Canonaco, F., Carbone, C., Cavalli, F.,

Coz, E., Cubison, M. J., Gietl, J. K., Green, D. C., Heikkinen, L., Lunder, C., Minguillón, M. C., Močnik, G., O'Dowd, C. D., Ovad- nevaite, J., Petit, J.-E., Petralia, E., Poulain, L., Prévôt, A. S. H., Priestman, M., Riffault, V., Ripoll, A., Sarda-Estève, R., Slowik, J., Setyan, A., and Jayne, J. T.: ACTRIS ACSM intercomparison: Part 1 – Intercomparison of concentration and fragment results from 13 individual co-located aerosol chemical speciation monitors (ACSM), Atmos. Meas. Tech. Discuss., submitted, 2015.

Cristofanelli, P., Marinoni, A., Arduini, J., Bonaf, U., Calzolari, F., Colombo, T., Decesari, S., Duchi, R., Facchini, M. C., Fierli, F., Finessi, E., Maione, M., Chiari, M., Calzolai, G., Messina, P., Orlandi, E., Roccato, F. and Bonasoni, P.: Significant variations of trace gas composition and aerosol properties at Mt . Cimone during air mass transport from North Africa – contributions from wildfire emissions and mineral dust, Atmos. Chem. Phys., 9(14), 4603–4619, doi:10.5194/acp-9-4603-2009, 2009.

Cusack, M., Alastuey, A., Pérez, N., Pey, J. and Querol, X.: Trends of particulate matter (PM2.5) and chemical composition at a regional background site in the Western Mediterranean over the last nine years (2002–2010), Atmos. Chem. Phys., 12(18), 8341–8357, doi:10.5194/acp-12-8341-2012, 2012.

Cusack, M.: Physical and chemical processes affecting atmospheric aerosols in the Western Mediterranean regional background, PhD Thesis, Universitat Autònoma de Barcelona (UAB), 2013.

Cusack, M., Pérez, N., Pey, J., Alastuey, A. and Querol, X.: Source apportionment of fine PM and sub-micron particle number concentrations at a regional background site in the western Mediterranean: a 2.5 year study, Atmos. Chem. Phys., 13(10), 5173–5187, doi:10.5194/acp-13-5173-2013, 2013a.

Cusack, M., Pérez, N., Pey, J., Wiedensohler, A., Alastuey, A. and Querol, X.: Variability of sub-micrometer particle number size distributions and concentrations in the Western Mediterranean regional background, Tellus, Ser. B Chem. Phys. Meteorol., 65(1), 1–19, doi:10.3402/tellusb.v65i0.19243, 2013b.

Daher, N., Hasheminassab, S., Shafer, M. M., Schauer, J. J. and Sioutas, C.: Seasonal and spatial variability in chemical composition and mass closure of ambient ultrafine particles in the megacity of Los Angeles, Environ. Sci. Process. Impacts, 15(1), 283-295, doi:10.1039/c2em30615h, 2013.

Daher, N., Saliba, N. A., Shihadeh, A. L., Jaafar, M., Baalbaki, R., Shafer, M. M., Schauer, J. J. and Sioutas, C.: Oxidative potential and chemical speciation of size-resolved particulate matter (PM) at near-freeway and urban background sites in the greater Beirut area., Sci. Total Environ., 417–426, doi:10.1016/j.scitotenv.2013.09.104, 2014.

Dall'Osto, M., Beddows, D. C. S., Pey, J., Rodriguez, S., Alastuey, A., Harrison, R. M. and Querol, X.: Urban aerosol size distributions over the Mediterranean city of

Barcelona, NE Spain, Atmos. Chem. Phys., 12(22), 10693–10707, doi:doi:10.5194/acp-12-10693-2012, 2012.

Dall'Osto, M., Querol, X., Alastuey, A., O'Dowd, C., Harrison, R. M., Wenger, J. and Gómez-Moreno, F. J.: On the spatial distribution and evolution of ultrafine particles in Barcelona, Atmos. Chem. Phys., 13(2), 741–759, doi:10.5194/acp-13-741-2013, 2013.

De Leeuw, G., Andreas, E. L., Anguelova, M. D., Fairall, C. W., Lewis, E. R., O'Dowd, C., Schulz, M. and Schwartz, S. E.: Production flux of sea spray aerosol, Rev. Geophys., 49(2), RG2001, doi:10.1029/2010RG000349, 2011.

Directive 2010/75/EC of the European Parliament and of the Council of 24 November 2010 on industrial emissions (integrated pollution prevention and control) (OJ L 334, 17.12.2010, pp. 17–119), available at: http://eur-lex.europa.eu/legal-content/EN/TXT/PDF/?uri=CELEX:32010L0075&from=EN (last access: 10 April 2015), 2010.

Directive 2008/50/EC of the European Parliament and of the Council of 21 May 2008 on ambient air quality and cleaner air for Europe (OJ L 152, 11.6.2008, pp. 1–44), available at: http://eur-lex.europa.eu/legal-content/EN/TXT/PDF/?uri=CELEX:32008L0050&from=EN (last access: 9 April 2015), 2008.

Directive 2008/1/EC of the European Parliament and of the Council of 15 January 2008 concerning integrated pollution prevention and control (OJ L 24, 29.1.2008, pp. 8–29), available at: http://eur-lex.europa.eu/LexUriServ/LexUriServ.do?uri=OJ:L:2008:024:0008:0029:en:PDF (last access: 9 April 2015), 2008.

Directive 2004/107/EC of the European Parliament and of the Council of 15 December 2004 relating to arsenic, cadmium, mercury, nickel and polycyclic aromatic hydrocarbons in ambient air (OJ L 23, 26.1.2005, pp. 3–16), available at: http://eur-lex.europa.eu/LexUriServ/LexUriServ.do?uri=OJ:L:2005:023:0003:0016 :EN:PDF (last access: 8 April 2015), 2004.

Draxler, R.R. and Rolph, G.D.: HYSPLIT (HYbrid Single-Particle Lagrangian Integrated Trajectory) Model access via NOAA ARL READY Website (http://www.arl.noaa.gov/HYSPLIT.php). NOAA Air Resources Laboratory, College Park, MD, 2014.

Easter, R. and Peters, L.: Binary Homogeneous Nucleation: Temperature and Relative Humidity Fluctuations, Nonlinearity, and Aspects of New Particle Production in the Atmosphere, J. Appl. Meteorol., 33, 775–784, 1994.

Escrig Vidal, A., Monfort, E., Celades, I., Querol, X., Amato, F., Minguillón, M. C. and Hopke, P. K.: Application of optimally scaled target factor analysis for assessing source contribution of ambient PM10, J. Air Waste Manag. Assoc., 59(11), 1296–1307, 2009.

Escudero, M., Querol, X., Pey, J., Alastuey, A., Pérez, N., Ferreira, F., Alonso, S., Rodríguez, S. and Cuevas, E.: A methodology for the quantification of the net African dust load in air quality monitoring networks, Atmos. Environ., 41(26), 5516–5524, doi:10.1016/j.atmosenv.2007.04.047, 2007.

Escudero, M., Stein, A., Draxler, R. R., Querol, X., Alastuey, A., Castillo, S. and Avila, A.: Determination of the contribution of northern Africa dust source areas to PM10 concentrations over the central Iberian Peninsula using the Hybrid Single-Particle Lagrangian Integrated Trajectory model (HYSPLIT) model, J. Geophys. Res., 111(D6), D06210, doi:10.1029/2005JD006395, 2006.

European Environment Agency (EEA) Technical report: European union emission inventory report 1990–2011 under the UNECE convention on long-range transboundary air pollution (LRTAP). Luxembourg: Publications Office of the European Union, ISBN: 978-92-9213-400-6, doi:10.2800/44480, 2013.

Forster, P., Ramaswamy, V., Artaxo, P., Berntsen, T., Betts, R., Fahey, D.W., Haywood, J., Lean, J., Lowe, D.C., Myhre, G., Nganga, J., Prinn, R., Raga, G., Schulz, M. and Van Dorland, R.: Changes in Atmospheric Constituents and in Radiative Forcing. In: Climate Change 2007: The Physical Science Basis. Contribution of Working Group I to the Fourth Assessment Report of the Intergovernmental Panel on Climate Change [Solomon, S., D. Qin, M. Manning, Z. Chen, M. Marquis, K.B. Averyt, M.Tignor and H.L. Miller (eds.)]. Cambridge University Press, Cambridge, United Kingdom and New York, NY, USA, 2007.

Freney, E. J., Sellegri, K., Canonaco, F., Boulon, J., Hervo, M., Weigel, R., Pichon, J. M., Colomb, A., Prévôt, A. S. H. and Laj, P.: Seasonal variations in aerosol particle composition at the puy-de-Dôme research station in France, Atmos. Chem. Phys., 11(24), 13047–13059, doi:10.5194/acp-11-13047-2011, 2011.

Fröhlich, R., Crenn, V., Setyan, A., Belis, C. A., Canonaco, F., Favez, O., Riffault, V., Slowik, J. G., Aas, W., Aijälä, M., Alastuey, A., Artiñano, B., Bonnaire, N., Bozzetti, C., Bressi, M., Carbone, C., Coz, E., Croteau, P. L., Cubison, M. J., Esser-Gietl, J. K., Green, D. C., Gros, V., Heikkinen, L., Herrmann, H., Jayne, J. T., Lunder, C. R., Minguillón, M. C., Močnik, G., O'Dowd, C. D., Ovadnevaite, J., Petralia, E., Poulain, L., Priestman, M., Ripoll, A., Sarda-Estève, R., Wiedensohler, A., Baltensperger, U., Sciare, J. and Prévôt, A. S. H.: ACTRIS ACSM intercomparison – Part 2: Intercomparison of ME-2 organic source apportionment results from 15 individual, co-located aerosol mass spectrometers, Atmos. Meas. Tech. Discuss., 8, 1559–1613, doi:10.5194/amtd-8-1559-2015, 2015.

Fu, P. P., Xia, Q., Hwang, H.-M., Ray, P. C. and Yu, H.: Mechanisms of nanotoxicity: generation of reactive oxygen species., J. food drug Anal., 22(1), 64–75, doi:10.1016/j.jfda.2014.01.005, 2014.

Garcia-Hurtado, E., Pey, J., Borrás, E., Sánchez, P., Vera, T., Carratalá, A., Alastuey, A., Querol, X. and Vallejo, V. R.: Atmospheric PM and volatile organic compounds

released from Mediterranean shrubland wildfires, Atmos. Environ., 89, 85–92, doi:10.1016/j.atmosenv.2014.02.016, 2014.

Gelencsér, A., May, B., Simpson, D., Sánchez-Ochoa, A., Kasper-Giebl, A., Puxbaum, H., Caseiro, A., Pio, C. and Legrand, M.: Source apportionment of PM2.5 organic aerosol over Europe: Primary/secondary, natural/anthropogenic, and fossil/biogenic origin, J. Geophys. Res., 112(D23), D23S04, doi:10.1029/2006JD008094, 2007.

Gianini, M. F. D., Gehrig, R., Fischer, A., Ulrich, A., Wichser, A. and Hueglin, C.: Chemical composition of PM10 in Switzerland: An analysis for 2008/2009 and changes since 1998/1999, Atmos. Environ., 54, 97–106, doi:10.1016/j.atmosenv.2012.02.037, 2012.

Gieré, R. and Querol, X.: Solid Particulate Matter in the Atmosphere, Elements, 6(4), 215–222, doi:10.2113/gselements.6.4.215, 2010.

Ginoux, P., Prospero, J. M., Gill, T. E., Hsu, N. C. and Zhao, M.: Global-scale attribution of anthropogenic and natural dust sources and their emission rates based on MODIS Deep Blue aerosol products, Rev. Geophys., 50, RG3005, doi:10.1029/2012RG000388, 2012.

Goldberg, E.D. Black carbon in the environment: properties and distribution, New York: John Wiley & Sons Inc., 1985.

GRIMM: Operating manual of the environmental dust monitor 1.107. Printed in Germany: Released July 2007.

Guarieiro, L. L. N. and Guarieiro, A. L. N.: Vehicle Emissions: What Will Change with Use of Biofuel?, Biofuels - Economy, Environment and Sustainability, Prof. Zhen Fang (Ed.), ISBN: 978-953-51-0950-1, InTech, doi:10.5772/52513, available at: http://www.intechopen.com/books/biofuels-economy-environment-and-sustainability/vehicle-emissions-what-will-change-with-use-of-biofuel- (last access: 9 April 2015), 2013.

Guenther, A., Geron, C., Pierce, T., Lamb, B., Harley, P. and Fall, R.: Natural emissions of non-methane volatile organic compounds, carbon monoxide, and oxides of nitrogen from North America, Atmos. Environ., 34(12-14), 2205–2230, doi:10.1016/S1352-2310(99)00465-3, 2000.

Hakala, J., Manninen, H. E., Petäjä, T. and Sipilä, M.: Counting Efficiency of a TSI Environmental Particle Counter Monitor Model 3783, Aerosol Sci. Technol., 47(5), 482–487, doi:10.1080/02786826.2013.766666, 2013.

Harrison, R. M. and Pio, C. a.: Size-differentiated composition of inorganic atmospheric aerosols of both marine and polluted continental origin, Atmos. Environ., 17(9), 1733–1738, doi:10.1016/0004-6981(83)90180-4, 1983.

Heal, M. R., Kumar, P. and Harrison, R. M.: Particles, air quality, policy and health., Chem. Soc. Rev., 41(19), 6606–30, doi:10.1039/c2cs35076a, 2012.

Hidy, G. M.: Atmospheric sulfur and nitrogen oxides: Eastern North America source receptor relationships, 447 pp., Academic Press Inc, San Diego, 1994.

Howarth, R. J. and Thompson, M.: Duplicate analysis in geochemical practice part II. Examination of proposed method and examples of its use, Analyst, 101(1206), 699–709, 1976.

Huneeus, N., Chevallier, F. and Boucher, O.: Estimating aerosol emissions by assimilating observed aerosol optical depth in a global aerosol model, Atmos. Chem. Phys., 12(10), 4585–4606, doi:10.5194/acp-12-4585-2012, 2012.

IUPAC 1995. International Union of Pure and Applied Chemistry. Nomenclature in evaluation of analytical methods including detection and qualification capabilities. Pure & Appl. Chem., 67, 1699-1723, 1995.

Jickells, T. D., An, Z. S., Andersen, K. K., Baker, A. R., Bergametti, G., Brooks, N., Cao, J. J., Boyd, P. W., Duce, R. A., Hunter, K. A., Kawahata, H., Kubilay, N., LaRoche, J., Liss, P. S., Mahowald, N., Prospero, J. M., Ridgwell, A. J., Tegen, I. and Torres, R.: Global Iron Connections Between Desert Dust, Ocean Biogeochemistry, and Climate, Science, 308(5718), 67–72, doi:10.1126/science.1105959, 2005.

Jimenez, J. L., Canagaratna, M. R., Donahue, N. M., Prevot, A. S. H., Zhang, Q., Kroll, J. H., DeCarlo, P. F., Allan, J. D., Coe, H., Ng, N. L., Aiken, A. C., Docherty, K. S., Ulbrich, I. M., Grieshop, A. P., Robinson, A. L., Duplissy, J., Smith, J. D., Wilson, K. R., Lanz, V. A., Hueglin, C., Sun, Y. L., Tian, J., Laaksonen, A., Raatikainen, T., Rautiainen, J., Vaattovaara, P., Ehn, M., Kulmala, M., Tomlinson, J. M., Collins, D. R., Cubison, M. J., Dunlea, E. J., Huffman, J. a, Onasch, T. B., Alfarra, M. R., Williams, P. I., Bower, K., Kondo, Y., Schneider, J., Drewnick, F., Borrmann, S., Weimer, S., Demerjian, K., Salcedo, D., Cottrell, L., Griffin, R., Takami, A., Miyoshi, T., Hatakeyama, S., Shimono, A., Sun, J. Y., Zhang, Y. M., Dzepina, K., Kimmel, J. R., Sueper, D., Jayne, J. T., Herndon, S. C., Trimborn, A. M., Williams, L. R., Wood, E. C., Middlebrook, A. M., Kolb, C. E., Baltensperger, U. and Worsnop, D. R.: Evolution of organic aerosols in the atmosphere., Science, 326(5959), 1525–1529, doi:10.1126/science.1180353, 2009.

Jimenez, J. L., Jayne, J. T., Shi, Q., Kolb, C. E., Worsnop, D. R., Yourshaw, I., Seinfeld, J. H., Flagan, R. C., Zhang, X., Smith, K. A., Morris, J. W. and Davidovits, P.: Ambient aerosol sampling using the Aerodyne Aerosol Mass Spectrometer, J. Geophys. Res., 108(D7), 8425, doi:10.1029/2001JD001213, 2003.

Jiménez, P., Lelieveld, J. and Baldasano, J. M.: Multiscale modeling of air pollutants dynamics in the northwestern Mediterranean basin during a typical summertime episode, J. Geophys. Res., 111(D18), D18306, doi:10.1029/2005JD006516, 2006.

Jorba, O., Pandolfi, M., Spada, M., Baldasano, J. M., Pey, J., Alastuey, A., Arnold, D., Sicard, M., Artiñano, B., Revuelta, M. a. and Querol, X.: Overview of the meteorology and transport patterns during the DAURE field campaign and their

impact to PM observations, Atmos. Environ., 77, 607–620, doi:10.1016/j.atmosenv.2013.05.040, 2013.

Junge, C. E.: Air chemistry and radioactivity, Academic Press, 1963.

Kallos, G.: The Regional weather forecasting system SKIRON. Proceedings, Symposium on Regional Weather Prediction on Parallel Computer Environments, pp. 9, Athens, Greece, 15-17 October, 1997.

Kent, G. S., Trepte, C. R. and Lucker, P. L.: Long-term stratospheric aerosol and gas experiment I and II measurements of upper tropospheric aerosol extinction, J. Geophys. Res., 103(D22), 28863, doi:10.1029/98JD02583, 1998.

Kerminen, V.-M., Pakkanen, T. A., Mäkelä, T., Hillamo, R. E., Sillanpää, M., Rönkkö, T., Virtanen, A., Keskinen, J., Pirjola, L., Hussein, T. and Hämeri, K.: Development of particle number size distribution near a major road in Helsinki during an episodic inversion situation, Atmos. Environ., 41(8), 1759–1767, doi:10.1016/j.atmosenv.2006.10.026, 2007.

Kloog, I., Ridgway, B., Koutrakis, P., Coull, B. A. and Schwartz, J. D.: Long- and short-term exposure to PM2.5 and mortality: using novel exposure models., Epidemiology, 24(4), 555–561, doi:10.1097/EDE.0b013e318294beaa, 2013.

Kok, J. F.: A scaling theory for the size distribution of emitted dust aerosols suggests climate models underestimate the size of the global dust cycle, Proc. Natl. Acad. Sci. U. S. A., 108(3), 1016–1021, doi:10.1073/pnas.1014798108/-/DCSupplemental.www.pnas.org/cgi/doi/10.1073/pnas.1014798108, 2011.

Kreyling, W. G., Semmler-Behnke, M. and Möller, W.: Health implications of nanoparticles, J. Nanoparticle Res., 8(5), 543–562, doi:10.1007/s11051-005-9068-z, 2006.

Krishnan, R. M., Adar, S. D., Szpiro, A. A., Jorgensen, N. W., Van Hee, V. C., Barr, R. G., O'Neill, M. S., Herrington, D. M., Polak, J. F. and Kaufman, J. D.: Vascular responses to long- and short-term exposure to fine particulate matter: MESA Air (Multi-Ethnic Study of Atherosclerosis and Air Pollution)., J. Am. Coll. Cardiol., 60(21), 2158–66, doi:10.1016/j.jacc.2012.08.973, 2012.

Kulmala, M. and Kerminen, V.-M.: On the formation and growth of atmospheric nanoparticles, Atmos. Res., 90(2-4), 132–150, doi:10.1016/j.atmosres.2008.01.005, 2008.

Kulmala, M., Kontkanen, J., Junninen, H., Lehtipalo, K., Manninen, H. E., Nieminen, T., Petäjä, T., Sipilä, M., Schobesberger, S., Rantala, P., Franchin, A., Jokinen, T., Järvinen, E., Äijälä, M., Kangasluoma, J., Hakala, J., Aalto, P. P., Paasonen, P., Mikkilä, J., Vanhanen, J., Aalto, J., Hakola, H., Makkonen, U., Ruuskanen, T., Mauldin, R. L., Duplissy, J., Vehkamäki, H., Bäck, J., Kortelainen, A., Riipinen, I., Kurtén, T., Johnston, M. V, Smith, J. N., Ehn, M., Mentel, T. F., Lehtinen, K. E. J., Laaksonen, A., Kerminen, V.-M. and Worsnop, D. R.: Direct observations of

atmospheric aerosol nucleation., Science, 339(6122), 943–946, doi:10.1126/science.1227385, 2013.

Kulmala, M., Toivonen, A., Makela, J. M. and Laaksonen, A.: Analysis of the growth of nucleation mode particles observed in Boreal forest, Tellus B, 50(5), 449–462, doi:10.1034/j.1600-0889.1998.t01-4-00004.x, 1998.

Laj, P., Klausen, J., Bilde, M., Plaß-Duelmer, C., Pappalardo, G., Clerbaux, C., Baltensperger, U., Hjorth, J., Simpson, D., Reimann, S., Coheur, P.-F., Richter, a., De Mazière, M., Rudich, Y., McFiggans, G., Torseth, K., Wiedensohler, a., Morin, S., Schulz, M., Allan, J. D., Attié, J.-L., Barnes, I., Birmili, W., Cammas, J. P., Dommen, J., Dorn, H.-P., Fowler, D., Fuzzi, S., Glasius, M., Granier, C., Hermann, M., Isaksen, I. S. A., Kinne, S., Koren, I., Madonna, F., Maione, M., Massling, A., Moehler, O., Mona, L., Monks, P. S., Müller, D., Müller, T., Orphal, J., Peuch, V.-H., Stratmann, F., Tanré, D., Tyndall, G., Abo Riziq, A., Van Roozendael, M., Villani, P., Wehner, B., Wex, H. and Zardini, a. a.: Measuring atmospheric composition change, Atmos. Environ., 43(33), 5351–5414, doi:10.1016/j.atmosenv.2009.08.020, 2009.

Lang-Yona, N., Rudich, Y., Mentel, T. F., Bohne, A., Buchholz, A., Kiendler-Scharr, A., Kleist, E., Spindler, C., Tillmann, R. and Wildt, J.: The chemical and microphysical properties of secondary organic aerosols from Holm Oak emissions, Atmos. Chem. Phys., 10(15), 7253–7265, doi:10.5194/acp-10-7253-2010, 2010.

Levin, Z. and Cotton, W. R. (Eds). Aerosol pollution impact on precipitation: A scientific review. Springer Netherlands, ISBN: 978-1-4020-8689-2, doi:10.1007/978-1-4020-8690-8, 2009.

Lim, S. S., Vos, T., Flaxman, A. D., Danaei, G., Shibuya, K., Adair-Rohani, H., Amann, M., Anderson, H. R., Andrews, K. G., Aryee, M., Atkinson, C., Bacchus, L. J., Bahalim, A. N., Balakrishnan, K., Balmes, J., Barker-Collo, S., Baxter, A., Bell, M. L., Blore, J. D., Blyth, F., Bonner, C., Borges, G., Bourne, R., Boussinesq, M., Brauer, M., Brooks, P., Bruce, N. G., Brunekreef, B., Bryan-Hancock, C., Bucello, C., Buchbinder, R., Bull, F., Burnett, R. T., Byers, T. E., Calabria, B., Carapetis, J., Carnahan, E., Chafe, Z., Charlson, F., Chen, H., Chen, J. S., Cheng, A. T. A., Child, J. C., Cohen, A., Colson, K. E., Cowie, B. C., Darby, S., Darling, S., Davis, A., Degenhardt, L., Dentener, F., Des Jarlais, D. C., Devries, K., Dherani, M., Ding, E. L., Dorsey, E. R., Driscoll, T., Edmond, K., Ali, S. E., Engell, R. E., Erwin, P. J., Fahimi, S., Falder, G., Farzadfar, F., Ferrari, A., Finucane, M. M., Flaxman, S., Fowkes, F. G. R., Freedman, G., Freeman, M. K., Gakidou, E., Ghosh, S., Giovannucci, E., Gmel, G., Graham, K. , Grainger, R., Grant, B., Gunnell, D., Gutierrez, H. R., Hall, W., Hoek, H. W., Hogan, A., Hosgood, H. D., Hoy, D., Hu, H., Hubbell, B. J., Hutchings, S. J., Ibeanusi, S. E., Jacklyn, G. L., Jasrasaria, R., Jonas, J. B., Kan, H., Kanis, J. a., Kassebaum, N., Kawakami, N., Khang, Y. H., Khatibzadeh, S., Khoo, J. P., Kok, C., et al.: A comparative risk assessment of burden of disease and injury attributable to 67 risk factors and risk factor clusters

in 21 regions, 1990-2010: A systematic analysis for the Global Burden of Disease Study 2010, Lancet, 380, 2224–2260, doi:10.1016/S0140-6736(12)61766-8, 2012.

Lingard, J. J. N., Agus, E. L., Young, D. T., Andrews, G. E. and Tomlin, A. S.: Observations of urban airborne particle number concentrations during rush-hour conditions: analysis of the number based size distributions and modal parameters, J. Environ. Monit., 8(12), 1203–1218, doi:10.1039/b611479b, 2006.

Liu, P. S. K., Deng, R., Smith, K. A., Williams, L. R., Jayne, J. T., Canagaratna, M. R., Moore, K., Onasch, T. B., Worsnop, D. R. and Deshler, T.: Transmission Efficiency of an Aerodynamic Focusing Lens System: Comparison of Model Calculations and Laboratory Measurements for the Aerodyne Aerosol Mass Spectrometer, Aerosol Sci. Technol., 41(February 2015), 721–733, doi:10.1080/02786820701422278, 2007.

Lopez-Bustins, J.-A., Martin-Vide, J. and Sanchez-Lorenzo, A.: Iberia winter rainfall trends based upon changes in teleconnection and circulation patterns, Glob. Planet. Change, 63(2-3), 171–176, doi:10.1016/j.gloplacha.2007.09.002, 2008.

Lucas, D. D. and Prinn, R. G.: Parametric sensitivity and uncertainty analysis of dimethylsulfide oxidation in the clear-sky remote marine boundary layer, Atmos. Chem. Phys., 5(6), 1505–1525, doi:10.5194/acp-5-1505-2005, 2005.

Marinoni, a, Cristofanelli, P., Calzolari, F., Roccato, F., Bonafè, U. and Bonasoni, P.: Continuous measurements of aerosol physical parameters at the Mt. Cimone GAW Station (2165 m asl, Italy), Sci. Total Environ., 391(2-3), 241–51, doi:10.1016/j.scitotenv.2007.10.004, 2008.

Marinoni, A., Cristofanelli, P., Laj, P., Duchi, R., Calzolari, F., Decesari, S., Sellegri, K., Vuillermoz, E., Verza, G. P., Villani, P. and Bonasoni, P.: Aerosol mass and black carbon concentrations, a two year record at NCO-P (5079 m, Southern Himalayas), Atmos. Chem. Phys., 10(17), 8551–8562, doi:10.5194/acp-10-8551-2010, 2010.

Marticorena, B.: Chapter 5: Dust Production Mechanisms, pp. 93-120, within Mineral Dust: A Key Player in the Earth System, [Knippertz, P. and Stuut, J.-B. W. (Eds.)], Springer Dordrecht Heidelberg New York London, doi:10.1007/978-94-017-8978-3_5, 2014.

McMurry, P.: A review of atmospheric aerosol measurements, Atmos. Environ., 34, 1959–1999, doi:10.1016/S1352-2310(99)00455-0, 2000.

Mészáros, E.: Fundamentals of atmospheric aerosol chemistry, 308 pp., Akademiai Kiado, Budapest, 1999.

Middlebrook, A. M., Bahreini, R., Jimenez, J. L. and Canagaratna, M. R.: Evaluation of Composition-Dependent Collection Efficiencies for the Aerodyne Aerosol Mass Spectrometer using Field Data, Aerosol Sci. Technol., 46(3), 258–271, doi:10.1080/02786826.2011.620041, 2012.

Millán, M. M., Salvador, R., Mantilla, E. and Kallos, G.: Photooxidant dynamics in the Mediterranean basin in summer: Results from European research projects, J. Geophys. Res., 102, 8811–8823, 1997.

Millán, M. M., Mantilla, E., Salvador, R., Carratalá, A., Sanz, M. J., Alonso, L., Gangoiti, G. and Navazo, M.: Ozone cycles in the western Mediterranean basin: Interpretation of monitoring data in complex coastal terrain, J. Appl. Meteorol., 39(4), 487–508, 2000.

Minguillón, M. C., Perron, N., Querol, X., Szidat, S., Fahrni, S. M., Alastuey, A., Jimenez, J. L., Mohr, C., Ortega, A. M., Day, D. A., Lanz, V. A., Wacker, L., Reche, C., Cusack, M., Amato, F., Kiss, G., Hoffer, A., Decesari, S., Moretti, F., Hillamo, R., Teinilä, K., Seco, R., Peñuelas, J., Metzger, A., Schallhart, S., Müller, M., Hansel, A., Burkhart, J. F., Baltensperger, U. and Prévôt, A. S. H.: Fossil versus contemporary sources of fine elemental and organic carbonaceous particulate matter during the DAURE campaign in Northeast Spain, Atmos. Chem. Phys., 11(8), 23573–23618, doi:10.5194/acp-11-12067-2011, 2011.

Minguillón, M. C., Ripoll, A., Pérez, N., Prévôt, A. S. H., Canonaco, F., Querol, X. and Alastuey, A.: Chemical characterization of submicron regional background aerosols in the Western Mediterranean using an Aerosol Chemical Speciation Monitor, Atmos. Chem. Phys. Discuss., 15, 965–1000, doi:10.5194/acpd-15-965-2015, 2015.

Mohr, C., DeCarlo, P. F., Heringa, M. F., Chirico, R., Slowik, J. G., Richter, R., Reche, C., Alastuey, a., Querol, X., Seco, R., Peñuelas, J., Jiménez, J. L., Crippa, M., Zimmermann, R., Baltensperger, U. and Prévôt, a. S. H.: Identification and quantification of organic aerosol from cooking and other sources in Barcelona using aerosol mass spectrometer data, Atmos. Chem. Phys., 12(4), 1649–1665, doi:10.5194/acp-12-1649-2012, 2012.

Mohr, C., Huffman, J. A., Cubison, M. J., Aiken, A. C., Docherty, K. S., Kimmel, J. R., Ulbrich, I. M., Hannigan, M. and Jimenez, J. L.: Characterization of Primary Organic Aerosol Emissions from Meat Cooking, Trash Burning, and Motor Vehicles with High-Resolution Aerosol Mass Spectrometry and Comparison with Ambient and Chamber Observations, Environ. Sci. Technol., 43(7), 2443–2449, doi:10.1021/es8011518, 2009.

Morawska, L., Thomas, S., Jamriska, M. and Johnson, G.: The modality of particle size distributions of environmental aerosols, Atmos. Environ., 33(27), 4401–4411, doi:10.1016/S1352-2310(99)00217-4, 1999.

Mordas, G., Manninen, H. E., Petäjä, T., Aalto, P. P., Hämeri, K. and Kulmala, M.: On Operation of the Ultra-Fine Water-Based CPC TSI 3786 and Comparison with Other TSI Models (TSI 3776, TSI 3772, TSI 3025, TSI 3010, TSI 3007), Aerosol Sci. Technol., 42(February 2015), 152–158, doi:10.1080/02786820701846252, 2008.

Moreno, T., Querol, X., Castillo, S., Alastuey, A., Cuevas, E., Herrmann, L., Mounkaila, M., Elvira, J. and Gibbons, W.: Geochemical variations in aeolian mineral particles from the Sahara-Sahel Dust Corridor., Chemosphere, 65(2), 261–70, doi:10.1016/j.chemosphere.2006.02.052, 2006.

Müller, T., Henzing, J. S., de Leeuw, G., Wiedensohler, A., Alastuey, A., Angelov, H., Bizjak, M., Collaud Coen, M., Engström, J. E., Gruening, C., Hillamo, R., Hoffer, A., Imre, K., Ivanow, P., Jennings, G., Sun, J. Y., Kalivitis, N., Karlsson, H., Komppula, M., Laj, P., Li, S.-M., Lunder, C., Marinoni, A., Martins dos Santos, S., Moerman, M., Nowak, A., Ogren, J. A., Petzold, A., Pichon, J. M., Rodriquez, S., Sharma, S., Sheridan, P. J., Teinilä, K., Tuch, T., Viana, M., Virkkula, A., Weingartner, E., Wilhelm, R. and Wang, Y. Q.: Characterization and intercomparison of aerosol absorption photometers: result of two intercomparison workshops, Atmos. Meas. Tech., 4(2), 245–268, doi:10.5194/amt-4-245-2011, 2011a.

Müller, T., Laborde, M., Kassell, G. and Wiedensohler, A.: Design and performance of a three-wavelength LED-based total scatter and backscatter integrating nephelometer, Atmos. Meas. Tech., 4(1996), 1291–1303, doi:10.5194/amt-4-1291-2011, 2011b.

Myhre, G., Shindell, D., Bréon, F.-M., Collins, W., Fuglestvedt, J., Huang, J., Koch, D., Lamarque, J.-F., Lee, D., Mendoza, B., Nakajima, T., Robock, A., Stephens, G., Takemura, T. and Zhang, H.: Anthropogenic and Natural Radiative Forcing. In: Climate Change 2013: The Physical Science Basis. Contribution of Working Group I to the Fifth Assessment Report of the Intergovernmental Panel on Climate Change [Stocker, T.F., D. Qin, G.-K. Plattner, M. Tignor, S.K. Allen, J. Boschung, A. Nauels, Y. Xia, V. Bex and P.M. Midgley (eds.)]. Cambridge University Press, Cambridge, United Kingdom and New York, NY, USA, 2013.

Ng, N. L., Canagaratna, M. R., Jimenez, J. L., Zhang, Q., Ulbrich, I. M. and Worsnop, D. R.: Real-Time Methods for Estimating Organic Component Mass Concentrations from Aerosol Mass Spectrometer Data, Environ. Sci. Technol., 45(3), 910–916, doi:10.1021/es102951k, 2011a.

Ng, N. L., Herndon, S. C., Trimborn, A., Canagaratna, M. R., Croteau, P. L., Onasch, T. B., Sueper, D., Worsnop, D. R., Zhang, Q., Sun, Y. L. and Jayne, J. T.: An Aerosol Chemical Speciation Monitor (ACSM) for routine monitoring of the composition and mass concentrations of ambient aerosol, Aerosol Sci. Technol., 45, 780–794, doi:10.1080/02786826.2011.560211, 2011b.

Nyeki, S., Baltensperger, U., Colbeck, I., Jost, D. T., Weingartner, E. and Gäggeler, H. W.: The Jungfraujoch high-alpine research station (3454 m) as a background clean continental site for the measurement of aerosol parameters, J. Geophys. Res., 103, 6097–6107, 1998.

Oberdörster, G., Sharp, Z., Atudorei, V., Elder, A., Gelein, R., Kreyling, W. and Cox, C.: Translocation of inhaled ultrafine particles to the brain., Inhal. Toxicol., 16(6-7), 437–445, doi:10.1080/08958370490439597, 2004.

Ostro, B., Broadwin, R., Green, S., Feng, W.-Y. and Lipsett, M.: Fine Particulate Air Pollution and Mortality in Nine California Counties: Results from CALFINE, Environ. Health Perspect., 114(1), 29–33, doi:10.1289/ehp.8335, 2006.

Ovrevik, J. and Schwarze, P. E.: Chemical composition and not only total surface area is important for the effects of ultrafine particles., Mutat. Res., 594(1-2), 201–202; author reply 199–200, doi:10.1016/j.mrfmmm.2005.10.002, 2006.

Paatero, P.: Least squares formulation of robust non-negative factor analysis, Chemom. Intell. Lab. Syst., 37(1), 23–35, doi:10.1016/S0169-7439(96)00044-5, 1997.

Paatero, P.: The multilinear engine - a table-driven, least squares program for solving multilinear problems, including the n-way parallel factor analysis model, J. Comput. Graph. Stat., 8(4), 854–888, doi:10.2307/1390831, 1999.

Paatero, P. and Hopke, P. K.: Rotational tools for factor analytic models, J. Chemom., 23(2), 91–100, doi:10.1002/cem.1197, 2009.

Paatero, P. and Tapper, U.: Positive matrix factorization: a non-negative factor model with optimal utilization of error estimates of data values, Environmetrics, 5(2), 111–126, 1994.

Pandolfi, M., Cusack, M., Alastuey, a. and Querol, X.: Variability of aerosol optical properties in the Western Mediterranean Basin, Atmos. Chem. Phys., 11(15), 8189–8203, doi:10.5194/acp-11-8189-2011, 2011.

Pandolfi, M., Martucci, G., Querol, X., Alastuey, a., Wilsenack, F., Frey, S., O'Dowd, C. D. and Dall'Osto, M.: Continuous atmospheric boundary layer observations in the coastal urban area of Barcelona during SAPUSS, Atmos. Chem. Phys., 13(9), 4983–4996, doi:10.5194/acp-13-4983-2013, 2013.

Pandolfi, M., Querol, X., Alastuey, A., Jimenez, J. L., Jorba, O., Day, D., Ortega, A., Cubison, M. J., Comerón, A., Sicard, M., Mohr, C., Prévôt, A. S. H., Minguillón, M. C., Pey, J., Baldasano, J. M., Burkhart, J. . F., Seco, R., Peñuelas, J., van Drooge, B. L., Artiñano, B., Di Marco, C., Nemitz, E., Schallhart, S., Metzger, A., Hansel, A., Lorente, J., Ng, S., Jayne, J. and Szidat, S.: Effects of sources and meteorology on particulate matter in the Western Mediterranean Basin: An overview of the DAURE campaign, J. Geophys. Res. Atmos., 119, 4978–5010, doi:10.1002/2013JD021079.Received, 2014a.

Pandolfi, M., Ripoll, a., Querol, X. and Alastuey, a.: Climatology of aerosol optical properties and black carbon mass absorption cross section at a remote high-altitude site in the western Mediterranean Basin, Atmos. Chem. Phys., 14(12), 6443–6460, doi:10.5194/acp-14-6443-2014, 2014b.

Papadopoulos, A., Katsafados, P. and Kallos, G.: Regional weather forecasting for marine application. Global Atmos. Ocean Syst., 8, No 2-3, 219-237, 2001.

Pérez, C., Sicard, M., Jorba, O., Comerón, A. and Baldasano, J. M.: Summertime re-circulations of air pollutants over the north-eastern Iberian coast observed from systematic EARLINET lidar measurements in Barcelona, Atmos. Environ., 38(24), 3983–4000, doi:10.1016/j.atmosenv.2004.04.010, 2004.

Perez, L., Tobias, A., Querol, X., Künzli, N., Pey, J., Alastuey, A., Viana, M., Valero, N., González-Cabré, M. and Sunyer, J.: Coarse Particles From Saharan Dust and Daily Mortality, Epidemiology, 19(6), 800–807, doi:10.1097/EDE.0b013e31818131cf, 2008.

Pérez, N., Pey, J., Castillo, S., Viana, M., Alastuey, a and Querol, X.: Interpretation of the variability of levels of regional background aerosols in the Western Mediterranean., Sci. Total Environ., 407(1), 527–40, doi:10.1016/j.scitotenv.2008.09.006, 2008.

Pérez, N.: Variability of atmospheric aerosols at urban, regional and continental backgrounds in the western Mediterranean basin, PhD Thesis, Universitat Autònoma de Barcelona (UAB), 2010.

Pérez, N., Pey, J., Cusack, M., Reche, C., Querol, X., Alastuey, A. and Viana, M.: Variability of Particle Number, Black Carbon, and PM10, PM2.5, and PM1 Levels and Speciation: Influence of Road Traffic Emissions on Urban Air Quality, Aerosol Sci. Technol., 44(7), 487–499, doi:10.1080/02786821003758286, 2010.

Perrino, C., Canepari, S., Pappalardo, S. and Marconi, E.: Time-resolved measurements of water-soluble ions and elements in atmospheric particulate matter for the characterization of local and long-range transport events. Chemosphere, 80(11), 1291–300, doi:10.1016/j.chemosphere.2010.06.050, 2010.

Petzold, A., Ogren, J. a., Fiebig, M., Laj, P., Li, S.-M., Baltensperger, U., Holzer-Popp, T., Kinne, S., Pappalardo, G., Sugimoto, N., Wehrli, C., Wiedensohler, a. and Zhang, X.-Y.: Recommendations for reporting “black carbon” measurements, Atmos. Chem. Phys., 13(16), 8365–8379, doi:10.5194/acp-13-8365-2013, 2013.

Pey, J.: Caracterización físico-química de los aerosols atmosféricos en el Mediterráneo Occidental, PhD Thesis, Universitat Politécnica de Catalunya (UPC), 2007.

Pey, J., Pérez, N., Castillo, S., Viana, M., Moreno, T., Pandolfi, M., López-Sebastián, J. M., Alastuey, a. and Querol, X.: Geochemistry of regional background aerosols in the Western Mediterranean, Atmos. Res., 94(3), 422–435, doi:10.1016/j.atmosres.2009.07.001, 2009.

Pey, J., Pérez, N., Cortés, J., Alastuey, A. and Querol, X.: Chemical fingerprint and impact of shipping emissions over a western Mediterranean metropolis : Primary and aged contributions, Sci. Total Environ., 463-464, 497–507, doi:10.1016/j.scitotenv.2013.06.061, 2013a.

Pey, J., Pérez, N., Querol, X., Alastuey, A., Cusack, M. and Reche, C.: Intense winter atmospheric pollution episodes affecting the Western Mediterranean., Sci. Total Environ., 408(8), 1951–1959, doi:10.1016/j.scitotenv.2010.01.052, 2010a.

Pey, J., Querol, X., Alastuey, A., Forastiere, F. and Stafoggia, M.: African dust outbreaks over the Mediterranean Basin during 2001–2011: PM10 concentrations, phenomenology and trends, and its relation with synoptic and mesoscale meteorology, Atmos. Chem. Phys., 13(3), 1395–1410, doi:10.5194/acp-13-1395-2013, 2013b.

Pey, J., Querol, X. and Alastuey, A.: Discriminating the regional and urban contributions in the North-Western Mediterranean: PM levels and composition, Atmos. Environ., 44(13), 1587–1596, doi:10.1016/j.atmosenv.2010.02.005, 2010b.

Pey, J., Rodríguez, S., Querol, X., Alastuey, A., Moreno, T., Putaud, J. P. and Van Dingenen, R.: Variations of urban aerosols in the western Mediterranean, Atmos. Environ., 42(40), 9052–9062, doi:10.1016/j.atmosenv.2008.09.049, 2008.

Pöschl, U.: Atmospheric aerosols: composition, transformation, climate and health effects, Angew. Chem. Int. Ed. Engl., 44(46), 7520–7540, doi:10.1002/anie.200501122, 2005.

Prospero, J. M., Ginoux, P., Torres, O., Nicholson, S. E. and Gill, T. E.: Environmental characterization of global sources of atmospheric soil dust identified with the NIMBUS 7 Total Ozone Mapping Spectrometer (TOMS) absorbing aerosol product, Rev. Geophys., 40(1), 1002, doi:10.1029/2000RG000095, 2002.

Putaud, J. P., Van Dingenen, R., Alastuey, A., Bauer, H., Birmili, W., Cyrys, J., Flentje, H., Fuzzi, S., Gehrig, R., Hansson, H. C., Harrison, R. M., Herrmann, H., Hitzenberger, R., Hüglin, C., Jones, A. M., Kasper-Giebl, A., Kiss, G., Kousa, A., Kuhlbusch, T. A. J., Löschau, G., Maenhaut, W., Molnar, A., Moreno, T., Pekkanen, J., Perrino, C., Pitz, M., Puxbaum, H., Querol, X., Rodriguez, S., Salma, I., Schwarz, J., Smolik, J., Schneider, J., Spindler, G., ten Brink, H., Tursic, J., Viana, M., Wiedensohler, A. and Raes, F.: A European aerosol phenomenology - 3: Physical and chemical characteristics of particulate matter from 60 rural, urban, and kerbside sites across Europe, Atmos. Environ., 44(10), 1308–1320, doi:doi:10.1016/j.atmosenv.2009.12.011, 2010.

Putaud, J.-P., Raes, F., Van Dingenen, R., Brüggemann, E., Facchini, M.-C., Decesari, S., Fuzzi, S., Gehrig, R., Hüglin, C., Laj, P., Lorbeer, G., Maenhaut, W., Mihalopoulos, N., Müller, K., Querol, X., Rodriguez, S., Schneider, J., Spindler, G., Brink, H. Ten, Tørseth, K. and Wiedensohler, A.: A European aerosol phenomenology—2: chemical characteristics of particulate matter at kerbside, urban, rural and background sites in Europe, Atmos. Environ., 38(16), 2579–2595, doi:10.1016/j.atmosenv.2004.01.041, 2004.

Querol, X., Alastuey, A., Ruiz, C. R., Artiñano, B., Hansson, H. C., Harrison, R. M., Buringh, E., ten Brink, H. M., Lutz, M., Bruckmann, P., Straehl, P. and Schneider,

J.: Speciation and origin of PM10 and PM2.5 in selected European cities, Atmos. Environ., 38(38), 6547–6555, doi:10.1016/j.atmosenv.2004.08.037, 2004.

Querol, X., Alastuey, A., Lopez-Soler, A., Mantilla, E. and Plana, F.: Mineral composition of atmospheric particulates around a large coal-fired power station, Atmos. Environ., 30(21), 3557–3572, doi:10.1016/1352-2310(96)00108-2, 1996.

Querol, X., Alastuey, A., Lopez-soler, A., Plana, F. and Puicercus, J. A.: Daily evolution of sulphate aerosols in a rural area , northeastern Spain - elucidation of an atmospheric reservoir effect, Environ. Pollut., 105(3), 397–407, doi:10.1016/S0269-7491(99)00037-8, 1999.

Querol, X., Alastuey, A., Pey, J., Cusack, M., Pérez, N., Mihalopoulos, N., Theodosi, C., Gerasopoulos, E., Kubilay, N. and Koçak, M.: Variability in regional background aerosols within the Mediterranean, Atmos. Chem. Phys., 9(14), 4575–4591, doi:10.5194/acp-9-4575-2009, 2009a.

Querol, X., Alastuey, A., Puicercus, J. A., Mantilla, E., Miro, J. V, Lopez-Soler, A., Plana, F. and Artiñano, B.: Seasonal evolution of suspended particles around a large coal-fired power station: particulate levels and sources, Atmos. Environ., 32(11), 1963–1978, 1998a.

Querol, X., Alastuey, A., Puicerdus, J. A., Mantilla, E., Ruiz, C. R., Lopez-soler, A., Plana, F. and Roberto, J.: Seasonal evolution of suspended particles around a large coal-fired power station: chemical characterization, Atmos. Environ., 32(4), 719–731, 1998b.

Querol, X., Alastuey, A., Rodriguez, S., Plana, F., Mantilla, E. and Ruiz, C. R.: Monitoring of PM10 and PM2.5 around primary particulate anthropogenic emission sources, Atmos. Environ., 35(5), 845–858, doi:10.1016/S1352-2310(00)00387-3, 2001a.

Querol, X., Alastuey, A., Rodriguez, S., Plana, F., Ruiz, C. R., Cots, N., Massagué, G. and Puig, O.: PM10 and PM2.5 source apportionment in the Barcelona Metropolitan area, Catalonia, Spain, Atmos. Environ., 35(36), 6407–6419, 2001b.

Querol, X., Pey, J., Pandolfi, M., Alastuey, A., Cusack, M., Pérez, N., Moreno, T., Viana, M., Mihalopoulos, N., Kallos, G. and Kleanthous, S.: African dust contributions to mean ambient PM10 mass-levels across the Mediterranean Basin, Atmos. Environ., 43(28), 4266–4277, doi:10.1016/j.atmosenv.2009.06.013, 2009b.

Querol, X., Viana, M., Alastuey, A., Amato, F., Moreno, T., Castillo, S., Pey, J., de la Rosa, J., Sánchez de la Campa, A., Artíñano, B., Salvador, P., García Dos Santos, S., Fernández-Patier, R., Moreno-Grau, S., Negral, L., Minguillón, M. C., Monfort, E., Gil, J. I., Inza, A., Ortega, L. A., Santamaría, J. M. and Zabalza, J.: Source origin of trace elements in PM from regional background, urban and industrial sites of Spain, Atmos. Environ., 41(34), 7219–7231, doi:10.1016/j.atmosenv.2007.05.022, 2007.

Raatikainen, T., Vaattovaara, P., Tiitta, P., Miettinen, P., Rautiainen, J., Ehn, M., Kulmala, M., Laaksonen, a. and Worsnop, D. R.: Physicochemical properties and origin of organic groups detected in boreal forest using an aerosol mass spectrometer, Atmos. Chem. Phys., 10(4), 2063–2077, doi:10.5194/acp-10-2063-2010, 2010.

Reche, C., Viana, M., Amato, F., Alastuey, A., Moreno, T., Hillamo, R., Teinilä, K., Saarnio, K., Seco, R., Peñuelas, J., Mohr, C., Prévôt, A. S. H. and Querol, X.: Biomass burning contributions to urban aerosols in a coastal Mediterranean city., Sci. Total Environ., 427-428, 175–90, doi:10.1016/j.scitotenv.2012.04.012, 2012a.

Reche, C., Viana, M., Moreno, T., Querol, X., Alastuey, A., Pey, J., Pandolfi, M., Prévôt, A., Mohr, C., Richard, A., Artiñano, B., Gomez-Moreno, F. J. and Cots, N.: Peculiarities in atmospheric particle number and size-resolved speciation in an urban area in the western Mediterranean: Results from the DAURE campaign, Atmos. Environ., 45(30), 5282–5293, doi:10.1016/j.atmosenv.2011.06.059, 2011.

Reche, C., Viana, M., Pandolfi, M., Alastuey, A., Moreno, T., Amato, F., Ripoll, A. and Querol, X.: Urban NH3 levels and sources in a Mediterranean environment, Atmos. Environ., 57, 153–164, doi:10.1016/j. atmosenv.2012.04.021, 2012b.

Regulation 582/2011 of 25 May 2011 implementing and amending Regulation 595/2009 of the European Parliament and of the Council with respect to emissions from heavy duty vehicles (Euro VI) (OJ L 167, 25.6.2011, pp. 1–168), available at: http://eur-lex.europa.eu/legal-content/EN/TXT/PDF/?uri=CELEX :32011R0582&from=en (last access: 10 April 2015), 2011.

Regulation 595/2009 of the European Parliament and of the Council of 18 June 2009 on type approval of motor vehicles and engines with respect to emissions from heavy duty vehicles (Euro VI) and on access to vehicle repair and maintenance information (OJ L 188, 18.7.2009, pp. 1–13), available at: http://eur-lex.europa.eu/legal-content/EN/TXT/PDF/?uri=CELEX:32009R0595&from=EN (last access: 10 April 2015), 2009.

Regulation 715/2007 of the European Parliament and of the Council of 20 June 2007 on type approval of motor vehicles with respect to emissions from light passanger and commercial vehicles (Euro 5 and Euro 6) and on access to vehicle repair and maintenance information (OJ L 171, 29.6.2007, pp. 1–16), available at: http://eur-lex.europa.eu/legal-content/EN/TXT/PDF/?uri=CELEX:32007R0715&from=EN (last access: 10 April 2015), 2007.

Ripoll, A., Minguillón, M. C., Pey, J., Jimenez, J. L., Day, D. A., Sosedova, Y., Canonaco, F., Prévôt, A. S. H., Querol, X. and Alastuey, A.: Long-term real-time chemical characterization of submicron aerosols at Montsec (southern Pyrenees, 1570 m a.s.l.), Atmos. Chem. Phys., 15(6), 2935–2951, doi:doi:10.5194/acp-15-2935-2015, 2015a.

Ripoll, A., Minguillón, M. C., Pey, J., Pérez, N., Querol, X. and Alastuey, A.: Joint analysis of continental and regional background environments in the Western

Mediterranean: PM1 and PM10 concentrations and composition, Atmos. Chem. Phys., 15, 1129–1145, doi:10.5194/acp-15-1129-2015, 2015b.

Ripoll, A., Pey, J., Minguillón, M. C., Pérez, N., Pandolfi, M., Querol, X. and Alastuey, A.: Three years of aerosol mass, black carbon and particle number concentrations at Montsec (southern Pyrenees, 1570 m a.s.l.), Atmos. Chem. Phys., 14(8), 4279–4295, doi:10.5194/acp-14-4279-2014, 2014.

Robinson, A. L., Donahue, N. M., Shrivastava, M. K., Weitkamp, E. A., Sage, A. M., Grieshop, A. P., Lane, T. E., Pierce, J. R. and Pandis, S. N.: Rethinking organic aerosols: semivolatile emissions and photochemical aging., Science, 315(5816), 1259–62, doi:10.1126/science.1133061, 2007.

Rodríguez, S., Alastuey, A., Alonso-Pérez, S., Querol, X., Cuevas, E., Abreu-Afonso, J., Viana, M., Pérez, N., Pandolfi, M. and de la Rosa, J.: Transport of desert dust mixed with North African industrial pollutants in the subtropical Saharan Air Layer, Atmos. Chem. Phys., 11(13), 6663–6685, doi:10.5194/acp-11-6663-2011, 2011.

Rodríguez, S., Van Dingenen, R., Putaud, J.-P., Martins-Dos Santos, S. and Roselli, D.: Nucleation and growth of new particles in the rural atmosphere of Northern Italy—relationship to air quality monitoring, Atmos. Environ., 39(36), 6734–6746, doi:10.1016/j.atmosenv.2005.07.036, 2005.

Rodríguez, S., Querol, X., Alastuey, A., Kallos, G. and Kakaliagou, O.: Saharan dust contributions to PM10 and TSP levels in Southern and Eastern Spain, Atmos. Environ., 35, 2433–2447, doi:10.1016/S1352-2310(00)00496-9, 2001.

Rodríguez, S., Querol, X., Alastuey, A. and Mantilla, E.: Origin of high summer PM10 and TSP concentrations at rural sites in Eastern Spain, Atmos. Environ., 36(19), 3101–3112, doi:10.1016/S1352-2310(02)00256-X, 2002a.

Rodríguez, S., Querol, X., Alastuey, A. and Plana, F.: Sources and processes affecting levels and composition of atmospheric aerosol in the western Mediterranean, J. Geophys. Res., 107(D24), 4777, doi:10.1029/2001JD001488, 2002b.

Rodríguez, S., Querol, X., Alastuey, A., Viana, M.-M. and Mantilla, E.: Events affecting levels and seasonal evolution of airborne particulate matter concentrations in the Western Mediterranean., Environ. Sci. Technol., 37(2), 216–222, doi:10.1021/es020106p, 2003.

Rolph, G.D.: Real-time Environmental Applications and Display sYstem (READY) Website (http://www.ready.noaa.gov). NOAA Air Resources Laboratory, College Park, MD, 2014.

Samet, J. M., Rappold, A., Graff, D., Cascio, W. E., Berntsen, J. H., Huang, Y.-C. T., Herbst, M., Bassett, M., Montilla, T., Hazucha, M. J., Bromberg, P. A. and Devlin, R. B.: Concentrated ambient ultrafine particle exposure induces cardiac changes in young healthy volunteers., Am. J. Respir. Crit. Care Med., 179(11), 1034–1042, doi:10.1164/rccm.200807-1043OC, 2009.

Scheuvens, D. and Kandler, K.: Chapter 2: On Composition, Morphology, and Size Distribution of Airborne Mineral Dust, pp. 15-49, within Mineral Dust: A Key Player in the Earth System, [Knippertz, P. and Stuut, J.-B. W. (Eds.)], Springer Dordrecht Heidelberg New York London, doi:10.1007/978-94-017-8978-3_2, 2014.

Seco, R., Peñuelas, J., Filella, I., Llusià, J., Molowny-Horas, R., Schallhart, S., Metzger, A., Müller, M. and Hansel, A.: Contrasting winter and summer VOC mixing ratios at a forest site in the Western Mediterranean Basin: the effect of local biogenic emissions, Atmos. Chem. Phys., 11(24), 13161–13179, doi:10.5194/acp-11-13161-2011, 2011.

Seinfeld, J. H. and Pandis, S. N.: Atmospheric chemistry and physics: From air pollution to climate change, 2nd Edition. 1232 pp., ISBN: 978-0-471-72018-8, September 2006.

Shindell, D., Kuylenstierna, J. C. I., Vignati, E., van Dingenen, R., Amann, M., Klimont, Z., Anenberg, S. C., Muller, N., Janssens-Maenhout, G., Raes, F., Schwartz, J., Faluvegi, G., Pozzoli, L., Kupiainen, K., Höglund-Isaksson, L., Emberson, L., Streets, D., Ramanathan, V., Hicks, K., Oanh, N. T. K., Milly, G., Williams, M., Demkine, V. and Fowler, D.: Simultaneously mitigating near-term climate change and improving human health and food security., Science, 335(6065), 183–189, doi:10.1126/science.1210026, 2012.

Sicard, M., Pérez, C., Rocadenbosch, F., Baldasano, J. M. and García-Vizcaino, D.: Mixed-Layer Depth Determination in the Barcelona Coastal Area From Regular Lidar Measurements: Methods, Results and Limitations, Boundary-Layer Meteorol., 119(1), 135–157, doi:10.1007/s10546-005-9005-9, 2006.

Sicard, M., Rocadenbosch, F., Reba, M. N. M., Comerón, A., Tomás, S., García-Vízcaino, D., Batet, O., Barrios, R., Kumar, D. and Baldasano, J. M.: Seasonal variability of aerosol optical properties observed by means of a Raman lidar at an EARLINET site over Northeastern Spain, Atmos. Chem. Phys., 11(1), 175–190, doi:10.5194/acp-11-175-2011, 2011.

Simpson, D., Winiwarter, W., Börjesson, G., Cinderby, S., Ferreiro, A., Guenther, A., Hewitt, C. N., Janson, R., Khalil, M. A. K., Owen, S., Pierce, T. E., Puxbaum, H., Shearer, M., Skiba, U., Steinbrecher, R., Tarrasón, L. and Öquist, M. G.: Inventorying emissions from nature in Europe, J. Geophys. Res. Atmos., 104(D7), 8113–8152, doi:10.1029/98JD02747, 1999.

Steinbrecher, R., Smiatek, G., Köble, R., Seufert, G., Theloke, J., Hauff, K., Ciccioli, P., Vautard, R. and Curci, G.: Intra- and inter-annual variability of VOC emissions from natural and semi-natural vegetation in Europe and neighbouring countries, Atmos. Environ., 43(7), 1380–1391, doi:10.1016/j.atmosenv.2008.09.072, 2009.

Sun, J., Zhang, Q., Canagaratna, M. R., Zhang, Y., Ng, N. L., Sun, Y., Jayne, J. T., Zhang, X., Zhang, X. and Worsnop, D. R.: Highly time- and size-resolved characterization of submicron aerosol particles in Beijing using an Aerodyne

Aerosol Mass Spectrometer, Atmos. Environ., 44(1), 131–140, doi:10.1016/j.atmosenv.2009.03.020, 2010.

Sun, Y., Wang, Z., Dong, H., Yang, T., Li, J., Pan, X., Chen, P. and Jayne, J. T.: Characterization of summer organic and inorganic aerosols in Beijing, China with an Aerosol Chemical Speciation Monitor, Atmos. Environ., 51, 250–259, doi:10.1016/j.atmosenv.2012.01.013, 2012.

Takahama, S., Schwartz, R. E., Russell, L. M., Macdonald, a. M., Sharma, S. and Leaitch, W. R.: Organic functional groups in aerosol particles from burning and non-burning forest emissions at a high-elevation mountain site, Atmos. Chem. Phys., 11(13), 6367–6386, doi:10.5194/acp-11-6367-2011, 2011.

Thermo: Operating instructions of the Black carbon monitor, CARUSSO / MMAP5012. SB-020-011010, Version 13.12.2004.

Thurston, G. D. and Spengler, J. D.: A quantitative assessment of source contributions to inhalable particulate matter pollution in metropolitan Boston, Atmos. Environ., 19, 9–25, 1985.

Toll, I. and Baldasano, J. M.: Modeling of photochemical air pollution in the Barcelona area with highly disaggregated anthropogenic and biogenic emissions, Atmos. Environ., 34(19), 3069–3084, doi:10.1016/S1352-2310(99)00498-7, 2000.

TSI: Operation and service manual of environmental particle counter model 3783. P/N 1981410, Revision B, September 2010.

TSI: Operation and service manual of electrostatic classifiers series 3080. P/N 1933792, Revision J, March 2009.

TSI: Operation and service manual of ultrafine condensation particle counter model 3776. P/N 1980522, Revision C, April 2007.

Van Dingenen, R., Raes, F., Putaud, J.-P., Baltensperger, U., Charron, A., Facchini, M.-C., Decesari, S., Fuzzi, S., Gehrig, R., Hansson, H.-C., Harrison, R. M., Hüglin, C., Jones, A. M., Laj, P., Lorbeer, G., Maenhaut, W., Palmgren, F., Querol, X., Rodriguez, S., Schneider, J., Brink, H. Ten, Tunved, P., Tørseth, K., Wehner, B., Weingartner, E., Wiedensohler, A. and Wåhlin, P.: A European aerosol phenomenology—1: physical characteristics of particulate matter at kerbside, urban, rural and background sites in Europe, Atmos. Environ., 38(16), 2561–2577, doi:10.1016/j.atmosenv.2004.01.040, 2004.

Venzac, H., Sellegri, K., Villani, P., Picard, D. and Laj, P.: Seasonal variation of aerosol size distributions in the free troposphere and residual layer at the puy de Dôme station , France, Atmos. Chem. Phys., 9, 1465–1478, 2009.

Viana, M., Pérez, C., Querol, X., Alastuey, A., Nickovic, S. and Baldasano, J. M.: Spatial and temporal variability of PM levels and composition in a complex summer atmospheric scenario in Barcelona (NE Spain), Atmos. Environ., 39(29), 5343–5361, doi:10.1016/j.atmosenv.2005.05.039, 2005.

Viana, M., Querol, X., Alastuey, A., Cuevas, E. and Rodríguez, S.: Influence of African dust on the levels of atmospheric particulates in the Canary Islands air quality network, Atmos. Environ., 36(38), 5861–5875, doi:10.1016/S1352-2310(02)00463-6, 2002.

Volkamer, R., Jimenez, J. L., San Martini, F., Dzepina, K., Zhang, Q., Salcedo, D., Molina, L. T., Worsnop, D. R. and Molina, M. J.: Secondary organic aerosol formation from anthropogenic air pollution: Rapid and higher than expected, Geophys. Res. Lett., 33(17), L17811, doi:10.1029/2006GL026899, 2006.

Vrekoussis, M., Liakakou, E., Koçak, M., Kubilay, N., Oikonomou, K., Sciare, J. and Mihalopoulos, N.: Seasonal variability of optical properties of aerosols in the Eastern Mediterranean, Atmos. Environ., 39, 7083–7094, doi:10.1016/j.atmosenv.2005.08.011, 2005.

Wall, S. M., John, W. and Ondo, J. L.: Measurement of aerosol size distributions for nitrate and major ionic species, Atmos. Environ., 22(8), 1649–1656, doi:10.1016/0004-6981(88)90392-7, 1988.

Watson, J. G., Robinson, N. F., Lewis, C., Coulter, T., Chow, J. C., Fujita, E. M., Lowenthal, D., Conner, T. L., Henry, R. C., and Willis, R. D.: Chemical Mass Balance Receptor Model Version 8 (CMB8) User's Manual, Prepared for US Environmental Protection Agency, Research Triangle Park, NC, by Desert Research Institute, Reno, NV, 1997.

Wiedensohler, A., Birmili, W., Nowak, A., Sonntag, A., Weinhold, K., Merkel, M., Wehner, B., Tuch, T., Pfeifer, S., Fiebig, M., Fjäraa, A. M., Asmi, E., Sellegri, K., Depuy, R., Venzac, H., Villani, P., Laj, P., Aalto, P., Ogren, J. A., Swietlicki, E., Williams, P., Roldin, P., Quincey, P., Hüglin, C., Fierz-Schmidhauser, R., Gysel, M., Weingartner, E., Riccobono, F., Santos, S., Grüning, C., Faloon, K., Beddows, D., Harrison, R., Monahan, C., Jennings, S. G., O'Dowd, C. D., Marinoni, A., Horn, H. G., Keck, L., Jiang, J., Scheckman, J., McMurry, P. H., Deng, Z., Zhao, C. S., Moerman, M., Henzing, B., De Leeuw, G., Löschau, G. and Bastian, S.: Mobility particle size spectrometers: Harmonization of technical standards and data structure to facilitate high quality long-term observations of atmospheric particle number size distributions, Atmos. Meas. Tech., 5(March), 657–685, doi:10.5194/amt-5-657-2012, 2012.

Wiedensohler, A., Covert, D. S., Swietlicki, E., Aalto, P., Heintzenberg, J. and Leck, C.: Occurrence of an ultrafine particle mode less than 20 nm in diameter in the marine boundary layer during Arctic summer and autumn, Tellus B, 48(2), 213-222, 1996.

World Health Organization (WHO): Review of Evidence on Health Aspects of Air Pollution – REVIHAAP, First Results, WHO's Regional Office for Europe, Copenhagen, 28 pp., available at: http://www.euro.who.int/_data/assets/pdf_file/0020/182432/ e96762-final.pdf (last access: 16 June 2014), 2013.

World Health Organization (WHO): Health effects of Black Carbon, WHO's Regional Office for Europe, Copenhagen, 86 pp., available at: http://www.euro.who.int/__data/assets/pdf_file/0004/162535/e96541.pdf (last access: 8 April 2015), 2012.

World Health Organization (WHO): Global health risk: mortality and burden of disease attributable to selected major risks, 62pp., available at: http://www.who.int/healthinfo/global_burden_disease/global_health_risks/en/ (last access: 8 April 2015), 2009.

Zhang, K. M. and Wexler, A. S.: Evolution of particle number distribution near roadways - Part I: Analysis of aerosol dynamics and its implications for engine emission measurement, Atmos. Environ., 38, 6643–6653, doi:10.1016/j.atmosenv.2004.06.043, 2004.

Zhang, Q., Jimenez, J. L., Canagaratna, M. R., Ulbrich, I. M., Ng, N. L., Worsnop, D. R. and Sun, Y.: Understanding atmospheric organic aerosols via factor analysis of aerosol mass spectrometry: a review., Anal. Bioanal. Chem., 401(10), 3045–3067, doi:10.1007/s00216-011-5355-y, 2011.

Zhang, R., Khalizov, A., Wang, L., Hu, M. and Xu, W.: Nucleation and growth of nanoparticles in the atmosphere., Chem. Rev., 112(3), 1957–2011, doi:10.1021/cr2001756, 2012.

Zhuang, H., Chan, C. K., Fang, M. and Wexler, A. S.: Formation of nitrate and non-sea-salt sulfate on coarse particles, Atmos. Environ., 33(26), 4223–4233, doi:10.1016/S1352-2310(99)00186-7, 1999a.

Zhuang, H., Chan, C. K., Fang, M. and Wexler, A. S.: Size distributions of particulate sulfate , nitrate , and ammonium at a coastal site in Hong Kong, Atmos. Environ., 33(6), 843–853, doi:10.1016/S1352-2310(98)00305-7, 1999b.

Agraïments/Acknowledgments

Aquí estic, escrivint la última secció de la tesi. Sembla impossible que ja faci més de 5 anys que vaig començar aquest projecte! Miro enrere i penso en totes les persones que m'han ajudat d'una manera o altra, en tot el que m'han ensenyat, en tot el que hem compartit, en totes les hores de viatges, de campanyes, de pensar, de llegir, d'escriure… Uf! Em poso nerviosa, inquieta, trista però contenta. Tancar etapes sempre m'ha generat una certa tristesa, però sé que després vindran nous reptes i això és motivador. Estic orgullosa de la feina ben feta, està clar que jo sola no ho hauria aconseguit, per això voldria agrair a cadascú de vosaltres el suport que m'heu regalat, tot i que no dubto que em deixi a algú. M'he pres la llibertat d'escriure aquesta secció en la meva llengua materna, encara que intentaré personalitzar els agraïments a cadascú en la llengua en la que ens hem comunicat.

En primer lloc, i saltant-me el protocol, si n'hi ha, vull puntualitzar que encara que no m'hagin deixat escriure el teu nom a la portada, Jorge Pey, para mí siempre serás uno de mis directores de tesis. La burocracia, las normativas y los papeles no entienden ni reflejan las relaciones humanas, pero por suerte las personas sí, y la amistad, la confianza, el apoyo y el conocimiento que me has dado desde el primer día reflejan, y de sobras, tu papel como codirector de esta tesis. Así que, ahora sí, esta tesis no habría sido posible sin la ayuda de Andrés Alastuey, Mari Cruz Minguillón y Jorge Pey, directores de tesis y amigos. Los tres formáis un equipo fantástico, una combinación única de rigurosidad y buen rollo. Os agradezco muchísimo vuestra dedicación, siempre con mucha paciencia, y la libertad que me habéis dado en todo

momento. Andrés, científico reconocido y mejor persona. Te agradezco el montón de oportunidades que me has dado para poder ir a cursos, escuelas y conferencias a nivel mundial. Mari Cruz, gracias por tu crítica siempre constructiva y tu sentido del humor, sin tu compañía las campañas, los viajes (profesionales y personales) y los congresos no habrían sido igual de divertidos. Jorge, gracias por enseñarme a "trastear" y a "destripar equipos", al final hasta arreglamos alguno! Pero sobretodo, gracias por introducirme en el "mundillo" de los aerosoles.

També vull agrair especialment la confiança del Xavier Querol. Sobre el paper, un investigador de renom mundial amb molta experiència en el món de la recerca. A la realitat, això i més, una persona propera, directa, honesta i que mai té un no per resposta. Xavi, tot i que no vas voler ser el meu director de tesi (és broma), moltes gràcies per la teva ajuda continuada i per obrir-me les portes d'aquesta casa.

A continuació vull donar les gràcies a totes les companyes i companys del grup, sou genials! ¡Sois geniales! You are all amazing! Des del primer dia m'heu fet sentir com a casa i sempre que he necessitat alguna cosa hi ha hagut algú disposat a ajudar-me. Gracias a los del despacho 1543 (a los de ahora y a los de antes), a las inmaduras (va, y a las maduras también), a las chicas del lab (aunque hay algunas que ya no estáis), a los que llevan desayuno para celebrar su cumple y a los que no también, y, sobretodo, a todos los que me habéis acompañado al Montsec (inclús als que no sou de la feina: família, Yolanda Sola, Ignasi Serra, Cris Mari, Alba Morros, Denis Ramos, Jaume Antonio i Jordi Lluis). A todos, ¡muchísimas gracias! Natalia i Mari Cruz, (bueno, y Michael), no oblidaré mai el viatge a Fuerteventura!

M'agradaria expressar el meu sincer agraïment a la gent de l'Observatori Astronòmic del Montsec (Josep Salse, Salvador Ribas, Pere Gil i Carlos) pel seu suport tècnic que tant ens ha ajudat quan hem tingut problemes, i al propi observatori per cedir-nos un lloc on posar l'estació de mesura. Aprofito també per donar les gràcies al Servei Meteorològic de Catalunya per proporcionar les dades meteorològiques de l'estació del Montsec d'Ares, i a la Direcció General de Qualitat Ambiental del Departament de Territori i Sostenibilitat de la Generalitat de Catalunya per proporcionar les dades dels gasos.

I would like to thank the CIRES people for a great three-months period in Boulder. Jose Jimenez and Doug Day, I learned a lot from you, thank you for your selfless help. Gràcies també a la família de Boulder, Mireies, Jordi, Albert, Roger, Mònica, María i Laia, per les excursions, sortides i birres al Dark Horse, sense vosaltres la meva estada no hauria estat el mateix.

Finalment, només em queda donar les gràcies a tots aquells que, sense saber-ho, també heu fet possible aquesta tesi, perquè m'heu acompanyat en aquest viatge, amics i família, la vostra companyia permanent m'ha ajudat a seguir caminant i a poder arribar fins aquí.

Amics de Sants: companys de classe al Proa o col·legues del lokal, han passat molts anys, alguns hem marxat, hem tornat, alguns us heu casat, heu tingut fills, però quan hi ha algun esdeveniment (aniversari, paella, barbacoa, cap d'any,...) sempre som una vintena! Sou collonuts!

Amics de la uni: ens vam conèixer estudiant ambientals entre viatges accidentats però molt divertits, i ens hem convertit en una gran família que no para de créixer! Gràcies pels nadals ambientals, les calçotades, les birres, ... que aquestes trobades no s'acabin mai.

I nenes d'Alcover: gràcies per ser-hi sense ser-hi. Tot i la distància sempre hem mantingut aquesta amistat tant sincera i directa que, entre crits i rialles, ens ha fet créixer plegades. No canvieu mai!

Ara sí, moltes moltes gràcies als meus pares, la Remei i el Joan, per la vostra estima incondicional, per la immensa llibertat que m'heu donat i per respectar sempre les meves decisions. També vull donar les gràcies a la meva germana, la Mireia, i al Pere, el "xispes" de la família, per la seva enorme hospitalitat, per fer de casa vostra la casa de tots! Sobretot ara que teniu dues filles incansables, la Nit i la Rut.

Jordi, per acabar vull donar-te les gracies a tu, perquè sense voler-ho t'has trobat amb aquest percal, i, com sempre, has sapigut desdramatitzar els meus problemes i les meves preocupacions. Estar al teu costat em dona pau i serenitat. La vida amb tu és millor!

This thesis was done with the financial support of a *Formación de Personal Investigador* (FPI) predoctoral fellowship (BES-2009-021012) funded by the *Ministerio de Economía y Competitividad* (MINECO) and FEDER funds under the projects of *Caracterización Integral de Aerosoles Troposféricos de Fondo Continental en el NE de Iberia* (CARIATI, CGL2008-06294/CLI) and *Propiedades ópticas y forzamiento radiativo de aerosoles atmosféricos en el Mediterráneo occidental en función de sus fuentes y composición química* (PRISMA, CGL2012-39623-C02-01), and by the *Agència de Gestió d'Ajuts Universitaris i de Recerca* (AGAUR, 2009SGR8 and 2014SGR33) from the *Generalitat de Catalunya*. A three-month stay in the Cooperative Institute for Research in Environmental Sciences (CIRES) at the University of Colorado Boulder was supported by a *Estancias Breves* fellowship (EEBB-I-12-04234) funded by the MINECO. The research received funding from the European Union Seventh Framework Programme (FP7/ 2007-2013) Aerosols, Clouds and Trace gases Research InfraStructure (ACTRIS) under grant agreement no. 262254.

Appendix

A. Appendix: List of acronyms and symbols

ACSM	Aerosol Chemical Speciation Monitor
ACTRIS	Aerosols, Clouds and Trace gases Research InfraStructure
AMS	Aerosol Mass Spectometer
a.s.l.	above sea level
BBOA	Biomass Burning Organic Aerosol
BC	Black Carbon
CCN	Cloud Condensation Nuclei
CE	Collection Efficiency
CPC	Condensation Particle Counter
CSIC	Consejo Superior de Investigaciones Científicas
DAURE	Determination of the sources of atmospheric Aerosols in Urban and Rural Environments in the western Mediterranean
DL	Detection Limit
DMA	Differential Mobility Analyzer
EC	Elemental Carbon
EMEP	European Monitoring and Evaluation Programme
FT	Free Troposphere
GAW	Global Atmosphere Watch
GADS1	Global Data Assimilation System 1

HOA	Hydrocarbon-like Organic Aerosol
HPLC	Ion High-Performance Liquid Chromatography
HYSPLIT	HYbrid Single Particle Lagrangian Integrated Trajectories
ICP-AES	Inductively Coupled Plasma Atomic Emission Spectroscopy
ICP-MS	Inductively Coupled Plasma Mass Spectrometry
IDAEA	Institut de Diagnosi Ambiental i Estudis de l'Aigua
IE	Ionization Efficiency
IN	Ice Nuclei
IP	Iberian Peninsula
IPCC	Intergovernmental Panel on Climate Change
LV-OOA	Low-Volatility Oxygenated Organic Aerosol
MAC	Mass Absorption Cross section
MAAP	Multi-Angle Absorption Photometer
ME-2	Multilinear Engine 2
MM	Mineral Matter
MSCS	Mass Scattering Cross Section
NAF	North African
NOAA	National Oceanic and Atmospheric Administration
NPF	New Particle Formation
OA	Organic Aerosol
OAdM	Observatori Astronòmic del Montsec
OM	Organic Matter
OOA	Oxygenated Organic Aerosol
OPC	Optical Particle Counter
PAH	Polycyclic Aromatic Hydrocarbons
PCA	Principal Component Analysis
PBL	Planetary Boundary Layer
PMF	Positive Matrix Factorization
POA	Primary Organic Aerosol
RIE	Relative Ionization Efficiency
SAE	Scattering Ångström Exponent
SMPS	Scanning Mobility Particle Sizer
s.n.m.	sobre el nivell del mar
SOA	Secondary Organic Aerosol
SoFi	Source Finder
SREG	Summer REGional
SS	Sea Salt

SSA	Single-Scattering Albedo
SV-OOA	SemiVolatile Oxygenated Organic Aerosol
UTC	Coordinated Universal Time
VOCs	Volatile Organic Compounds
WHO	World Health Organization
WREG	Winter REGional
XVPCA	Xarxa de Vigilància i Previsió de la Contaminació Atmosfèrica
σ_{bsp}	Aerosol particle backscattering coefficient
σ_{ap}	Aerosol particle light-absorption coefficient
σ_{sp}	Aerosol particle light-scattering coefficient
g	Asymmetry parameter
m/z	Atomic mass unit
B/S	Backscattering-to-scattering ratio
Dp	Particle diameter
N	Particle number
NH_3	Ammonia
NH_4^+	Ammonium
NO_3^-	Nitrate
NO_x	Nitrogen oxides
nss-Na	non-sea-salt Na
O_3	Ozone
PM	Particle mass
SO_4^{2-}	Sulfate
SO_2	Sulfur dioxide
ss-Na	sea-salt sodium

B. Appendix: List of detection limit and uncertainty for PM components

Table B.1. Detection limit estimated for PM components.

DL (µg m^{-3})	PM_{10}	PM_1
EC	0.0201	0.0205
OC	0.0201	0.0205
NO_3^-	0.0369	0.0377
NH_4^+	0.0152	0.0155
S	0.0004	0.0004
Cl^-	0.0308	0.0314
Al	0.0006	0.0006
Ca	0.0004	0.0004
K	0.0005	0.0005
Na	0.0004	0.0004
Mg	0.0004	0.0004
Fe	0.0004	0.0004

DL (ng m^{-3})	PM_{10}	PM_1
P	0.4102	0.4186
Li	0.0156	0.0159
Ti	0.0158	0.0161
V	0.0156	0.0159
Cr	0.0162	0.0165
Mn	0.0159	0.0162
Co	0.0156	0.0159
Ni	0.0162	0.0165
Cu	0.0157	0.0161
Zn	0.0173	0.0177
As	0.0156	0.0159
Se	0.0156	0.0159
Rb	0.0156	0.0159
Sr	0.0157	0.0160
Zr	0.136	0.1388
Nb	0.0156	0.0159
Cd	0.0156	0.0159
Sn	0.0156	0.0159
Sb	0.0156	0.0159
Cs	0.0156	0.0159
Ba	0.0187	0.0192
La	0.0156	0.0159
Ce	0.0156	0.0159
Pr	0.0156	0.0159
Nd	0.0156	0.0159
Hf	0.1353	0.1381
Tl	0.0156	0.0159
Pb	0.0156	0.0159
Bi	0.0156	0.0159
Th	0.0156	0.0159
U	0.0156	0.0159

Table B.2. Uncertainty estimated for PM components.

σ^2_{ij} (µg m^{-3})	PM_{10}	PM_1
EC	0.0153	0.0164
OC	0.1965	0.2337
NO_3^-	0.0909	0.0403
NH_4^+	0.0836	0.1036
S	0.0521	0.0675
Cl^-	0.0762	0.0756
Al	0.1178	0.1094
Ca	0.0498	0.0254
K	0.0595	0.0585
Na	0.0226	0.0111
Mg	0.0151	0.0112
Fe	0.0215	0.0116

σ^2_{ij} (ng m^{-3})	PM_{10}	PM_1
P	1.6060	1.6383
Li	0.0243	0.0072
Ti	2.0178	0.7206
V	0.1533	0.1368
Cr	1.0604	1.0851
Mn	0.9742	0.8010
Co	0.0216	0.0209
Ni	1.0539	1.0819
Cu	0.5573	0.5308
Zn	1.9936	2.0630
As	0.0258	0.0221
Se	0.0285	0.0277
Rb	0.0483	0.0233
Sr	0.4508	0.3804
Zr	3.914	4.1940
Nb	0.0780	0.0698
Cd	0.0175	0.0177
Sn	0.0641	0.0561
Sb	0.0783	0.0790
Cs	0.0062	0.0053
Ba	2.5756	2.5976
La	0.0744	0.0688
Ce	0.1588	0.1480
Pr	0.0213	0.0203
Nd	0.0744	0.0702
Hf	0.2025	0.2123
Tl	0.0053	0.0053
Pb	0.1712	0.1795
Bi	0.0070	0.0068
Th	0.0738	0.0746
U	0.1003	0.1027